INFORMATION TO USERS

This manuscript has been reproduced from the microfilm master. UMI films the text directly from the original or copy submitted. Thus, some thesis and dissertation copies are in typewriter face, while others may be from any type of computer printer.

The quality of this reproduction is dependent upon the quality of the copy submitted. Broken or indistinct print, colored or poor quality illustrations and photographs, print bleedthrough, substandard margins, and improper alignment can adversely affect reproduction.

In the unlikely event that the author did not send UMI a complete manuscript and there are missing pages, these will be noted. Also, if unauthorized copyright material had to be removed, a note will indicate the deletion.

Oversize materials (e.g., maps, drawings, charts) are reproduced by sectioning the original, beginning at the upper left-hand corner and continuing from left to right in equal sections with small overlaps. Each original is also photographed in one exposure and is included in reduced form at the back of the book.

Photographs included in the original manuscript have been reproduced xerographically in this copy. Higher quality 6" x 9" black and white photographic prints are available for any photographs or illustrations appearing in this copy for an additional charge. Contact UMI directly to order.

UMI

A Bell & Howell Information Company
300 North Zeeb Road, Ann Arbor MI 48106-1346 USA
313/761-4700 800/521-0600

STUDIES ON THE INTERCONVERSION AND REARRANGEMENT OF C_4H_6 AND C_8H_{12} RADICAL CATIONS

by

Hubrecht Johan Peter de Lijser

B.Sc., Van Leeuwenhoek Institute, Delft
M.Sc., Leiden University

Submitted in partial fulfillment of the requirements
for the degree of Doctor of Philosophy

at

Dalhousie University
Halifax, Nova Scotia
July, 1997

DALHOUSIE UNIVERSITY

FACULTY OF GRADUATE STUDIES

The undersigned hereby certify that they have read and recommend to the Faculty of Graduate Studies for acceptance a thesis entitled "Studies on the Interconversion and Rearrangement of C_4H_6 and C_8H_{12} Radical Cations"

by Hubrecht Johan Peter de Lijser

in partial fulfillment of the requirements for the degree of Doctor of Philosophy.

Dated: July 17, 1997

External Examiner

Research Supervisor

Examining Committee

DALHOUSIE UNIVERSITY

DATE: July 17, 1997

AUTHOR: Hubrecht Johan Peter de Lijser

TITLE: Studies on the Interconversion and Rearrangement of C_4H_6 and C_8H_{12} radical cations

DEPARTMENT OR SCHOOL: Department of Chemistry

DEGREE: Ph.D. CONVOCATION: October YEAR: 1997

Permission is herewith granted to Dalhousie University to circulate and to have copied for non-commercial purposes, at its discretion, the above title upon the request of individuals or institutions.

[redacted]

Signature of Author

To my parents

Live and don't learn, that's us.[0]

Table of Contents

List of Figures

Chapter 1

Chapter 2

Chapter 3

Chapter 4

Appendix II

List of Schemes

Chapter 1

Chapter 3

List of Tables

Chapter 1

Chapter 2

Chapter 3

Chapter 4

Appendix I

Appendix II

Abstract

The structure and reactivity of the radical cations of methylenecyclopropane (**1**), 1,4-bis(methylene)cyclohexane (**2**), tricyclo[2.2.2.$0^{1,4}$]octane (**3**), dispiro[2.0.2.2]octane (**4**), and dispiro[2.1.2.1]octane (**5**) were studied by theoretical and experimental methods. *Ab initio* molecular orbital calculations show that several interconversions and rearrangements of these radical cations are energetically favourable. Structural limitations, however, will prevent most of these from actually taking place. Experimental studies included photochemical (PET) and electrochemical (EC) techniques under a number of distinctive conditions. Generation of $\mathbf{2}^{+\bullet}$ by PET in the presence of a nucleophile leads to nucleophilic addition to the radical cation. In the absence of a nucleophile several other pathways are followed; the mechanisms for these are complicated and involve radical ions, radicals, and ionic species. Electrochemical oxidation of **2** in the presence of a nucleophile leads to nucleophilic addition to the initially formed radical cation, often followed by a second oxidation and nucleophilic addition (ECE). In the absence of a nucleophile, multiple oxidation steps, as well as acid catalyzed reactions, lead to the formation of aromatic species. Deprotonation is commonly observed under all conditions but is favoured when no nucleophile is present. Photochemical reactions of **1** in the presence of an electron-acceptor (1,4-dicyanobenzene, **33**) in acetonitrile lead to cycloadditions rather than products from electron transfer (ET). ET was predicted to occur based on the measured (CV) oxidation potential. It was shown that the measured oxidation potential of **1** represents the adiabatic ionization potential. For PET processes the value for the vertical ionization potential must be used. Generation of $\mathbf{1}^{+\bullet}$ (EC) without a nucleophile present results in the formation of one product: *tert*-butyl acetamide (**92**). A series of rearrangements leading to the *tert*-butyl cation is proposed. Addition of a nucleophile (methanol) to the mixture leads to the formation of 3-methoxy-2-(methoxymethyl)-1-propene (**93**). This product most likely arises from trapping of the initially formed ring-opened (trimethylenemethane) radical cation ($\mathbf{1a}^{+\bullet}$) which undergoes a second oxidation and nucleophilic addition (ECE). Under these conditions, the *tert*-butyl cation is not expected to be an important intermediate.

List of Abbreviations and Symbols used

AM1	Austin model 1
BPA	benzophenone azine
BPI	benzophenone imine
C	Coulomb
CRIP	contact radical ion pair
CT	charge transfer
CV	cyclic voltammetry
d	doublet (nmr)
dcfc	dry column flash chromatography
DCM	dichloromethane
ΔG	change in free (Gibbs) energy
ε	molar extinction coefficient
$E_{½}^{ox}$	half-wave oxidation potential
$E_{½}^{red}$	half-wave reduction potential
EC	electrochemistry
esr	electron spin resonance
ET	electron transfer
eV	electron volt
F	Faraday's constant
fid	flame ionization detector

gc	gas chromatography
HOMO	highest occupied molecular orbital
Hz	hertz
IP	ionization potential
ir	infrared
ISC	intersystem crossing
λ	reorganizational energy
	wavelength
LFP	laser flash photolysis
LUMO	lowest unoccupied molecular orbital
m	medium (ir)
	multiplet (nmr)
Me	methyl
MeCN	acetonitrile
MeOH	methanol
MCP	methylenecyclopropane
mp	melting point
mplc	medium pressure liquid chromatography
ms	mass spectrometry
m/z	mass to charge ratio
nmr	nuclear magnetic resonance
p-CAPA	*p*-cyanoacetophenone azine

PET	photoinduced electron transfer
photo-NOCAS	photochemical nucleophile-olefin combination, aromatic substitution reaction
q	quartet (nmr)
s	singlet (nmr)
	strong (ir)
sce	saturated calomel electrode
SET	single electron transfer
SIM	selected ion monitoring
SSRIP	solvent separated radical ion pair
t	triplet (nmr)
TEAP	tetraethylammonium perchlorate
tert	tertiairy
TMM	trimethylenemethane
TS	transition state
uv	ultraviolet
V	volt
vis	visible
w	weak (ir)

All other abbreviations are standard.

Acknowledgements

I sincerely thank my supervisor, Dr. Donald R. Arnold, for all his help, guidance, suggestions, enthusiasm, and inspiration. The many crazy ideas he shared with me these past four years will be precious memories. Thanks for "recruiting" me; it has been a wonderful and rewarding experience.

I would not have made it this far without the help of the many members (old and new) of the research group: Mary Chan, Dino Mangion, Allyson Perrott, and especially my best buddy Kim McManus. Good luck to all of you.

I would like to thank all the members of my supervisory committee: Dr. Pincock, Dr. Hooper, and Dr. Boyd for their interest and help throughout my stay at Dalhousie.

The laser flash photolysis experiments described in this thesis were accomplished thanks to the very valuable help of Dr. Fran Cozens, Dr. Norm Schepp and their research group.

There are several members of the Department that I am grateful to: Dr. Cameron (DalX) provided many X-ray structures on short notice; Jürgen Müller not only made beautiful and useful things out of glass, he also provided lots of non-chemistry related entertainment. Exact mass measurements were provided by Dr. Kim.

I thank Darrell Young and his Tiger squad for making my last year at Dalhousie an unforgettable one. Go Tigers! I also have met a lot of people and new friends through The Friends of Dalhousie Hockey Society.

A very special thanks goes to Linda Tingley as well as to her relatives who have been like a family far away from home for me.

I also thank Tim and Jill for putting up with me all this time and for all the smiles you've given me. Last but not least I want to thank my parents and family for their love and support.

Financial support from the Izaak Walton Killam foundation, the Department of Chemistry, and Dalhousie University (Faculty of Graduate Studies) is gratefully acknowledged.

Chapter 1

General Introduction

1.1 Radical Cations

Radical cations are important intermediates in many chemical and biological reactions.[1] They are easily generated by removal of an electron from a neutral molecule using techniques such as electrochemical oxidation,[2-4] radiolytic oxidation,[5-13] photo-induced electron transfer,[14-19] laser flash photolysis,[20,21] chemical oxidation,[22-27] and mass spectrometry.[28-33] A commonly used technique for detecting and studying radical ions (often in combination with radiolytic irradiation) is electron spin resonance.[34]

Radical cations can undergo a wide variety of reactions. Many examples have been documented, including deprotonation,[35-38] bond cleavage,[39-44] cyclization,[45-51] nucleophilic addition,[21,39-43,52] dimerization,[19a,21,24,25,27,53] and *cis/trans* isomerization.[51] There are several examples of radical cations undergoing interconversions or other rearrangements,[54-57] including the interesting rearrangement to distonic radical cations.[31-33] In addition to these experimental methods, theoretical methods have proven to be very useful for studying the structure and reactivity of radical cations.[58-61]

In this Chapter, some of the methods for generating radical cations, as well as some of the reactions of these species that are relevant to the work described in this thesis, will be discussed.

1.2 Generation of Radical Ions

Many techniques for generating radical ions are used on a routine basis. The most common techniques are photoinduced electron transfer (PET), electrochemical oxidation or reduction, and radiolytic irradiation. More recently techniques such as laser flash photolysis and chemical oxidation have become more popular. There are many examples in the literature of reactions involving radical cations generated by the techniques mentioned above. The two techniques that are used in this thesis, photoinduced electron transfer (PET) and electrochemical oxidation, will be briefly discussed.

1.2.1 Electrochemical Oxidation

One of the easiest ways to generate radical ions is by means of electrochemistry.[2] Several electrochemical techniques are known but all of these fall into two classes: bulk electrolysis (coulometric) techniques and micro-electrode (voltammetric) techniques. Of the latter, cyclic voltammetry (CV) is the most frequently applied. Both reversible and irreversible electron transfer (ET) reactions can be studied. In CV, a cyclic (or triangular) potential-time waveform is used (Figure 1.1a). A plot of the resulting current as a function of the potential of the working electrode is recorded on an X-Y recorder or an oscilloscope (Figure 1.1b). Initially the potential has such a value that no current flows, i.e. no oxidation takes place. When the potential is increased, the current will rise exponentially until nearly all the material near the electrode (anode) is depleted. Even though the potential still increases, the flux of material to the electrode is diffusion-limited. The maximum (peak) current (i_{pa}) will be reached when the concentration of the reactant is

almost zero. This potential is called the anodic peak potential (E_{pa}). The current then decreases until the diffusion-limited value is reached. After reaching the value of E_2 (Figure 1.1b), the potential will change in a negative direction and the radical cation will be reduced. In this case one observes a maximum cathodic current (i_{pc}) at a certain potential (E_{pc}) after which the diffusion-limited value is reached again. This process can be repeated to obtain more accurate values; however, changes in the concentrations of reactants (and products) will be reflected in the i-E profiles. The above described cyclic voltammogram is typical for a reversible electrochemical reaction; it will only be obtained when the radical cation is stable within the time frame of the experiment.

For reversible systems, assuming linear diffusion to the electrode surface, the peak potential (E_p) can be related to the half-wave potential ($E_{½}$):

$$E_p = E_{½} \pm 1.11\ RT/nF = E_{½} \pm 0.0285/n\ V \ \text{(at 25°C)} \qquad (1.1)$$

The formal electrode potential of the reversible couple ($E^{o'}$) can be approximated by the average of the two peak potentials (E_{pa} and E_{pc}), i.e. $E^{o'} \approx E_{½}$. The half-peak potential ($E_{p/2}$; the potential at which $i = ½i_p$) can be related to the half-wave potential by Eq. 1.2:

$$E_{p/2} = E½ \pm 0.0280/n\ V \ \text{(at 25°C)} \qquad (1.2)$$

Organic systems are often irreversible, i.e. no cathodic wave is observed. The measured half-wave potential does therefore not have any thermodynamic significance. The complete description of these types of systems is much more complicated as can be seen from the expression for the anodic peak potential (Eq. 1.3):

$$E_{pa} = E^{o'} + RT/[(1-\alpha)n_aF]\,[0.780 + \tfrac{1}{2}\ln(F/RT)\,(1-\alpha)n_aD\nu - \ln k_s] \qquad (1.3)$$

where $E^{o'}$ is the formal potential of the couple, α is the transfer coefficient, n_a is the number of electrons in the rate determining step, F is Faraday's constant, D is the diffusion coefficient of the electroactive species, ν is the sweep rate, and k_s is the heterogeneous rate constant for the electrode reaction at the formal potential.

It is also possible to estimate half-wave potentials from the measured peak potentials.[3]

CV is commonly used for determining oxidation and reduction potentials of compounds. However, to study reactions of the initially formed radical ions, bulk electrolysis is more suitable.[2] This experiment is also known as controlled-potential electrolysis. The apparatus used for these experiments is essentially the same as the one used in CV except for the fact that the scale is larger (i.e. larger cell, larger electrodes), and the solutions are usually stirred. A technique often used in these types of experiments is coulometry.[4] This experiment involves the measurement of the amount of electricity (coulombs = Ax˙s) in the electrolysis reaction. The number of coulombs (Q) consumed in

the reaction can be measured with great accuracy. This value (Q) is obtained by equation (1.4).

$$Q = \int_0^t i \, dt \tag{1.4}$$

The number of electrons (n) consumed per mol of electroactive compound can then be calculated from equation (1.5),

$$x = Q/(96{,}485*n) \tag{1.5}$$

where x is the number of moles of electrolyzed material.

A typical experiment consists of a reaction at a constant potential which will be stopped after a certain amount of coulombs has been consumed.

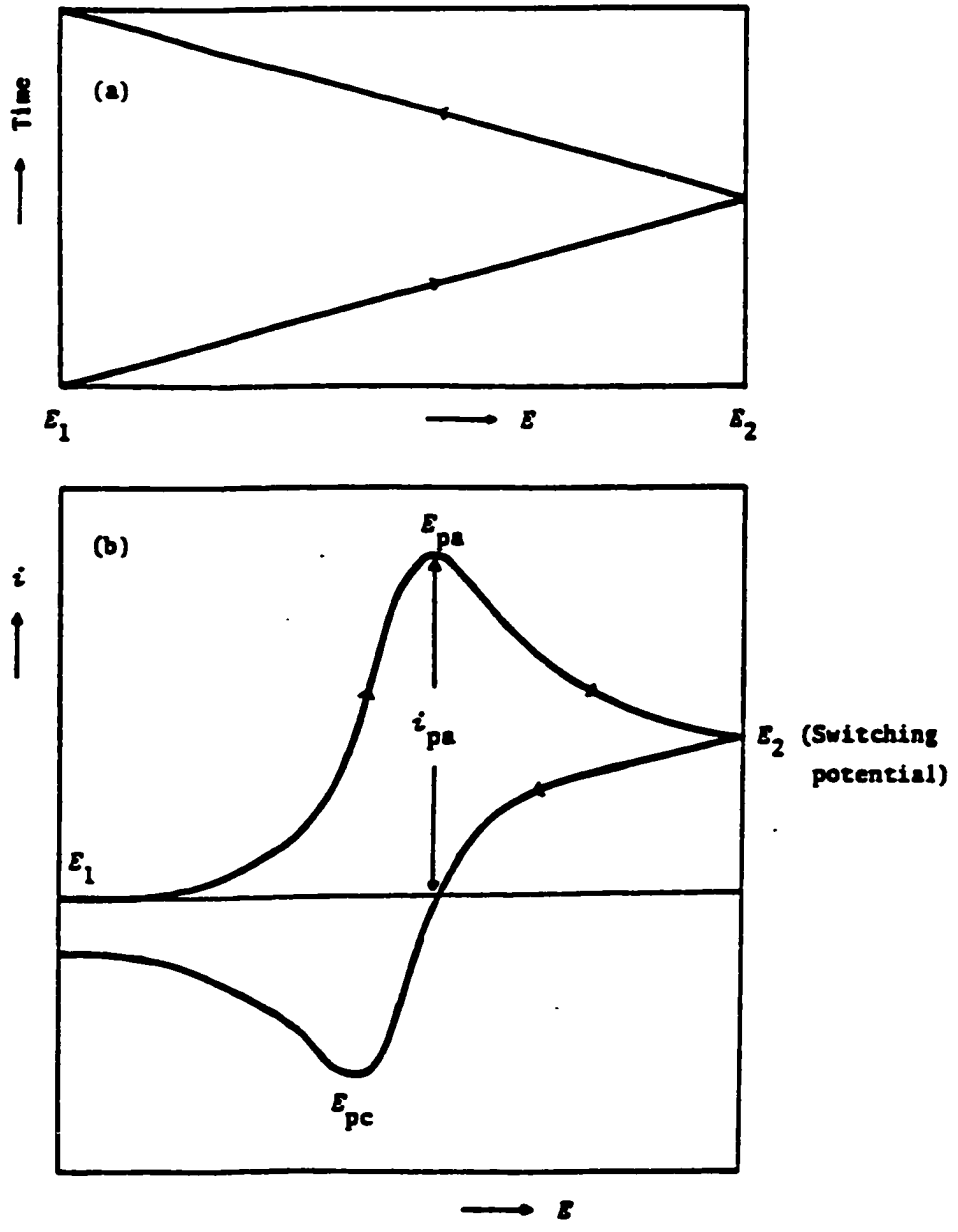

Figure 1.1. Cyclic potential sweep (a). Resulting cyclic voltammogram (b) (from ref. 2b)

1.2.2 Photoinduced Electron Transfer (PET)

Absorption of light by a molecule can bring the molecule to an electronically excited state. An electron is promoted from the highest occupied molecular orbital (HOMO) to an unoccupied orbital of higher energy. Relaxation processes are rapid and the electron will fall down to the lowest unoccupied molecular orbital (LUMO), and, depending on its ground state configuration, will give the first excited singlet state (S_1) or the first excited triplet state (T_1) of the molecule.

Promotion of an electron from the HOMO to the LUMO results in a reduced ionization potential (IP) as well as in an increased electron affinity (EA) for the molecule. This is schematically shown in Figure 1.2.

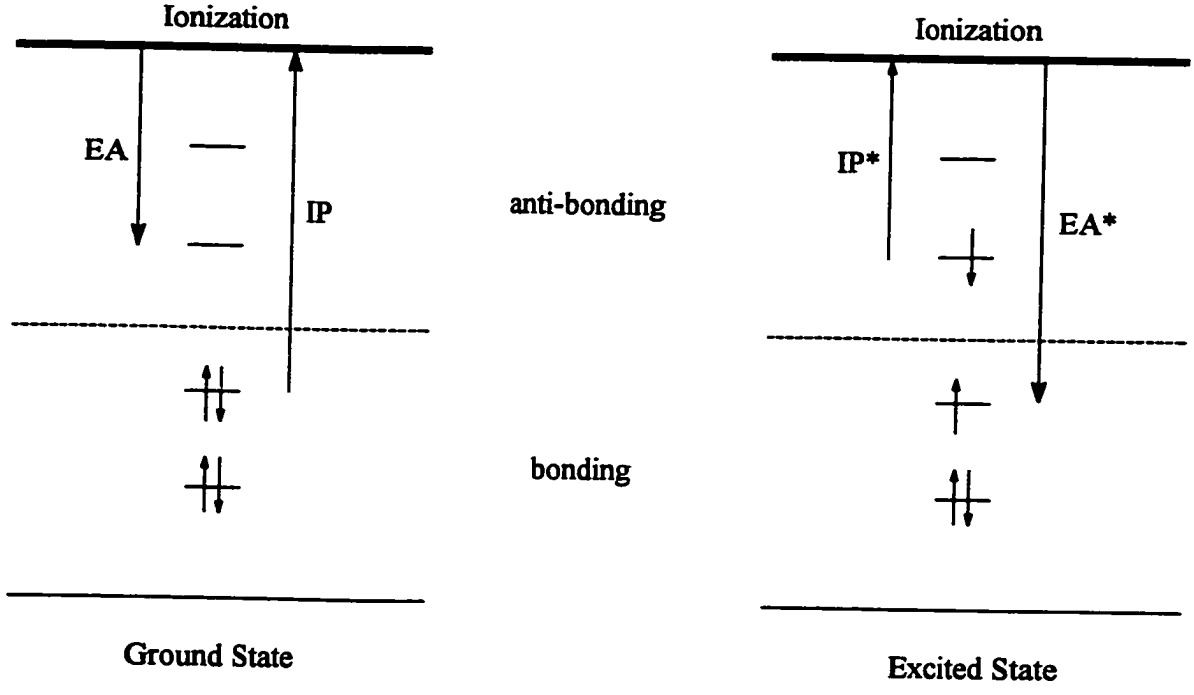

Figure 1.2 Schematic representation of the changes in IP and EA upon excitation.

There are a number of processes that can take place with the excited state molecule. Common photophysical processes are fluorescence, internal conversion (radiationless decay), intersystem crossing, and phosphorescence. In addition to these energy-wasting steps there are a number of other processes that can quench the excited state. These include energy transfer, chemical reaction, and electron transfer. Energy transfer can happen when a second molecule, having a lower excited state energy than the excited molecule, is present. A chemical reaction can take place if the lifetime of the excited state is sufficiently long to undergo that particular reaction. Examples include dimerization, isomerization, hydrogen atom abstraction, and bond homolysis reactions. Electron transfer (ET) can occur if a suitable electron donor (e.g. an alkene) and electron acceptor (e.g. arene) are present together. This last process is called photoinduced electron transfer (PET).[14]

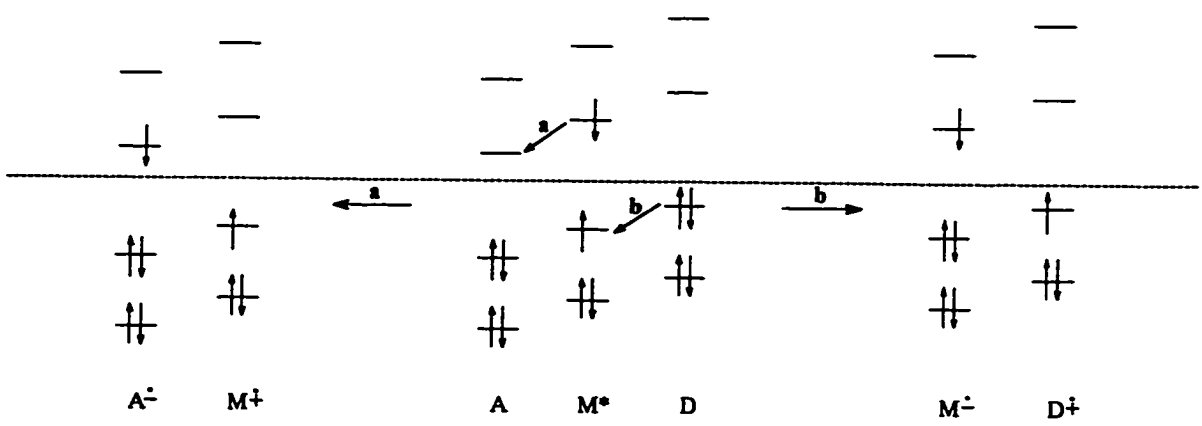

Scheme 1.1 Schematic representation of electron transfer from an excited molecule to an acceptor (pathway **a**) or from a donor to the excited molecule (pathway **b**).

As mentioned above, an excited state molecule has a lower IP and a higher EA, making electron transfer more feasible, independent of the fact whether the molecule will act as an electron acceptor or an electron donor (Scheme 1.1).

An empirical formula for determining whether electron transfer will occur was developed by Weller and Rehm (Equation 1.6).[15]

$$\Delta G_{ET} = F[E_{½}^{ox}(D) - E_{½}^{red}(A) - e/\varepsilon\alpha] - \Delta E_{0,0} \qquad (1.6)$$

where ΔG_{ET} = free energy of electron transfer (kcal/mol)
F = Faraday's constant (96,485 C/mol)
$E_{½}^{ox}(D)$ = oxidation potential of the donor (V)
$E_{½}^{red}(A)$ = reduction potential of the acceptor (V)
$e/\varepsilon\alpha$ = free enthalpy gained by encounter of the radical ion pair at a distance α in a medium of dielectric constant ε (e = electron charge)
$\Delta E_{0,0}$ = singlet excitation energy

Electron transfer can occur when $\Delta G < 0$ (i.e. an exergonic process). In the case of an endergonic reaction ($\Delta G > 0$) energy transfer will occur. The process of electron transfer and subsequent reactions is schematically shown in Scheme 1.2. Advanced spectroscopic techniques are being used to study these intermediates and the rate constants for most of these processes can be measured.[16c,d]

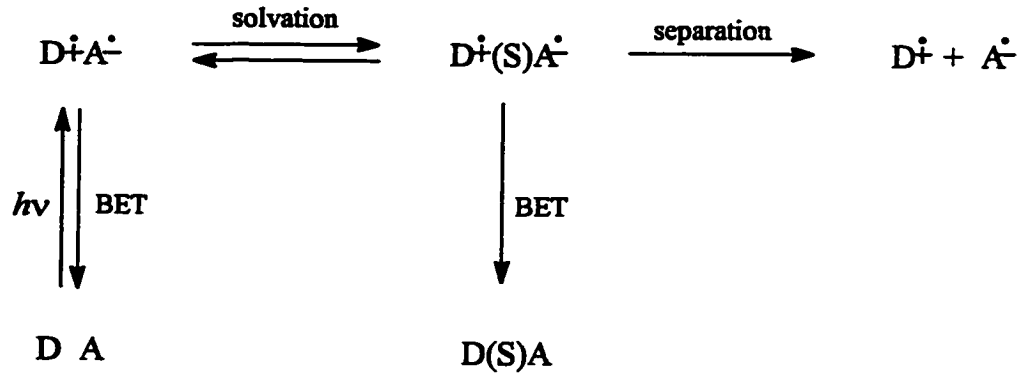

Scheme 1.2 Electron transfer between a donor (D) and an acceptor (A) molecule and subsequent reactions.

A major mode of deactivation of the initially formed radical ion pair is back electron transfer (BET), which can occur from both the contact radical ion pair (CIP, $D^{+\bullet}A^{-\bullet}$) and from the solvent separated ion pair (SSIP, $D^{+\bullet}(S)A^{-\bullet}$). The rate of BET was shown to be dependent on the exothermicity of the reaction and to decrease with increasing exothermicity.[16a] This corresponds to the Marcus "inverted region", an empirical formulation by Marcus[17] predicting that the rate of electron transfer increases with increasing free energy, reaches a maximum at the point where the solvent reorganizational energy equals the free energy, and then decreases even though the free energy for the reaction further increases (equation 1.7).

$$k_{ET} = A' \exp\{-[(\Delta G^{\circ}+\lambda_s)^2 (4\lambda_s k_B T)^{-1}]\} \qquad (1.7)$$

where A' is the exponential factor ($M^{-1}s^{-1}$), k_B is the Boltzman constant, and T is the absolute temperature. There now are several examples available in the literature proving the existence of the Marcus "inverted region".[16a,b, 18]

Rehm and Weller[15] have tested the Marcus theory for electron transfer and they showed that the inverted region could not be observed for the bimolecular electron transfer quenching of excited states. It was argued that these exothermic reactions are often diffusion controlled (when electron transfer is exothermic enough) and for very exothermic reactions the initial electron transfer could lead to the formation of (low lying electronic) excited states of the radical ions. Other processes (e.g. exciplex formation or proton transfer) might also play a role.

Normally, BET is considered to be an energy-wasting step. However, recently a system was designed in which BET was used to assist in the cleavage of a carbon-carbon bond.[16e] This process (dissociative return electron transfer (DRET)) is schematically shown in Scheme 1.3.

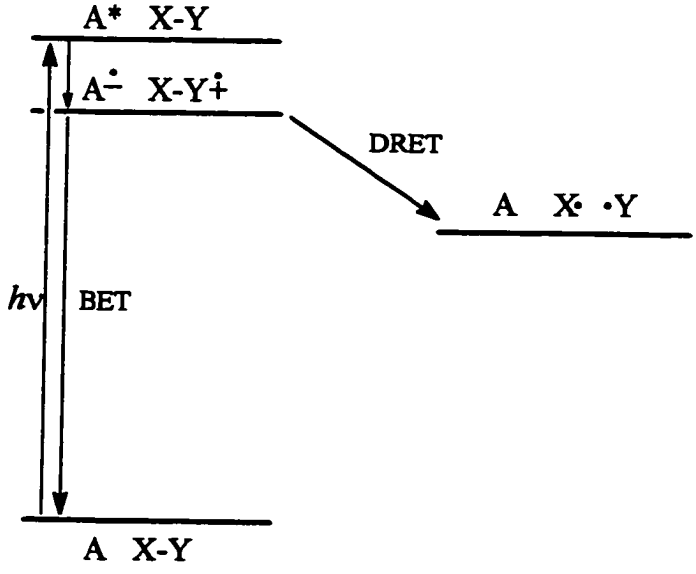

Scheme 1.3 Schematic representation of the photoinduced dissociative return electron transfer (DRET) process.[16e]

A requirement for this reaction is that the energy of the radical ion pair must be greater than the bond dissociaton energy of the bond to be cleaved. Naturally, this puts some restrictions on the system. An example of this dissociative return electron transfer process is shown in Scheme 1.4.

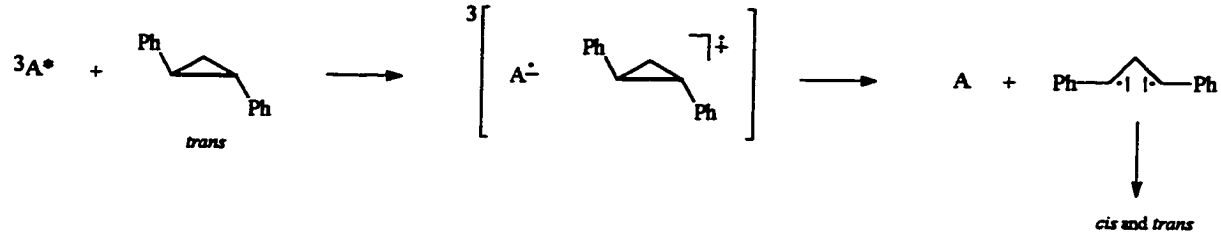

Scheme 1.4 Example of dissociative return electron transfer in *trans*-1,2-diphenylcyclopropane using 3,3',4,4'-benzophenonetetracarboxylic dianhydride as the triplet sensitizer.[16e]

Attempts have been made to reduce the yield of BET. Addition of a codonor (e.g. biphenyl) is believed to result in the formation of the codonor radical cation. The oxidation potential of biphenyl is high (+1.8 eV vs. sce), i.e. the electron transfer reaction with 1,4-dicyanobenzene acting as the electron acceptor ($E^{½}_{red}$ = -1.66 eV vs. sce) is exergonic by 19 kcal/mol.[52d] Back electron transfer for this process, however, will be highly exergonic (energy of the radical ion pair is ≈ 3.5 eV; ΔG_{BET} = -80 kcal/mol) and is therefore disfavoured (i.e. it falls in the Marcus "inverted region"). In addition to this, the reorganizational energy for reduction of the biphenyl radical cation is small and also disfavours back electron transfer. Oxidation of an alkene by the biphenyl radical cation is believed to be an equilibrium process. This reaction is favoured when the oxidation

potential of the alkene is lower than that of biphenyl. However, there are many examples of situations where the oxidation potential of the alkene is actually higher than that of biphenyl.[52d] Even in these cases addition of biphenyl results in more efficient reactions. It has been suggested that the biphenyl radical cation forms a charge-transfer complex with the alkene, allowing electron transfer to happen more easily.[52d]

1.3 Reactions of Radical Ions

In the previous sections several examples of radical cation reactions were mentioned. These species can undergo a wide variety of reactions and some of the more interesting examples are discussed below.

1.3.1 Deprotonation

It has been well established that the acidity of a radical cation is much greater than that of the neutral precursor.[35,36] For example, the pK_a value of the radical cation of toluene was calculated to be -11,[36] whereas that of the neutral molecule is 41.[37] In order for deprotonation to take place the singly occupied molecular orbital (SOMO) of the radical cation must overlap with the C-H bond that is cleaving. In these types of molecules, the SOMO will be largely associated with the phenyl ring. Therefore, the angle between the plane of the phenyl ring and the benzylic C-H bond will be important. When this angle is 90°, overlap between the SOMO and the benzylic C-H bond will be 100%. An

angle of 0° indicates that the SOMO and the C-H bond are perpendicular and overlap will be 0%.

Several examples have been reported that confirm this conformational requirement. For example, when *cis*-1-methyl-2-phenylcyclopentane is irradiated in the presence of an electron-accepting photosensitizer (1,4-dicyanobenzene) and a non-nucleophilic base (collidine) in acetonitrile, the *trans* isomer is formed in good yield. However, irradiating the *trans* isomer under the same conditions does not give any reaction (Reactions [1.1] and [1.2]).[38]

Reaction [1.1]

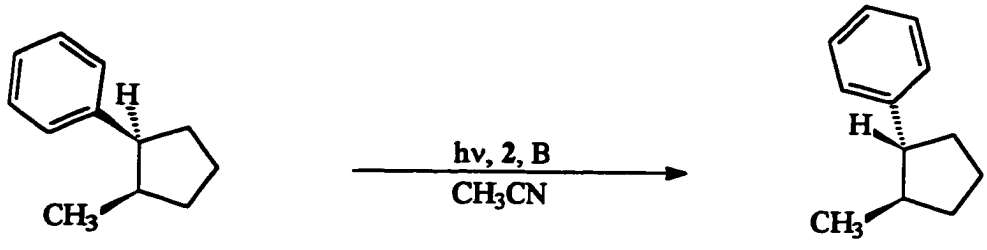

B = 2,4,6-collidine

Reaction [1.2]

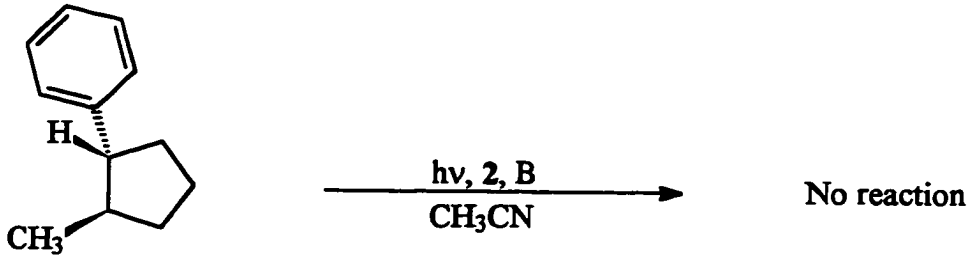

B = 2,4,6-collidine

Using molecular mechanics calculations it was shown that in the *trans* isomer the angle between the benzylic C-H bond and the SOMO is 1°. The calculated overlap in the cis isomer is 31% (MM3, angle: 34°).[38]

1.3.2 Carbon-carbon bond cleavage

Several examples of photosensitized (electron transfer) carbon-carbon bond cleavage have been reported.[39] One of the first examples of this type of reaction was the C-C bond cleavage of methyl 2,2-diphenylethyl ether when irradiated in the presence of 1,4-dicyanobenzene in an acetonitrile-methanol (3:1) solution (Reaction [1.3]).[39a]

Reaction [1.3]

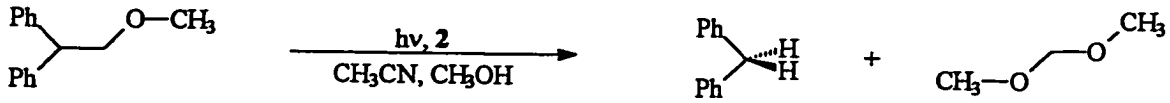

2 = 1,4-dicyanobenzene

The mechanism proposed for the photosensitized (electron transfer) bond cleavage is shown in Scheme 1.5 where A is an electron-accepting photosensitizer (e.g. 1,4-dicyano-benzene). Step 4 shows the actual cleavage of the radical cation to yield radical and cationic fragments. Cleavage can occur in two ways and the preferred mode can be predicted based on the oxidation potentials of the alternative radical fragments.[39a,40]

The feasibility of photosensitized (electron transfer) carbon-carbon bond cleavage is known to depend on the dissociation energy of the vulnerable bond in the radical cation

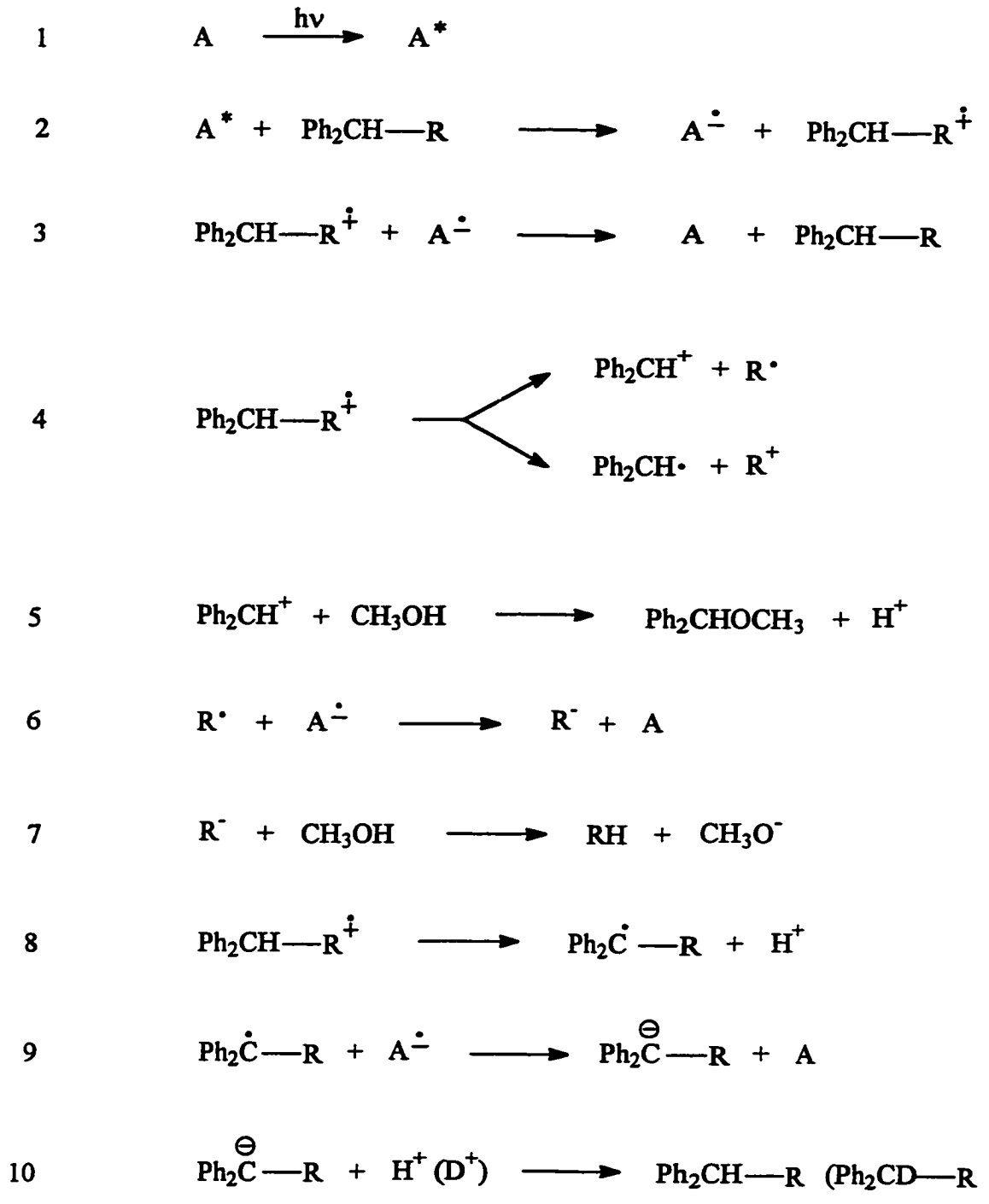

Scheme 1.5 Proposed mechanism for the photosensitized (electron transfer) carbon-carbon bond cleavage reaction of radical cations.

and on the conformation of the radical cation. From previous studies, an upper threshold of 55 kJ/mol has been estimated for the bond dissociation energy (BDE) in the radical cation.[40] When the BDE in the radical cation is well below this threshold, cleavage of the bond in the radical cation usually occurs readily. If the BDE is above the threshold, no cleavage is observed. Generalizations are more difficult when the BDE approaches the threshold value and using the BDE as the only criterion for cleavage has led to some erroneous predictions. For example, although the calculated BDE for cleavage of the radical cation of *cis*-1-methoxy-2-phenylcyclopentane is only 18 kJ/mol,[38] no bond cleavage was observed experimentally (Reaction [1.4]). Deprotonation of the radical cation, reduction of the radical, and reprotonation leads ultimately to the *trans*-isomer. In order to improve the predictive power of the hypothesis, conformational criteria were included.

Reaction [1.4]

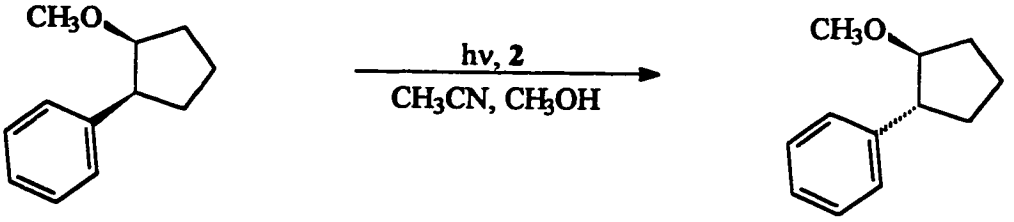

Based on the results for C-H bond cleavage (see above) it seemed reasonable to suggest that, in order for C-C bond cleavage to occur, the SOMO must also overlap with the vulnerable C-C bond; methyl *cis*- and *trans*-2-phenylcyclohexylether and 6-phenyl-1,4-dioxaspiro[4.5]decane were therefore expected to cleave. However, whereas the diphenyl

systems did show C-C bond cleavage, the monophenyl systems did not (Reactions [1.5] - [1.8]).[39i]

Reaction [1.5]

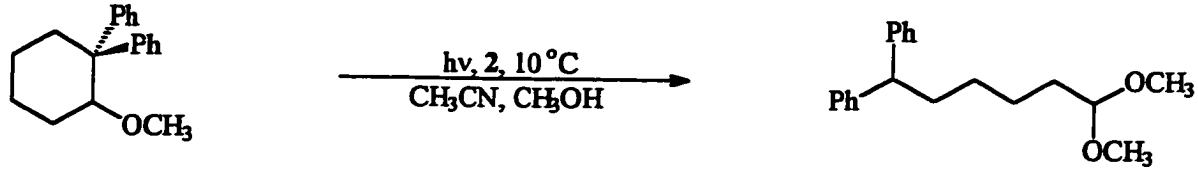

Reaction [1.6]

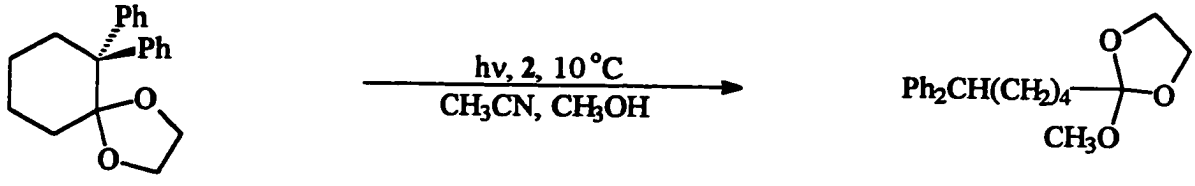

Reaction [1.7]

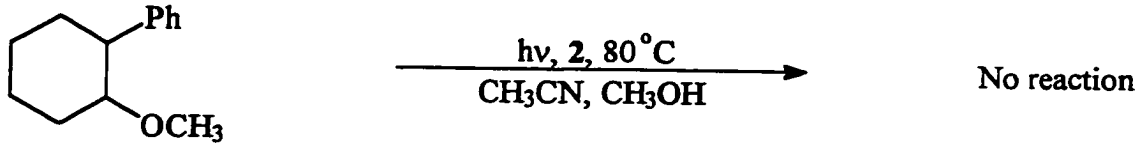

(*cis* and *trans*)

Reaction [1.8]

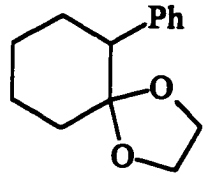

$$\xrightarrow[CH_3CN,\ CH_3OH]{h\nu,\ 2,\ 80\,^{\circ}C}$$

No reaction

The new hypothesis that was formulated recognized that in order for the radical cation of a β-phenylethyl ether to cleave, the alkoxy group must also be oriented so that a lone pair of electrons on the oxygen can overlap with the C-C *sigma* antibonding (σ*) orbital. The preferred conformation for cleavage is shown in Figure 1.3.[39i]

Additional examples of C-C bond cleavage that confirm the hypothesis were recently reported.[41] The reactivity of the four β-phenylethyl ethers (the diastereomers of 2-methoxy-3-phenylbutane and the *cis* and *trans* isomers of 2-methyl-3-phenyltetrahydro-pyran) is governed by conformational effects; the BDE values of the vulnerable C-C bond in the radical cation were below the threshold value of 55 kJ/mol. Based on the calculated angles and overlap between orbitals it was predicted that the global-minimum conformers of the diastereomers would not give C-C bond cleavage or deprotonation to any significant extent. In good agreement with the calculations, cleavage of these two ethers when irradiated in the presence of an electron-accepting photosensitizer (1,4-dicyano-benzene) was not efficient and deprotonation or isomerization was not observed. The global minimum of the *trans* ether is well oriented for C-C cleavage but not for deprotonation. The global minimum of the *cis* ether is not suitably oriented for C-C

a

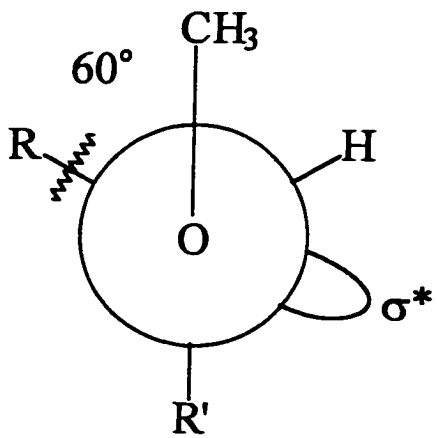

b

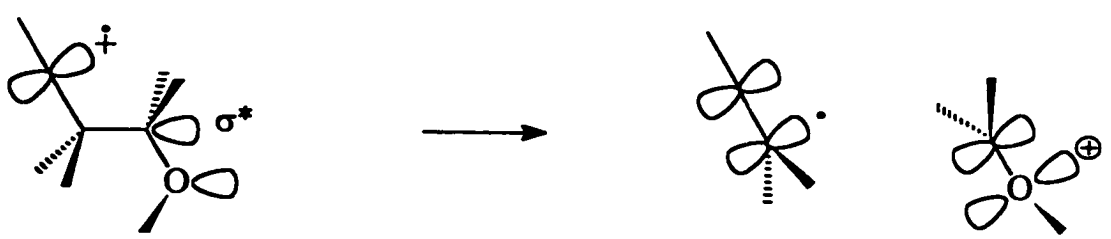

Figure 1.3 Preferred conformation for carbon-carbon bond cleavage of the radical cation illustrated with a Newman projection along the O-C bond (a); illustrated with dashed-wedged line notation (b).

cleavage but some deprotonation was expected. Upon irradiation in the presence of 1,4-dicyanobenzene reasonable amounts of cleavage products were obtained from both the *cis* and the *trans* isomer. In fact, the *cis* isomer cleaved more efficiently than the *trans* isomer (Reaction [1.9]). This was explained by the fact that another conformer of the *cis* isomer, only 4.35 kJ/mol higher in energy than the global minimum, is perfectly aligned for cleavage. In good agreement with the calculations, no deprotonation was observed in the *trans* isomer and some deprotonation was observed in the *cis* isomer.

Reaction [1.9]

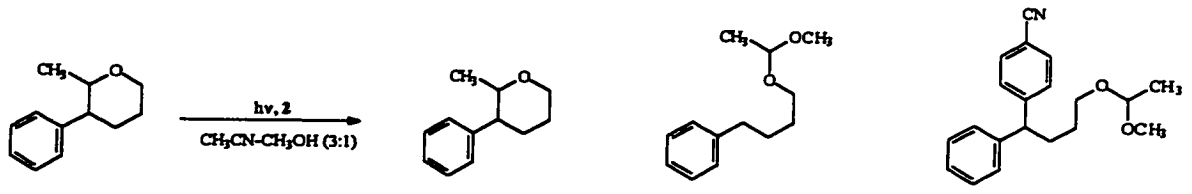

[a]	*cis*	*trans*: 6%	20%	31%
[b]	*trans*	*cis*: 1%	23%	37%

Bond cleavage is also expected to occur when an electron is removed from a strained molecule, thereby weakening one of the C-C bonds. Typical examples are three- and four-membered ring systems in naturally occuring molecules such as 2-carene, and α- and β-pinene. Irradiation of a solution of (+)-2-carene and 1,4-dicyanobenzene in acetonitrile-methanol (3:1) leads to the formation of products resulting from C1-C7 bond

cleavage. (Reaction [1.10]).[42] However, in the absence of a nucleophile, partial racemization of the starting material is observed, indicating that cleavage of the C1-C6 bond has occured.

Reaction [1.10]

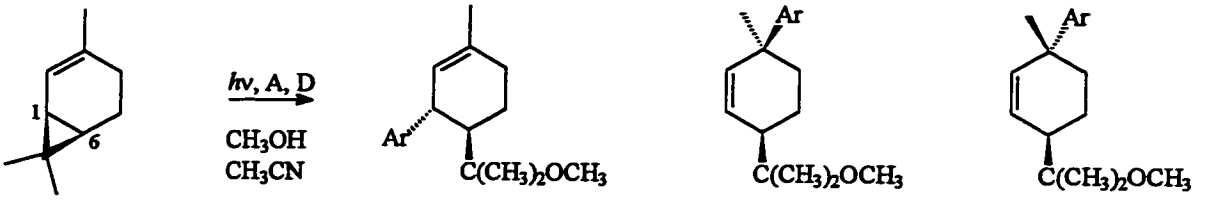

(+)-2-carene (-) (48%) (*cis*) (-) (16%) (*trans*) (+) (16%)

A = 1,4-dicyanobenzene
B = biphenyl

Similar results are obtained from studies on the radical cations of α- and β-pinene (Reactions [1.11] and [1.12]).[43] The cyclobutane ring cleaves irreversibly before addition of the nucleophile to the radical cation takes place.

Reaction [1.11]

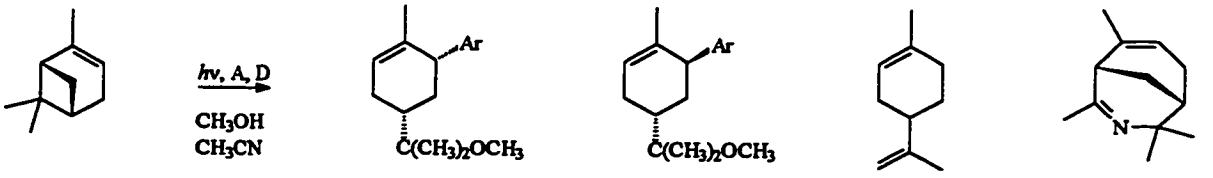

(-)-α-pinene (±) (23%) (±) (16%) (±)

A = 1,4-dicyanobenzene
B = biphenyl

Reaction [1.12]

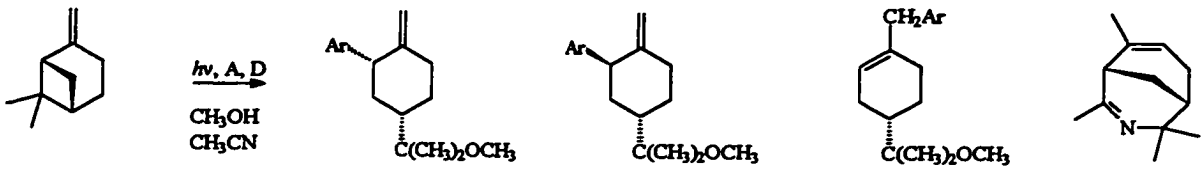

(-)-β-pinene (±) (3%) (-) (9%) (-) (9%) (+)

A = 1,4-dicyanobenzene
B = biphenyl

Ab initio molecular orbital calculations predict that the ring-closed radical cation is more stable than the ring opened radical cation. This indicates that addition of the nucleophile (methanol) is relatively slow. Using a better nucleophile (e.g. azide) might result in addition of the nucleophile to the ring closed radical cation. Addition of nucleophiles to radical cations will be discussed below.

In some cases C-C bond cleavage was shown to be assisted by the attack of the nucleophile.[44] For example, the reaction (nucleophilic cleavage of one-electron σ bonds) of arylcyclopropanes radical cations with nucleophiles leads to inversion of configuration at carbon (Reaction [1.13]). The relative rate constants for addition of methanol, iso-propanol, and tert-butanol are ≈5:3:1, indicating that these reactions are relatively insensitive to steric effects.[44a]

Reaction [1.13]

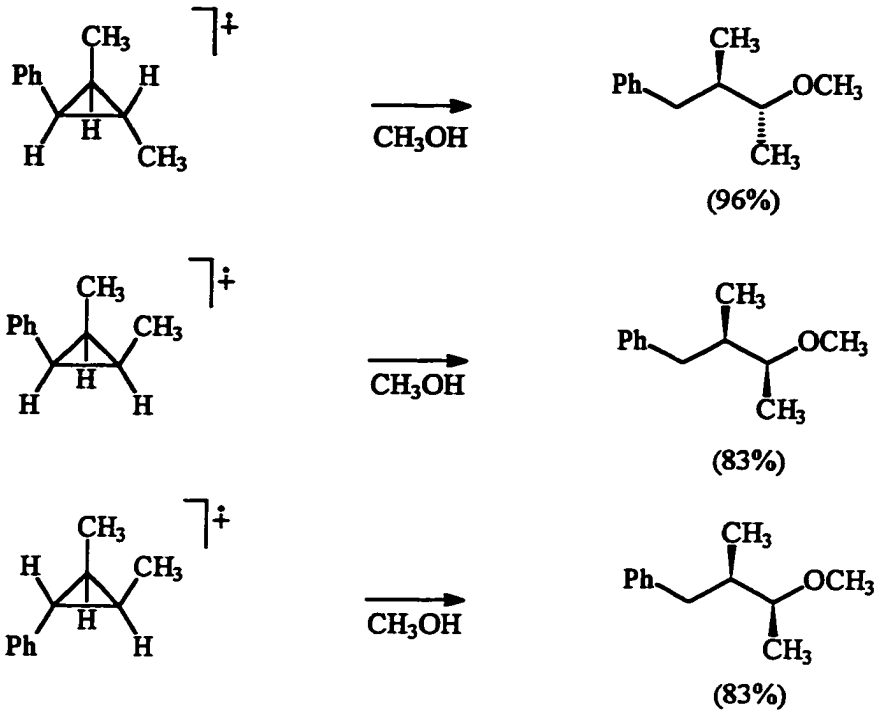

Reaction [1.14]

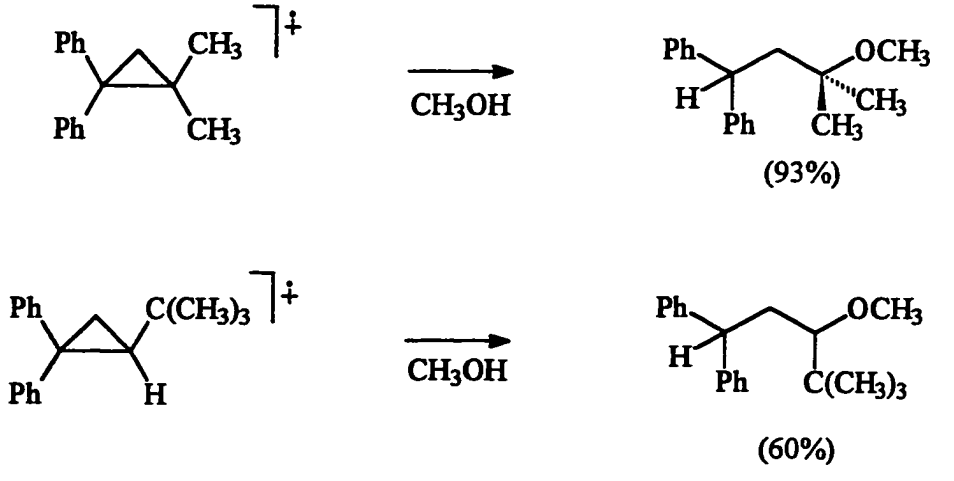

Including bulky substituents on C2 of the cyclopropane ring provided additional proof that in these reactions steric effects are small (Reaction [1.14]).[44c] These are

examples of reactions where the addition of the nucleophile is directed by electronic effects rather than steric effects.

1.3.3 Cyclization

The cyclization of radicals[45] and of ionic species[46] are well-studied reactions and rules have been formulated for both of these processes. The cyclization of radical cations, however, has received far less attention. Several examples have been reported and a recent review lists most of the published work.[47]

In order for cyclization to take place, a molecule needs a donor and an acceptor site. In many of the examples, the acceptor site is olefinic. Some of the possible donor sites include olefins and alcohols. Cyclization can occur from the radical cation intermediate or, in the presence of a nucleophile, from the intermediate β-alkoxyalkyl radical.

When a series of nonconjugated dienes (1,5-hexadiene, 2-methyl-1,5-hexadiene, and 2,5-dimethyl-1,5-hexadiene) was studied, it was found that only the radical cation of 2,5-dimethyl-1,5-hexadiene formed cyclized products (Reaction [1.15]).[48] Based on the observed products, it was concluded that cyclization occurs from the radical cation intermediate only; the mode of cyclization is 1,6-*endo*, *endo*. There was no evidence for cyclization of the intermediate β-alkoxyalkyl radical.

When this study was extended to include 2,6-dimethyl-1,6-heptadiene, two types of cyclized products were found (Reaction [1.16]).[49] Cyclization of the radical cation is a 1,7-*endo*, *endo* process and results in the formation of seven-membered ring species.

Reaction [1.15]

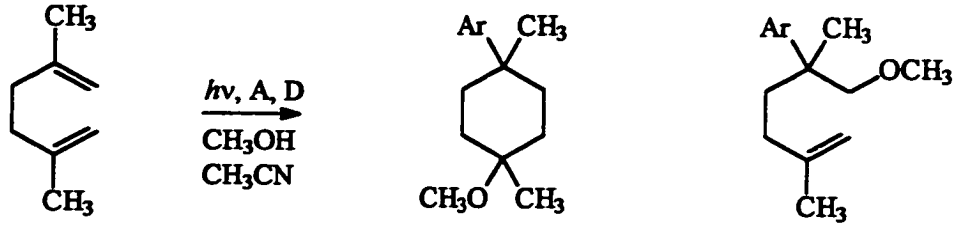

cis (9%)
trans (4%)

(16%)

A = 1,4-dicyanobenzene
D = biphenyl

Ar = 4-cyanophenyl

Cyclization also occurs from the intermediate β-alkoxyalkyl radical which is formed by addition of the nucleophile (methanol) to the radical cation. This mode of cyclization is 1,6-*endo* and yields cyclohexane derivatives.

Reaction [1.16]

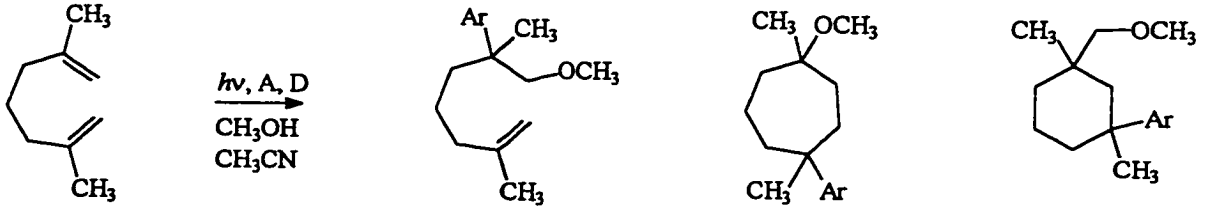

(5%)

cis (12%)
trans (10%)

cis (12%)
trans (11%)

A = 1,4-dicyanobenzene
D = biphenyl

Ar = 4-cyanophenyl

The cylization of 6-methyl-5-hepten-2-ol radical cation only proceeds to give products from the 1,5-*exo* intermediate (Reaction [1.17]).[50] Under similar conditions, the cyclization of 5-methyl-5-hexen-2-ol involves both 1,5-*exo* and 1,6-*endo* radical intermediates (Reaction [1.18]).[50] This observation more closely resembles the results of the cyclization of the corresponding alkyl radicals than those of the corresponding alkoxy radicals. The explanation for this result is that the C-O bond length is shorter than the C-C bond length and therefore favours the formation of a 1,5-*exo* intermediate. The longer C-C bond length can give rise to both 1,5-*exo* and 1,6-*endo* intermediates. The C-O bond in the alkenol radical cations are longer than the C-O bond in the alkoxy radicals and their reactivity therefore resembles that of the alkyl radicals. Similar results were obtained when (R)-(+)-α-terpineol was used as the substrate (Reaction [1.19]).[51]

Cyclization has also been observed in the electrochemical oxidation of several substrates (these will be discussed in more detail in Chapter 3).[47] However, since a secondary oxidation usually occurs rapidly, the cyclized products might have arisen from carbocation intermediates rather than radical cation intermediates.

Reaction [1.17]

A = 1,4-dicyanobenzene
D = biphenyl

Ar = 4-cyanophenyl

Reaction [1.18]

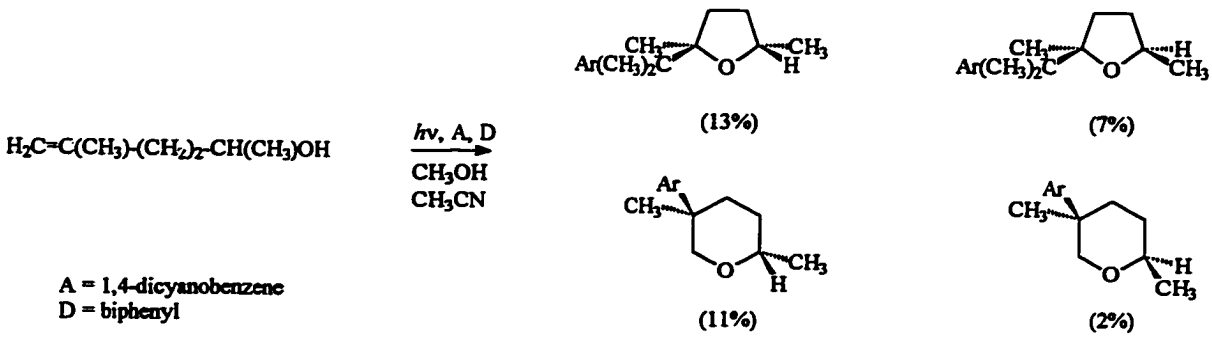

A = 1,4-dicyanobenzene
D = biphenyl

Ar = 4-cyanophenyl

Reaction [1.19]

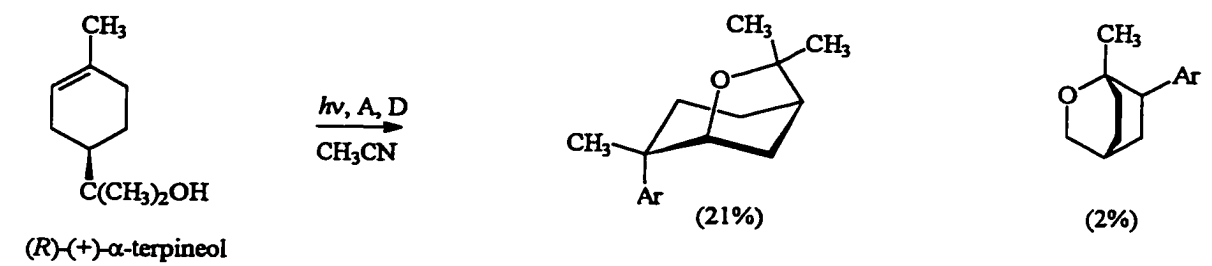

(*R*)-(+)-α-terpineol

A = 1,4-dicyanobenzene
D = biphenyl

Ar = 4-cyanophenyl

1.3.4 Nucleophilic addition

Generation of an alkene radical cation in the presence of a nucleophile usually leads to products arising from addition of the nucleophile to the radical cation. In general the addition leads to anti-Markovnikov products, i.e. the nucleophile adds to the least

substituted end of the alkene. The first example of this type was reported by Arnold and co-workers.[39a] The mechanism is shown in Scheme 1.6.[39e-i,40-43,52] Step 4 shows the addition of the nucleophile to the radical cation. In the case of a neutral nucleophile (e.g. methanol) deprotonation occurs from the intermediate β-distonic radical cation. The resulting radical can, depending on the circumstances, undergo several reactions. Reduction of the radical by the radical anion of the photosensitizer yields an anion which is subsequently protonated (steps 5,6). Coupling with the electron-accepting radical anion followed by rearomatization (loss of cyanide anion) leads to photo-NOCAS (photochemical nucleophile-olefin combination, aromatic substitution) products (step 7). This reaction has been studied extensively and the scope and limitations have been extended to include a variety of alkenes, electron-acceptors, and nucleophiles.[52]

Laser flash photolysis experiments have shown that the reaction of substituted styrene radical cations with several different anions proceed at or near the diffusion controlled rate.[21] It is important to note that in some cases, instead of addition of the nucleophile to the radical cation, electron transfer from the nucleophile to the styrene radical cation occurs. When the oxidation potential of the nucleophile is lower than that of the alkene, electron transfer from the nucleophile to the alkene will occur at the diffusion controlled rate. This has been observed for both azide anion[21] and for cyanide anion.[52h] Changing the solvent can have a dramatic effect on the results. For example, the oxidation potential of azide anion in trifluoroethanol is significantly higher than in acetonitrile.[21] When the radical cations of substituted styrenes were studied in the presence of azide

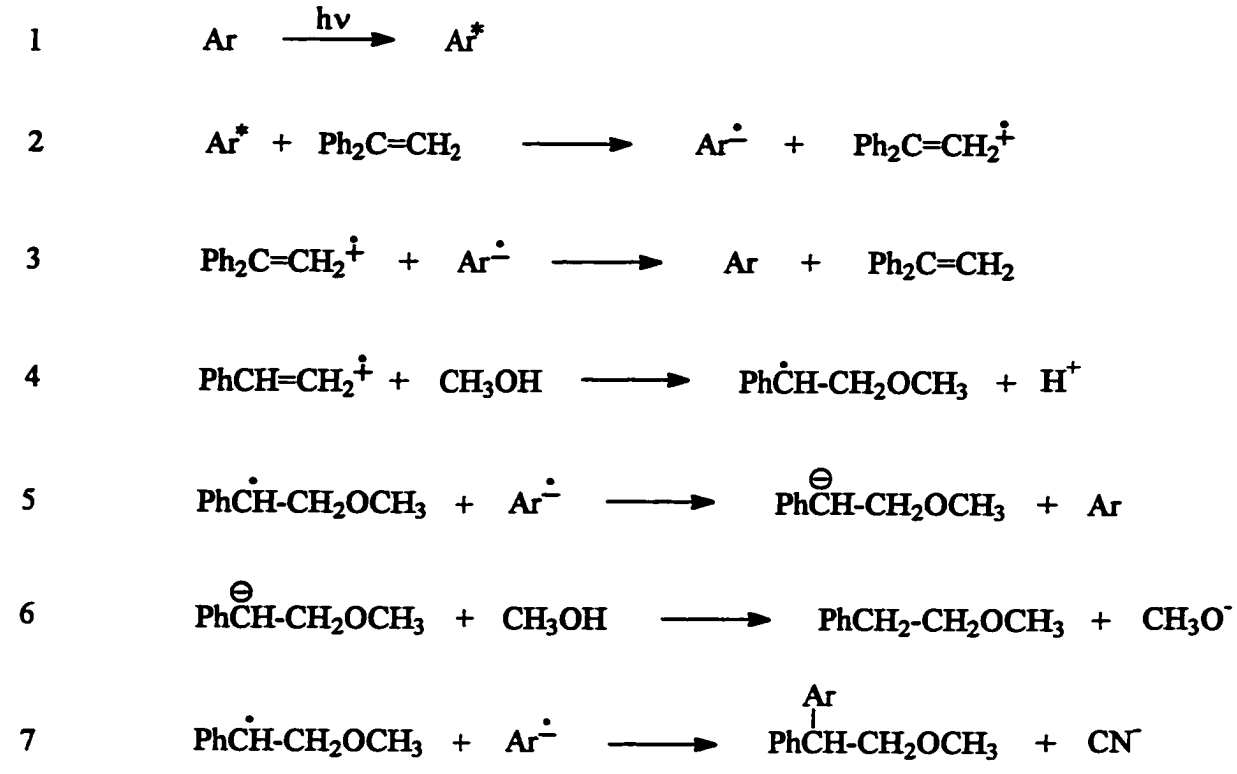

Ar = an electron-accepting photosensitizer (e.g. 1,4-dicyanobenzene)

Scheme 1.6 Proposed mechanism for the nucleophilic addition to alkene radical cations.

anion, a shift towards addition products is observed when the solvent is changed from acetonitrile to trifluoroethanol.[21]

Methanol, the nucleophile most often used in the photo-NOCAS reactions,[52] is a relatively poor nucleophile. The rate constants for the addition of methanol to substituted styrene radical cations measured by laser flash photolysis are in the range of 10^4 - 10^8

$M^{-1}s^{-1}$.[21] This has both advantages and disadvantages. When addition of the nucleophile is slow, the radical cation can undergo reactions before it is trapped by the nucleophile. In the case of studies on the cyclization of radical cations this can be advantageous since C-C bond formation might be faster than attack of the nucleophile on the initially formed radical cation. However, it was pointed out earlier that calculations have shown that the initially formed radical cations of 2-carene and α- and β-pinene are the ring-closed species.[42,43] If the addition of the nucleophile is too slow to compete with bond cleavage, the initially formed radical cation will not be trapped. In cases like these, careful consideration of the use (and implications) of the chosen nucleophile is necessary. Knowledge of the rate constants for the addition process as well as information on the oxidation potentials of the nucleophiles and alkenes is of extreme importance.

1.3.5 Reaction with a neutral substrate (dimerization)

Dimerization reactions of radical cations have been reported.[1,21,53] The dimerization of several substituted styrenes to give cyclobutane derivatives was studied by laser flash photolysis.[21] The rate constants that were obtained indicate that these dimerization reactions often are quite rapid (Table 1.1). Important factors influencing the rates are steric effects and stability of the monomeric radical cation.

The cross-reactions between (substituted) alkene radical cations and other (substituted) alkenes are synthetically useful reactions. Typical examples are the radical cation Diels-Alder reactions.[24,25] It was mentioned above that these radical cation reactions often proceed much faster at milder conditions than their classic counterparts.

Table 1.1. Rate constants for the dimerization of substituted styrenes in cyclohexane measured by laser flash photolysis.[a]

alkene	k_{dim} ($M^{-1}s^{-1}$)[b]
4-chlorostyrene	6.0×10^9
styrene	8.0×10^9
4-methylstyrene	1.0×10^{10}
4-methoxystyrene	1.0×10^{10}
β-methylstyrene	$<6 \times 10^7$
α-methylstyrene	1.0×10^{10}
β-methyl-4-methoxystyrene	$<6 \times 10^7$
1,1-diphenylethylene	1.2×10^{10}

[a] data from reference; [b] rate constant for dimerization.

Studies on the reaction of substituted styrene radical cations with substrates (alkenes, dienes, and vinyl ethers) have shown that instead of addition of the substrate to the radical cation, electron transfer from the substrate to the radical cation can occur. This strongly resembles the addition of nucleophiles to styrene radical cations (see above). The rate constants for addition range from $<1\times10^5$ - 4×10^9 $M^{-1}s^{-1}$. Addition will occur when the oxidation potential of the substrate is greater than that of the styrene.

The mechanism for the dimerization reactions as well as that for the radical cation cycloaddition (Diels-Alder) reaction is thought to go through a long-bond cyclobutane radical intermediate (concerted mechanism, Reaction [1.20])[27] although earlier investigations supported the existence of a distonic 1,4-acyclic radical cation (step-wise mechanism, Reaction [1.21]).[19a] Due to the diversity of these reactions it is likely that there is more than just one clear-cut reaction pathway. Differences in substrate, solvent, and other conditions, will lead to the formation of different intermediates and alternative pathways may then be followed.

Reaction [1.20]

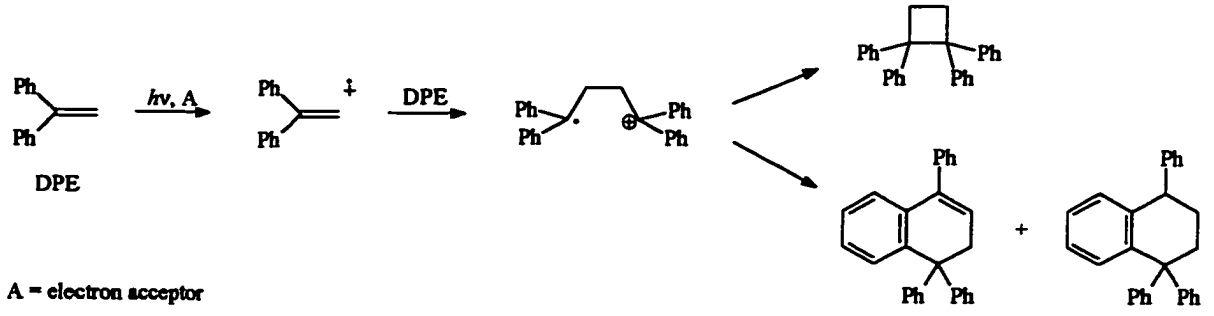

A = electron acceptor

Reaction [1.21]

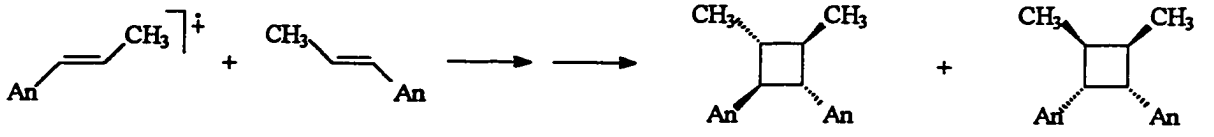

An = 4-$CH_3OC_6H_4$-

1.3.6 Interconversion and rearrangement

Rearrangements of radical cations occur frequently and many examples have been documented.[31-33,54-57] In the gas phase, the formation of distonic radical cations is a well-known phenomenon.[31-33] A distonic radical cation is an open-shell ion in which the spin and charge sites are separated.[31] The proximity of the two sites is indicated by a Greek letter, i.e. an α-distonic radical cation has the spin and charge sites on adjacent atoms (e.g. $^{\bullet}CH_2OH_2^{+}$).

Radical cations are often thought to have the same connectivity as their neutral precursors. However, in many cases a rearrangement leading to a distonic radical cation is observed. Some examples of these rearrangements are given in Figure 1.4.[32]

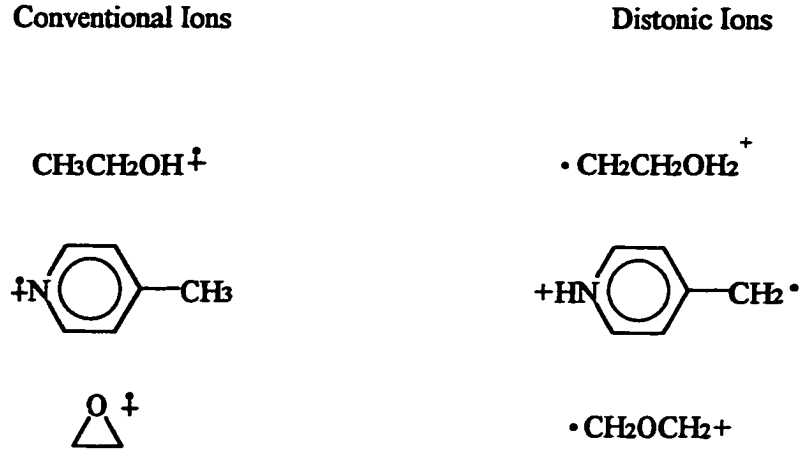

Figure 1.4 Examples of distonic radical cations and the corresponding conventional species.

Distonic radical cations undergo a wide variety of ion-molecule reactions.[33] Their reactivity is different from that of the conventional radical cations. Most distonic radical cations can be considered as protonated radicals since bimolecular reactions of these ions seems to involve the charge site of the ion. Distonic radical cations with an unreactive charge site can undergo radical-type reactions. A commonly observed bimolecular reaction of distonic radical cations is the transfer of a charged odd spin group to a neutral reagent (Reaction [1.22]).

Reaction [1.22]

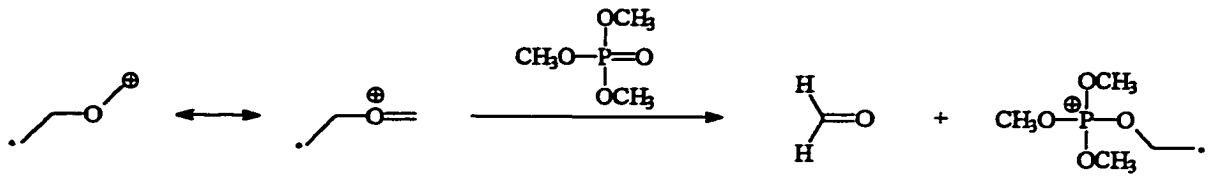

Distonic radical cations are important intermediates in radical ion chemistry. They are frequently observed in solution as well as in the gas phase.

Strictly speaking, the examples discussed in the previous sections (cyclization, bond cleavage) are also examples of rearrangements. Often these rearrangements occur spontaneously but in some cases extra energy (e.g. light or heat) needs to be provided. Examples of isomerization and rearrangement of radical cations in solution, and in solid matrices are given below. Examples of isomerizations in the gas phase (distonic radical cations) were given above.

One of the most common isomerization reactions is the *cis/trans* isomerization (tautomerization) of alkenes.[54] It was mentioned above that radical cations are much more acidic than their neutral precursors and in the presence of a non-nucleophilic base deprotonation is rapid. The resulting allylic radical can be reduced, and reprotonation will give the final product. Tautomerization can be achieved when the starting material is the alkene with the lower oxidation potential. Isomerization will give an alkene with a higher oxidation potential and oxidation of this alkene will not proceed (Reaction [1.23]).

Reaction [1.23]

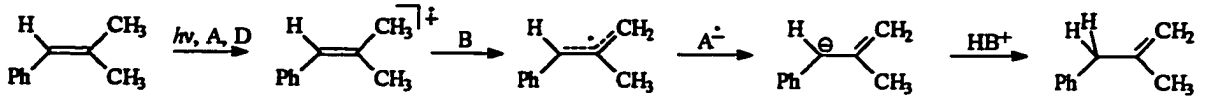

A = electron acceptor
B = base
D = codonor

Formation of the radical cation of *cis*- and *trans*-1-*p*-anisyl-2-(E-2-buten-2-yl)-2-methylcyclopropane leads to a rearrangement yielding *trans*- and *cis*-1-*p*-anisyl-2,3,4-trimethylcyclopent-3-ene in a 6:1 ratio (Reaction [1.24]).[55] These ring expansion reactions were shown to proceed by a stepwise radical cation mechanism.

Reaction [1.24]

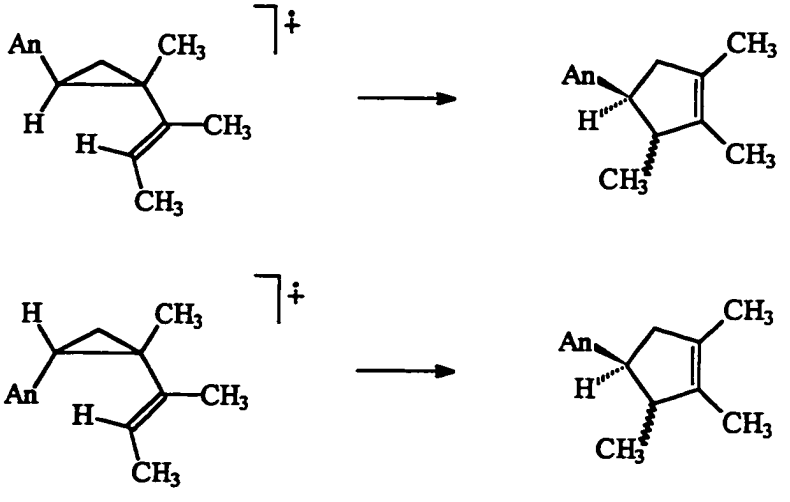

An = 4-$CH_3OC_6H_4$-

Another interesting example is the 4-vinylcyclohexene/bicyclo[3.2.1]oct-2-ene rearrangement.[56] The radical cation of vinylcyclohexene was generated by radiolytic irradiation but upon annealing of the matrix a (thermal) rearrangement to the bicyclo[3.2.1]octene radical cation was observed (ESR).[56a] The results were confirmed by mass spectrometry studies.[56b] However, it was suggested that the distonic bicyclo[2.2.2]-oct-2-yl-5-ylium radical cation could be a possible intermediate. A Wagner-Meerwein rearrangement followed by a vicinal hydride shift would account for the formation of the final product (Reaction [1.25]).[56a]

Reaction [1.25]

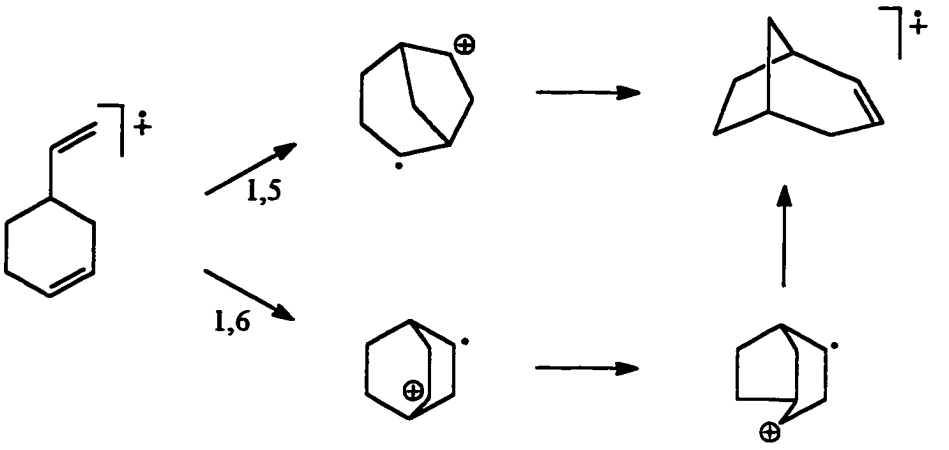

The results from the photo-NOCAS reaction on terpineol strengthen the idea that 1,6-ring closure product might be an intermediate.[51] As described above (Reaction [1.19]), the radical cation of terpineol reacts to give two cyclized products: a 1,5-ring closure and a 1,6-ring closure product (10:1 ratio). The reaction of limonene (structurally related to vinylcyclohexene) in the presence of a nucleophile does not lead to the formation of ring

closed products.[51] However, this reaction was not done in the absence of a nucleophile. Prolonging the lifetime of the radical cation by eliminating nucleophilic attack on the radical cation might lead to cyclized products.

1.4 Theoretical Methods

In addition to the experimental methods described above, theoretical methods have gained much popularity in recent years. Often they are combined with experimental studies. Both *ab initio* molecular orbital (MO) calculations and semi-empirical calculations have proven to be useful tools for understanding and predicting reaction pathways and structures of radical cations. Their use is mainly in predicting structures as well as spin and charge distributions in the radical cation. Molecular orbital calculations are used to obtain a set of molecular orbitals which are occupied by the electrons assigned to the molecule. There are several ways to achieve this, however, the most convenient method is to use a set of atomic orbitals centered on individual atoms. Combining the atomic orbitals (finding the combinations of the orbitals that have the correct symmetries and that will give the lowest energies) builds up the molecular orbitals. This method is known as the linear combination of atomic orbitals (LCAO). For larger systems these types of calculations become more time consuming because more electrons are present and therefore more orbitals will have to be taken into account. For example, for a carbon atom, there are 1s, 2s, and 2p electrons. The 1s electrons are called the core electrons. The core electrons do not take any part in bonding and are therefore ignored in semi empirical calculations. Only the valence electrons are considered which leads to much faster results. Another major

difference between the two methods described here is the fact that semi empirical methods are parameterized. Parameters obtained from both experiments and *ab initio* calculations are used in the semi empirical methods in order to obtain accurate results within short periods of time.[59]

There are many examples available of the use of theoretical methods in radical ion chemistry. It is, however, beyond the scope of this thesis to give an extensive overview of this type of work. Some of the studies where theory has been applied succesfully to radical ion chemistry are (*a*) the structure of the oxirane radical cation,[10] (*b*) the structure of the cyclopropane radical cation,[12] (*c*) the pathway of the radical cation Diels-Alder reaction of s-*cis*-1,3-butadiene radical cation with ethylene,[58e] (*d*) reactions of nucleophiles with alkene radical cations,[52i,58m] (*e*) predicting esr spectra (hyperfine coupling constants) of radical cations,[58a,d,j,n] (*f*) rearrangements of radical cations,[58f,o] (*g*) predicting thermodynamic properties (this is especially useful if the species cannot be easily studied experimentally),[58p] (*h*) predicting the reactivity (e.g. bond cleavage, deprotonation, cyclization, etc.) of radical cations based on the calculated structure (spin and charge densities).[58c,k]

It is evident that the use of theoretical methods in radical cation chemistry is important and that it adds a great deal of information to the experimental results. More examples will be discussed in the following chapters.

1.5 Outline of Research

The research described in this thesis is concerned with the rearrangement and interconversion of C_4H_6 and C_8H_{12} radical cations. The species that will be investigated are methylenecyclopropane (**1**), 1,4-bis(methylene)cyclohexane (**2**), tricyclo[2.2.2.$0^{1,4}$]octane (**3**), dispiro[2.0.2.2]octane (**4**), and dispiro[2.1.2.1]octane (**5**) (Figure 1.5).

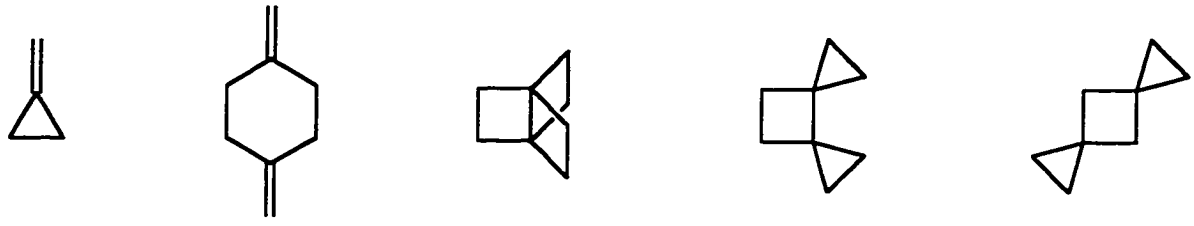

1 **2** **3** **4** **5**

Figure 1.5 Compounds of interest for the work described in this thesis.

Dimerization of $\mathbf{1}^{+\bullet}$ could yield all four dimers, depending on its orientation in the transition state. Polymerization of $\mathbf{1}^{+\bullet}$ might lead to the formation of a highly ordered system. The dimeric radical cations $\mathbf{2}^{+\bullet}$ - $\mathbf{5}^{+\bullet}$ could undergo bond cleavage to give the monomer. Cyclization of **2** leads to **3**, a highly unstable species; however, there is a possibility of trapping the radical cation. The radical cations of **4** and **5** are likely to rearrange.

The structure and reactivity of the radical cations were investigated by theoretical and experimental methods. *Chapter 2* reports on the structure of the neutral species and the radical cations as well as on the energetics of the possible interconversions and

rearrangements of the radical cations, calculated by *ab initio* molecular orbital and semiempirical methods. Photochemical and electrochemical techniques were used to generate the radical cations of 1,4-bis(methylene)cyclohexane (**2**, *Chapter 3*) and methylenecyclopropane (**1**, *Chapter 4*). Additional studies involved the generation of iminyl radicals (*Chapter 3*) and the PET reactions of isobutylene (*Chapter 4*).

Chapter 2

Theoretical studies on the interconversion and rearrangement of the radical cations of methylenecyclopropane, 1,4-bis(methylene)cyclohexane, tricyclo[2.2.2.0^{1,4}]octane, dispiro[2.0.2.2]octane, and dispiro[2.1.2.1]octane

2.1 Introduction

In Chapter 1 it was shown that radical cations are reactive species that can undergo a wide variety of reactions. The reactivity of radical cations will be largely governed by their structure (e.g. spin and charge densities). In order to be able to make predictions about the reactivity of radical cations in general, it will be necessary to determine their (electronic) structures.

This study is concerned with the structure and reactivity (interconversion and rearrangement) of $C_4H_6^{+\bullet}$ and $C_8H_{12}^{+\bullet}$, the radical cations of methylenecyclopropane (**1**) 1,4-bis(methylene)cyclohexane (**2**), tricyclo[2.2.2.0^{1,4}]octane (**3**), dispiro[2.0.2.2]octane (**4**), and dispiro[2.1.2.1]octane (**5**) (Figure 2.1a). Important factors governing these transformations are the energetics and the orientation (entropy) of the radical cations involved. These factors can be studied using theoretical methods which have proven to be useful in the study of other radical cations.[58] For relatively small systems, high level *ab initio* molecular orbital calculations will undoubtedly give the most accurate results. For larger systems smaller basis-sets have to be used due to limited computer time. As a compromise, semi-empirical methods such as MINDO/3,[62a] AM1,[62b] (and others) have

been developed. Although not as sophisticated as the *ab initio* methods, useful results can be obtained with much less computer time.[62b]

A first indication of the energetics for bond cleavage and rearrangement of the radical cations was obtained by performing AM1 calculations on the radical cations of **1-5** and related species. Higher level *ab initio* calculations were then performed on selected species in order to get more accurate numbers for the energetics involving the interconversion of the radical cations $\mathbf{1}^{+\bullet}$ - $\mathbf{5}^{+\bullet}$. High level *ab initio* methods were also used to study the dimerization of methylenecyclopropane; reaction of the radical cation ($\mathbf{1}^{+\bullet}$) and the radical cation of trimethylenemethane ($\mathbf{1a}^{+\bullet}$) with its neutral precursor (**1**).

2.2 Computational

Calculations were carried out using the Gaussian 92 package of programs,[63] installed on Silicon Graphics 40420S and IBM RISC 6000 work stations, with the STO-3G and 6-31G* basis sets,[59b] without imposing any symmetry constraints. For closed-shell species the restricted Hartree-Fock (RHF) formalism was used whereas the unrestricted (UHF) formalism was used for open-shell species. Input orientations for the AM1 calculations were generally obtained by using PC Model.[64] For the radical cations $\mathbf{1}^{+\bullet}$, $\mathbf{2}^{+\bullet}$ (2 conformers), $\mathbf{3}^{+\bullet}$, $\mathbf{4}^{+\bullet}$, and $\mathbf{5}^{+\bullet}$ the starting structures were obtained by taking one electron from the optimized geometry for the corresponding neutral species. After minimization was completed, a frequency calculation was performed in order to confirm that the structure obtained was a minimum (zero imaginary frequencies), not a transition state (TS, one imaginary frequency). Spin and charge densities were calculated using the Mulliken population analysis.[60]

For the *ab initio* calculations PC Model was used to obtain the input orientations for the neutral compounds. Removing one electron from the optimized structure of the neutral compound gave the input orientation for the radical cations. The energies for all of the optimized structures were corrected for electron correlation by single point energy calculations at the MP2/6-31G* level.[61] In some cases spin contamination was large and therefore all energies reported here for the open-shell species are projected energies (PUHF, PMP2). Frequency analyses were done after every optimization in order to determine whether the species are true minima or transition states.

2.3 Results and Discussion

Interconversion and rearrangement of the radical cations of compounds 1-5.

AM1 calculations were performed on the species shown in Figures 2.1a (neutrals) and 2.1b (radical cations). The numbering of the atoms is shown in Figure 2.1a.

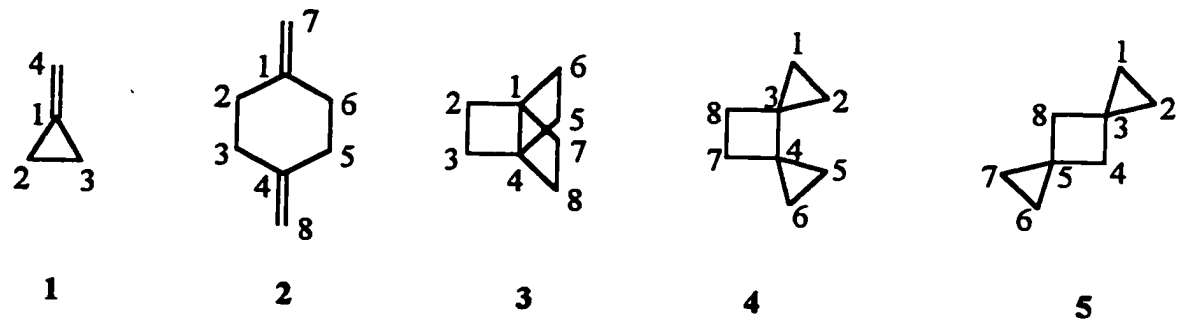

Figure 2.1a Neutral compounds studied using AM1 and ab initio methods.

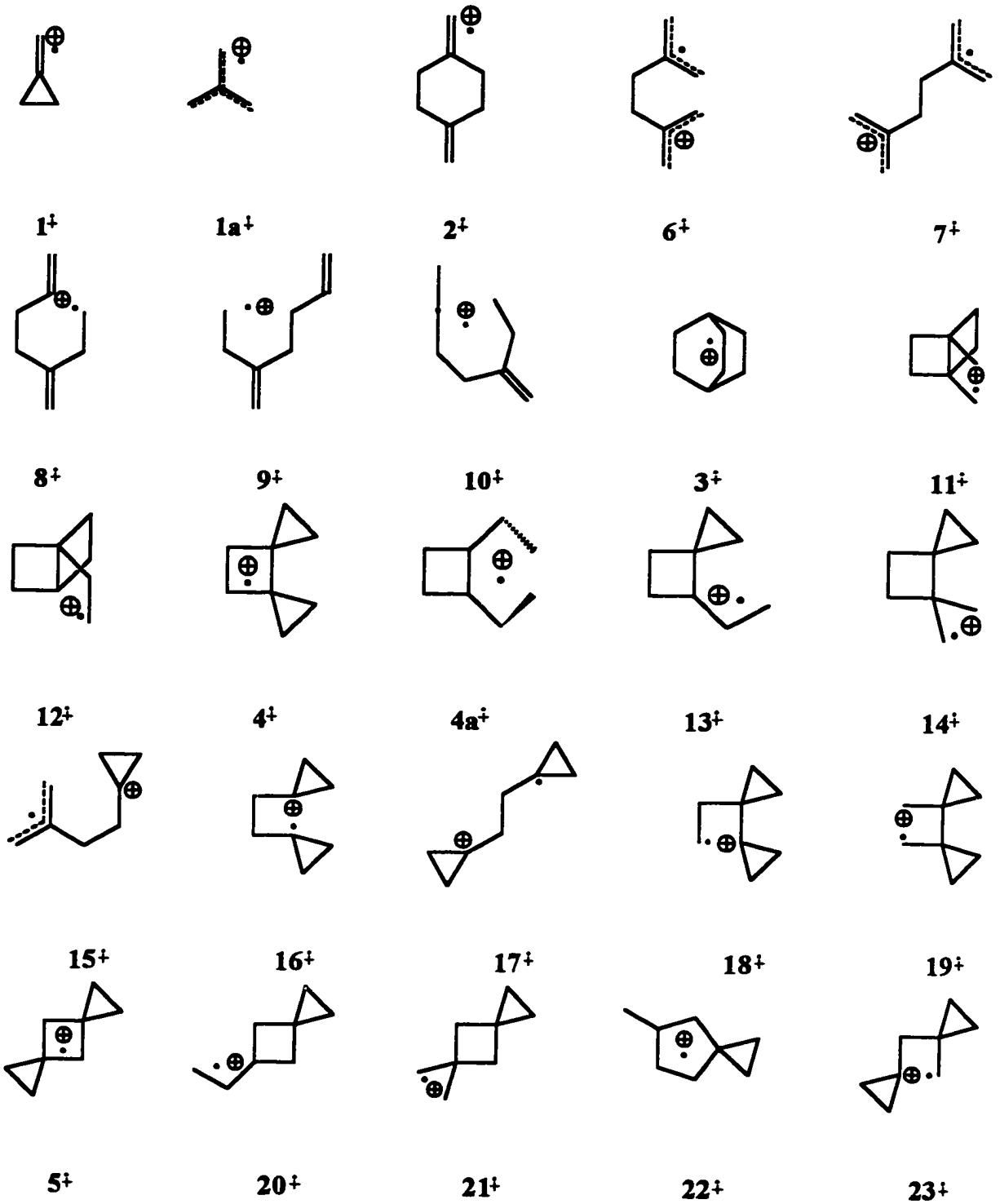

Figure 2.1b Radical cations studied using AM1 (all) and *ab initio* (selected) methods (see text for details).

Table 2.1 Calculated AM1 energies for several neutral species and radical cations.

species[a]	energy[b]	species[a]	energy[b]	species[a]	energy[b]
1	104.9	**2b**$^{+\bullet}$	327.1	**13**$^{+\bullet}$	373.0
2a	127.7	**6**$^{+\bullet}$	358.5	**14**$^{+\bullet}$ (**15**$^{+\bullet}$)	374.6
2b	128.4	**7**$^{+\bullet}$	358.3	**16**$^{+\bullet}$	398.7
3	181.6	**8**$^{+\bullet}$	328.4	**17**$^{+\bullet}$	399.1
4	181.3	**9**$^{+\bullet}$ (**10**$^{+\bullet}$)	359.1	**18**$^{+\bullet}$	389.8
5	180.5	**3**$^{+\bullet}$	344.3	**19**$^{+\bullet}$	395.7
1$^{+\bullet}$	330.7	**11**$^{+\bullet}$ (**8**$^{+\bullet}$)	328.4	**5**$^{+\bullet}$	375.8
1a$^{+\bullet}$	302.5	**12**$^{+\bullet}$	392.4	**21**$^{+\bullet}$ (**22**$^{+\bullet}$)	343.3
2a$^{+\bullet}$	327.8	**4**$^{+\bullet}$	392.4	**23**$^{+\bullet}$	396.8

[a] Numbers in brackets indicate that a rearrangment was observed
[b] Hartree-Fock (HF) + thermal energy; values in kcal/mol

The calculated energies for all species are shown in Table 2.1. The spin and charge densities are given in Table 2.2. Selected properties of the optimized structures (bond lengths, bond angles and dihedral angles) can be found in Appendix I (Tables 2.8-2.12).

Ab initio calculations were performed on **1-5** (neutrals) and **1**$^{+\bullet}$-**7**$^{+\bullet}$(radical cations). The calculated energies (HF/6-31G* and MP2/6-31G*//HF/6-31G*) are given in Table 2.3. The spin and charge densities can be found in Table 2.4. The results presented here are generally in agreement with those reported,[65] considering the differences in the calculations used and the fact that previous calculations have imposed symmetry constraints.

Methylenecyclopropane (1).

Methylenecyclopropane (**1**; MCP) is a symmetric (C_{2v}) species. The results for **1** obtained with AM1 calculations are similar to those obtained by *ab initio* (STO-3G,

Table 2.2 Calculated (AM1) spin and charge densities of the radical cations.[a]

Species		atom no. 1	2	3	4	5	6	7	8
$\mathbf{1}^{+\bullet}$	charge	-0.212	0.388	0.388	0.436				
	spin	0.613	0.198	0.198	-0.008				
$\mathbf{1a}^{+\bullet}$	charge	-0.187	0.297	0.297	0.594				
	spin	-0.232	0.719	0.718	-0.205				
$\mathbf{2a}^{+\bullet}$	charge	0.141	0.144	0.146	-0.207	0.146	0.144	0.317	0.168
	spin	0.162	0.055	0.009	-0.034	0.009	0.055	0.707	0.037
$\mathbf{2b}^{+\bullet}$	charge	-0.203	0.142	0.150	0.135	0.150	0.142	0.160	0.323
	spin	-0.015	0.005	0.059	0.152	0.059	0.005	0.017	0.718
$\mathbf{6}^{+\bullet}$	charge	-0.263	0.553	0.057	-0.156	0.107	0.117	0.515	0.070
	spin	0.001	-0.013	0.808	-0.611	0.035	-0.016	0.011	0.785
$\mathbf{7}^{+\bullet}$	charge	-0.127	0.066	0.535	-0.265	0.120	0.064	0.075	0.531
	spin	-0.610	0.800	-0.003	0.002	-0.019	0.050	0.790	0.000
$\mathbf{8}^{+\bullet}$	charge	0.146	0.143	0.148	-0.209	0.148	0.137	0.318	0.170
	spin	0.161	0.060	0.006	-0.033	0.015	0.035	0.719	0.036
$\mathbf{10}^{+\bullet}$	charge	-0.094	0.024	0.092	-0.192	0.201	0.349	0.468	0.154
	spin	0.362	0.002	0.003	-0.003	0.046	0.332	0.250	0.007
$\mathbf{3}^{+\bullet}$	charge	-0.099	0.182	0.115	0.211	0.114	0.182	0.182	0.115
	spin	0.974	-0.085	0.021	0.213	0.021	-0.085	-0.085	0.021
$\mathbf{12}^{+\bullet}$	charge	0.227	0.013	0.171	-0.136	0.187	0.180	0.181	0.179
	spin	-0.001	1.024	-0.030	0.010	-0.001	0.000	0.000	-0.003
$\mathbf{4}^{+\bullet}$	charge	0.253	0.253	-0.181	-0.181	0.254	0.253	0.174	0.174
	spin	0.161	0.158	0.162	0.162	0.162	0.158	0.019	0.019
$\mathbf{13}^{+\bullet}$	charge	0.235	0.235	-0.328	0.266	0.065	0.191	0.152	0.184
	spin	-0.001	-0.001	-0.005	0.055	1.030	-0.077	-0.001	0.002
$\mathbf{15}^{+\bullet}$	charge	0.219	0.201	0.203	-0.151	0.072	0.086	0.133	0.236
	spin	0.000	-0.001	0.003	-0.609	0.804	0.785	0.037	-0.018
$\mathbf{16}^{+\bullet}$	charge	0.145	0.093	-0.320	0.208	0.198	0.221	0.237	0.218
	spin	-0.047	-0.047	1.109	-0.002	0.001	0.000	0.017	-0.032
$\mathbf{17}^{+\bullet}$	charge	0.150	0.104	-0.320	0.192	0.205	0.215	0.245	0.209
	spin	-0.049	-0.051	1.122	-0.004	0.001	0.000	0.011	-0.030
$\mathbf{18}^{+\bullet}$	charge	0.273	0.269	-0.265	0.155	0.214	0.183	0.014	0.156
	spin	0.000	-0.002	0.013	-0.005	0.001	0.001	1.024	-0.031
$\mathbf{19}^{+\bullet}$	charge	0.106	0.120	-0.154	-0.301	0.304	0.321	0.543	0.061
	spin	0.093	0.062	-0.166	0.014	-0.001	0.000	-0.007	1.005
$\mathbf{20}^{+\bullet}$	charge	0.137	0.137	-0.220	0.215	0.232	0.218	0.078	0.203
	spin	0.000	0.000	0.001	-0.004	0.048	-0.059	1.017	-0.003
$\mathbf{22}^{+\bullet}$	charge	0.110	0.109	-0.207	0.149	0.133	0.160	0.339	0.208
	spin	0.003	-0.001	-0.001	0.000	0.172	0.054	0.716	0.056
$\mathbf{23}^{+\bullet}$	charge	0.133	0.098	-0.185	0.048	0.205	0.197	0.224	0.280
	spin	0.098	0.055	-0.164	1.004	-0.004	0.001	0.000	0.010

[a] Hydrogen atoms are summed with the carbon atoms.

6-31G*) methods.[65] Removing an electron from **1** results in radical cation $\mathbf{1}^{+\bullet}$, a second order stationairy point (two imaginary frequencies). The energy difference between these two states is 225.8 kcal/mol, a value close to the experimentally determined (vertical) ionization potential (221.4 kcal/mol; 9.6 eV).[66a] A stable intermediate on the potential energy surface of $\mathbf{1}^{+\bullet}$ is trimethylenemethane (TMM) radical cation, $\mathbf{1a}^{+\bullet}$, a species with C_S symmetry. The (C2-C3) bond of the cyclopropane is broken and all four atoms lie in the same plane. The charge in $\mathbf{1a}^{+\bullet}$ is mainly localized on C4 whereas the spin density is distributed over C2 and C3. The bond between C1 and C4 (1.399 Å) is slightly shorter than the bonds between C1 and C2 (1.414 Å), and C1 and C3 (1.413 Å). The bond angle C2-C1-C3 (121.2°) is somewhat larger than the bond angles C3-C1-C4 and C2-C1-C4 (119.4°).

The *ab initio* calculations on **1** agree with the results of the AM1 calculations and are also consistent with those previously reported by Feller, et al.,[65a] as well as with the results of the investigation of the microwave spectrum of this species.[65d]

Ionization of the optimized geometry (HF/6-31G*) of **1** leads immediately to the TMM radical cation $\mathbf{1a}^{+\bullet}$, a minimum with a ring opened structure. This is consistent with the findings of Du and Borden[65b] who have calculated that ring opening from both the $^2B_1$ π ground state and the $^2A_1$ σ state of MCP radical cation is exothermic and the disrotatory pathway requires no (or only a small) activation energy (2 kcal/mol).

Further efforts to find a ring closed radical cation without constraining the molecule lead to $\mathbf{1}^{+\bullet}$, a second order stationairy point (two imaginairy frequencies) with an energy 14.5 kcal/mol higher than $\mathbf{1a}^{+\bullet}$. Du and Borden[65b] found the same species ($^2B_2$

Table 2.3. Calculated energies of several neutral species and radical cations using *ab initio* methods.

species	UHF/6-31G*[a]	MP2/6-31G*[a]	$E_{relative}$[b]
1	-154.88734	-155.39579	84.2
2a	-309.90132	-310.92580	0.0
2b	-309.89371	-310.91789	5.0
2c	-309.89274	-310.91741	8.4
3	-309.80932	-310.84861	48.4
4	-309.83304	-310.86990	35.1
5	-309.83354	-310.86917	35.5
$\mathbf{1}^{+\bullet}$	-154.57974	-155.04594	303.8
$\mathbf{1a}^{+\bullet}$	-154.61388	-155.06903	289.3
$\mathbf{2a}^{+\bullet}$	-309.62894	-310.60870	199.0
$\mathbf{2b}^{+\bullet}$	-309.62452	-310.60347	202.3
$\mathbf{2c}^{+\bullet}$	-309.60668	-310.61121	197.4
$\mathbf{6}^{+\bullet}$	-309.60356	-310.56284	227.8
$\mathbf{7}^{+\bullet}$	-309.60013	-310.55305	233.9
$\mathbf{3}^{+\bullet}$	-309.61056	-310.59988	204.5
$\mathbf{4a}^{+\bullet}$	-309.56601	-310.57770	218.4
$\mathbf{21}^{+\bullet}$	-309.54493	-310.54110	241.5

[a] Reported energies are in atomic units (1 a.u. ≡ 627.5 kcal/mol) and, in case of open-shell species, have been corrected for spin contamination; [b] relative energies in kcal/mol.

state). According to their results the first order TS ($^2B_1$ state) has an energy that is 6.6 kcal/mol higher than the planar TMM radical cation ($^2B_1$ state; $\mathbf{1a}^{+\bullet}$). The spin density in $\mathbf{1}^{+\bullet}$ is located on C1 (C4 has a large negative spin density); the charge density is delocalized over C2, C3, and C4. Breaking the C2-C3 bond leads to the formation of the TMM radical cation ($\mathbf{1a}^{+\bullet}$). This radical cation deviates from C_{2v} symmetry. One carbon-carbon bond is distinctly longer than the other two (1.452 vs 1.385 Å) which is in contrast with the AM1 results. Distances between non-bonded carbons are nearly identical (C2-C4, 2.495 Å; C3-C4, 2.494 Å; and C2-C3, 2.321 Å). One bond angle is different from the other two: C2-C1-C3: 113.8°; C3-C1-C4 and C2-C1-C4: 123.1°.

Table 2.4. Calculated (HF/6-31G*) spin and charge densities of the radical cations.[a]

species		atom no. 1	2	3	4	5	6	7	8
$\mathbf{1}^{+\bullet}$	charge	0.082	0.375	0.375	0.168				
	spin	1.117	0.172	0.320	-0.608				
$\mathbf{1a}^{+\bullet}$	charge	0.022	0.419	0.419	0.140				
	spin	-0.281	0.143	0.141	0.997				
$\mathbf{2a}^{+\bullet}$	charge	0.072	0.088	0.090	0.231	0.090	0.088	0.025	0.316
	spin	-0.160	0.036	-0.028	0.286	-0.028	0.036	0.146	0.710
$\mathbf{2b}^{+\bullet}$	charge	0.069	0.088	0.093	0.246	0.092	0.089	0.009	0.314
	spin	-0.022	0.009	-0.007	0.274	-0.007	0.007	-0.008	0.726
$\mathbf{2c}^{+\bullet}$	charge	0.143	0.090	0.107	0.143	0.090	0.107	0.161	0.161
	spin	-0.219	0.054	0.060	-0.219	0.054	0.060	0.605	0.605
$\mathbf{6}^{+\bullet}$	charge	0.002	0.432	0.021	0.054	0.071	0.077	0.363	-0.018
	spin	0.016	0.066	0.879	-0.753	0.061	-0.022	-0.067	0.822
$\mathbf{7}^{+\bullet}$	charge	0.094	-0.005	0.411	-0.007	0.087	0.013	-0.005	0.411
	spin	-0.790	0.874	0.000	-0.003	-0.019	0.065	0.874	0.000
$\mathbf{3}^{+\bullet}$	charge	0.056	0.122	0.123	0.208	0.124	0.122	0.122	0.123
	spin	1.123	-0.113	0.060	0.033	0.083	-0.135	-0.135	0.083
$\mathbf{4a}^{+\bullet}$	charge	0.064	0.065	-0.011	0.123	-0.059	0.348	0.348	0.123
	spin	0.008	0.009	-0.009	0.053	-0.224	0.555	0.554	0.053
$\mathbf{21}^{+\bullet}$	charge	0.064	0.065	-0.011	0.123	-0.059	0.348	0.348	0.123
	spin	0.008	0.009	-0.009	0.053	-0.224	0.554	0.555	0.053

[a] Hydrogen atoms are summed with the carbon atoms

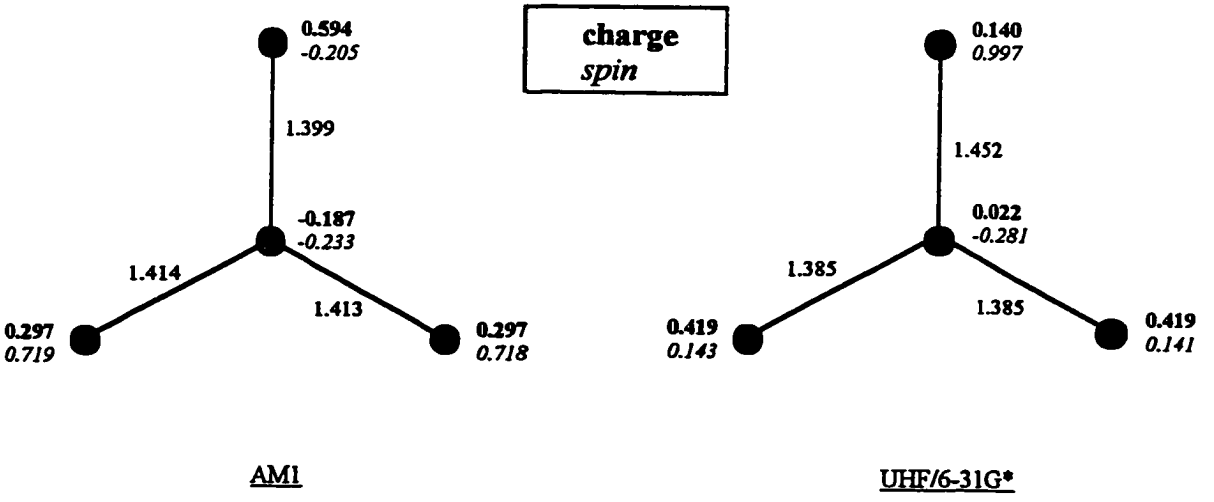

Figure 2.2. Spin and charge density distribution in $\mathbf{1a}^{+\bullet}$ as calculated by AM1 and *ab initio* methods.

The charge in $\mathbf{1a}^{+\bullet}$ is distributed primarily over C2 and C3, while the spin is essentially localized on C4, again different from the AM1 results (Figure 2.2).

In order to determine whether the calculated energies are correct, the ionization potential (IP) of the molecules can be calculated and compared to the experimentally determined values. Two different methods can be used to calculate the IP. The difference in energy between the neutral species and the first order TS upon removal of an electron from this neutral is equal to the vertical IP. For MCP (**1**) this would be the $^1B_2$ state which we were unable to locate. However, the energy difference between the second order stationairy point ($\mathbf{1}^{+\bullet}$) and **1** (219.5 kcal/mol) is very close to the experimentally determined value of 221.4 kcal/mol (9.6 eV). The energy difference between the neutral species (**1**) and the minimized (0 imaginary frequencies) radical cation ($\mathbf{1a}^{+\bullet}$), derived from the neutral, is taken to be the adiabatic IP.

The second method is to calculate the energy needed for the removal of an electron from the HOMO of the ground state species. This number should also be equal to the vertical IP. For **1** this accounts to 0.35927 au (225.4 kcal/mol), a value also very close to the experimental number. The calculated and experimental numbers are listed in Table 2.5.

The dominant factor for isomerization and rearrangement (including dimerization) of the radical cations will be the energy (ΔH). The calculated ΔH values can therefore be used to predict whether these interconversions are likely to take place. From Figure 2.3 it

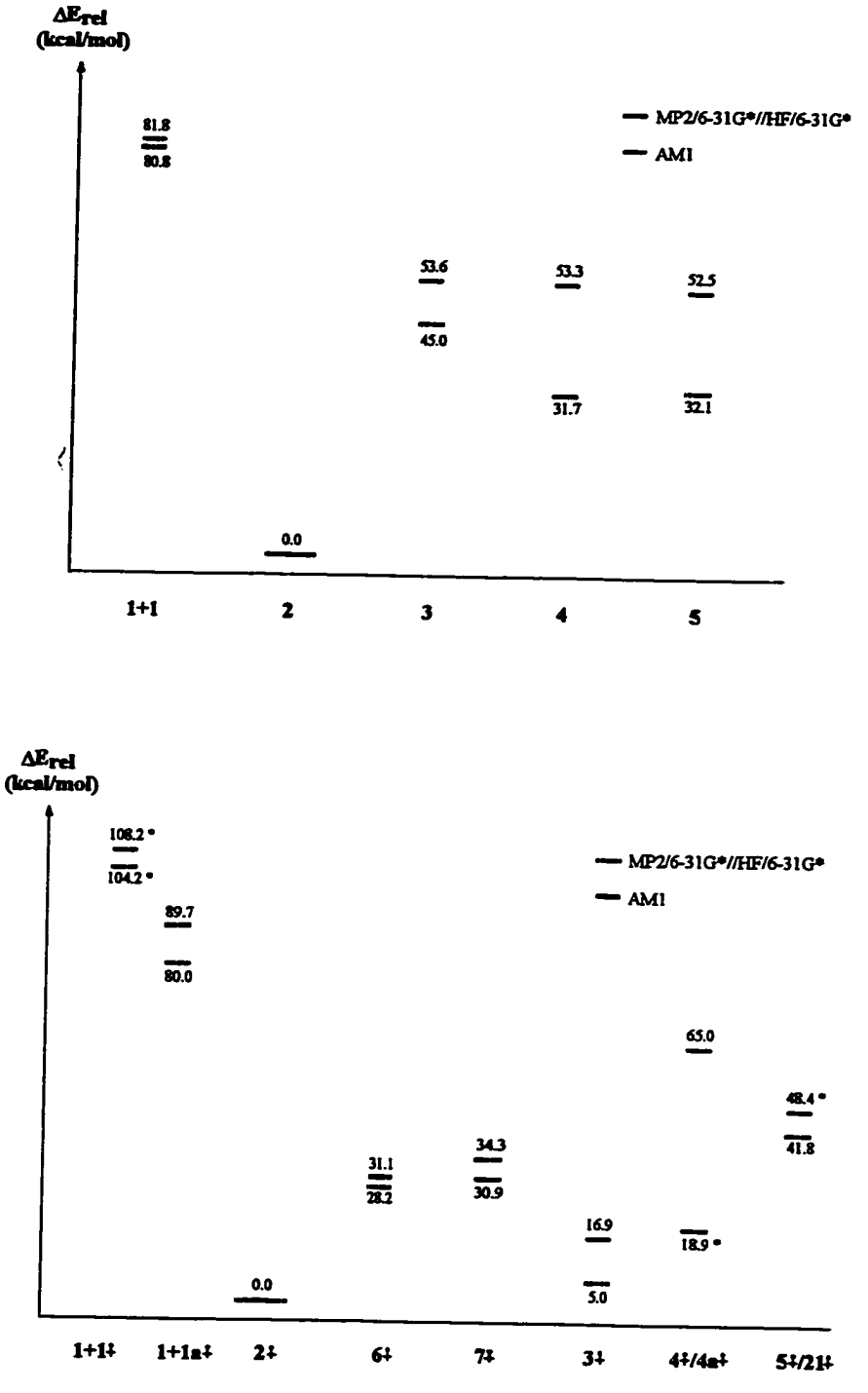

Figure 2.3. Relative energies (AM1 and MP2/6-31G*//HF/6-31G*) of the neutrals **1-5** (a); Relative energies (AM1 and MP2/6-31G*//HF/6-31G*) of the radical cations (b) (an asterisk next to the energy level indicates that this optimized geometry is not a minimum) (see text for details).

Table 2.5. Calculated Ionization Potentials using AM1 and Hartree-Fock (HF) Theory.[a]

species	Ionization Potential			HOMO[b]
	HF[c]	AM1	exptl[d]	HF[c]
1	219.5	225.8	221.4	225.4
2	196.2[e]	199.4[f]	207.5	212.2[e]
3	156.1	162.8	na[g]	210.9
4	183.4	211.1	208.0	225.4
5	205.9	195.3	212.4	234.5

[a] Energies are given in kcal/mol; [b] energy necessary to remove an electron from the highest occupied molecular orbital (HOMO); [c] MP2/6-31G*//HF/6-31G* level of theory; corrected for spin contamination; [d] experimental values (ref. 66); [e] average of three values; [f] average of two values; [g] not available.

is clear that reactions of **1** with its radical cation ($\mathbf{1}^{+\bullet}$ or $\mathbf{1a}^{+\bullet}$) to give a dimeric radical cation ($\mathbf{2}^{+\bullet}$, $\mathbf{6}^{+\bullet}$, $\mathbf{7}^{+\bullet}$, $\mathbf{3}^{+\bullet}$, $\mathbf{4}^{+\bullet}$, or $\mathbf{5}^{+\bullet}$) are all exothermic and can be expected to happen. Which product forms may depend upon the initial orientation of the orbitals involved in the bonding, i.e. the conformation of the initially formed radical cation. The (dimerization) reactions of **1** with its radical cation ($\mathbf{1}^{+\bullet}$ and $\mathbf{1a}^{+\bullet}$) using different orientations for the reactants were studied separately and will be discussed below.

Three types of dimerization involving **1** have been reported. After generation of the triplet of TMM ($\mathbf{7}^{t}$), formation of **2** is observed.[67] Triplet TMM has no favourable unimolecular decay mechanism; thus, the concentration of the triplet can increase to the point where bimolecular reaction leading to **2** can occur.[68] The dimerization of **1** to give **4** and **5** will be discussed below.

1,4-Bis(methylene)cyclohexane (2).

A thorough search for conformers of the neutral species **2** using AM1 found two: the chair (**2a**) and *pseudo* chair (**2b**) conformers. The chair conformer is the lower in

energy but the difference is only 0.7 kcal/mol. A boat conformer, which is thought to be a likely precursor for a ring closure reaction, could not be found and it is undoubtedly of higher energy. The calculated adiabatic IP's of **2a** and **2b** (200.1 and 198.7 kcal/mol respectively), are close to the experimental (vertical) IP (207.5 kcal/mol; 9.0 eV) (Table 2.5).[66a] The structural changes resulting upon ionization are small. One double bond has lengthened and carries most of the spin and charge densities (Table 2.2). The energy difference between the conformers of the radical cations $\mathbf{2a}^{+\bullet}$ and $\mathbf{2b}^{+\bullet}$ is also 0.7 kcal/mol (Table 2.1).

Although no lengthening of the C2-C3 bond was observed in $\mathbf{2}^{+\bullet}$, cleavage of this bond seems possible (*a priori*) since this would give the bis-allylic radical cations $\mathbf{6}^{+\bullet}$ and/or $\mathbf{7}^{+\bullet}$. However, calculations on these species show that they are ca. 30 kcal/mol higher in energy than $\mathbf{2}^{+\bullet}$. Note that these numbers do not take into account the activation energies for these processes. The barriers for interconversion will be higher than the calculated energy differences between the species.

Breaking the C1-C2 bond in **2** is highly unlikely as shown by calculations performed on $\mathbf{8}^{+\bullet}$. This species undergoes ring closure to give a third conformer of $\mathbf{2}^{+\bullet}$. Structurally this species is very similar to the chair ($\mathbf{2a}^{+\bullet}$) but it has a slightly higher energy (Table 2.1).

Optimization of structure $\mathbf{9}^{+\bullet}$ (obtained from $\mathbf{2}^{+\bullet}$ by breaking the C1-C2 bond and rotation around the C5-C6 bond by 180°) gives $\mathbf{10}^{+\bullet}$ (an allene radical cation) which is the result of a hydrogen atom migration process. The energy of this species is almost 32 kcal/mol higher than $\mathbf{2}^{+\bullet}$.

Using the *ab initio* methods, three conformers were found for neutral 1,4-bis(methylene)cyclohexane (**2**): the chair conformer (**2a**) is the global minimum, 5.0 kcal/mol (MP2/6-31G*//HF/6-31G*) more stable than the *pseudo*-chair conformer (**2b**). The twist-boat conformer (**2c**) is only 5.3 kcal/mol above the global minimum. Removing an electron from **2a** requires 199.0 kcal/mol, 197.3 kcal/mol from **2b** and 192.2 kcal/mol from **2c**; therefore, the energy difference between the radical cations of the chair and *pseudo*-chair conformers is reduced to 3.3 kcal/mol, and the difference between the chair and twist-boat conformers is 1.6 kcal/mol but now in favour of the twist-boat conformer (Table 2.3). The reported ionization potential for **2**, determined from the photoelectron spectra, is 207.5 kcal/mol (9.0 eV),[66a] in good agreement with the calculated value (Table 2.5). All three radical cations were proven to be minima by frequency analyses and therefore the calculated IP's must be the adiabatic IP's. Using the HOMO energies of **2a**, **2b**, and **2c** we can calculate IP's for these species of 210.8, 212.4, and 213.5 kcal/mol respectively. These numbers are also very close to the experimental values, taking into account the relative error of the experiment (± 0.1 eV) (Table 2.5).[66a]

The structures of the radical cations $\mathbf{2a}^{+\bullet}$, $\mathbf{2b}^{+\bullet}$, and $\mathbf{2c}^{+\bullet}$ are very similar to those of the neutral species; ionizing this molecule has little effect on its structure. Results from the lower level calculations (HF/STO-3G) give the spin and charge densities delocalized over the entire molecule. With the higher level calculations, however, the spin and charge densities of $\mathbf{2a}^{+\bullet}$ and $\mathbf{2b}^{+\bullet}$ are essentially localized on one methylene group (C1-C7 or C4-C8). For $\mathbf{2c}^{+\bullet}$ the high level calculations still predict complete delocalization of spin and charge. Complete delocalization of spin and charge will lead to a lower energy in the gas

phase whereas in polar solvent a localized charge can be stabilized to give a lower energy. Comparison with the neutral molecule in configurations **2a** and **2b**, shows that one of the carbon-carbon double bonds of the radical cation lengthens, from 1.321 Å to 1.418 Å, while the other double bond remains unchanged, 1.321 Å. In the case of $\mathbf{2c}^{+\bullet}$, both double bonds are now 1.372 Å. Other structural changes are minimal; the chair, *pseudo*-chair, and twist-boat conformations are maintained. Ionizing **2c** moves the two methylene groups slightly towards one another. This structure ($\mathbf{2c}^{+\bullet}$) is, however, still far from a true boat conformation. The symmetric boat conformation for the neutral molecule could not be optimized. This species is undoubtedly significantly less stable than **2a**, **2b** and **2c**. Furthermore, since neither **2a**, **2b**, nor **2c** showed any tendency to relax toward a boat conformation upon ionization, the boat conformation was not considered further.

Formation of the bisallyl (distonic) radical cations $\mathbf{6}^{+\bullet}$ and $\mathbf{7}^{+\bullet}$ in the gas phase is not favoured. Besides a considerable barrier for carbon-carbon bond cleavage, these species are also ca. 30-36 kcal/mol higher in energy than $\mathbf{2}^{+\bullet}$. According to these calculations the *gauche* conformer is more stable than the *anti* confomer by 6.1 kcal/mol. The spin and charge in these species are separated, delocalized over the two allylic systems.

The results from the calculations described above indicate that, as expected, isomerization of $\mathbf{2}^{+\bullet}$ is endothermic; however, $\mathbf{3}^{+\bullet}$ is only a few kcal/mol higher in energy than $\mathbf{2}^{+\bullet}$ and this interconversion may occur. Obviously, the conformation required for ring closure across the double bonds is not ideal (*i.e.* a symmetric boat conformation). To get to this transition state may require an additional 6-8 kcal/mol beyond the thermodynamic

barrier, as well as some loss in entropy.[69] In the gas phase, ionization of **2** may bring the radical cation initially to a higher vibrationally excited state, with enough excess energy to overcome this barrier.

Carbon-carbon bond breaking to give ($\mathbf{1}^{+\bullet}$+**1**) or (**1**+$\mathbf{1a}^{+\bullet}$) is highly unlikely. Although some bond lengthening is observed in $\mathbf{2}^{+\bullet}$, breaking these two bonds is a significantly endothermic process (ca. 80-90 kcal/mol).

Breaking only one carbon-carbon bond might seem more likely, especially since the result would be a double allylic (one for the spin and one for the charge) system ($\mathbf{6}^{+\bullet}$ or $\mathbf{7}^{+\bullet}$). From Table 2.3 and Figure 2.3b it can be seen that this process is not as favourable as might have been expected. These species are ca. 30-35 kcal/mol higher in energy than $\mathbf{2}^{+\bullet}$ and therefore significant extra energy would have to be given to the molecule (**2**) upon ionization. This might still be achieved by using mass spectrometry or high energy irradiation.

Rearrangement of $\mathbf{2}^{+\bullet}$ to give $\mathbf{4}^{+\bullet}$ or $\mathbf{5}^{+\bullet}$ is even more unlikely since these processes are endothermic (ca. 20-40 kcal/mol) and would require multiple rearrangements including carbon-carbon bond breaking and formation of two cyclopropane rings.

It is recognized that radical cations are generally much stronger acids than their neutral precursors (eg. the pK_a of the radical cation of toluene is -11).[36] Therefore, another possible reaction of $\mathbf{2}^{+\bullet}$ is deprotonation to the allylic radical. The charge density on the allylic hydrogens on C3 and C5 is high; there is also a high charge density on C4. These allylic protons are certainly acidic and deprotonation is possible.

Tricyclo[2.2.2.0^{1,4}]octane (3).

Tricyclo[2.2.2.0^{1,4}]octane (**3**, commonly referred to as [2.2.2]propellane) has been (and still is) of considerable interest both from a theoretical[71] and a synthetic[72] point of view. Some calculations (SCF energy as a function of the central carbon-carbon bond length) have been reported on this compound as well as on the bicyclo[2.2.2]octane-1,4-diradical.[71a-d,h] In all of these calculations the D_{3h} symmetry was imposed on these structures. The difference in energy (calculated) between **3** and the diradical varies widely depending upon the type of calculation used; however, all of the calculations agree: the diradical is more stable than the bonded structure **3**, but the energy difference between the two ranges from 6 - 38 kcal/mol! Eaton and Temme have reported the synthesis of a substituted [2.2.2]propellane (2-(N,N-dimethylcarboxamide)tricyclo[2.2.2.0^{1,4}]octane).[72a] The activation energy for ring-opening was measured, 22 kcal/mol, and is in reasonable agreement with the barrier of 29 kcal/mol, going from **3** to the diradical, as calculated by Newton and Schulman.[71b] Feller and Davidson have reported 3-21G, 6-31G*, and two-configuration SCF (TCSCF) calculations on **3**, as a function of the C1-C4 bond distance.[71h] The potential energy surface resulting from lengthening the C1-C4 distance indicates a barrier of ca. 10 kcal/mol at the 3-21G level (14 kcal/mol at the 6-31G* level) separating the two minima. When configuration interaction was included in these calculations (3-21G), the double minimum disappears and a single minimum was found with a central C1-C4 distance of 2.5 Å. However, the potential energy surface was now a broad flat region and this might contain another minimum at a shorter bond length. If the potential energy surface is as flat as these calculations indicate, ring opening of **3** to give **2**

should proceed without an activation barrier. In fact, attempts (this work) to optimize the diradical, **without the D_{3h} symmetry constraint**, failed; the diradical isomerizes directly to the twist-boat conformer of the 1,4-bis(methylene)cyclohexane (**2c**). Clearly, there is little or no barrier for the conversion of the 1,4-diradical to **2c**.

The interconversion (**3** → **2c**) mentioned above is the only one observed experimentally. The radical cations $\mathbf{2}^{+\bullet}$ and $\mathbf{3}^{+\bullet}$ have not been prepared nor have there been any previous theoretical studies on these species.

AM1 calculations predict that tricyclo[2.2.2.$0^{1,4}$]octane (**3**) has a symmetrical structure (D_{3h}) with a relatively long central bond (1.616 Å). The three C-C bonds parallel to the central bond are also longer (1.568 Å) than normal C-C bonds indicating that this molecule is significantly strained. It is interesting that upon removal of an electron from **3** a stable species ($\mathbf{3}^{+\bullet}$) results. The central C-C 'bond' is now 2.271 Å and the parallel C-C bonds have also lengthened, from 1.568 to 1.597 Å. The spin in $\mathbf{3}^{+\bullet}$ is mainly located on C1, while the charge is delocalized over several atoms, 55% can be found on C3, C4, C5, and C8.

The calculated IP of **3** is 162.8 kcal/mol (Table 2.5), a relatively low number which seems consistent with the large strain energy present in **3**. However, the frequency analysis shows that $\mathbf{3}^{+\bullet}$ is not a TS and therefore the calculated value for the IP must represent the adiabatic IP (i.e. the energy of the radical cation after relaxation). The value for the vertical IP will be higher than the one given here. Neither the vertical nor the adiabatic IP are known.

Forcing the C2-C3 bond to break ($\mathbf{11}^{+\bullet}$) results in the formation of the same product as from $\mathbf{8}^{+\bullet}$. In contrast, breaking the C1-C2 bond does not result in a rearrangement ($\mathbf{12}^{+\bullet}$) and the final geometry is close to that of the starting material. The energy content of this species, however, is ca. 50 kcal/mol higher than that of $\mathbf{3}^{+\bullet}$.

The results of the *ab initio* calculations for **3** are in good agreement with those of the AM1 calculations; both methods predict a symmetric (D_{3h}) structure. The central C-C bond is somewhat shorter (1.511 Å) than was derived from the AM1 calculations (1.616 Å). Removal of an electron from **3** leads to a ring-opened species ($\mathbf{3}^{+\bullet}$) which was also indicated by AM1.[70] Full optimization (without symmetry constraint) of the radical cation $\mathbf{3}^{+\bullet}$ leads to a stable bicyclic species (C_1 point group). The short central carbon-carbon bond of the neutral molecule **3** (1.511 Å) has become substantially longer (2.292 Å) in the radical cation. The three bridging bonds also lengthen (1.569 to 1.626 Å) whereas the other carbon-carbon bonds become shorter (1.548 → 1.468 Å and 1.548 → 1.511 Å). The charge and spin in $\mathbf{3}^{+\bullet}$ are not equally distributed over the molecule; there is greater charge density on one half of the molecule while the spin density is delocalized over the other half. This structure can formally be regarded as a distonic radical cation.

The calculated energy for ionization of **3**, using the energies of **3** and $\mathbf{3}^{+\bullet}$, is 156.1 kcal/mol. This, however, is the adiabatic IP, since $\mathbf{3}^{+\bullet}$ is a minimum. Using the HOMO energy of **3** the IP is calculated to be 210.9 kcal/mol, a surprisingly large number for such a highly strained molecule (Table 2.5). There is no reported experimental value; however, the earlier calculated IP's (**1** and **2**) are in good agreement with experimentally determined values.

The radical cation $\mathbf{3}^{+\bullet}$ has an energy close to that of $\mathbf{2}^{+\bullet}$ and therefore interconversion may occur rapidly as in the neutral molecule. However, $\mathbf{3}^{+\bullet}$ is now a minimum (unlike the 1,4-diradical) and it seems likely that, in the presence of a good nucleophile, $\mathbf{3}^{+\bullet}$ could be trapped. As in the case of $\mathbf{2}^{+\bullet}$, reaction to give $(\mathbf{1}+\mathbf{1}^{+\bullet})$ or $(\mathbf{1}+\mathbf{1a}^{+\bullet})$ is unlikely as the barrier is too high. Again, some bond lengthening is observed but it seems unlikely that this is enough to make this interconversion favourable.

Rearrangement of $\mathbf{3}^{+\bullet}$ to give either $\mathbf{4}^{+\bullet}$ or $\mathbf{5}^{+\bullet}$ seems highly unlikely since, upon ionization of **3**, the central carbon-carbon bond immediately breaks leading to a bicyclooctane derivative rather than the required cyclobutane.

Dispiro[2.0.2.2]octane (4).

According to the AM1 calculations, this symmetric molecule (C_{2v}) has a short central bond (C3-C4: 1.507 Å) and a longer external bond (C7-C8: 1.550 Å). In contrast to a normal cyclobutane ring, the torsional angle C3-C8-C7-C4 shows that the ring in **4** is essentially planar (0.05°). Removing an electron from **4** gives structure ($\mathbf{4}^{+\bullet}$) which is geometrically similar to the neutral molecule. The central bond (C3-C4) has become shorter (1.507 → 1.451 Å) whereas some of the bonds in the cyclopropane rings have become slightly longer (C1-C3: 1.495 → 1.559 Å; C2-C3: 1.494 → 1.558 Å). Despite these changes, the molecule remains intact. The spin and charge in $\mathbf{4}^{+\bullet}$ are delocalized over the entire molecule. The calculated energy difference between the radical cation and the neutral compound is 211.1 kcal/mol. The experimentally determined (vertical) IP is 208.0

kcal/mol (9.0 eV) (Table 2.5).[66b] The calculated value must represent the adiabatic IP since we are not dealing with a TS species; nevertheless it is close to the measured value.

Breaking the C4-C5 bond in $\mathbf{4}^{+\bullet}$ gives a species ($\mathbf{13}^{+\bullet}$) that is of lower energy by almost 20 kcal/mol (Table 2.1). The cyclobutane remains planar and is unsymmetric: C4-C7: 1.503 Å and C3-C8: 1.538 Å; C3-C4: 1.451 Å and C7-C8: 1.558 Å.

Breaking the C5-C6 bond in $\mathbf{4}^{+\bullet}$ and optimizing the resulting structure ($\mathbf{14}^{+\bullet}$) leads to $\mathbf{15}^{+\bullet}$ (bond cleavage of C3-C4). This species is also of lower energy than $\mathbf{4}^{+\bullet}$ (ca. 18 kcal/mol, Table 2.1).

Cleavage of the C3-C4 bond gives structure $\mathbf{16}^{+\bullet}$. The cyclopropane rings do not open up. Two conformers can be found (cf. $\mathbf{6}^{+\bullet}$ and $\mathbf{7}^{+\bullet}$): *gauche* ($\mathbf{16}^{+\bullet}$) and *anti* ($\mathbf{17}^{+\bullet}$). The torsional angle C4-C7-C8-C3 is -69° in $\mathbf{16}^{+\bullet}$ and 179.5° in $\mathbf{17}^{+\bullet}$. The energies of these species are slightly higher (6.3 and 6.7 kcal/mol, respectively) than that of $\mathbf{4}^{+\bullet}$. Ring opening to give $\mathbf{6}^{+\bullet}$ and $\mathbf{7}^{+\bullet}$ is exothermic (ca. 40 kcal/mol); however, since both species have intact cyclopropyl groups, the barrier for this process must be high. Frequency analyses show that both $\mathbf{16}^{+\bullet}$ and $\mathbf{17}^{+\bullet}$ are transition structures.

Two more possibilities for bond breaking in $\mathbf{4}^{+\bullet}$ exist: the C4-C7 bond (to give $\mathbf{18}^{+\bullet}$) and the C7-C8 bond (to give $\mathbf{19}^{+\bullet}$). Compound $\mathbf{18}^{+\bullet}$ has an energy slightly below that of $\mathbf{4}^{+\bullet}$ (ΔE = -2.6 kcal/mol). According to the frequency analysis this species is a TS.

Breaking the C7-C8 bond ($\mathbf{19}^{+\bullet}$) is less endothermic than breaking the C3-C4 bond ($\mathbf{16}^{+\bullet}$), probably because the C7-C8 bond in $\mathbf{4}^{+\bullet}$ is already longer than the C3-C4 bond (1.550 vs. 1.507 Å). As in the case with $\mathbf{18}^{+\bullet}$, this species is a TS.

The results of the optimization of dispiro[2.0.2.2]octane (**4**) with the HF/6-31G* basis set are in good agreement with those obtained by the AM1 calculations and lead to a symmetric (C_{2v}) species. The C3-C4 bond is shorter (1.521 Å) than the C7-C8 bond (1.553 Å) and the dihedral angle C3-C4-C7-C8 is -0.1°. One-electron oxidation of **4** leads to a structure (**4a**$^{+\bullet}$) with both C1-C3 and C4-C5 bonds lengthened (1.728 Å). The energy difference between **4** and **4a**$^{+\bullet}$ is 183.4 kcal/mol, significantly less than the actual measured IP of 208.0 kcal/mol obtained from the photoelectron spectrum.[66b] Using the HOMO energy of **4** the IP is calculated to be 225.4 kcal/mol which is significantly higher than the experimental value (Table 2.5). The frequency analysis for species **4** gave one small negative frequency (-50.1566 cm^{-1}) indicating that this geometry might not be the absolute minimum. However, since small geometrical changes can result in large differences in the frequency analyses, we are confident that the geometry of **4** as presented here is likely to be very similar to that of the actual molecule.

A frequency analysis showed that **4a**$^{+\bullet}$ is a TS (one imaginary frequency); however, it is quite clear that this is not the expected species. The AM1 calculations did give a 'TS like' species (**4**$^{+\bullet}$) with an energy close to the value expected for this species. The fact that the *ab initio* calculations cannot reproduce this result could mean that upon ionization **4**$^{+\bullet}$ will relax to another species. However, from these results it is not clear what that species would be.

A number of reports concerning *cis*-dispiro[2.0.2.2]octane (**4**) have been published.[66b,73] Compound **4** has been studied using the Maximum Overlap Method,[73d] Consistent Force Field,[73i] MINDO/3 and *ab initio* (4-31G basis set) calculations;[66b]

however, geometrical parameters were only reported for the MINDO/3 calculations. Our results (both AM1 and *ab initio*) are quite different from those reported using the MINDO/3 program. All methods predict a planar cyclobutane ring; however, the central carbon-carbon bond (C3-C4) is, according to our calculations, a shorter bond (1.512 Å) than the C7-C8 bond (1.553 Å). MINDO/3 predicts a long C3-C4 bond (1.559 Å) and a short C7-C8 bond (1.516 Å). No structural (experimental) data have been reported for this compound; however, since both the AM1 and the *ab initio* calculations arrive at the same conclusion, we believe that these new numbers are more likely than those reported previously.

One type of interconversion involving compound **4** has been reported. It was shown that the thermal dimerization of **1** leads to the formation of **4**.[73] The radical cation has not been prepared or studied.

The results presented here show that ionization of **4** gives $\mathbf{4a}^{+\bullet}$, a species with two lengthened carbon-carbon bonds. It is not clear what the resulting species would be if these bonds were to break completely. The AM1 calculations on $\mathbf{13}^{+\bullet}$, a species with only one of these carbon-carbon bonds broken, show that it is a relatively stable species, i.e. no rearrangement took place upon optimizing this structure. Rearrangement of $\mathbf{4a}^{+\bullet}$ is unlikely to give any of the other species mentioned ($\mathbf{1+1}^{+\bullet}$, $\mathbf{1+1a}^{+\bullet}$, $\mathbf{2}^{+\bullet}$, $\mathbf{3}^{+\bullet}$, $\mathbf{5}^{+\bullet}$, $\mathbf{6}^{+\bullet}$, or $\mathbf{7}^{+\bullet}$) even though the energetics for most of these reactions are favourable. A rearrangement of this nature is probably too constraining for the radical cation.

Dispiro[2.1.2.1]octane (5).

The geometry optimization of *trans*-dispiro[2.1.2.1]octane (**5**) using AM1 leads to a symmetric species (D_{2h}) with a planar cyclobutane ring. The bonds in the cyclobutane ring are all 1.528 Å long; the bonds in the cyclopropane ring are 1.492 Å (C1-C3; C2-C3; C5-C6 and C5-C7) and 1.503 Å (C1-C2 and C6-C7) long. Ionization of **5** leads to cleavage of the C5-C7 bond ($\mathbf{20}^{+\bullet}$) in contrast to the *cis* compound (**4**) which gave a ring closed species ($\mathbf{4}^{+\bullet}$). The energy difference between **5** and $\mathbf{20}^{+\bullet}$ is 195.3 kcal/mol, significantly less than the reported (vertical) IP (212.4 kcal/mol; 9.2 eV) (Table 2.5).[66b] Ring opening of $\mathbf{4}^{+\bullet}$ to give $\mathbf{13}^{+\bullet}$ is an exothermic process ($\Delta E = -19.4$ kcal/mol). Using the same value for the ring opening of $\mathbf{5}^{+\bullet}$ to $\mathbf{20}^{+\bullet}$, we can propose a ring closed structure (a transition state: $\mathbf{5}^{+\bullet}$) with an energy of ca. 214.7 kcal/mol. This, indeed, is very close to the experimentally observed vertical IP. The spin in $\mathbf{20}^{+\bullet}$ is localized on C7; the charge is delocalized over the molecule. Ionization does not lead to a distortion of the planar cyclobutane ring. The distance between C5 and C7 in $\mathbf{20}^{+\bullet}$ is 2.461 Å.

Other possibilities for bond breaking in $\mathbf{5}^{+\bullet}$ are the C6-C7 bond and the C4-C5 bond. Optimization of the structure where the C6-C7 bond was broken ($\mathbf{21}^{+\bullet}$) again leads to a rearrangement ($\mathbf{22}^{+\bullet}$). A five membered ring is formed by making a new bond between C4 and C6, and breaking the C4-C5 bond. This species has a low energy compared to $\mathbf{20}^{+\bullet}$ ($\Delta E = -32.5$ kcal/mol). It is interesting to note that the neutral alkene (**22**) was observed as a side product in the metal-catalyzed dimerization of **5** from **1**.[73g,74b]

Structure $23^{+\bullet}$ is obtained after breaking the bond C4-C5 in $5^{+\bullet}$. This species has an energy which is higher than $20^{+\bullet}$, indicating the difficulty of breaking this bond. A frequency analysis showed that this species is a minimum.

Based on the *ab initio* results, **5** is a symmetric (D_{2h}) species with (again) a planar cyclobutane ring, in good agreement with the results from the AM1 calculations. Ionization of **5** leads to a species with a long C6-C7 bond (1.844 Å), a species similar to $21^{+\bullet}$ rather than the expected TS $5^{+\bullet}$. The energy difference between **5** and $21^{+\bullet}$ is 205.9 kcal/mol, close to the measured IP of **5** (212.4 kcal/mol).[66b] Using the HOMO energy of **5** again leads to a much higher IP (234.5 kcal/mol) than the measured value. Similar to species **4**, the frequency analysis on **5** gives one small negative frequency (-13.7222 cm^{-1}). The spin and charge are localized on carbons 6 and 7: each carbon has 35% of the total charge density and 55% of the (positive) spin density. Other changes with respect to the neutral compound are minimal. The cyclobutane ring in $21^{+\bullet}$ remains planar. In contrast to the AM1 results, no rearrangement to $22^{+\bullet}$ was indicated. Compound $21^{+\bullet}$ is a TS (one imaginary frequency), however, it was not determined whether $22^{+\bullet}$ results directly from $21^{+\bullet}$.

trans-Dispiro[2.1.2.1]octane (**5**) has been studied previously with MINDO/3[66b] and both our AM1 and *ab initio* results are in reasonable agreement with those reported earlier. Similar to compound **4**, compound **5** can be obtained from **1** by catalytic dimerization.[73]

The calculations presented here show that isomerizations involving the radical cation ($\mathbf{5}^{+\bullet}$) are energetically favourable (similar to $\mathbf{4a}^{+\bullet}$); however, due to geometrical constraints are unlikely to happen.

Dimerization of methylenecyclopropane radical cation.

From the results described above it is clear that relatively few of the possible interconversions might actually occur. The (dimerization) reactions of MCP radical cation ($\mathbf{1}^{+\bullet}$) or TMM radical cation ($\mathbf{1a}^{+\bullet}$) with its neutral precursor (**1**) to give any of the dimeric radical cations are all exothermic and therefore most likely to occur. However, besides the energetics of these reactions, the orientations of the reactants will be important in determining which of the possible products will eventually be formed.

The dimerization of MCP radical cation ($\mathbf{1}^{+\bullet}$) with its neutral precursor (**1**) was studied using four different starting orientations ($\mathbf{24}^{+\bullet}$ - $\mathbf{27}^{+\bullet}$; Figure 2.4a). The same starting orientations were used for the study on the dimerization of TMM radical cation ($\mathbf{1a}^{+\bullet}$) with **1** ($\mathbf{28}^{+\bullet}$ - $\mathbf{31}^{+\bullet}$; Figure 2.4b). In every case the initial distance between the two reactants was 4 Å. No constraints were imposed and a full optimization at the HF/6-31G* level of theory was carried out in order to see whether bonding would occur and, if so, how it would occur.

The energies of the final structures are given in Table 2.6. For reference the values of the energies of ($\mathbf{1}+\mathbf{1}^{+\bullet}$) and ($\mathbf{1}+\mathbf{1a}^{+\bullet}$) are also given. The spin and charge densities are shown in Table 2.7. Selected bond lengths, bond angles, and dihedral angles can be found in Table 2.18 (Appendix I). In five cases ($\mathbf{24}^{+\bullet}$, $\mathbf{25}^{+\bullet}$, $\mathbf{28}^{+\bullet}$, $\mathbf{29}^{+\bullet}$, and $\mathbf{31}^{+\bullet}$) bonding

a

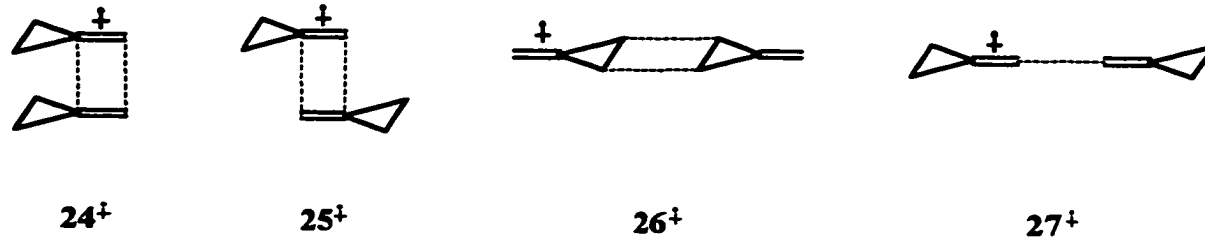

$24^{\ddagger}$ $25^{\ddagger}$ $26^{\ddagger}$ $27^{\ddagger}$

b

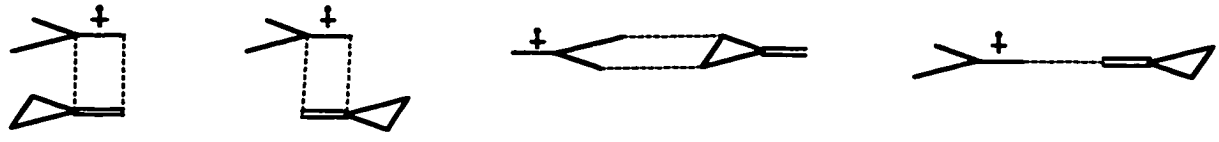

$28^{\ddagger}$ $29^{\ddagger}$ $30^{\ddagger}$ $31^{\ddagger}$

Figure 2.4. Orientations studied in the dimerization of **1** and $\mathbf{1}^{+\bullet}$ (a). Orientations studied in the dimerization of **1** and $\mathbf{1a}^{+\bullet}$ (b).

between the two species was observed (Figure 2.5). All final structures were shown to be minima. It is clear from Table 2.6 that in every case, except $\mathbf{27}^{+\bullet}$, the energy of the final structure is lower than the summed energy of the two separate molecules, indicating that even in the non-bonded cases some stabilizing interaction is taking place. These non-bonded species are referred to as complexes.

The final structure starting with $\mathbf{24}^{+\bullet}$ is bonded between C4 and C5 (Figure 2.5). Both cyclopropane rings remain intact which contributes to the relatively high energy of this species (Table 2.6). Another destabilizing factor is the deformation at C1: the dihedral angle C1-C2-C3-C4 is 121.5° instead of the expected 180°. The spin density is largely localized on C1 which could explain this deformation. The charge is delocalized over C5,

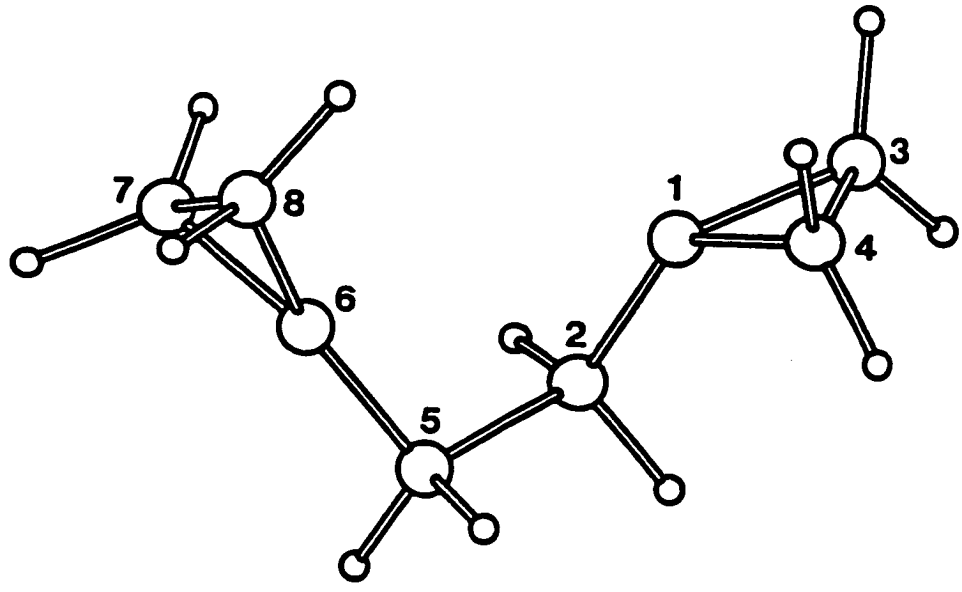

24

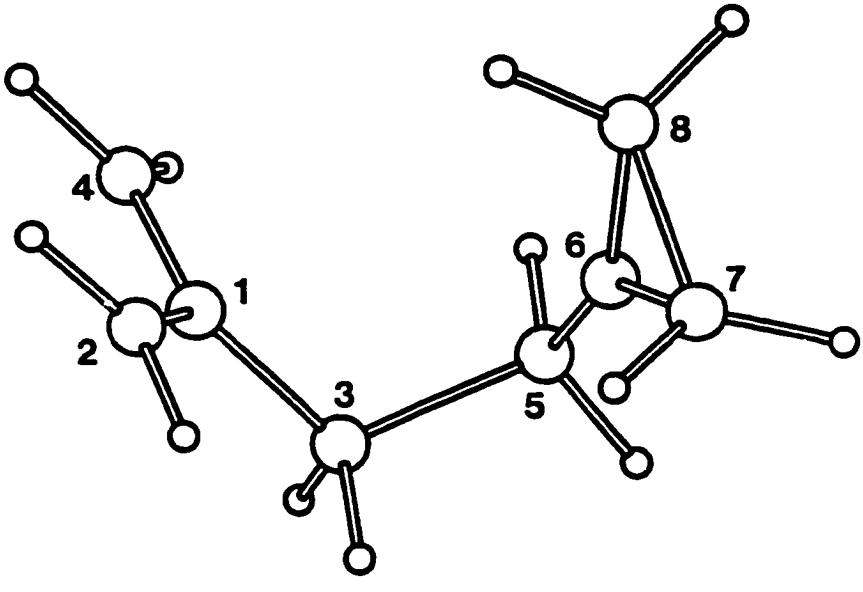

25

Figure 2.5. Optimized geometries ($24^{+\bullet}$ - $31^{+\bullet}$) from the dimerizations of **1** with $\mathbf{1}^{+\bullet}$, and **1** with $\mathbf{1a}^{+\bullet}$.

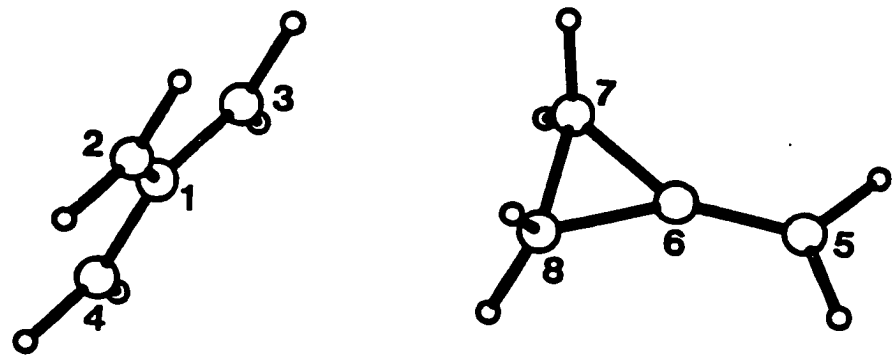

26

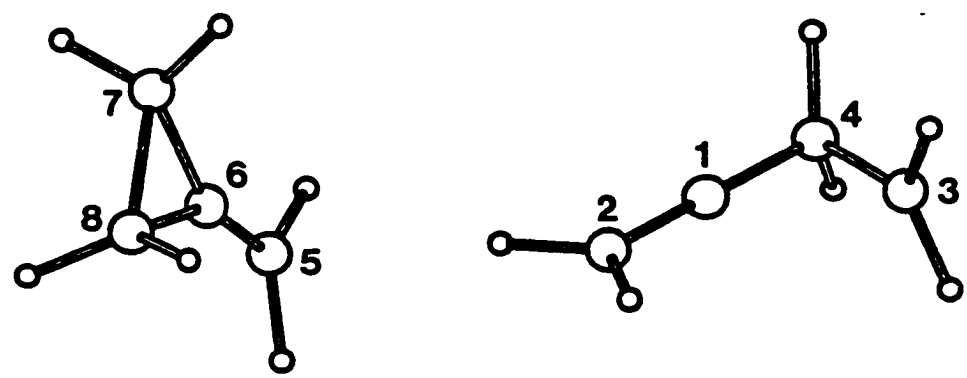

27

Figure 2.5. Optimized geometries ($24^{+\bullet}$ - $31^{+\bullet}$) from the dimerizations of 1 with $1^{+\bullet}$, and 1 with $\mathbf{1a}^{+\bullet}$ (cont.).

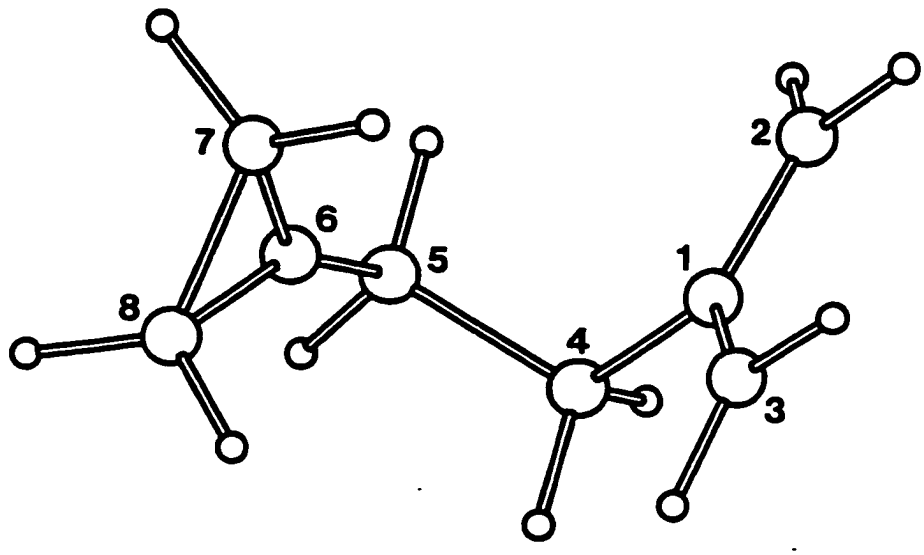

28

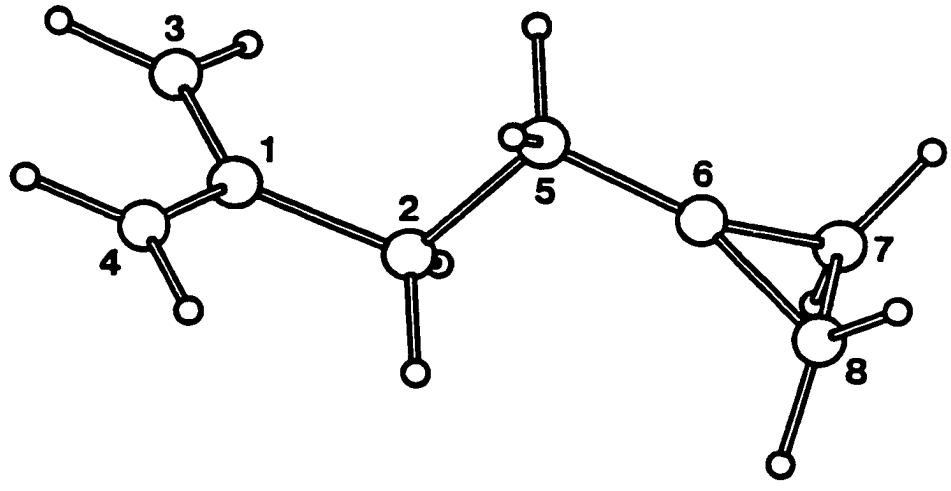

29

Figure 2.5. Optimized geometries ($24^{+\bullet}$ - $31^{+\bullet}$) from the dimerizations of **1** with $\mathbf{1}^{+\bullet}$, and **1** with $\mathbf{1a}^{+\bullet}$ (cont.).

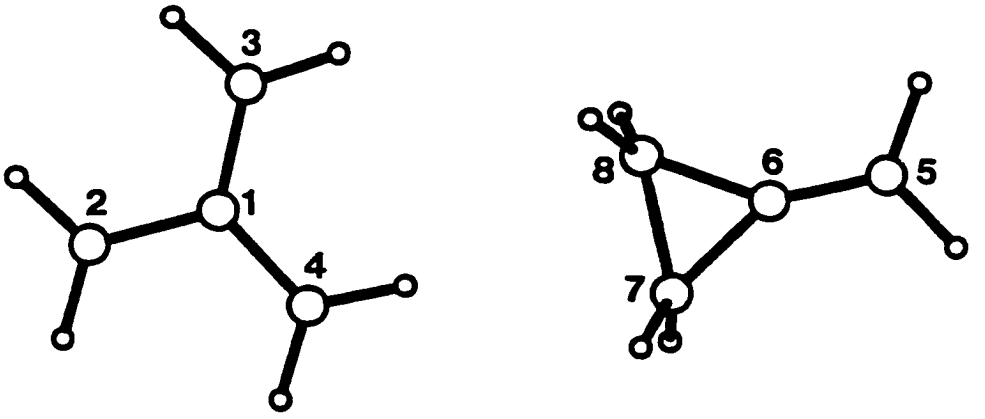

30

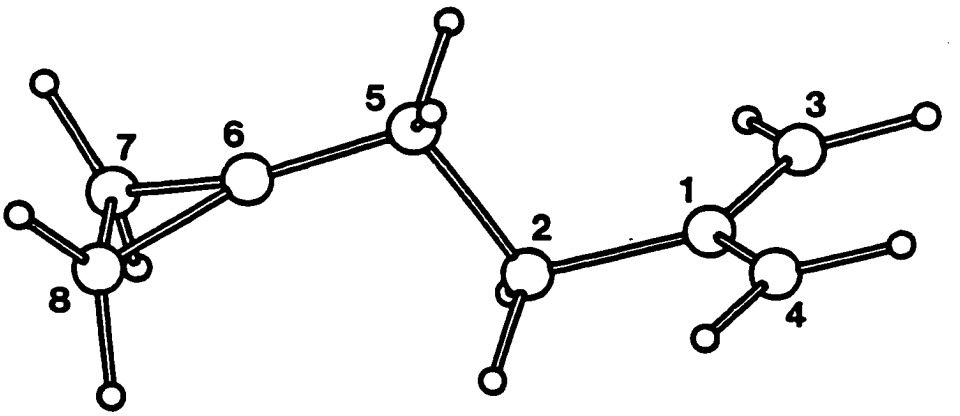

31

Figure 2.5. Optimized geometries ($24^{+\bullet}$ - $31^{+\bullet}$) from the dimerizations of 1 with $1^{+\bullet}$, and 1 with $\mathbf{1a}^{+\bullet}$ (cont.).

Table 2.6 Calculated energies (*ab initio*) for the dimerization of **1** with $\mathbf{1}^{+\bullet}$ and of **1** with $\mathbf{1a}^{+\bullet}$.

species	UHF/6-31G*[a]	MP2/6-31G*[a]	$E_{relative}$[b]
$\mathbf{24}^{+\bullet}$	-309.51453	-310.49442	24.5
$\mathbf{25}^{+\bullet}$	-309.57468	-310.53344	0.0
$\mathbf{26}^{+\bullet}$	-309.50485	-310.47250	38.2
$\mathbf{27}^{+\bullet}$	-309.48347	-310.45996	46.1
$\mathbf{28}^{+\bullet}$	-309.57468	-310.53344	0.0
$\mathbf{29}^{+\bullet}$	-309.57416	-310.53295	0.3
$\mathbf{30}^{+\bullet}$	-309.52651	-310.47358	37.6
$\mathbf{31}^{+\bullet}$	-309.57415	-310.53295	0.3
$\mathbf{1+1}^{+\bullet}$	-309.46708	-310.44173	57.5
$\mathbf{1+1a}^{+\bullet}$	-309.50122	-310.46482	43.1

[a] Energies reported are in atomic units (1 a.u. ≡ 627.5 kcal/mol) and, in case of open-shell species, are corrected for spin contamination; [b] relative energies in kcal/mol

C6, C7, and C8. The dihedral angle C1-C2-C5-C6 is 58.0° and the distance between C1 and C6 is 2.884 Å.

Starting with orientation $\mathbf{25}^{+\bullet}$ gives a final structure which resembles $\mathbf{15}^{+\bullet}$ (Figure 2.5). Bonding has taken place between C3 and C5. This structure is also quite similar to $\mathbf{24}^{+\bullet}$ except for the fact that in one of the cyclopropane rings a carbon-carbon bond was cleaved. Consequently, both dihedral angles (C1-C2-C3-C4 and C5-C6-C7-C8) are close to 180°. The spin is almost completely localized on C2 and C4; the charge is distributed over C5-C6-C7-C8. The dihedral angle C1-C3-C5-C6 is 59.8° (*gauche*) and the distance C1-C6 is 2.968 Å, values very close to those observed in $\mathbf{24}^{+\bullet}$. However, structure $\mathbf{25}^{+\bullet}$ is 24.5 kcal/mol lower in energy than $\mathbf{24}^{+\bullet}$ (MP2/6-31G*//HF/6-31G*; Table 2.6).

No bonding is observed starting with $\mathbf{26}^{+\bullet}$ (Figure 2.5). In this complex, one of the MCP units does undergo ring opening to give the TMM radical cation ($\mathbf{1a}^{+\bullet}$). Both spin and charge are largely localized on this ring opened species: C3 and C4 carry ca. 80% of

Table 2.7. Calculated (HF/6-31G*) spin and charge densities of the dimeric radical cations.[a]

species		atom no. 1	2	3	4	5	6	7	8
24$^{+\bullet}$	charge	-0.004	0.096	0.059	0.027	0.103	0.370	0.179	0.170
	spin	1.099	-0.030	-0.046	-0.033	0.006	0.001	0.004	0.000
25$^{+\bullet}$	charge	0.064	0.000	0.093	0.031	0.093	0.375	0.180	0.165
	spin	-0.777	0.854	0.061	0.883	-0.021	0.000	0.001	0.000
26$^{+\bullet}$	charge	0.021	0.132	0.424	0.407	-0.027	0.147	-0.065	-0.040
	spin	-0.277	0.998	0.184	0.094	-0.001	0.002	-0.001	0.000
27$^{+\bullet}$	charge	0.253	0.168	0.280	0.259	-0.125	0.127	0.017	0.020
	spin	0.624	-0.249	0.760	-0.138	-0.006	0.009	-0.001	-0.001
28$^{+\bullet}$	charge	0.064	0.031	-0.001	0.093	0.093	0.375	0.165	0.180
	spin	-0.777	0.883	0.854	0.061	-0.021	0.000	0.001	0.001
29$^{+\bullet}$	charge	0.095	0.048	0.025	0.025	0.110	0.353	0.172	0.172
	spin	-0.782	0.072	0.873	0.873	-0.018	-0.021	0.001	0.001
30$^{+\bullet}$	charge	0.103	0.445	0.216	0.227	-0.043	0.140	-0.061	-0.026
	spin	-0.242	-0.413	0.838	0.817	0.001	-0.002	0.000	0.000
31$^{+\bullet}$	charge	0.095	0.047	0.025	0.025	0.110	0.353	0.172	0.172
	spin	-0.782	0.072	0.873	0.873	-0.018	-0.021	0.001	0.002

[a] Hydrogen atoms are summed with carbon atoms.

the positive charge density; C2 has essentially all the spin. The distance between the two moieties is ca. 3 Å (C3-C8: 3.342 Å; C3-C7: 3.252 Å). The bond lengths and bond angles in the TMM radical cation unit in **26**$^{+\bullet}$ are different from those in **1a**$^{+\bullet}$: C1-C2: 1.453 Å; C1-C3: 1.389 Å; C1-C4: 1.381 Å; C3-C1-C4: 114.0°. The total energy of **26**$^{+\bullet}$ is 38.2 kcal/mol higher than **25**$^{+\bullet}$ but still 4.8 kcal/mol more stable than the summed energies of **1** and **1a**$^{+\bullet}$. A frequency analysis of this complex indicates that it is a minimum.

The resulting structure from **27**$^{+\bullet}$(Figure 2.5) is also a non-bonded configuration (complex). In this case, however, the C1-C3 bond is partially broken (1.933 Å) giving rise

to an allene type radical cation (C2-C1-C4: 179.2°). Spin and charge are on the ring opened moiety: C1 and C3 have a large positive spin density (62 and 76% respectively); 96% of the charge is equally divided over C1-C2-C3-C4. The distance between the moieties is ca. 3.5 Å and the energy is, as expected, the highest in this series: 46.1 kcal/mol higher than $\mathbf{25}^{+\bullet}$ (Table 2.6). This type of bond cleavage seems highly unlikely;[74] however, optimization of the sub unit with an elongated C1-C3 bond at the HF/6-31G* level gave essentially the same structure. A frequency analysis showed that this species is a minimum. The energy (MP2/6-31G*//HF/6-31G*) of this species is only 9.1 kcal/mol higher than $\mathbf{1a}^{+\bullet}$ so this cleavage is not as unfavourable as it seemed at first.

The final structure from $\mathbf{28}^{+\bullet}$ is the same as the one obtained from $\mathbf{25}^{+\bullet}$ (Table 2.6; Figure 2.5). Bonding has taken place between C4 and C5.

The structure resulting from $\mathbf{29}^{+\bullet}$ (Figure 2.5) can be compared to $\mathbf{25}^{+\bullet}$ (and $\mathbf{28}^{+\bullet}$) as can $\mathbf{6}^{+\bullet}$ to $\mathbf{7}^{+\bullet}$, and $\mathbf{16}^{+\bullet}$ to $\mathbf{17}^{+\bullet}$, i.e. these species are conformers (*gauche* and *anti*). The energy difference between $\mathbf{29}^{+\bullet}$ and $\mathbf{25}^{+\bullet}$ is only 0.3 kcal/mol, indicating once again that in the gas phase the *gauche* conformer is more stable than the *anti* conformer. A new bond is formed between C2 and C5 giving a molecule with the spin localized on C3 and C4 and the charge largely distributed over C5-C6-C7-C8.

The non-bonded complex $\mathbf{30}^{+\bullet}$ (Figure 2.5) consists of a ring closed MCP unit and a ring opened TMM unit. The geometry of this complex is similar to that of $\mathbf{26}^{+\bullet}$ but has a lower energy (Table 2.6). The TMM unit carries most of the spin and charge (as in $\mathbf{26}^{+\bullet}$) but the bond lengths, bond angles and spin distribution are different again from those in $\mathbf{26}^{+\bullet}$ and $\mathbf{1a}^{+\bullet}$. The units remain ca. 4 Å apart.

Optimization of **31**$^{+\bullet}$ leads to a bonded (between C2 and C5) structure equivalent to that of **29**$^{+\bullet}$ (Table 2.6; Figure 2.5).

The results decribed above show that of the eight starting geometries considered only five gave a product in which a new carbon-carbon bond was formed. As can be seen from Figure 2.5, none of the expected products were observed. Four of the five products (**25**$^{+\bullet}$, **28**$^{+\bullet}$, **29**$^{+\bullet}$, and **31**$^{+\bullet}$) are conformers of the same species, the difference being the orientation around the single (C2-C5, C3-C5 or C4-C5) bond: the products from **25**$^{+\bullet}$ and **28**$^{+\bullet}$ have the *gauche* orientation while those from **29**$^{+\bullet}$ and **31**$^{+\bullet}$ have the *anti* orientation. The *anti* conformer is of slightly higher energy than the *gauche* conformer (0.3 kcal/mol) indicating that there is some form of attractive interaction between the orbitals in the *gauche* form that helps stabilize this conformation. The *gauche* conformer was also observed after breaking the C1-C2 bond in **4**$^{+\bullet}$ (giving rise to **15**$^{+\bullet}$) using AM1. This species is of much higher energy (12-18 kcal/mol) than **6**$^{+\bullet}$ or **7**$^{+\bullet}$ (which have both cyclopropane rings opened), indicating that the barrier for ring opening to give a doubly allylic system is high. This was also observed with the AM1 calculations on **16**$^{+\bullet}$ and **17**$^{+\bullet}$; ring opening of the two cyclopropyl groups (to give **6**$^{+\bullet}$ and **7**$^{+\bullet}$) was calculated to be exothermic by ca. 40 kcal/mol but, due to the high barrier, did not occur.

The fact that no cyclization product was observed could be due to the fact that these calculations simulate gas phase conditions. Studying the dimerization of **1** with **1**$^{+\bullet}$ or **1a**$^{+\bullet}$ in the gas phase (*e.g.* mass spectrometry) will most likely give products such as **25**$^{+\bullet}$, **28**$^{+\bullet}$, **29**$^{+\bullet}$, or **31**$^{+\bullet}$. It is interesting to learn that the *gauche* conformations (**25**$^{+\bullet}$ and **28**$^{+\bullet}$) are more stable in the gas phase than the *anti* conformations (**29**$^{+\bullet}$ and **31**$^{+\bullet}$). The

gauche conformations more closely resemble the cyclized dimers than do the *anti* conformations. Experiments in the liquid phase (polar solvent) will not only change the relative energies of the species but will also have a significant influence on the structures of the compounds when these have a large dipole moment. The dipole moments of the bonded dimeric species are 4.88 D for the *gauche* conformer and 6.80 D for the *anti* conformer. Including solvent interactions might therefore have a significant effect on the structures of these dimeric radical cations.

2.4 Conclusions

The effects of ionization of compounds **1-5**, have been examined using semi-empirical (AM1) and *ab initio* (MP2/6-31G*//HF/6-31G*) methods. Special attention was given to the possible isomerization and rearrangement of the radical cations as well as the ion-molecule reactions of methylenecyclopropane radical cation ($\mathbf{1}^{+\bullet}$ or $\mathbf{1a}^{+\bullet}$) with its neutral precursor (**1**). This study has shown that several interconversions are energetically favourable but, due to geometrical constraints, are unlikely to take place. Some rearrangements seem to occur 'spontaneously'; in these cases no transition state was found. The reaction of **1** with $\mathbf{1}^{+\bullet}$ or with $\mathbf{1a}^{+\bullet}$ (to give $\mathbf{2}^{+\bullet}$, $\mathbf{3}^{+\bullet}$, $\mathbf{4}^{+\bullet}$, $\mathbf{5}^{+\bullet}$, or species derived from these radical cations) was found to be the most exothermic interconversion. Further consideration of this dimerization reaction has shown that, in the gas phase, only one type of dimer can be expected. It must be emphasized that electron-transfer reactions (chemical, photochemical, or electrochemical) are usually carried out in the liquid phase using polar solvent. The energy of solvation associated with these radical ions may alter

the order of stability of the species relevant to the gas phase calculated here. For example, in solution the radical cation of 1,1-diphenyl-2-methoxyethane undergoes carbon-carbon bond cleavage to give the diphenylmethyl radical and the methoxymethyl cation.[75] However, the mass spectrum of 1,1-diphenyl-2-methoxyethane has a base peak at m/z 167 showing that in the gas phase formation of the diphenylmethyl cation is preferred. Performing calculations with the molecules enclosed in a solvent cage should allow more realistic predictions for the experiments carried out in solution. Studies in the gas phase (e.g. mass spectrometry) should give results that can be explained on the basis of the calculations reported here. Also, results from matrix isolation techniques are usually considered as being on the isolated species, without significant solvent interaction and gas phase calculational results have been very useful in these cases as well.[5,6,53d,56a,58i]

Chapter 3

Photoinduced electron transfer and electrochemical oxidation of 1,4-bis(methylene)cyclohexane

3.1 Introduction

In the previous Chapter the possible interconversions and rearrangements of some $C_4H_6^{+\bullet}$ and $C_8H_{12}^{+\bullet}$ radical cations (Figure 3.1) were investigated with *ab initio* molecular orbital calculations.[76a]

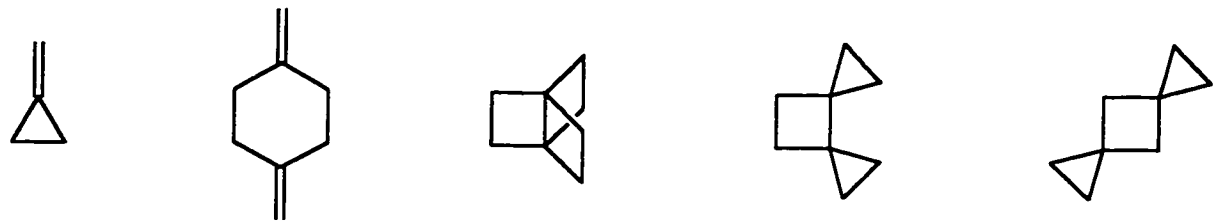

1 2 3 4 5

Figure 3.1. Molecules of interest studied by *ab initio* molecular orbital calculations

It was shown that some interconversions are energetically favourable and several of these radical cations are expected to undergo spontaneous rearrangements and/or bond cleavage. Some of the reaction pathways of these five isomeric species are briefly indicated in Scheme 3.1 (relative energies of the species given in kcal/mol).

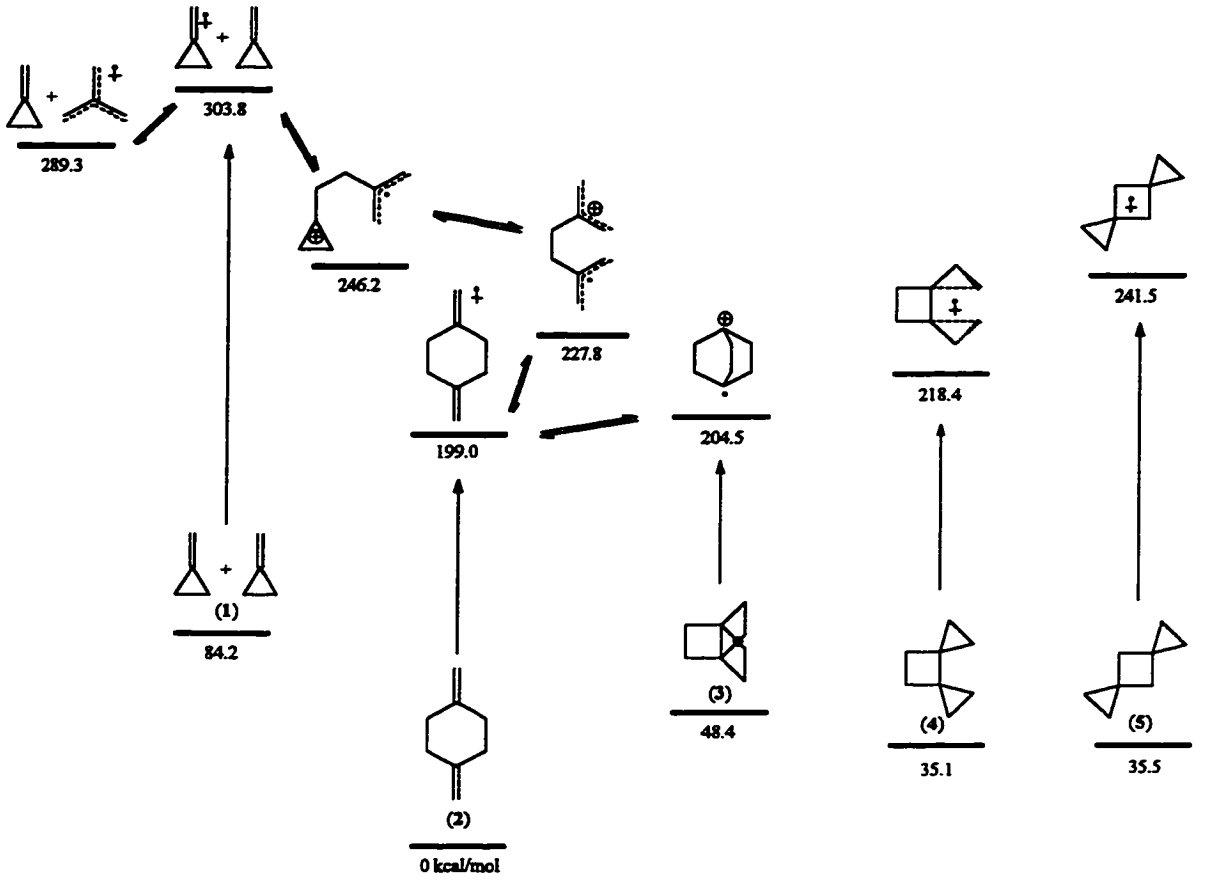

Scheme 3.1. Energetics of selected interconversion and rearrangement of C_4H_6 and C_8H_{12} radical cations as calculated by *ab initio* molecular orbital calculations.

The long range objective of this study is to understand the mechanisms for the interconversion and rearrangement of these $C_8H_{12}^{+\bullet}$ radical cations. The most stable of these structures is the 1,4-bis(methylene)cyclohexane radical cation ($\mathbf{2}^{+\bullet}$). Note, however, that the [2.2.2]propellane radical cation ($\mathbf{3}^{+\bullet}$) is only 5 kcal/mol higher in energy. The most exothermic reactions are those combining methylenecyclopropane (**1**) with its radical cation ($\mathbf{1}^{+\bullet}$) or with trimethylenemethane radical cation ($\mathbf{1a}^{+\bullet}$). The calculations, relevant to the gas phase, identified only one type of dimeric radical cation.

Relevant experimental work has been limited and there are no reports involving the reactivity of these radical cations. Most of the previous work has focussed on [2.2.2]propellane (**3**).[72] The parent molecule has never been isolated but the synthesis of a substituted propellane (2-(*N*,*N*-dimethylcarboxamide)tricyclo[2.2.2.$0^{1,4}$]octane) was reported.[72a] In one of the attempts to synthesize **3**, **2** was used as the starting material.[72c] However, the 1,4-diradical (**32**) is also a minimum on the potential energy surface,[71] and the barrier between **3** and **32** is small which leads to a rapid cleavage back to **2** (Scheme 3.2).[71h]

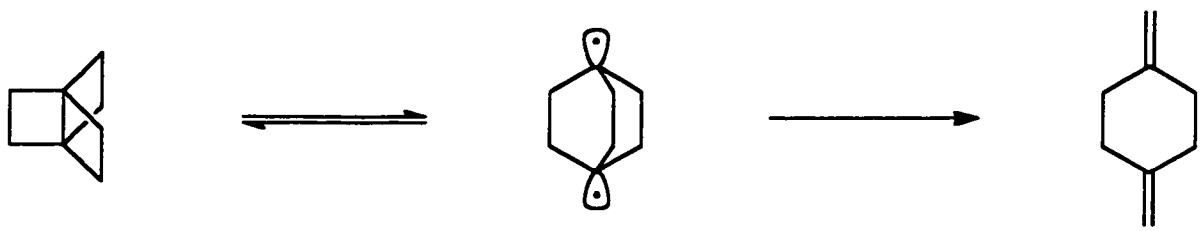

3 **32** **2**

Scheme 3.2. Rearrangement of tricyclo[2.2.2.$0^{1,4}$]octane to 1,4-bis(methylene)cyclohexane through the 1,4-diradical intermediate.

Reaction of triplet **1** ($\mathbf{1}^t$) with $\mathbf{1}^t$ results in the formation of **2** since $\mathbf{1}^t$ has no other favourable decay mechanism.[67] Thermal dimerization of **1** results in the formation of **4**,[73b,c] whereas **5** can be formed by the metal-catalyzed dimerization.[73b,c,g,h]

As discussed in Chapter 1, in the presence of a nucleophile, radical cations usually undergo rapid nucleophilic addition.[21,44,52] Under standard conditions for the photochemical nucleophile-olefin combination, aromatic substitution (photo-NOCAS) reaction, methanol is present and acts as the nucleophile; the 1:1:1 adduct (olefin-

nucleophile-aromatic) is usually the major product.[52] In the absence of a nucleophile other processes take place.[48,77] For example, when a radical cation is oriented properly, cyclization can occur,[26,47-51] usually in competition with other reactions. Cyclized products were observed in the photo-NOCAS reaction of 2,5-dimethyl-1,5-hexadiene (**35**),[48] 2,6-dimethyl-1,6-heptadiene,[49] 6-methyl-5-hepten-2-ol and 5-methyl-5-hexen-2-ol,[50] and (R)-(+)-α-terpineol.[51] It is interesting to note that 1,5-hexadiene (**36**) does not give cyclized products upon irradiation in the presence of 1,4-dicyanobenzene (**33**, electron acceptor) and biphenyl (**34**, codonor) in acetonitrile or in acetonitrile-methanol mixtures.[48] However, in the radiolytic oxidation of **36** in a CF_3CCl_3 matrix the cyclized radical cation ($37^{+\bullet}$) was observed.[78] This species then rearranged to give the cyclohexene radical cation ($38^{+\bullet}$) upon photobleaching or annealing of the matrix (Scheme 3.3).

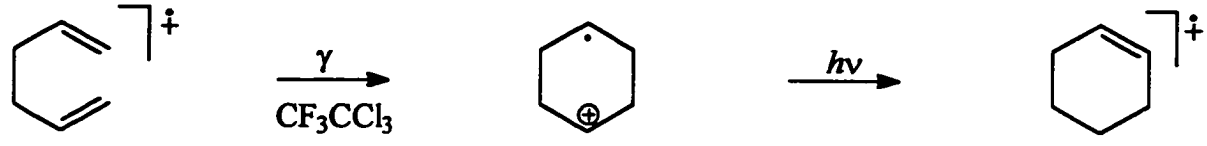

36$^{+\bullet}$ **37**$^{+\bullet}$ **38**$^{+\bullet}$

Scheme 3.3. Rearrangement of 1,5-hexadiene radical cation to cyclohexene radical cation observed upon radiolytic irradiation.

Under similar radiolytic conditions the cyclized product from 2,5-dimethyl-1,5-hexadiene radical cation ($35^{+\bullet}$), *trans*-3,6-dimethylcyclohexene radical cation ($39^{+\bullet}$), was observed.[79] However, the products from the photo-NOCAS reaction of **35** clearly indicate that $35^{+\bullet}$ cyclizes to $40^{+\bullet}$(Scheme 3.4).[48] No rearrangement was observed under these

conditions.

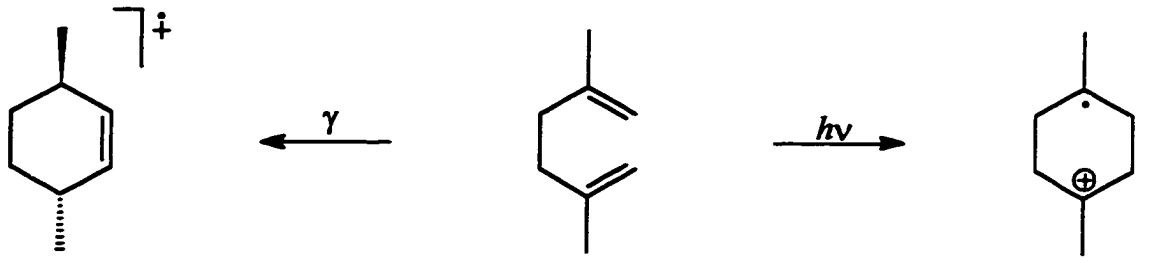

39$^{+\bullet}$ **35** **40**$^{+\bullet}$

Scheme 3.4. Rearrangements of the radical cation of 2,5-dimethyl-1,5-hexadiene observed upon photoinduced electron transfer (*hυ)* or radiolytic irradiation (γ).

From these results it is clear that generation of an alkene radical cation can lead to a wide variety of reactions, depending on the circumstances (solvent, method of generation, etc.) In this Chapter, the reactivity of the most stable $C_8H_{12}^{+\bullet}$ isomer, the radical cation of 1,4-bis(methylene)cyclohexane (**2**$^{+\bullet}$), under four distinct reaction conditions is reported. The major products from the electrochemical anodic oxidation in acetonitrile solution with and without added nucleophile (methanol) have been identified, as well as the major products resulting from the photochemical electron transfer to the singlet excited state of 1,4-dicyanobenzene (**33**) in the presence and absence of a nucleophile (methanol). Several interesting (unexpected) products were formed and the possible mechanisms for the formation of these products are discussed.[76b]

This work provides the foundation for the next phase of the continuing study; that is, subjecting the higher energy species to these same reaction conditions.

3.2 Results and Discussion

Photoinduced electron transfer of 1,4-bis(methylene)cyclohexane (2) in the presence of a nucleophile.

1,4-Bis(methylene)cyclohexane (**2**) reacts under photo-NOCAS conditions to give two products in low yields (Reaction [3.1]): the 1:1 (alkene-methanol) adduct 4-(methoxymethyl)-1-methylenecyclohexane (**41**) and the 1:1:1 (alkene-methanol-aromatic) adduct 4-(4-cyanophenyl)-4-(methoxymethyl)-1-methylenecyclohexane (**42**).

Reaction [3.1]

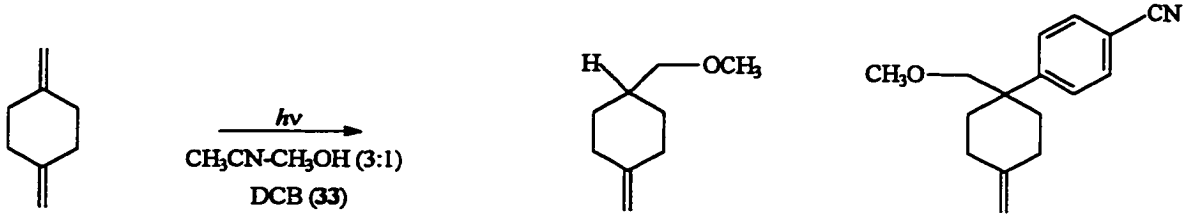

41 (3%) **42** (2%)

The progress of the reaction was followed by capillary column gas chromatography with either a flame ionization detector (gc/fid) or mass selective (gc/ms) detector. The ratio of the products did not change during the irradiation. Both products arise from methanol attack on the terminal end of the methylene group of the initially formed radical cation ($\mathbf{2}^{+\bullet}$) to form the (methoxymethyl)methylenecyclohexyl radical. The 1:1 (alkene-methanol) adduct, 4-(methoxymethyl)-1-methylenecyclohexane (**41**, m/z = 140), results from

reduction of this β-methoxy radical to the anion by **33**$^{-\bullet}$, followed by protonation. This mechanism was confirmed by performing the same experiment in acetonitrile-methanol-O-*d*. The mass spectrum of **41** obtained from this experiment showed a molecular ion at m/z 141. Reduction of the β-methoxy radical to the anion, followed by deuteration (by methanol-O-*d*) can account for this molecular ion ($C_9H_{15}DO$).

The (1:1:1) photo-NOCAS adduct, 4-(4-cyanophenyl)-4-(methoxymethyl)-1-methylenecyclohexane (**42**), is a result of a coupling of the β-methoxy radical with **39**$^{-\bullet}$, and subsequent loss of cyanide anion. These results are in good agreement with the mechanism proposed for the photo-NOCAS reaction.[52] Adduct (**42**) can be described as the *anti*-Markovnikov product.[52a] Attempts to detect the other regioisomer, the Markovnikov product, using gc/ms in the selected ion monitoring (sim) mode were unsuccessful; only one product with molecular weight 241 was formed. The photo-NOCAS reaction of the structurally related compound, isobutylene (2-methylpropene), gave two 1:1:1 adducts in a 26:1 ratio;[52c,d] the major product was the *anti*-Markovnikov regioisomer. The total yield in this reaction was 54%. Since the yields in Reaction [3.1] are low, it is possible that the Markovnikov regioisomer was formed below the detection limit. The spin and charge densities in **2**$^{+\bullet}$, calculated at the MP2/6-31G*//HF/6-31G* level of theory,[76] are almost equally distributed over both carbons of one of the methylene groups; solely based on this fact, one would expect some attack of the nucleophile on the tertiary carbon. This, however, would lead to a primary radical in contrast to attack on the terminal carbon which results in the formation of a tertiary radical. Obviously, radical stability is important.[52i]

The low yields and efficiency of this reaction are understandable in view of the relatively high oxidation potential of **2** (2.49 V vs. sce; Table 3.1) which influences the rate of electron transfer. The initial electron transfer will occur at the diffusion controlled limit when the ΔG_{et} for the process is exergonic by more than 5 kcal/mol.[15] The ΔG_{et} can be calculated using the Weller equation (Equation (3.1)):[15]

$$\Delta G_{et} = F[E_{1/2}^{ox}(D) - E_{1/2}^{red}(A) - e/\varepsilon\alpha] - E_{0,0}(A) \qquad (3.1)$$

The oxidation potentials and calculated ΔG_{et} values for several compounds are given in Table 3.1. For **2** the rate of electron transfer will be close to the diffusion controlled limit.

Adding biphenyl (**34**) to the reaction mixture is known to increase both the yield and the efficiency of the photo-NOCAS reaction.[52] This could, in part, be due to the fact that addition of biphenyl to the reaction mixture leads to an enhanced absorbtion of the incident light. This would explain the fact that increased product yields are obtained with increasing biphenyl concentration. In the photo-NOCAS reaction of **2** the yields of **41** and **42** approximately doubled with a shorter irradiation time when **34** was used as the codonor. Other explanations for the role of **34** have been proposed as well. The explanation that is frequently used is that separation of the radical ion pair becomes more efficient since back electron transfer (BET) between $\mathbf{34}^{+\bullet}$ and $\mathbf{33}^{-\bullet}$ is slower because of the small reorganization energy for $\mathbf{34}^{+\bullet}$ going back to **34**. Reducing the BET prolongs the lifetime of the radical cation and this may lead to other (side) reactions such as cyclization.

Table 3.1. Oxidation potentials of selected compounds and the calculated free energy change (ΔG_{et}) for the electron transfer process involving the singlet excited state of 1,4-dicyanobenzene (**33**) as the electron acceptor and the alkene or diene as the electron donor.

Compound	$E_{1/2}^{ox}$ (V)[a]	ΔG_{et} (kcal/mol)[b]
2,5-Dimethyl-1,5-hexadiene (**35**)	2.60[c]	-0.7
1,4-Bis(methylene)cyclohexane (**2**)	2.49[d]	-3.2
2-Methylpropene	2.99[e]	+8.3

[a] see experimental for details; [b] based upon the Weller equation[15]: $E_{0,0}$ (**33**) 97.6 kcal/mol, $E_{1/2}^{red}$(**33**) -1.66 V, the Coulombic attraction term was taken to be 1.3 kcal/mol[52d]; [c] ref. 48; [d] this work; [e] ref. 52c

For example, when 2,5-dimethyl-1,5-hexadiene (**35**) was irradiated in the presence of **39** and **34**, both acyclic and cyclic products were observed whereas without the codonor (**34**) only acyclic products were formed.[48] The ratio of cyclic to acyclic product increased withincreasing biphenyl concentration. This ratio also increased with decreasing methanol concentration. The mode of cyclization was shown to be 1,6-*endo*-*endo*. Cyclization of **2**, which obviously has some structural similarities to **35**, could therefore give $\mathbf{3}^{+\bullet}$ (Scheme 3.5).

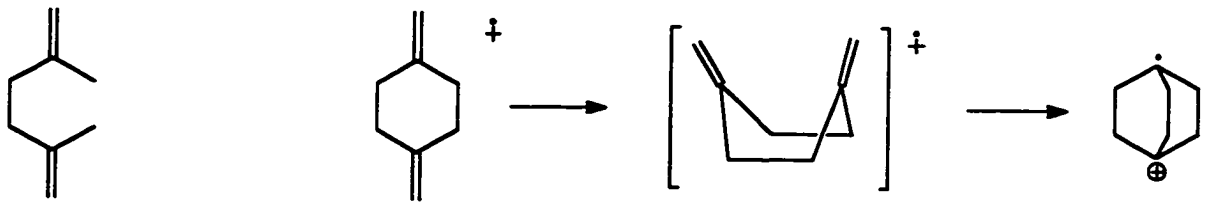

35 **2**$^{+\bullet}$ **3**$^{+\bullet}$

Scheme 3.5. Expected mode of cyclization for 1,4-bis(methylene)cyclohexane radical cation based on results of 2,5-dimethyl-1,5-hexadiene radical cation.

Table 3.2. Influence of the methanol concentration on the product ratio **41**:**42**.

$[CH_3OH]^a$	ratio **41**:**42**
6.0	1.0
3.6	1.0
1.2	0.8
0.5	0.8
0.25	0.5
0.1	0.3

[a] concentrations in mol L^{-1}; concentration of **34** in these experiments was 0.05 mol L^{-1}

Table 3.3. Influence of the biphenyl (**34**) concentration on the product ratio **41**:**42**.

[**34**][a]	ratio **41**:**42**
0.2	0.6
0.1	1.1
0.05	1.0

[a] concentrations in mol L^{-1}; methanol concentration in these experiments was 6.0 mol L^{-1}

Calculations have shown that $\mathbf{3}^{+\bullet}$ is only 5 kcal/mol higher in energy than $\mathbf{2}^{+\bullet}$.[76] It was, however, noted that cyclization of $\mathbf{2}^{+\bullet}$ would require a boat-like transition state which would further increase the reaction barrier by about 7 kcal/mol.[69,80] Experiments with **2** where the methanol concentration was lowered (0.1 - 6 M) and where the biphenyl concentration was increased (0.05 - 0.2 M) did not result in the formation of cyclized products. In all of these experiments only two products were formed: **41** and **42**. The ratio of these products (as determined by calibrated gc/fid) was dependent on the conditions used (Tables 3.2 and 3.3). Lowering the methanol concentration leads to increased amounts of the 1:1:1 adduct (**41**:**42** = 0.3 - 1.0). The same result is obtained when the biphenyl concentration is increased (**41**:**42** = 0.6 - 1.0). It must be noted that the relative yields of the products **41** and **42** are low and this could affect the calculated ratios.

However, the two product peaks were clearly visible (S/N > 100) and separated from other (minor) compounds and therefore the relative error will be small.

Small amounts of other products were detected and, based on the gc/ms data, these compounds are believed to be 1:1 (alkene-aromatic) adducts. When the biphenyl (**34**) concentration was increased products arising from **34** were also observed. These products, 2-cyanobiphenyl, 4-cyanobiphenyl, and 3,5-dimethoxy-4-phenylcyclohexane-carbonitrile, have been observed before.[48]

Photoinduced electron transfer of 1,4-bis(methylene)cyclohexane (2) in the absence of a nucleophile.

When the nucleophile, methanol, is omitted from the reaction mixture different products, derived from both **2** and **33**, are formed (Reaction [3.2]). Products derived from **33** include benzonitrile (**43**), 4-cyanotoluene (**44**), and 4-cyanoacetophenone (**45**). The cyclohexyl structure is found in spiro[(1-methylene)cyclohexane-4,3'-(2'methyl-4'-oxo)-1'-pyrroline] (**46**), 4-(4-cyanophenyl)-1-methylenecyclohexane (**47**), 2-(4-cyanophenyl)-1,4-bis(methylene)cyclohexane (**48**), bis(1'-methylenecyclohexane)-1,4',2,4'-cyclobutane (**49**), and 1-(4'-methylbenzene)-2-(1'-methylene-4'-cyclohexyl)ethane (**50**).

In the absence of a nucleophile the major products of this reaction are often 1:1 (alkene-aromatic) adducts. The mechanism for the formation of these products is believed to involve deprotonation of the alkene radical cation followed by coupling of the resulting allylic radical with the radical anion of **33** and subsequent loss of cyanide anion.

Reaction [3.2]

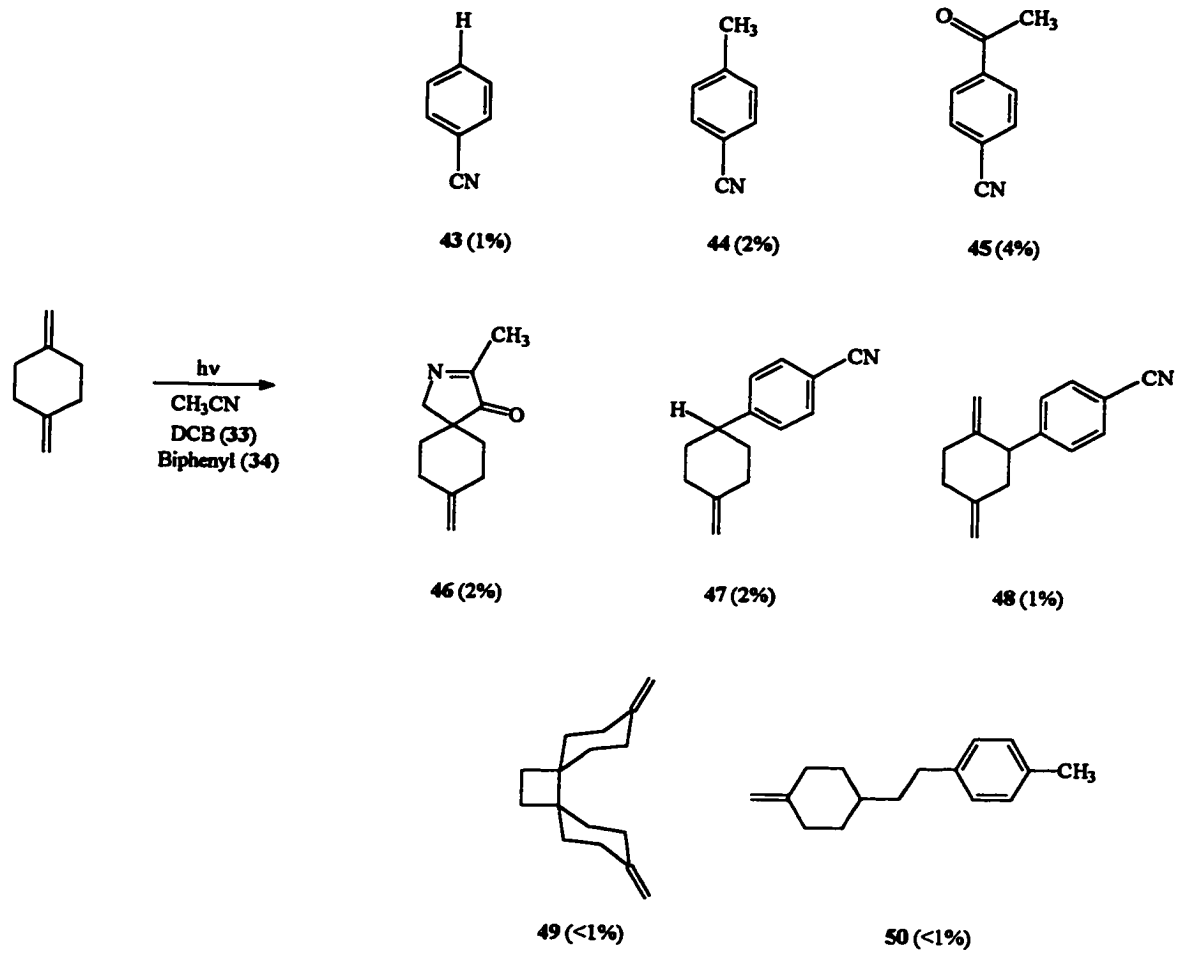

43 (1%) 44 (2%) 45 (4%)

46 (2%) 47 (2%) 48 (1%)

49 (<1%) 50 (<1%)

From **2**, two products (**49** and **51**) were expected; only one (**49**) was isolated from the reaction mixture. In the early stages of the irradiation, gc/ms analysis of the photolysate indicates that both 1:1 adducts were present. After prolonged irradiation only **49** remained. Compound **51** has a lower oxidation potential than **49** because of the internal double bond and will therefore be more reactive towards further oxidation than **49**. There is some evidence that this secondary reaction takes place. One of the products found in the reaction mixture is 4-cyanotoluene (**44**) which is likely to be the result of the *p*-

cyanobenzyl radical (**44**$^{\bullet}$). A hydrogen atom abstraction from a suitable donor or reduction by **33**$^{-\bullet}$ (to give the benzyl anion) followed by protonation would then give **44**. To verify this, the reaction was also carried out in CD_3CN. The mass spectrum of **44** indicates that deuterium was incorporated. It is unlikely that the benzyl radical abstracts a deuterium form acetonitrile, however reduction to the benzyl anion followed by deuteration (D-donor is D_2O; present in ca 10 mM concentration in CD_3CN) can explain the formation of **44-*d***. Also, analysis of the product mixture by gc/ms indicated the presence of a small amount of a product with a mass of (m/z) 232. Based on the mass spectrum of this compound we conclude that this is the coupling product of two *p*-cyanobenzyl radicals. The benzylic radical (**44**$^{\bullet}$) is thought to arise by deprotonation of **51**$^{+\bullet}$ (a result of electron transfer from **51** to **33***) leading to a conjugated diene which could then get further oxidized and undergo bond cleavage to give the *p*-cyanobenzyl radical (**44**$^{\bullet}$) (Scheme 3.6).

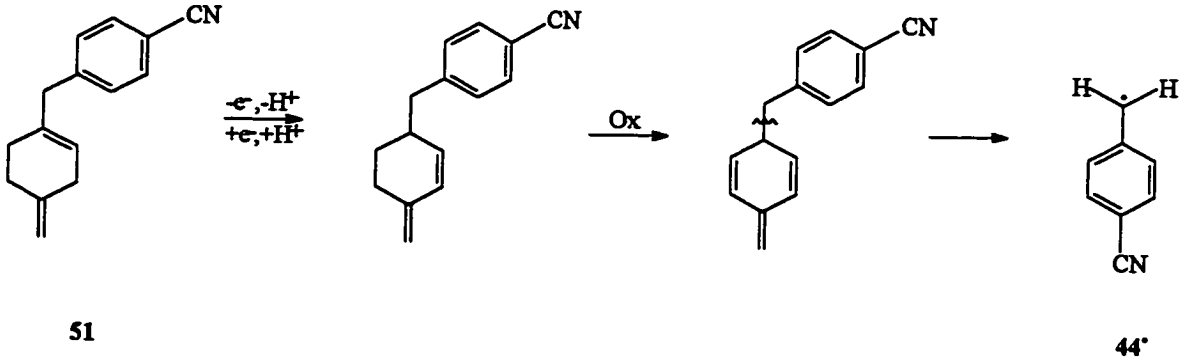

51 **44**$^{\bullet}$

Scheme 3.6. Possible route for the formation of *p*-cyanobenzyl radical.

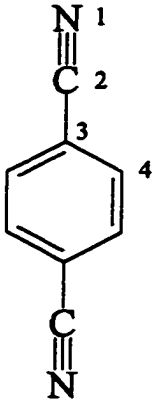

Table 3.4. Calculated (STO-3G) spin and charge densities for the radical anion of 1,4-dicyanobenzene ($33^{-\bullet}$)

atom[a]	spin density[b]	charge density[b]
1	+0.849	-0.296
2	-0.792	+0.022
3	+0.536	-0.084
4	-0.047	-0.071

[a] See Figure 3.2 for numbering of atoms. [b] Hydrogens summed with heavy atoms.

Figure 3.2. Atom numbering for the radical anion of 1,4-dicyanobenzene ($33^{-\bullet}$). See Table 3.4 for the calculated (STO-3G) spin and charge densities.

The formation of **43** and **45** could be explained on the basis of both radical and ionic mechanisms. In general the conditions will be relatively acidic due to deprotonation of the radical cation. Acetonitrile can serve as the base and reaction of protonated acetonitrile with **33** or $33^{-\bullet}$ would lead to the observed products. The calculated[52f] charge densities in $33^{-\bullet}$ show that the negative charge is mainly on the nitrogens and not on the *ipso* carbon (Figure 3.2; Table 3.4) and reaction between these two species would therefore not lead to the observed product. However, protonation of the two sites of high charge density (N1 and C2; Fig. 3.4) would not give any reaction whereas protonation of C3 would give a reaction! Even though protonation of C3 might be slower than protonation of N1 or C2, eventually this is the only process that will lead to products. This is a similar process to that of the photo-NOCAS reaction. Formation of the NOCAS products proceeds by coupling between the radical anion of the sensitizer ($33^{-\bullet}$) and the β-

alkoxy radical at the *ipso* position. It can be seen from Table 3.4 that the spin density on C3 (*ipso*) is much smaller than that on C2 and N1, yet only products from reaction at C3 are observed. The explanation for this observation is similar to one given above.

A radical mechanism is likely to involve *p*-cyanophenyl radical. The formation of this species is most likely a complex process and **not** just a simple loss of CN^- from $\mathbf{33}^{-\bullet}$ (it is known that the lifetime of $\mathbf{33}^{-\bullet}$ is on the order of days in very dry solvents). Hydrogen atom abstraction would lead to **43** whereas addition to acetonitrile and further oxidation (hydrolysis) would give **45**. There is no absolute proof for the fact that this reaction actually takes place, because the mass spectrum of this compound from the reaction that was carried out in CD_3CN was not analyzed. However, the proposed mechanism seems to be the most likely pathway.

These are not common products of this type of reaction. A possible explanation for their formation could be the fact that under these conditions $\mathbf{2}^{+\bullet}$ is quite unreactive. Other (normally unlikely) pathways may therefore become more active. The formation of **45** was further investigated and the results of this study can be found below.

An intramolecular radical addition to a nitrile group can be used to explain the formation of **46**. The sequence of events involves addition of acetonitrile to $\mathbf{2}^{+\bullet}$ followed by attack of cyanide ion on the intermediate radical cation, and an intramolecular radical addition to the carbon of the nitrile (a 1,5-exo cyclization). The final product could be obtained by hydrogen atom abstraction followed by hydrolysis or by reduction to the iminyl anion (using $\mathbf{33}^{-\bullet}$ as the reducing agent) followed by protonation (Scheme 3.7). Another possible pathway could be reduction of the radical followed by nucleophilic

attack on the carbon of the nitrile and hydrolysis of the imine. From the data available here it is not possible to distinguish between these two pathways. However, it must be noted that reduction of a tertiary alkyl radical by $33^{-\bullet}$ is usually an endergonic reaction.

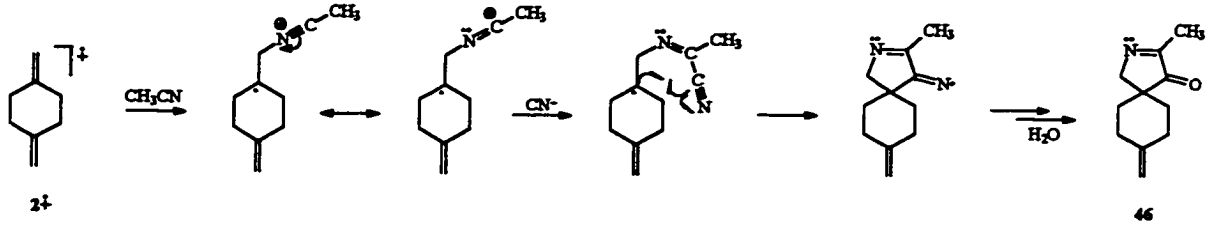

Scheme 3.7. Proposed mechanism for the formation of spiro compound **46**: an example of an intramolecular radical addition to the carbon of a nitrile group.

The formation of **47** remains unexplained. From experiments performed in CD_3CN it is evident that deuterium is incorporated and therefore radical **47**$^{\bullet}$ could be an intermediate (Scheme 3.8). Reduction of the intermediate radical to the anion followed by protonation would give the observed product. It is, however, unclear how this intermediate is formed from **2**.

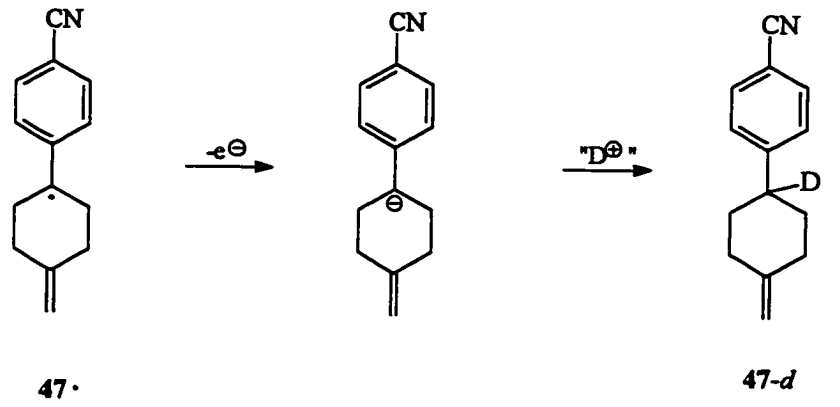

Scheme 3.8. Radical intermediate in the formation of aromatic substitution product **47**.

It is interesting to note that the formation of **47** is more dependent on the presence of biphenyl (**34**) than is the formation of **48**. In the absence of **34**, the formation of **47** is six times less favourable than when **34** is present.

Dimerization products are commonly observed in radical ion reactions.[21,53] The mechanism of this type of reaction is thought to be either a stepwise or a concerted mechanism. There is evidence for both mechanisms but the concerted mechanism to give a long-bond cyclobutane intermediate is favoured. We can assume that the two isolated dimerization products from this reaction (**49** and **50**) stem from the same radical cation intermediate. This intermediate then undergoes a ring closure reaction to yield **49** or a deprotonation (plus additional oxidation steps) to give **50** (Scheme 3.9).

Deprotonation of $\mathbf{2}^{+\bullet}$ is fast when a base (2,4,6-collidine) is added to the solution. The major product under these conditions is **48**; however, small amounts of **47** were also present.

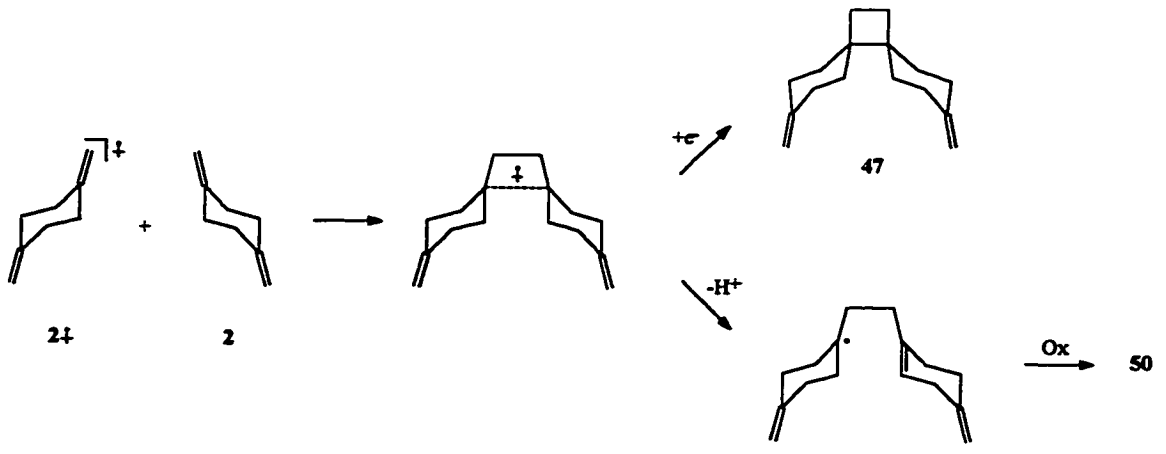

Scheme 3.9. Formation of cyclic and acyclic dimers arising from the common long bond cyclobutane intermediate dimeric radical cation.

Electrochemical oxidation of 1,4-bis(methylene)cyclohexane (2) in the presence of a nucleophile.

There are several reports in the literature concerning the anodic oxidation of alkenes in the presence of a nucleophile.[81] For example, the electrochemical oxidation of cyclic alkenes (cyclohexene, methylcyclohexenes, and cyclopentene) in the presence of methanol yielded allylically substituted products.[81a] In the case of cyclohexene a rearranged disubstituted product ((dimethoxymethyl)cyclopentane) was also observed. The electrochemical oxidation of α- and β-pinene in methanol gave only ring-opened products. This is in good agreement with the studies of the photo-NOCAS reaction on these species,[43] indicating that in these photochemical and electrochemical reactions the same intermediates are involved. The initially formed radical cation is a ring closed species but its lifetime is too short to be trapped by the nucleophile. In their electrochemical oxidation studies of non-conjugated dienes,[81b] Shono et al. found that several dienes showed transannular interaction. For example, electrooxidation of norbornadiene and cyclo[2.2.2]octadiene gave cyclized products whereas limonene and 4-vinylcyclohexene did not.

Performing a controlled potential electrolysis experiment on **2** (0.1 M) in acetonitrile-methanol (3:1) (0.1 M TEAP) at 2.55 V ($E_{1/2}^{ox}$(**2**) = 2.49 vs. sce; Table 3.1) resulted in the formation of several products (Reaction [3.3]). None of these products give any indication of transannular interaction in $\mathbf{2}^{+\bullet}$.

The products can be divided into three categories: mono substitutions or additions, double substitutions or additions, and multiple substitutions or additions. The first group

consists of 2-methoxy-1,4-bis(methylene)cyclohexane (**52**), 4-methoxy-4-methyl-1-methylenecyclohexane (**53**), and 1-(methoxymethyl)-4-methylenecyclohex-1-ene (**54**). These products account for 50% of the total yield based on the initial amount of **2** present. The second group includes 1-(methoxymethyl)-4-methylenecyclohexanol (**55**), 4-(di-methoxymethyl)-1-methylenecyclohexane (**56**), 4-methoxy-4-(methoxymethyl)-1-methyl-enecyclohexane (**57**), and (1-methoxy-4-methylenecyclohexyl)methanol (**58**). The sum of these four compounds accounts for 42% of the total yield. Two of the products (8% of the total yield) can be placed in the last group: 4-methoxy-4-(methoxymethyl)-cyclohex-2-en-1-one (**59**) and 3,6-dimethoxy-3,6-bis(methoxymethyl)-cyclohex-1-ene (**60**). This last compound (**60**) was isolated as a mixture of diastereomers.

Products **52** and **54** are typical allylic substitution products, however, **52** can only be formed by deprotonation of the radical cation ($\mathbf{2}^{+\bullet}$). The resulting allylic radical is further oxidized to the carbocation which undergoes nucleophilic attack at carbon 2.

It is clear that several deprotonation steps take place and that the acidity of the solution will increase. Methanol will, in general, serve as the base but the double bonds in **2** can also serve as the base. Protonation of **2** leads to the relatively stable tertiary carbocation ($\mathbf{2}^{+}$) which will then undergo nucleophile attack. Examination of the product mixture shows that only **53** may have arisen from this type of 'acid-catalysis'. In a control experiment in which **2**, dissolved in an acetonitrile-methanol (3:1) mixture, was treated with concentrated sulphuric acid, several products were formed but only **53** was a common product, present in both (acid-catalyzed and electrochemical) reaction mixtures.

Reaction [3.3]

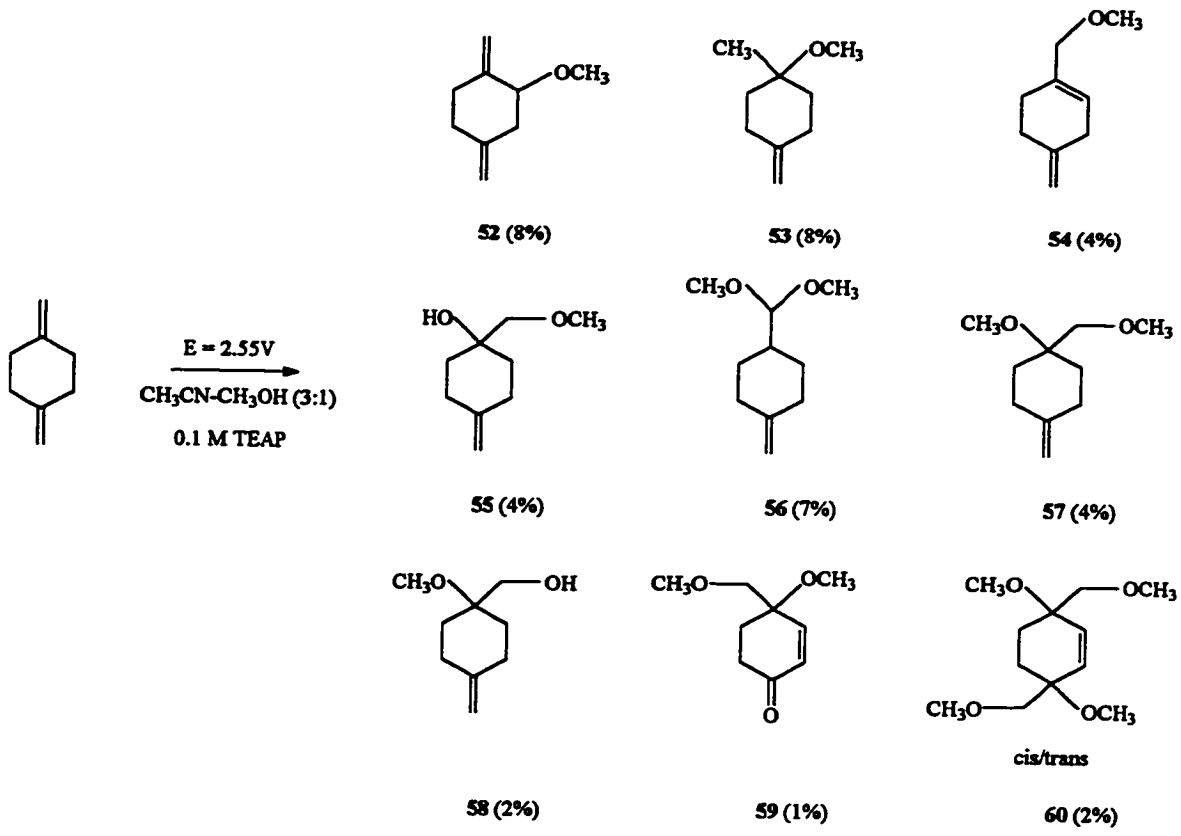

Products **55-58** are the result of a second nucleophilic addition. The important intermediate is the carbocation **61**$^+$ which is a result of an oxidation of the initially formed radical (**61**$^\bullet$). Nucleophilic (methanol or water) attack at carbon 4 will give products **55**, **57** and **58**. Product **56** is formed following a hydride transfer from carbon 8 to carbon 4 and subsequent nucleophilic attack on carbon 8 (Scheme 3.10). The relative yields (**56**, 7%; **55**, **57**, and **58** combined: 10%) suggest that this hydride shift is a facile process. This is not surprising since the positive charge in **62**$^+$ is stabilized by the adjacent oxygen.

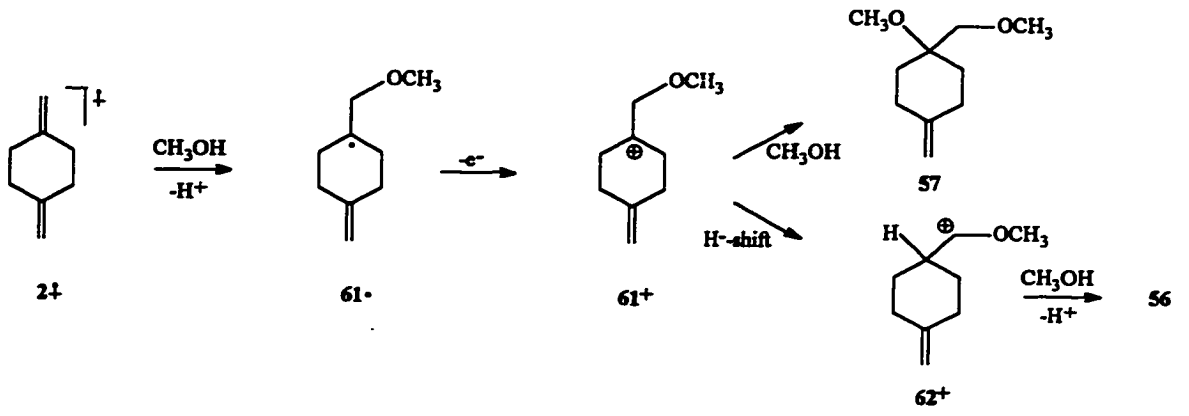

Scheme 3.10. Formation of acetal **56** as the result of a hydride shift in the intermediate cation $\mathbf{61}^{+}$.

Formation of **59** and **60** involves a more complicated process. There are two possible pathways that lead toward product **60**. Pathway I involves subsequent oxidation of both double bonds and a deprotonation in the final step. Pathway II involves oxidation of the first double bond, deprotonation to give a conjugated diene which is then further oxidized (Scheme 3.11).

Pathway I involves intermediate **62**, which resembles the isolated product **54**; however, **62** was not isolated from the reaction mixture. The conjugated diene **63** (an intermediate in pathway II) is likely to be very reactive under these (oxidative) conditions and **60** will be formed rapidly. The presence of **59** is also an indication that **63** is an intermediate. Compound **59** results from **63** as well; however, the nucleophile in this case is water and several subsequent deprotonation steps lead to the ketone.

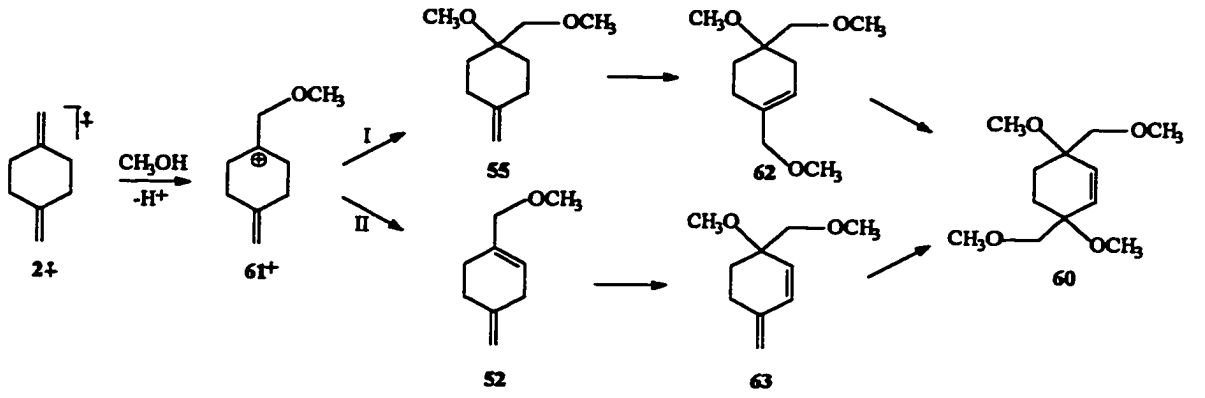

Scheme 3.11. Possible mechanism for the formation of the diastereomers of **60**.

The overall electrooxidation of **2** in an acetonitrile-methanol (3:1) solution is a two-electron process. As explained in Chapter 1, this number can be derived using the total amount of current that was consumed in this reaction (3800 Coulombs), and the conversion of **2**, as determined by calibrated gc/fid (Equation (3.2)).

$$n = (Q*M)/(a*F) \qquad (3.2)$$

In this equation n is the number of electrons involved in the oxidation process per molecule substrate, Q is the total number of coulombs consumed, M is the molecular weight of the substrate, a is the amount of substrate that has been converted (in grams), and F is Faraday's constant.

Using calibrated gc/fid, the conversion of **2** was determined to be 86%. From Equation (3.2) we then get the value for n which is 2.0. This is consistent with the observed product mixture. Formation of products **52**, **54**, **55**, **56**, **57**, and **58** each requires

2 oxidation steps. These compounds account for ca. 75% of the total yield. The formation of **59** and **60** requires more oxidation steps but this is compensated for by product **53** which only requires only one oxidation step. As mentioned above, compound **53** can be formed by protonation of the methylene group by $\mathbf{2}^{+\bullet}$ (or indirectly by $CH_3OH_2^+$). In order for one molecule of **53** to be formed, one molecule of **2** needs to undergo a one-electron oxidation. This leaves $\mathbf{2}^{\bullet}$, an allylic radical, which will undergo a second oxidation, followed by nucleophilic attack to give **52** and/or **54**.

Electrochemical oxidation of 1,4-bis(methylene)cyclohexane (2) in the absence of a nucleophile.

The results discussed above clearly show that following formation of the radical cation, nucleophilic attack is rapid and there is no evidence for rearrangements, cyclization or bond cleavage. Extending the lifetime of the radical cation by inhibiting nucleophilic attack might lead to different reactions. With this in mind, the electrochemical oxidation of **2** was carried out in the absence of a nucleophile (methanol). Three of the isolated products, 1,4-dimethylbenzene (**64**), 4-methylbenzaldehyde (**65**), and N-[4-methylbenzyl]-acetamide (**66**), are the result of multiple oxidation leading to aromatic molecules. The other two products, N-(4-[4-methyl-1-methylene-cyclohexyl])acetamide (**67**) and N-(4-[1,4-dimethylcyclohexenyl])acetamide (**68**), have the cyclohexyl moiety (partially) intact (Reaction [3.4]). Analysis of the reaction mixture with gc/ms indicated the presence of several other products with m/z 108 (C_8H_{12}). These are thought to be isomeric dimethylcyclohexadienes.

Reaction [3.4]

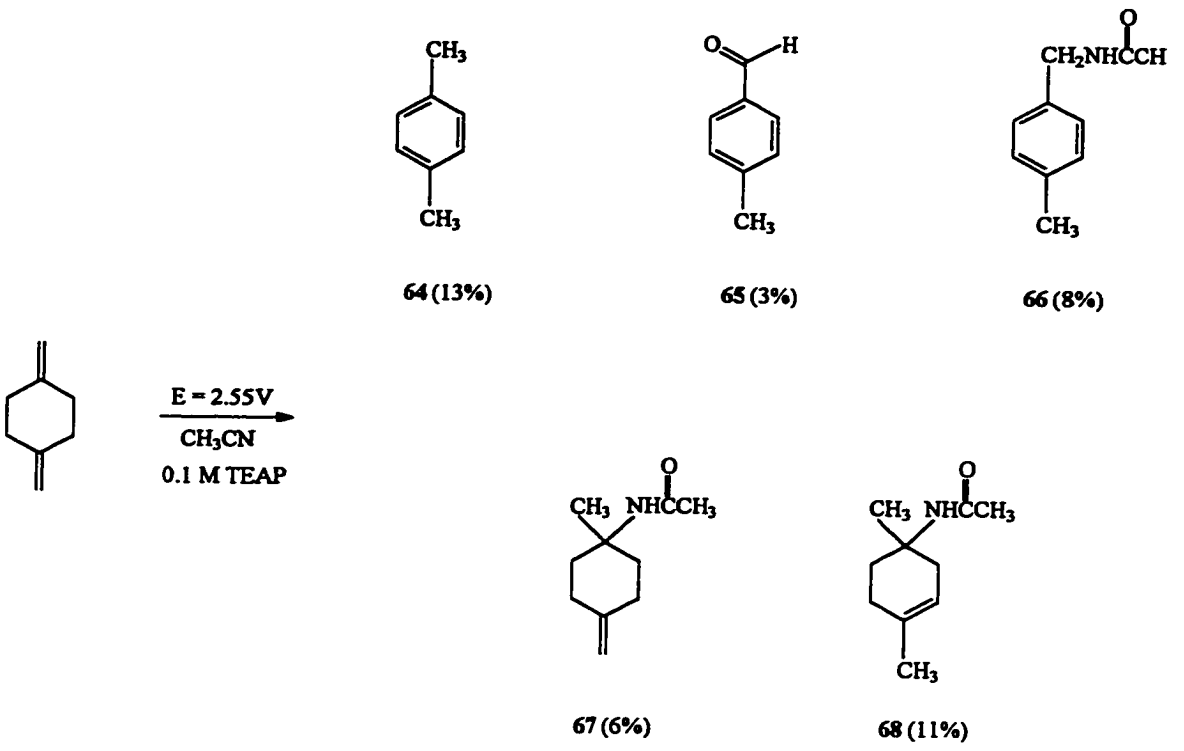

The formation of aromatic products upon electrochemical oxidation is a well known phenomenon.[2,81a] These products are usually explained on the basis of the mechanism for the Ritter reaction, i.e. cationic intermediates are formed. The initial step is formation of the radical cation $2^{+\bullet}$. This species is highly acidic and, in the absence of a nucleophile, will rapidly deprotonate. Both acetonitrile and **2** can serve as the base; protonating **2** leads to the formation of a relatively stable (tertiary) carbocation and the allylic radical. The carbocation then is deprotonated (by acetonitrile or **2**) to give a diene. The oxidation potential of the diene is lower than that of the alkene and further oxidation is facile. This sequence is repeated until an aromatic product is obtained. The product at

this stage is 1,4-dimethylbenzene (**64**), one of the major constituents of the reaction mixture (Reaction [3.4]).

The reaction does not necessarily stop at this point. Aromatic compounds undergo anodic oxidation as well; often this involves substitution of the side chain. For example, oxidation of polymethylbenzenes in acetonitrile leads to N-substituted acetamides.[2] Product **66** obviously is a secondary product arising from the oxidation of **64** with acetonitrile acting as the nucleophile (another nucleophile, water, is also necessary for the formation of the acetamides). Oxidation of **64** also leads to **65** but in this case water is the initial nucleophile reacting with the benzylic cation.

The aliphatic products **67** and **68** are formed by nucleophilic attack of acetonitrile on the tertiary carbocation formed by protonation of **2** (by $\mathbf{2}^{+\bullet}$ and/or CH_3CNH^+). Another control experiment showed that this is indeed the case. Reaction of **2** in acetonitrile with concentrated sulphuric acid resulted in the formation of three products (**64**, **67**, and **68**) in a ratio of 10:5:1.

The ratio of the products (**64**+**65**):(**66**+**67**+**68**) obtained from Reaction [3.4] indicates that, under these reaction conditions, deprotonation is about 1.4 times as fast as nucleophilic attack. Radical cations are known to have much lower pK_a values than their neutral precursors, i.e. they are strong acids.[36] Deprotonation of the radical cation is therefore expected to be a fast process. Since the ratio, deprotonation/nucleophilic attack, is only 1.4 this must mean that acetonitrile, under these conditions, is also an effective nucleophile.

After 21 days only 2047 C had been consumed in this reaction. However, the conversion of **2** at this point is 87% (calibrated gc/fid); i.e. the reaction is quite efficient. Using Equation (3.2), we find that n = 1.1. Again, this is consistent with the observed products and the mechanisms proposed for their formation. At first glance, the formation of aromatic compounds looks like a six-electron oxidation process. However, as discussed above, the aromatic compounds result from the Ritter reaction which involves carbocations. One-electron oxidation of **2** leads to the radical cation ($2^{+\bullet}$) which will deprotonate to another molecule of **2**. This sequence of oxidation-deprotonation can continue until aromatic products are formed. Overall, a one-electron oxidation (n = 1) reaction is the result.

Photochemistry of substituted 2,3-diaza-1,3-butadienes (azines): preliminary studies on the formation and reactivity of iminyl radicals.

Earlier in this Chapter it was mentioned that one of the products from the photoinduced electron transfer reactions of 1,4-bis(methylene)cyclohexane (**2**) is *p*-cyanoacetophenone (**45**). The mechanism for the formation is thought to be as shown below in Scheme 3.12.

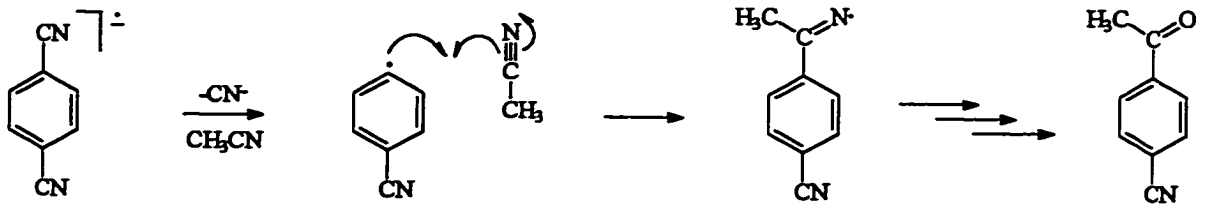

Scheme 3.12 Proposed mechanism for the formation of *p*-cyanoacetophenone through the iminyl radical intermediate.

Other possible evidence for the intermediacy of *p*-cyanophenyl radical is the presence of benzonitrile (**44**) in the product mixture although it was pointed out earlier that this could also arise from protonation of **33**$^{-\bullet}$. Step 2 in Scheme 3.12 involves the addition of a carbon centered (phenyl) radical to the carbon of a nitrile group. Intermolecular radical additions to nitriles are not very well known. In fact, Ingold and co-workers[85a] found that the phenyl radical (and others) did not add to pivalonitrile. On the other hand, Shelton and Uzelmeier[85b] found that both phenyl and cyclohexyl radicals added to benzonitrile. There are several examples of intramolecular radical additions to nitriles.[85c] For example, Ogibin et al.[85d] found that upon generation of the 4-cyanobutyl radical in an aqueous medium, cyclopentanone was the major product. Additions of carbon-centered radicals to acetonitrile are rarely observed. The only other example of a radical (adamantane) addition to acetonitrile was reported by Engel et al.[86] There are, however, several examples in the literature of heteroatom radicals adding to acetonitrile: hydrogen atoms add to the CN triple bond in acetonitrile,[87a,b] tertiary amine-boryl radicals add to nitriles to give iminyl radicals ($R_3N{\rightarrow}BH_2C(R')=N^{\bullet}$)[87c,d] as do primary amine-boryl radicals,[87e] and the ammonia-boryl radical.[113f] Reaction of the β-distonic radical cation $^{\bullet}CH_2\text{-}CH_2\text{-}O\text{-}CH_2^{+}$ with acetonitrile is thought to proceed by either a 'head on" radical addition to the carbon of acetonitrile or a "side on" electrophilic addition to the nitrogen.[87g]

It must be noted that product **45** could also arise from reaction of **33**$^{-\bullet}$ with acetonitrile. This reaction, however, should also be governed by spin density (radical) rather than charge density (ionic). Another possible pathway could involve reduction of *p*-

cyanophenyl radical by **33**$^{-\bullet}$ to *p*-cyanophenyl anion. This anion could then attack acetonitrile. Recently, Arnold and co-workers[48] found that irradiation of an acetonitrile-methanol solution of **33** and 2-methyl-1,5-hexadiene or **33** and 2,5-dimethyl-1,5-hexadiene resulted in the formation of imines. The involvement of radical intermediates was considered but based on calculated (STO-3G) spin and charge densities in **33**$^{-\bullet}$ (Figure 3.2; Table 3.4) it was concluded that reduction of the intermediate β-methoxy radical to the anion and subsequent attack on **33** was a more plausible mechanism. In this case, however, generation of *p*-cyanophenyl anion, an extremely strong base, would very likely result in the formation of benzonitrile (**43**) rather than acetophenone (**45**).† The product ratio (**43**:**45** = 1:4) that was observed does not comply with that mechanism.

Addition of a carbon-centered radical to acetonitrile yields an iminyl radical. Relatively little is known about iminyl radicals and their reactivity.[88,89] There are a number of reactions that they can undergo and examples of these are available in the literature.[88] The major pathways are hydrogen atom abstraction (to give an imine), β-cleavage (or ring opening in small ring systems) to give a nitrile, dimerization to give an azine, and addition to alkenes or aromatics (homolytic aromatic substitution). Only a few studies on the reactivity of iminyl radicals have been reported. For example, Ingold and Griller[90] have studied the reactions of iminyl radicals (generated from the parent imines by reaction with *t*-butoxide radicals) by ESR. The only process believed to take place was dimerization; the measured rate constant for dimerization of the benzophenone iminyl radical is 2×10^8 $M^{-1}s^{-1}$ at -35°C. Suehiro et al.[91] have measured a rate constant of 5×10^2 $M^{-1}s^{-1}$ for the

† In order to find out whether it is the radical or the anion adding to acetonitrile, one could add p-cyano-phenyllithium to acetonitrile and identify the products (deprotonation or addition).

hydrogen atom abstraction process of benzophenone iminyl radical from toluene at 50°C. No other spectroscopic techniques have been applied to these species.

Iminyl radicals can be generated by a number of ways.[88-93] Known methods are photolysis of azines (N-N bond homolysis; Scheme 3.13)),[92] hydrogen atom abstraction from imines (see above),[90] and deprotonation of an imine radical cation.[88f]

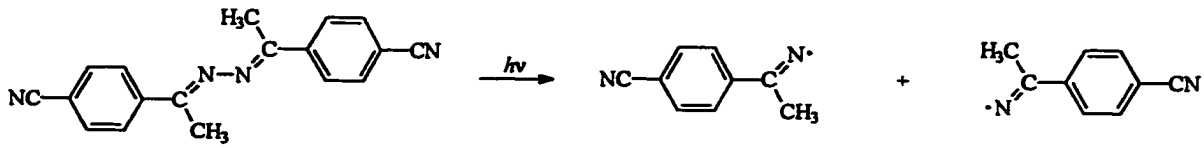

Scheme 3.13. Photochemical generation of *p*-cyanoacetophenone iminyl radical by N-N bond homolysis of *p*-cyanoacetophenone azine.

In this part of the thesis, the results of a preliminary investigation on the generation and reactivity of iminyl radicals will be described and discussed. In the first section, steady-state photolyses of a number of azines and imines were carried out to determine the proper conditions for the nanosecond laser flash photolysis (LFP) experiments. The second section contains the results from the LFP experiments.

Steady-state photolysis of azines and imines.

The compounds chosen for this study are *p*-cyanoacetophenone azine (*p*-CAPA, **69**), benzophenone azine (BPA, **70**), and benzophenone imine (BPI, **74**). The solvent chosen for most of these studies was dichloromethane (DCM). Other solvents (MeCN, MeOH, and benzene) were not suitable since the azines did not dissolve very well in these

solvents. Irradiations were carried out in quartz tubes in order to reduce reaction times. Irradiation through Pyrex did result in some conversion of the azines but only after much longer irradiation times.

Irradiation through quartz of a solution of *p*-CAPA (**69**) in dichloromethane (DCM) leads to only one product: *p*-cyanoacetophenone (**45**, 60% yield; 51% conversion after 4 days; Reaction [3.5]).

Reaction [3.5]

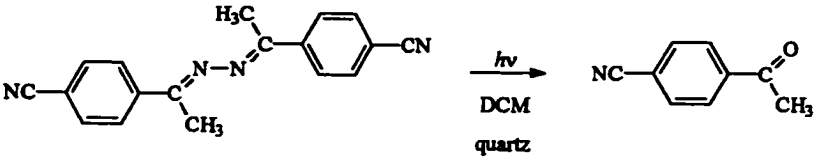

69 **45**

This result, in agreement with other observations reported in the literature, indicates that upon irradiation, the N-N bond is cleaved resulting in the formation of two iminyl radicals which are then further hydrolyzed to give *p*-cyanoacetophenone (**45**). At this stage, it must be pointed out that this result can also be seen as a photoinduced hydrolysis. However, this process would most likely proceed through the hydrazone intermediate. Binkley[92d] has shown that irradiation of benzophenone hydrazone gives different products than irradiateion of benzophenone azine (see below). Nevertheless, the photoindiuced hydrolysis process cannot be completely ruled out.

Steady-state photolysis of BPA (**70**) in DCM results in the formation of benzophenone (**71**) as the major product (60% yield at ca. 50% conversion). Minor products include benzophenone hydrazone (**72**), 1,3,3-triphenylisoindole (**73**), and benzophenone imine (**74**), (Reaction [3.6]).

Reaction [3.6]

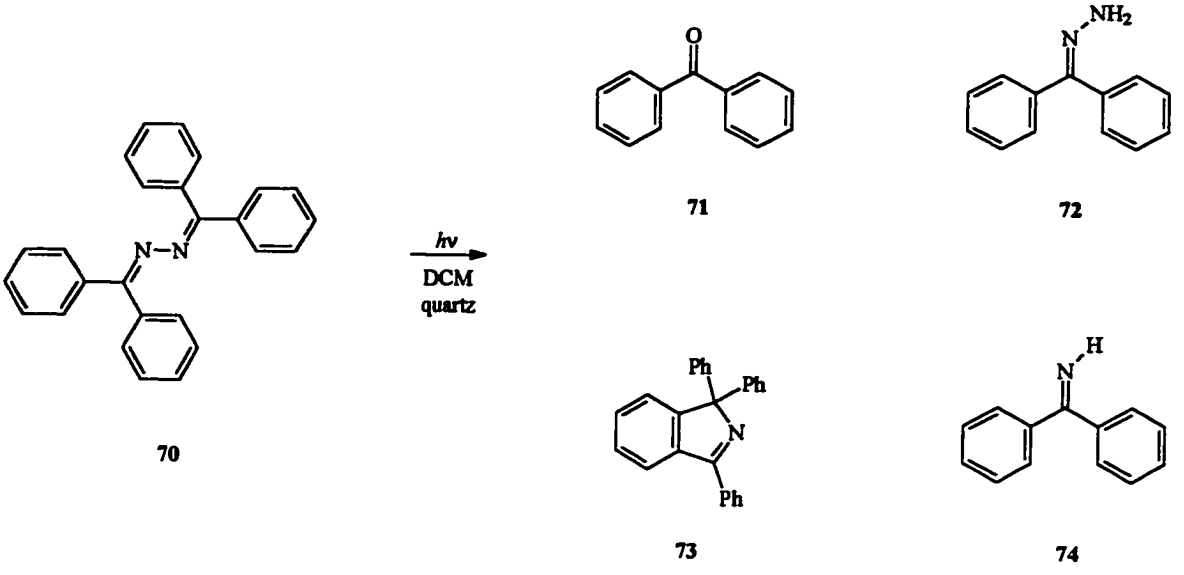

70 71 72 73 74

These results, however, are in sharp contrast with those reported in the literature.[94] Binkley reported that in contrast to all other acyclic azines, BPA does not undergo N-N bond homolysis upon irradiation in methanol. Instead a molecular rearrangement and a photoreduction account for the product formation in this reaction. The major product under these conditions (methanol solution) is 1,3,3-triphenylisoindole (**73**), a product also observed when the reaction is carried out in DCM (Reaction [3.6]). However, the formation and involvement of the benzophenone iminyl radical was not thought to take

place. The mechanism for formation of the indole, as proposed by Binkley, is shown in Scheme 3.14. As can be seen from Scheme 3.15, iminyl radicals and a radical mechanism can account for the formation of the indole as well.

The different reactivity of benzophenone azine as compared to other acyclic azines was believed to be due to the fact that a different excited state was formed.[94] Because of the extended π-system the lowest excited state was believed to be the result of a $\pi \rightarrow \pi^*$ transition. For other azines, the lowest excited state is the result of an $n \rightarrow \pi^*$ transition. The UV-spectrum of *p*-CAPA, however, does not show an $n \rightarrow \pi^*$ transition but this could be due to the fact that the molar extinction coefficients (ε) of these azines are very high ($\approx 10^4$ L mol^{-1} cm^{-1}; see experimental section), and the $\pi \rightarrow \pi^*$ absorption might overlap with the weak $n \rightarrow \pi^*$ absorption.

The products that are observed when BPA in photolyzed in DCM are similar to those observed in the photolysis of benzophenone hydrazone (**72**).[92d] Because the hydrazone is an expected hydrolysis product of BPA, this result could indicate that the photolysis of BPA does not give N-N bond homolysis, but rather a photoinduced hydrolysis. In favour of the radical pathway, however, are the observations that the solvent effects are small (expected for radical reactions, unexpected for ionic reactions) and the fact that thermal decomposition of azines (N-N bond homolysis) yields similar products.[92]

The possibility of an acid catalyzed process when carrying out the photoreaction in DCM due to the *in situ* formation of HCl was tested by carrying out two further experiments. An experiment in which an acid (trifluoroacetic acid, TFA) was added to the

solution yielded, upon irradiation, the three major products that had been observed before: benzophenone (**71**), benzophenone imine (**74**), and 1,3,3-triphenylisoinole (**73**). A second experiment in which a radical trap (2,6-di-*tert*-butyl-4-methylphenol (DBMP) was added to the solution yielded the exact same products upon irradiation. The radical trap had been consumed completely after 24 hrs irradiation. In both experiments the relative ratio of the three products (**71**:**74**:**73**) is about 2:2:1. However, this ratio is very different from that observed in the photoreaction of BPA under normal conditions (ratio **71**:**74**:**73** = 10:3:1). These results do not clarify the picture; in fact, both mechanisms (ionic and radical) can be defended on the basis of these preliminary results. The possibility that the products arise from a photoinduced hydrolysis cannot be ruled out either.

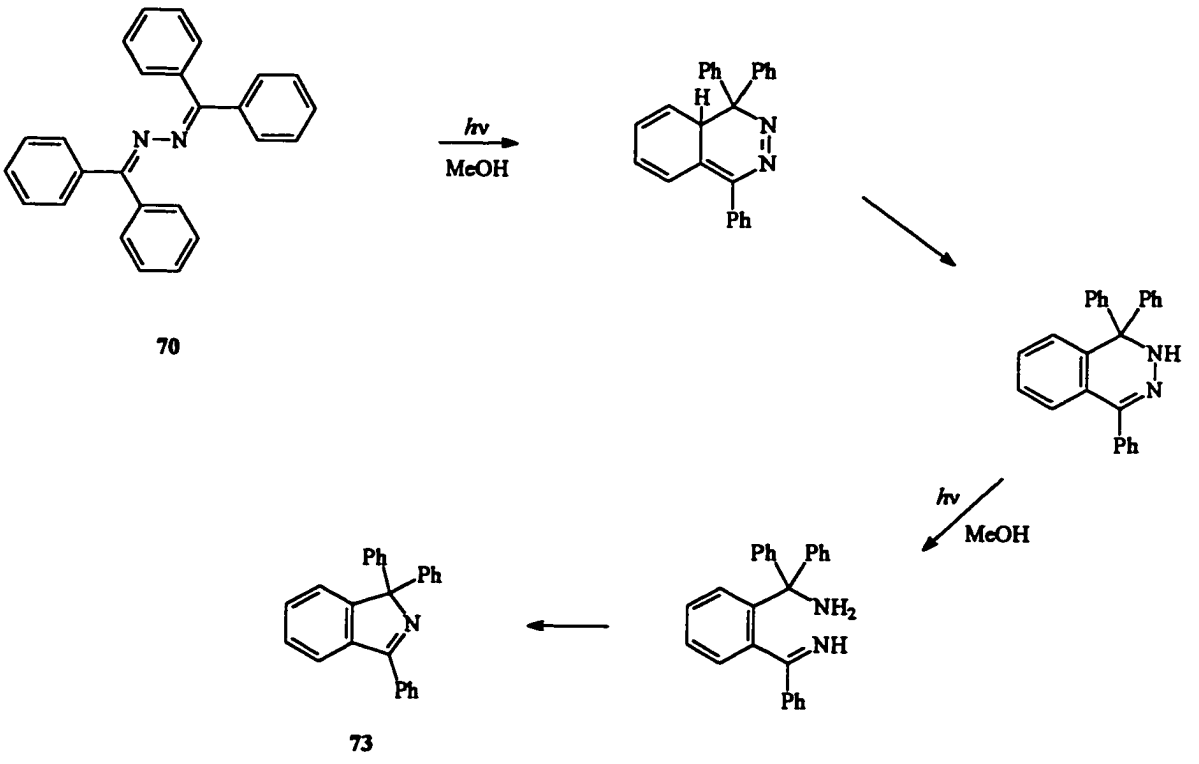

Scheme 3.14 Formation of 1,3,3-triphenylisoindole (**73**) in the photochemical reaction of benzophenone azine as proposed by Binkley.[94]

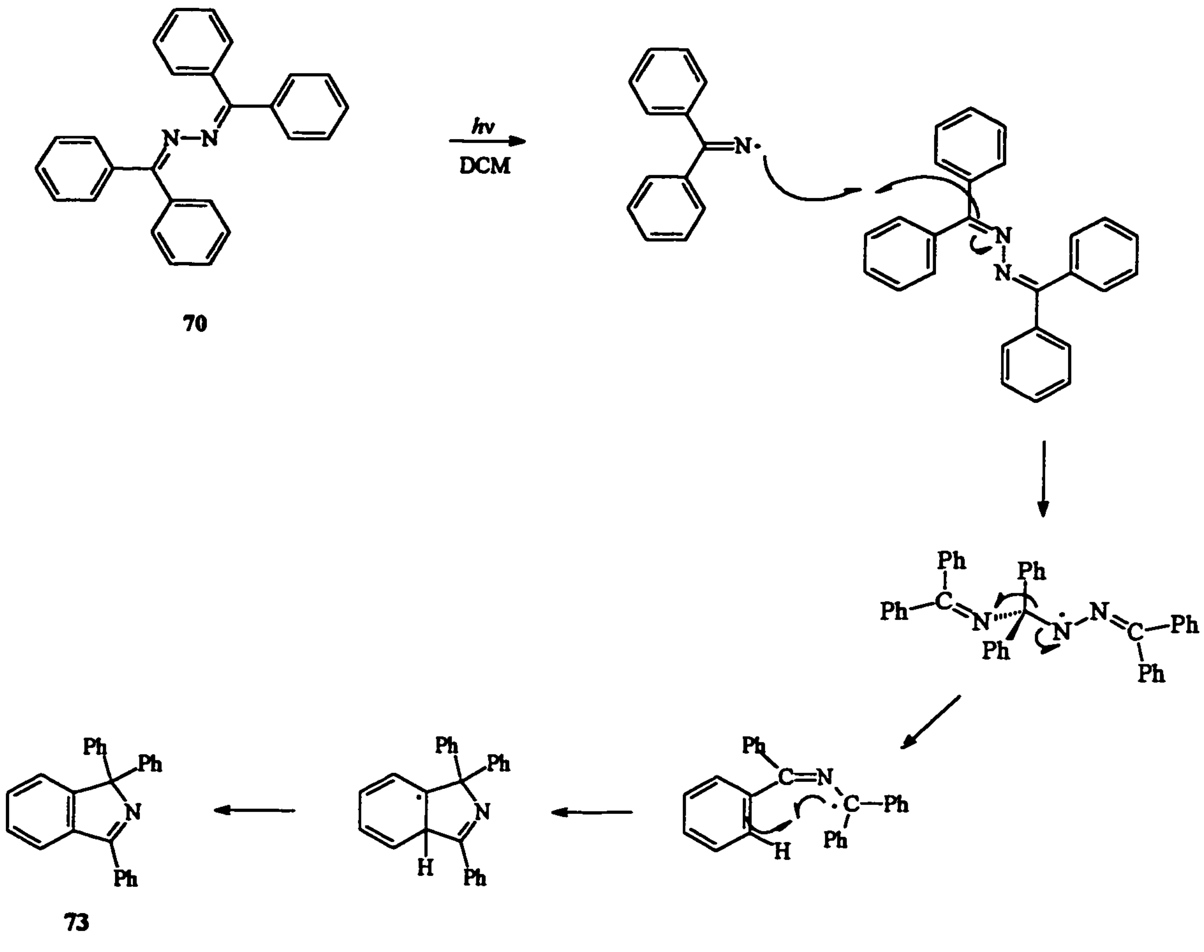

Scheme 3.15 Formation of 1,3,3-triphenylisoindole (73) by a radical mechanism involving the benzophenone iminyl radical.

Another method for generating iminyl radicals was mentioned above. Ingold and co-workers[90] generated the benzophenone iminyl radical by reacting benzophenone imine (BPI) with *tert*-butoxy radicals. Steady-state photolysis of a DCM solution of *tert*-butyl peroxide and benzophenone imine resulted in some conversion of the imine, however, benzophenone was not the major product. A small amount of benzophenone azine could be detected. Irradiation of a DCM solution containing only benzophenone imine did not result in any conversion of the starting material, indicating that conversion of the imine in the former reaction is a radical induced process. It must be noted that the radical reactions could also involve the solvent since it contains abstractable hydrogens as well as chlorine atoms. Also, irradiation through quartz might give rise to unwanted side reactions. The former experiment was therefore repeated in benzene; the experiments were done in Pyrex tubes. The major products after five hours irradiation are now biphenyl, benzophenone, and benzophenone azine. Clearly, these products must arise from radical intermediates. In order to see whether the biphenyl results from coupling of two phenyl radicals produced by a β-cleavage in the benzophenone iminyl radical, or from phenyl radicals derived from the solvent, the same experiment was carried out in benzene-d_6. The mass spectrum of biphenyl indicates that no deuterium was present in the molecule and it must, therefore, arise by dimerization of two phenyl radicals formed by a β-cleavage reaction (Reaction [3.7]). Interestingly, no benzonitrile could be detected in the product mixture. This could mean that β-cleavage in benzophenone iminyl radical occurs (simultaneously) for both phenyl groups resulting in the formation of two phenyl radicals and a cyano radical. Biphenyl could also be the result of an in-cage reaction between phenyl radical and

benzonitrile. Another precursor of biphenyl could be benzophenone. However, this process (α-cleavage) is highly unlikely.

Reaction [3.7]

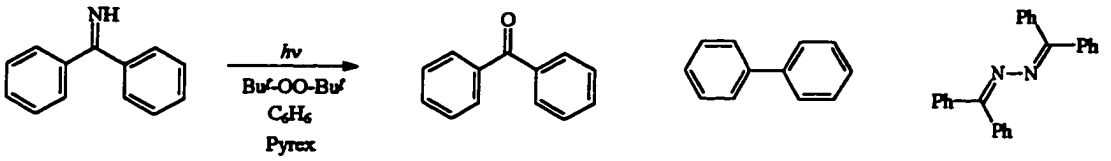

74 71 34 70

From the results on the steady-state photolyses of azines **69** and **70** described above it can be concluded that a major pathway in the photochemical decomposition of these compounds in DCM is N-N bond homolysis. An ionic mechanism or a photoinduced hydrolysis cannot be completely ruled out and it is possible that several pathways are followed. From these results it is not possible to assess to what extend these individual pathways contribute to the decomposition of the azines. However, since N-N bond homolysis is believed to be a major pathway, the conditions described above seem suitable for LFP studies. The photochemical decomposition of benzophenone imine in benzene initiated by *tert*-butoxide radicals is clearly a radical pathway. The reaction is relatively fast and this method for generating iminyl radicals seems promising for the LFP studies.

Laser flash photolysis experiments.

According to Scheme 3.12, the *p*-cyanobenzophenone iminyl radical is formed by addition of the *p*-cyanophenyl radical to acetonitrile. *p*-Cyanobromobenzene (*p*-CBB) was chosen as a precursor of the *p*-cyanophenyl radical. Photolysis of *p*-CBB in acetonitrile (266 nm) resulted in the formation of a transient with a weak absorption at 280 nm. A first- order growth with a rate constant of approximately 1×10^5 s^{-1} was observed. This rate constant is close to the number observed by Scaiano and Stewart[95] for the reaction of phenyl radical[96] with acetonitrile. In order to determine whether this signal is due to the formation of the *p*-cyanobenzophenone iminyl radical, photolysis of *p*-CAPA, under similar conditions, was attempted. Photolysis (266 nm) of a solution of *p*-CAPA in DCM did not result in the formation of any detectable transients. The signal at 280 nm, observed in the previous experiment, could not be seen due to strong photobleaching in this region. A similar result was obtained when BPA was photolyzed.

Laser flash photolysis (308 nm) of a benzene solution containing benzophenone imine and *tert*-butylperoxide resulted in the formation of a strong transient at around 300 nm; this signal, however, corresponds to that of the *tert*-butoxy radical. Based on the results described above, the signal of the iminyl radical is expected in the same region and could therefore not be observed since it is much weaker than that of the *tert*-butoxy radical.

It is somewhat surprising that the absorption spectra of iminyl radicals are weak and have a maximum at short wavelengths. However, it must be noted that the single

electron of the iminyl radical does not have extensive delocalization throughout the molecule since it is localized in an orbital perpendicular to the π-system (Figure 3.3).

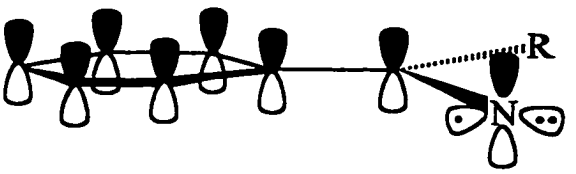

Figure 3.3 Schematic representation of the orientation of the orbitals in iminyl radicals.

Calculations (AM1) showed that 80% of the spin density in benzophenone iminyl radical is localized on the nitrogen. A small amount of spin density can be found on the *ipso* carbons of the two phenyl rings. A similar result was obtained for *p*-cyanoacetophenone iminyl radical. For comparison, the spin density in the benzhydrol radical is largely delocalized over the entire molecule; only 45% is localized on the benzylic carbon. Due to this delocalization this radical has a very distinctive absorption spectrum. Although delocalization is not always a requirement for enhanced absorption, in this case it is probably the major reason for not being able to observe any transients upon generation of the radical. Obviously, doing kinetic studies on these intermediates using LFP will be considerably more difficult than was anticipated.

3.3 Conclusions

Two major reaction pathways for the radical cation of 1,4-bis(methylene)-cyclohexane ($2^{+\bullet}$) have been identified by studying the photoinduced electron transfer and

the electrochemical oxidation of **2**. The behaviour of the radical cation was studied both with and without nucleophile present. While the photochemical and electrochemical experiments yield different products, the major reaction pathways of $\mathbf{2}^{+\bullet}$ in these experiments are understandably similar. In the presence of a good nucleophile the products arise from nucleophilic attack on the radical cation. This is the case in both the photochemical and the electrochemical experiments. In the absence of a nucleophile, the electrooxidation experiments show that there is a preference for deprotonation. However, the solvent that was used in this experiment (acetonitrile) can, and does, act as a nucleophile resulting in the formation of N-acetamides. It was shown using a control experiment that these products arise from Ritter-type reactions, i.e. the intermediates are carbocations and the products are formed by acid-catalyzed processes. This is not surprising since the radical cations are highly acidic species and deprotonation of $\mathbf{2}^{+\bullet}$ leads (directly or indirectly) to $\mathbf{2}^{+}$. The photoinduced electron transfer experiments in the absence of a nucleophile leads to the formation of some interesting products, including two dimeric species (**49** and **50**). Another interesting observation is the presence of *p*-cyanoacetophenone (**45**), which is thought to arise by addition of *p*-cyanophenyl radical to acetonitrile (yielding an iminyl radical), followed by hydrolysis. More evidence for this pathway was obtained from steady-state photolysis experiments using azines and imines as precursors of the iminyl radicals.

The differences observed between the electrochemical and the photochemical reactions are most likely due to the fact that in the electrochemical experiments the initially formed radical cation ($\mathbf{2}^{+\bullet}$) is close (or adsorbed) to the electrode and a second oxidation

of the resulting radical (formed after deprotonation or nucleophilic attack) is therefore often inevitable.

The previous calculations, summarized in Scheme 1, have indicated that 1,4-bis(methylene)cyclohexane (**2**) and its radical cation ($\mathbf{2}^{+\bullet}$) are the most stable of the C_8H_{12} and $C_8H_{12}^{+\bullet}$ isomers considered.[76] This study therefore provides the foundation for future characterization of the higher energy isomers which we expect/predict will dimerize, rearrange, cyclize, or fragment to some of the same intermediates observed in this study.

3.4 Experimental

General Information

^1H and ^{13}C nmr spectra were obtained on a Bruker 250 MSL spectrometer. Spectra were recorded in parts per million and frequencies are relative to tetramethylsilane. Infrared spectra (ir) were recorded on a Nicolet 205 spectrometer and are reported in wavenumbers (cm^{-1}). Elemental analyses were performed by Canadian Microanalytical Service Ltd., Delta, B.C. Exact mass determinations were obtained using a CEC 21-110B spectrometer. Melting points were determined using a Cybron Corporation Thermolyne apparatus with a digital thermocouple and are corrected. Product yields were determined using a Hewlett-Packard (HP) 5890 gas chromatograph with a DB-1701 fused silica WCOT column (30 m x 0.25 mm, 0.25-μm film thickness) and a calibrated flame ionization detector (gc/fid) and, for consistency, are based upon 1,4-bis-(methylene)cyclohexane (**2**). An HP 3392A integrator was interfaced with the gc/fid to obtain peak areas. An HP 5890 gas chromatograph with a 5% phenyl methyl silicone fused

silica WCOT column (25 m x 0.20 mm, 0.33-μm film thickness) interfaced with an HP 5970 mass selective detector (gc/ms) was also used for product analyses. Mass spectra are reported as *m/z* (relative intensity). Separation of product mixtures was generally carried out using preparative medium-pressure liquid chromatography (mplc), followed by dry column flash chromatography (dcfc)[82] and preparative-GC. The mplc consists of a 2.5 cm x 1 m column packed with thin-layer chromatography (tlc) grade silica gel (Rose Scientific Ltd., Silica Gel G/UV-254 with Gypsum binder, cat. no. 81632) at a pressure of 18 psi using helium (1psi= 6.9 kPa). Connected to the mplc was a uv spectrophotometer-fraction collector that collects ca. 10-mL fractions. For dcfc the column was packed with thin-layer chromatography grade silica gel (Rose Scientific Ltd., Silica Gel G/UV-254 with Gypsum binder, cat. no. 81632). Fraction sizes were ca. 5 mL. Preparative gas chromatography (prep-gc) was carried out using a Varian Aerograph 920 equiped with a 20% SE-30 on Chromosorb W 60/80 column (6′ × ¼″).

Materials

Acetonitrile (Fisher ACS grade) was distilled twice, first from sodium hydride and then from phosphorus pentoxide. It was then passed through a column of basic alumina, refluxed over calcium hydride for 24 h (under a nitrogen atmosphere), fractionally distilled (under nitrogen) and stored over molecular sieves (3 Å).[39f] Anhydrous acetonitrile (Aldrich) was stored over molecular sieves (3 Å) upon arrival and used without further purification. Methanol was distilled and then stored over molecular sieves (3 Å). Anhydrous methanol (Aldrich) was stored over molecular sieves (3 Å) upon arrival and

used without further purification. 1,4-Dicyanobenzene (**33**) (Aldrich) was purified by treatment with Norite in methylene chloride, followed by recrystallization from 95% ethanol. Biphenyl (**34**) (Eastman Kodak) was recrystallized from methanol. Tetraethylammonium perchlorate (TEAP) (Fisher) was recrystallized three times from water and then dried in a vacuum oven for 15 h, 70°C, 0.25 Torr (1 Torr = 133.3 Pa). Dichloromethane (BDH) was distilled and stored over molecular sieves (3 Å). *p*-Bromobenzonitrile, benzophenone imine, trifluoroacetic acid, 2,6-di- *tert*-butyl-4-methylphenol, and *tert*-butyl peroxide were purchased from Aldrich and used as received. 1,4-Bis(methylene)cyclohexane, 99% (**2**) was purchased from Wiley Organics and used without further purification. *p*-Cyanoacetophenone azine (**69**) and benzophenone azine (**70**) were prepared according to literature procedures with some slight modifications.

Irradiations

Irradiations were generally carried out on solutions of acetonitrile-methanol (3:1) with 1,4-dicyanobenzene, the alkene, and with or without a codonor. In certain experiments methanol was omitted. Solutions were irradiated in either 2 cm i.d. Pyrex tubes or 5 mm Pyrex nmr tubes, which were degassed by nitrogen ebullition. The samples were irradiated at 10°C using a CGE 1-kW medium-pressure mercury vapor lamp contained in a water-cooled quartz immersion well.

Cyclic Voltammetric Measurements

Cyclic voltammetry at a sweep rate of 100 mV/s was used to obtain the oxidation potential of the alkene. The apparatus has been described.[83] The working electrode was a platinum sphere (1 mm diameter) and the counter electrode was a platinum wire. The reference electrode was a saturated calomel electrode (sce), which was connected to the solution (TEAP 0.1 M, acetonitrile) through a Luggin capillary. The alkene concentration was ca. 0.005 M. Since the anodic wave was irreversible, the half-wave potential was taken as 0.028 V before the anodic peak potential.[3]

Controlled Potential Electrolyses

Controlled potential electrolyses of **2** were performed with a customized two-electrode cell (total volume 200 mL), containing the working electrode and the reference electrode. The counter electrode compartment, containing the counter electrode, was fitted into the cell; the two compartments are connected by means of fine glass frit. Both the working electrode and counter electrode were platinum mesh (6.5 cm^2). The reference electrode was the standard calomel electrode (sce). All experiments were performed at room temperature.

The electrochemical measurements were obtained with a Princeton Applied Research (PAR) 173 potentiostat in combination with a PAR 175 universal programmer and a PAR 179 digital coulometer.

Irradiation of a mixture of 1,4-bis(methylene)cyclohexane (2) and 1,4-dicyanobenzene (33) in acetonitrile-methanol (3:1).

A mixture of 1,4-bis(methylene)cyclohexane (**2**) (2.2 g, 2.0×10^{-2} mol) and 1,4-dicyanobenzene (**33**) (1.3 g, 1.0×10^{-2} mol) dissolved in 200 mL acetonitrile-methanol (3:1) was irradiated for 12 days. The solvent was removed by rotary evaporation and the residue was chromatographed on silica gel (mplc) using a linear solvent gradient (hexanes - 50% diethylether/50% hexanes). Compound **41** was further purified by prep-gc.

4-(Methoxymethyl)-1-methylenecyclohexane (**41**): ir (liquid film) ν: 3071 (w), 2981 (m), 2923 (s), 2854 (s), 2809 (w), 1650 (m), 1448 (m), 1387 (w), 1212 (w), 1195 (w), 1124 (s), 1102 (s), 966 (w), 944 (w), 888 (s); ^{1}H nmr ($CDCl_3$, AC250) δ: 4.59 (s, 2H), 3.31 (s, 3H), 3.18 (d, 6.71 Hz, 2H), 2.29 (d, 13.43 Hz, 2H), 2.01 (td, 4.27 Hz, 13.43 Hz, 2H), 1.87-1.80 (m, 2H), 1.77-1.63 (m, 1H), 1.04 (qd, 4.27 Hz, 12.20 Hz, 2H); ^{13}C nmr ($CDCl_3$, AC250) δ: 149.53 (s), 106.92 (t), 78.05 (t), 58.81 (q), 37.53 (d), 34.14 (t), 31.16 (t); ms *m/z*: 140 ($M^{+\bullet}$,1%), 108 (38), 93 (100), 91 (25), 80 (47), 79 (67), 77 (25), 67 (40), 55 (21), 53 (25).

4-(4-Cyanophenyl)-4-(methoxymethyl)-1-methylenecyclohexane (**42**): ir (liquid film) ν: 3071 (m), 2981 (m), 2933 (s), 2875 (s), 2228 (s), 1651 (m), 1607 (m), 1506 (m), 1450 (m), 1404 (w), 1382 (w), 1191 (m), 1116 (s), 979 (w), 958 (w), 892 (m), 836 (m); ^{1}H nmr ($CDCl_3$, AC250) δ: 7.63 (d, 8.54 Hz, 2H), 7.51 (d, 8.54 Hz, 2H), 4.61 (s, 2H), 3.31 (s, 2H), 3.17 (s, 3H), 2.23-2.17 (3 line multiplet, 6.11 Hz, 10.37 Hz, 4H), 2.09-1.97 (m, 2H), 1.83-1.66 (m, 2H); ^{13}C nmr ($CDCl_3$, AC250) δ: 150.09 (s), 148.07 (s), 132.02 (d), 128.10

(d), 119.10 (s), 109.81 (s), 107.50 (t), 81.53 (t), 59.43 (q), 43.31 (s), 33.75 (t), 30.63 (t); ms *m/z*: 241 ($M^{+\bullet}$, 6%), 209 (51), 196 (41), 195 (21), 181 (25), 180 (25), 168 (19), 154 (51), 142 (21), 140 (19), 117 (19), 116 (100), 115 (21), 93 (38), 89 (19), 79 (21), 77 (23), 67 (41); Anal. Calcd. for $C_{16}H_{19}NO$: C 79.63, H 7.94, N 5.80; Found: C 78.75, 80.28, H 7.85, 7.89, N 5.75, 5.91.

Irradiation of a mixture of 1,4-bis(methylene)cyclohexane (2) and 1,4-dicyanobenzene (33) in acetonitrile-methanol-O-d (3:1).

A mixture of 1,4-bis(methylene)cyclohexane (**2**) (0.0440 g, 4.1×10^{-4} mol) and 1,4-dicyanobenzene (**33**) (0.0365 g, 2.9×10^{-4} mol) dissolved in 4 mL acetonitrile-methanol-O-*d* (3:1) was irradiated for 6 hours. Deuterium incorporation was checked by gc/ms analysis. Identification of the products was based on the mass spectra and the retention times (gc/ms and gc/fid) of the compounds.

Irradiation of a mixture of 1,4-bis(methylene)cyclohexane (2), 1,4-dicyanobenzene (33), and biphenyl (34) in acetonitrile.

A solution of 1,4-bis(methylene)cyclohexane (**2**) (2.3 g, 2.1×10^{-2} mol), 1,4-dicyanobenzene (**33**) (2.6 g, 2.0×10^{-2} mol), and biphenyl (**34**) (3.1 g, 2.0×10^{-2} mol) in 200 mL acetonitrile was irradiated for 41 days. The solvent was removed by rotary evaporation and the residue was chromatographed on silica gel (mplc) using a linear solvent gradient (hexanes - diethylether). Mixtures of compounds were further purified by dcfc using cyclohexane or a cyclohexane - 5% diethylether/95% cyclohexane gradient.

Benzonitrile (**43**): this compound was not isolated but identification is based on its mass spectrum: *m/z*: 103 ($M^{+\bullet}$, 100%), 77 (12), 76 (82), 75 (23), 74 (12), 64 (4), 63 (8), 62 (4), 52 (14), 51 (27); retention time (gc/fid and gc/ms) and mass spectrum were compared to that of an authentic sample (Aldrich).

4-Cyanotoluene (**44**): identification of this compound is based on its mass spectrum: *m/z*: 117 ($M^{+\bullet}$, 100%), 116 (76), 91 (12), 90 (50), 89 (39), 76 (5), 75 (7), 64 (11), 63 (24), 62 (12), 51 (12); retention time (gc/fid and gc/ms) and mass spectrum were compared to that of the pure compound (Aldrich).

4-Cyanoacetophenone (**45**): ^{1}H nmr ($CDCl_3$, AC250) δ: 8.05 (d, 8.54 Hz, 2H), 7.78 (d, 8.54 Hz, 2H), 2.65 (s, 3H); ^{13}C nmr ($CDCl_3$, AC250) δ: 196.50 (s), 139.82 (s), 132.45 (d), 128.63 (d), 117.88 (s), 116.31 (s), 26.72 (q); ms *m/z*: 145 ($M^{+\bullet}$, 16%), 130 (100), 102 (57), 76 (12), 75 (19), 74 (6), 63 (4), 62 (3), 51 (15); retention time (gc/fid and gc/ms) and mass spectrum were compared to that of an authentic sample (Aldrich).

5'-Methyl-4-methylene-4'-oxospiro[cyclohexane-1,3'-pyrroline] (**46**): ir ($CDCl_3$) ν: 3098 (m), 3054 (m), 2930 (s), 2854 (m), 1728 (s), 1681 (w), 1651 (m), 1501 (m), 1442 (m), 1405 (w), 1377 (w), 1345 (w), 1276 (w), 1197 (w), 1115 (w), 1022 (w), 841 (s); ^{1}H nmr ($CDCl_3$, AC250) δ: 4.72 (s, 2H), 4.16-4.10 (m, 2H), 2.47-2.38 (dt (unresolved), observed splittings: 3.67 Hz, 4.27 Hz, 13.43 Hz, 14.04 Hz, 2H), 2.15 (t, 2.44 Hz, 3H), 2.16-2.05

(td, partially under triplet at 2.15 ppm, 4.88 Hz, 13.43 Hz, 2H), 1.67-1.56 (td (unresolved), observed splittings: 4.27 Hz, 12.20 Hz, 12.82 Hz, 2H), 1.50-1.41 (m, 2H); ^{13}C nmr ($CDCl_3$, AC250) δ: 206.79 (s), 170.91 (s), 146.16 (s), 108.64 (t), 67.13 (t), 45.73 (s), 33.75 (t), 31.25 (t), 13.95 (q); ms *m/z*: 177 ($M^{+\bullet}$, 6%), 108 (83), 93 (100), 91 (33), 80 (32), 79 (61), 78 (11), 77 (30), 67 (12), 65 (12), 55 (13), 54 (16), 53 (18).

4-(4-Cyanophenyl)-1-methylenecyclohexane (**47**): ir ($CDCl_3$) ν: 3070 (w), 2979 (w), 2930 (s), 2856 (m), 2228 (s), 1650 (m), 1607 (m), 1505 (m), 1444 (m), 1410 (w), 1180 (w), 1079 (w), 978 (w), 893 (s), 838 (s); ^1H nmr ($CDCl_3$, AC250) δ: 7.57 (d, 7.93 Hz, 2H), 7.30 (d, 7.93 Hz, 2H), 4.70 (s, 2H), 2.79-2.67 (m, 1H), 2.46-2.41 (m, 2.44 Hz, 11.59 Hz, 2H), 2.24-2.13 (m, 2H), 1.97 (d, 12.82 Hz, 2H), 1.61-1.44 (qd (unresolved), observed splittings: 3.67 Hz, 4.27 Hz, 12.21 Hz, 12.81 Hz, 2H); ^{13}C nmr ($CDCl_3$, AC250) δ: 152.22 (s), 147.72 (s), 131.62 (d), 127.61 (d), 119.02 (s), 109.72 (s), 107.95 (t), 44.17 (d), 34.91 (t), 34.71 (t); ms *m/z*: 197 ($M^{+\bullet}$, 60%), 182 (33), 168 (81), 155 (37), 142 (21), 129 (61), 116 (38), 103 (17), 89 (21), 79 (40), 68 (100), 53 (35); actual mass of ion $C_{14}H_{15}N$: 197.1204; measured: 197.1202.

2-(4-Cyanophenyl)-1,4-bis(methylene)cyclohexane (**48**): ir ($CDCl_3$) ν: 3075 (w), 2982 (w), 2937 (s), 2847 (m), 2227 (s), 1651 (m), 1607 (m), 1504 (w), 1442 (m), 1410 (w), 899 (s), 845 (s); ^1H nmr ($CDCl_3$, AC250) δ: 7.61 (d, 7.94 Hz, 2H), 7.36 (d, 8.54 Hz, 2H), 4.83 (s, 1H), 4.81 (s, 1H), 4.79 (s, 1H), 4.23 (s, 1H), 3.44 (t, 7.32 Hz, 1H), 2.55 (d, 7.93 Hz, 2H), 2.46-2.38 (m, 2H), 2.19-2.28 (m, 2H); ^{13}C nmr ($CDCl_3$, AC250) δ: 149.94 (s),

148.24 (s), 146.29 (s), 132.00 (d), 129.14 (d), 119.01 (s), 110.21 (t), 110.14 (s), 109.80 (t), 50.19 (d), 40.75 (t), 35.84 (t), 35.67 (t); ms *m/z*: 209 ($M^{+\bullet}$, 53%), 194 (13), 180 (15), 166 (19), 153 (21), 140 (26), 127 (21), 116 (22), 102 (74), 93 (100), 91 (32), 80 (56), 77 (38), 63 (15), 51 (20); actual mass of ion $C_{15}H_{15}N$: 209.1204; measured: 209.1194.

4,4"-Bis(methylene)dispiro[cyclohexane-1,1'-cyclobutane-2',1"-cyclohexane] (**49**): ir ($CDCl_3$) ν: 3071 (w), 2927 (s), 2855 (s), 1652 (w), 1458 (m), 1376 (w), 886 (m); ^1H nmr ($CDCl_3$, AC250) δ: 4.56 (s, 4H), 2.24-1.94 (m, 8H), 1.84-1.71 (m, 8H), 1.74 (s, 4H); ^{13}C nmr ($CDCl_3$, AC250) δ: 150.04 (s), 105.89 (t), 42.76 (s), 33.87 (t), 29.71 (t), 26.43 (t); ms *m/z*: 216 ($M^{+\bullet}$, 2%), 201 (3), 160 (8), 120 (7), 109 (25), 108 (24), 106 (61), 93 (100), 91 (42), 79 (71), 77 (36), 67 (31), 53 (21).

1-(4'-Methylphenyl)-2-(4-methylenecyclohexyl)ethane (**50**): ir ($CDCl_3$) ν: 3064 (m), 3034 (m), 2927 (s) 2854 (m), 1481 (m), 1431 (m), 1078 (w), 908 (s); ^1H nmr ($CDCl_3$, AC250) δ: 7.07 (s, 4H), 4.59 (s, 2H), 2.59 (t, 7.93 Hz, 2H), 2.31 (s, 3H), 2.26 (s, 2H), 2.10-1.93 (m, 2H), 1.93-1.80 (m, 2H), 1.53 (s, 2H), 1.25 (s, br, 3H (CH_2 + CH)); ^{13}C nmr ($CDCl_3$, AC250) δ: 150.02 (s), 139.85 (s), 134.98 (s), 128.95 (d), 128.17 (d), 106.55 (t), 38.61 (t), 36.70 (d), 34.56 (t), 34.33 (t), 32.89 (t), 29.69 (t), 20.97 (q); ms *m/z*: 214 ($M^{+\bullet}$, 20%), 157 (6), 143 (5), 119 (11), 118 (58), 105 (100), 91 (24), 79 (25), 77 (24), 67 (19), 53 (12).

Analysis of the mixture by gc/ms also indicated the presence of *1,2-bis(4-cyanophenyl)-ethane*: ms *m/z*: 232 ($M^{+\bullet}$, 29%), 141 (100), 115 (28), 91 (9), 77 (3), 65 (7), 51 (5).

Irradiation of a mixture of 1,4-bis(methylene)cyclohexane (2), 1,4-dicyanobenzene (33), and biphenyl (34) in acetonitrile-d_3.

A solution of 1,4-bis(methylene)cyclohexane (**2**) (0.0110 g, 1.0×10^{-4} mol), 1,4-dicyanobenzene (**33**) (0.0085 g, 6.6×10^{-5} mol), and biphenyl (**34**) (0.0074 g, 4.8×10^{-5} mol) in 1 mL acetonitrile-d_3 was irradiated for 5 days. Deuterium incorporation was checked by gc/ms analysis. Identification of the products was based on the mass spectra and the retention times (gc/ms and gc/fid) of the compounds.

Electrolysis of a solution of 1,4-bis(methylene)cyclohexane (2) in acetonitrile-methanol (3:1).

A solution of tetraethylammonium perchlorate (TEAP) (4.6 g, 0.1 M) in 200 mL acetonitrile-methanol (3:1) was degassed by nitrogen ebullition for 30 min. After this period 1,4-bis(methylene)cyclohexane (**2**) (2.5 g, 2.3×10^{-2} mol) was added to the solution and the mixture was electrolyzed (ΔV = 2.55 V) for 75 hours at room temperature. During this period 3800 C were consumed. The solvent was evaporated and the residue was chromatographed on silica gel (mplc) using hexanes. Further purification of the products and mixtures was achieved by prep-gc.

2-Methoxy-1,4-bis(methylene)cyclohexane (**52**): ir ($CDCl_3$) ν: 3079 (m), 2979 (m), 2938 (s), 2855 (m), 2825 (m), 1654 (m), 1446 (m), 1095 (s), 901 (s), 842 (m), 746 (s), 712

(w); ^{1}H nmr ($CDCl_3$, AC250) δ: 4.93 (s, 2H), 4.79 (d, 6.71 Hz, 2H), 3.69 (dd (unresolved), observed splittings: 4.27 Hz, 4.88 Hz, 1H), 3.26 (s, 3H), 2.42 (d, 4.27 Hz, 2H), 2.35-2.26 (m, 2H), 2.19-2.14 (m, 2H); ^{13}C nmr ($CDCl_3$, AC250) δ: 146.60 (s), 144.63 (s), 110.48 (t), 110.36 (t), 81.66 (d), 56.00 (q), 41.95 (t), 35.67 (t), 31.83 (t); ms *m/z*: 138 ($M^{+\bullet}$, 23%), 123 (15), 106 (44), 93 (27), 91 (100), 79 (51), 77 (36), 71 (19), 67 (27), 55 (25), 53 (30).

4-Methoxy-4-methyl-1-methylenecyclohexane (**53**): ir ($CDCl_3$) ν: 2924 (s), 2853 (m), 1737 (m), 1649 (w), 1462 (w), 1078 (w), 912 (w), 886 (w), 743 (m); ^{1}H nmr ($CDCl_3$, AC250) δ: 4.61 (s, 2H), 3.21 (s, 3H), 2.36-2.24 (td (unresolved), observed splittings: 4.27 Hz, 4.88 Hz, 11.59 Hz, 12.21 Hz, 13.43 Hz, 2H), 2.11-2.02 (dt, 4.27 Hz, 13.43 Hz, 2H), 1.89-1.80 (m, 2H), 1.43-1.31 (m, 2H), 1.13 (s, 3H); ^{13}C nmr ($CDCl_3$, AC250) δ: 148.90 (s), 106.78 (t), 72.85 (s), 48.60 (q), 36.91 (t), 30.44 (t), 23.73 (q); ms *m/z*: 140 ($M^{+\bullet}$, 0.6%), 125 (21), 111 (35), 108 (76), 93 (100), 91 (29), 85 (15), 79 (41), 77 (29), 72 (24), 67 (32), 55 (38).

1-(Methoxymethyl)-4-methylenecyclohexene (**54**): ir ($CDCl_3$) ν: 3072 (w), 2982 (m), 2908 (s), 2843 (m), 2817 (m), 1654 (m), 1449 (m), 1378 (w), 1359 (w), 1278 (w), 1215 (w), 1193 (m), 1152 (m), 1102 (s), 1053 (w), 958 (w), 936 (w), 909 (m), 887 (s), 815 (w); ^{1}H nmr ($CDCl_3$, AC250) δ: 5.64 (s, 1H), 4.76 (s, 2H), 3.79 (s, 2H), 3.29 (s, 3H), 2.81 (s, 2H), 2.36-2.31 (3 line pattern (unresolved), observed splittings: 6.71 Hz, 6.11 Hz, 2H), 2.16 (d, br. 5.49 Hz, 2H); ^{13}C nmr ($CDCl_3$, AC250) δ: 145.45 (s), 134.91 (s), 123.87

(d), 107.85 (t), 76.62 (t), 57.60 (q), 33.23 (t), 31.42 (t), 27.98 (t); ms *m/z*: 138 ($M^{+\bullet}$, 9%), 123 (5), 106 (36), 93 (30), 91 (100), 79 (32), 78 (52), 77 (46), 71 (23), 65 (20), 53 (18), 51 (19); actual mass of ion $C_9H_{14}O$: 138.1045; measured: 138.1060.

1-(Methoxymethyl)-4-methylenecyclohexanol (**55**): ir ($CDCl_3$) ν: 3438 (s), 3070 (w), 2979 (m), 2934 (s), 2891 (m), 2854 (m), 2827 (m), 1715 (w), 1683 (m), 1650 (m), 1445 (m), 1408 (w), 1372 (w), 1330 (w), 1273 (w), 1230 (w), 1195 (m), 1105 (s), 954 (m), 914 (s), 889 (m), 745 (m); ^1H nmr ($CDCl_3$, AC250) δ: 4.64 (s, 2H), 3.40 (s, 3H), 3.25 (s, 2H), 2.74-2.34 (m, 2H), 2.22 (s, 1H), 2.17-2.08 (dt (unresolved), observed splittings: 4.27 Hz, 4.88 Hz, 13.43 Hz, 14.04 Hz, 2H), 1.79-1.71 (m, 2H), 1.50-1.38 (m, 2H); ^{13}C nmr ($CDCl_3$, AC250) δ: 148.81 (s), 107.07 (t), 80.35 (t), 70.53 (s), 59.40 (q), 35.50 (t), 30.04 (t); ms *m/z*: 138 (8%), 111 (100), 106 (9), 93 (41), 91 (28), 81 (21), 77 (21), 69 (14), 67 (18), 55 (18), 53 (17).

4-(Dimethoxymethyl)-1-methylenecyclohexane (**56**): ir ($CDCl_3$) ν: 3071 (w), 2983 (m), 2936 (s), 2860 (m), 2832 (m), 1650 (m), 1445 (m), 1382 (m), 1249 (w), 1220 (w), 1186 (m), 1134 (s), 1102 (m), 1076 (s), 1054 (s), 1011 (w), 970 (m), 891 (s); ^1H nmr ($CDCl_3$, AC250) δ: 4.61 (3 line multiplet, 1.84 Hz, 13.43 Hz, 2H), 4.02 (d, 7.32 Hz, 1H), 3.34 (s, 6H), 2.35-2.29 (m, 2H), 2.07-1.95 (dt (unresolved), observed splittings: 3.66 Hz, 4.27 Hz, 12.82 Hz, 13.43 Hz, 2H), 1.94-1.83 (m, 2H), 1.82-1.68 (10 line pattern, 1H), 1.19-1.03 (qd (unresolved), observed splittings: 3.66 Hz, 4.27 Hz, 11.59 Hz, 12.21 Hz, 12.82 Hz, 2H); ^{13}C nmr ($CDCl_3$, AC250) δ: 149.14 (s), 107.99 (d), 106.92 (t), 53.52 (q), 39.63

(d), 34.98 (t), 29.25 (t); ms *m/z*: 170 ($M^{+\bullet}$, 0.7%), 139 (7), 138 (6), 107 (16), 91 (15), 79 (25), 75 (100), 71 (23), 67 (13), 55 (13), 53 (17).

4-Methoxy-4-(methoxymethyl)-1-methylenecyclohexane (**57**): ir ($CDCl_3$) ν: 3071 (w), 2980 (m), 2934 (s), 2880 (s), 2829 (m), 1650 (m), 1457 (m), 1442 (m), 1196 (m), 1144 (m), 1103 (s), 1076 (s), 979 (w), 889 (m), 734 (m); ^1H nmr ($CDCl_3$, AC250) δ: 4.62 (s, 2H), 3.37 (s, 3H), 3.31 (s, 2H), 3.27 (s, 3H), 2.37-2.25 (td (unresolved), observed splittings: 3.66 Hz, 4.27 Hz, 12.20 Hz, 12.82 Hz, 13.43 Hz, 2H), 2.13-2.04 (dt, 4.27 Hz, 13.42 Hz, 2H), 1.94-1.86 (m, 2H), 1.44-1.32 (td (unresolved), observed splittings: 4.27 Hz, 4.88 Hz, 12.21 Hz, 12.82 Hz, 13.43 Hz, 2H); ^{13}C nmr ($CDCl_3$, AC250) δ: 148.75 (s), 106.89 (t), 76.06 (t), 74.41 (s), 59.36 (q), 49.21 (q), 32.20 (t), 29.79 (t); ms *m/z*: 142 (0.1%), 138 (1), 125 (100), 109 (4), 93 (62), 91 (38), 79 (13), 77 (32), 71 (7), 67 (17), 53 (15).

4-(1-Methoxy-4-methylenecyclohexyl)methanol (**58**): ir ($CDCl_3$) ν: 3447 (s), 3071 (w), 2936 (s), 1706 (m), 1651 (m), 1607 (w), 1459 (m), 1442 (m), 1072 (s), 1050 (s), 888 (s), 852 (m), 745 (m), 715 (m), 671 (m); ^1H nmr ($CDCl_3$, AC250) δ: 4.65 (s, 2H), 3.50 (s, 2H), 3.25 (s, 3H), 2.35-2.23 (td (unresolved), observed splittings: 4.27 Hz, 11.60 Hz, 13.43 Hz, 2H), 2.17-2.08 (dt, 4.88 Hz, 13.43 Hz, 2H), 1.76 (s, br. 1H), 1.46-1.31 (m, 2H); ^{13}C nmr ($CDCl_3$, AC250) δ: 148.30 (s), 107.40 (t), 75.23 (s), 64.75 (t), 48.68 (q), 31.83 (t), 29.89 (t); ms *m/z*: 125 (100%), 109 (2), 95 (5), 93 (49), 91 (30), 79 (8), 77 (24), 67 (13), 55 (7), 53 (9).

4-Methoxy-4-(methoxymethyl)cyclohex-2-en-1-one (**59**): ir ($CDCl_3$) ν: 2936 (w), 2894 (w), 2831 (w), 1679 (s), 1455 (w), 1384 (w), 1199 (w), 1099 (w), 910 (s), 807 (w), 734 (s); ^1H nmr ($CDCl_3$, AC250) δ: 6.84 (d, 10.38 Hz, 1H), 6.12 (d, 10.37 Hz, 1H), 3.52 (s, 2H), 3.42 (s, 3H), 3.34 (s, 3H), 2.73-2.40 (m, 2H), 2.32-2.04 (m, 2H); ^{13}C nmr ($CDCl_3$, AC250) δ: 198.83 (s), 150.15 (d), 131.93 (d), 75.88 (t), 74.74 (s), 59.64 (q), 51.30 (q), 34.41 (t), 27.80 (t); ms *m/z*: 170 ($M^{+\bullet}$, 5%), 140 (7), 125 (100), 107 (8), 97 (54), 79 (23), 77 (17), 67 (25), 65 (14), 55 (16), 53 (23); actual mass of ion $C_9H_{14}O_3$: 170.0943; measured: 170.0943.

3,6-Dimethoxy-3,6-bis(methoxymethyl)cyclohex-1-ene (**60**), mixture of diastereomers: ir ($CDCl_3$) ν: 2980 (m), 2933 (s), 2887 (s), 2828 (s), 1686 (w), 1457 (m), 1394 (w), 1253 (w), 1196 (m), 1155 (w), 1105 (s), 1081 (s), 1007 (w), 961 (w), 913 (s), 879 (w), 781 (w), 733 (s); ^1H nmr ($CDCl_3$, AC250) δ: 5.89 (d, 8.54 Hz, 2H), 3.40 (s, 5H), 3.38 (s, 3H), 3.33 (s, 2H), 3.30 (s, 3H), 3.25 (s, 3H), 2.06-1.89 (m, 1H), 1.88-1.82 (m, 2H), 1.75-1.61 (m, 1H); ^{13}C nmr ($CDCl_3$, AC250) δ: 133.65 (d), 133.46 (d), 77.03 (t), 76.93 (t), 75.26 (s), 74.45 (s), 59.66 (q), 59.52 (q), 50.91 (q), 50.56 (q), 25.32 (t), 25.25 (t); ms *m/z*: 185 (42%), 153 (42), 140 (16), 127 (14), 125 (35), 123 (18), 121 (100), 97 (17), 95 (15), 91 (16), 79 (12), 77 (16), 75 (20), 65 (10), 53 (10); actual mass of ion $C_{10}H_{17}O_3$: 185.1178; measured: 185.1183.

Acid-catalyzed reaction of 1,4-bis(methylene)cyclohexane in an acetonitrile-methanol (3:1) mixture.

1,4-Bis(methylene)cyclohexane (**2**) (0.21 g, 1.9×10^{-3} mol) was dissolved in 16 mL of an acetonitrile-methanol (3:1) mixture and concentrated sulphuric acid (0.18 g, 1.8×10^{-3} mol) was added dropwise. The mixture was stirred for 24 hours and the products were analyzed by gc/ms and gc/fid. The identification of **53** was based on the mass spectrum and on the retention times (gc/ms and gc/fid).

Electrolysis of a solution of 1,4-bis(methylene)cyclohexane (2) in acetonitrile.

A solution of tetraethylammonium perchlorate (TEAP (4.6 g, 0.1 M) in 200 mL acetonitrile was degassed for 30 minutes by nitrogen ebullition. 1,4-Bis(methylene)-cyclohexane (**2**) (2.5 g, 2.3×10^{-2} mol) was then added to the solution and the mixture was electrolyzed (ΔV = 2.55 V) for 21 days. A total of 1728 C were consumed during this period. The solvent was evaporated and the residue was chromatographed on silica gel (mplc) using a hexanes - diethylether gradient. The products and some mixtures were further purified by dcfc using hexanes or a hexanes - 5% diethylether/95% hexanes gradient. Compound **65** was further purified by prep-gc.

1,4-Dimethylbenzene (**64**): identified on basis of its mass spectrum: *m/z*: 106 ($M^{+\bullet}$, 57%), 105 (29), 103 (8), 91 (100), 79 (11), 78 (10), 77 (19), 65 (10), 63 (9), 53 (5), 52 (7), 51 (18); retention time (gc/fid and gc/ms) and mass spectrum compared to that of an authentic sample (Aldrich).

4-Methylbenzaldehyde (**65**): ^{1}H nmr ($CDCl_3$, AC250) δ: 9.97 (s, 1H), 8.00 (d, 7.94 Hz, 2H), 7.28 (d, 7.93 Hz, 2H), 2.44 (s, 3H); ^{13}C nmr ($CDCl_3$, AC250) δ: 192.03 (d), 145.55 (s), 134.16 (s), 129.85 (d), 129.70 (d), 21.88 (q); ms *m/z*: 120 ($M^{+\bullet}$, 77%), 119 (94), 91 (100), 89 (12), 74 (3), 65 (40), 64 (5), 63 (24), 62 (11), 51 (16); retention time (gc/fid and gc/ms), mass spectrum and ^{1}H and ^{13}C spectra compared to those of the pure compound (Aldrich).

N-[4-Methylbenzyl]acetamide (**66**): recrystallized from cyclohexane; mp: 107-108°C (lit:[84] 111-112 °C); ir ($CDCl_3$) ν: 3291 (s), 3076 (w), 2923 (m), 2854 (w), 1646 (s), 1635 (s), 1553 (s), 1518 (m), 1463 (w), 1436 (w), 1374 (w), 1356 (w), 1290 (w), 1279 (w), 1094 (w), 1024 (w), 806 (w), 731 (w); ^{1}H nmr ($CDCl_3$, AC250) δ: 7.20-7.12 (m, 8.55 Hz, 4H), 5.77 (s, br. 1H), 4.38 (d, 5.49 Hz, 2H), 2.34 (s, 3H), 2.01 (s, 3H); ^{13}C nmr ($CDCl_3$, AC250) δ: 169.80 (s), 137.26 (s), 135.14 (s), 129.35 (d), 127.86 (d), 43.50 (t), 23.28 (q), 21.07 (q); ms *m/z*: 163 ($M^{+\bullet}$, 62%), 148 (11), 120 (45), 106 (100), 105 (34), 91 (23), 77 (22), 65 (13); actual mass of ion $C_{10}H_{13}NO$: 163.0997; measured: 163.1000.

N-(1-Methyl-4-methylenecyclohexyl)acetamide (**67**): mp: 94 - 95 °C; ir ($CDCl_3$) ν: 3316 (s), 3077 (w), 2966 (m), 2934 (m), 2852 (w), 1647 (s), 1553 (s), 1442 (m), 1371 (m), 1323 (w), 1299 (w), 1271 (w), 1132 (w), 951 (w), 885 (w); ^{1}H nmr ($CDCl_3$, AC250) δ: 5.22 (s, br. 1H), 4.64 (s, 2H), 2.16 (t, 4.88 Hz, 2H), 2.14 (s, 2H), 2.08 (t, 4.27 Hz, 2H), 1.96 (s, 3H), 1.57-1.45 (m, 2H), 1.40 (s, 3H); ^{13}C nmr ($CDCl_3$, AC250) δ: 169.70 (s),

147.47 (s), 107.73 (t), 53.09 (s), 37.71 (t), 30.40 (t), 25.67 (q), 24.61 (q); ms *m/z*: 167 ($M^{+\bullet}$, 8%), 110 (29), 108 (87), 93 (100), 91 (20), 79 (27), 70 (18), 60 (63); actual mass of ion $C_{10}H_{17}NO$: 167.1310; measured: 167.1295.

N-(1,4-Dimethylcyclohex-3-enyl)acetamide (**68**): ir ($CDCl_3$) ν: 3303 (s), 3077 (w), 2964 (m), 2923 (s), 2852 (w), 1650 (s), 1551 (s), 1442 (m), 1372 (m), 1301 (w), 1277 (w); ^1H nmr ($CDCl_3$, AC250) δ: 5.24 (s, br. 1H), 2.31 (dt, 5.49 Hz, 1H), 2.13 (s, 2H), 1.92 (s, 5H, CH_3 + CH_2), 1.66 (s, 3H), 1.51 (dt, 7.33 Hz, 1H), 1.41 (s, 3H); ^{13}C nmr ($CDCl_3$, AC250) δ: 169.86 (s), 134.26 (s), 117.62 (d), 51.52 (s), 38.59 (t), 31.49 (t), 27.55 (t), 25.07 (q), 24.49 (q), 23.26 (q); ms *m/z*: 108 (96%), 99 (7), 93 (100), 91 (22), 77 (15), 60 (24), 57 (68); actual mass of ion $C_{10}H_{17}NO$: 167.1310; measured: 167.1287.

Acid-catalyzed reaction of 1,4-bis(methylene)cyclohexane (2) in acetonitrile.

Concentrated sulphuric acid (0.20 g, $1.8x10^{-3}$ mol) was added dropwise to a solution of 1,4-bis(methylene)cyclohexane (**2**) (0.18 g, $1.9x10^{-3}$ mol) in acetonitrile (15 mL). The mixture was stirred for 14 hours. Analysis of the product mixture by gc/ms and gc/fid showed that three products (**64**, **67**, and **68**) were formed in a ratio of 10:5:1 (gc/fid). This ratio changed to 48:22:1 after 24 hours. The identification of the products was based on their mass spectra and their retention times (gc/ms and gc/fid).

Synthesis of p-cyanoacetophenone azine (69).

p-Cyanoacetophenone (10 g, 6.9×10^{-2} mol) was added to a stirred solution of hydrazine hydrate (85% solution, 2 mL, 3.5×10^{-2} mol) in 50 mL ethanol and the mixture was refluxed for 2 days. After cooling, a solid material (azine) formed which was removed by filtration. The azine was recrystallized from ethanol-dichloromethane (orange needles); yield: 4.2 g (43%). Crystal data obtained by X-ray crystallography were consistent with those reported in the literature.[97]

1,4-di-(4-cyanophenyl)-1,4-dimethyl-2,3-diaza-1,3-butadiene (**69**)

mp (corrected): 242 - 243°C; uv (CH_2Cl_2): $\varepsilon_{292} = 6.2 \times 10^4$ L mol^{-1} cm^{-1}; ir (Nicolet, KBr) ν: 3406 (w), 3062 (w), 3016 (w), 2220 (s), 1602 (s), 1551 (m), 1500 (m), 1405 (m), 1366 (s), 1284 (s), 839 (s); ^1H nmr ($CDCl_3$, 400.13 MHz) δ: 8.01 (d, 8.45 Hz, 4H), 7.72 (d, 8.40 Hz, 4H), 2.32 (s, 6H) ; ^{13}C nmr ($CDCl_3$, 100.61 MHz) δ: 156.77 (s), 141.99 (s), 132.22 (d), 127.22 (d), 118.54 (s), 113.32 (s), 15.02 (q); ms *m/z*: 287 ($M^{+\bullet}$+1, 7%), 286 (34), 244 (4), 230 (7), 184 (12), 157 (8), 143 (16), 129 (8), 116 (5), 102 (38), 75 12), 51 (9); calculated for $C_{18}H_{14}N_4$: C 75.51, H 4.93, N 19.57; found: C 75.23, H 4.90, N 19.64; actual mass of ion $C_{18}H_{14}N_4$: 286.1218; measured: 286.1210.

Synthesis of benzophenone azine (70).

Benzophenone (18 g, 1.0×10^{-1} mol) and hydrazine hydrate (85% solution, 4.0 g, 6.8×10^{-2} mol) were added to 50 mL ethanol. After the addition of 10 drops of concentrated HCl, the solution was refluxed for 5 hours and then cooled overnight. The

crystals (hydrazone) were collected and dissolved in 50 mL ethanol with 4 g (2.2×10^{-2} mol) benzohenone and 15 drops of conc. HCl. The solution was refluxed for 5 hours and then cooled overnight. The crystals (azine) were collected and recrystallized from ethanol-dichloromethane (small off-white plates); yield: 17 g (78%). Crystal data obtained by X-ray crystallography were consistent with those reported in the literature.[98]

1,1,4,4-tetraphenyl-2,3-diaza-1,3-butadiene (70)

mp (corrected): 164 - 165°C; uv (CH_2Cl_2): $\varepsilon_{280} = 3.2 \times 10^4$ L mol^{-1} cm^{-1}, $\varepsilon_{316} = 2.7 \times 10^4$ L mol^{-1} cm^{-1}; ir (Nicolet, KBr) ν: 3083 (m), 3054 (m), 3025 (m), 1583 (m), 1564 (s), 1487 (m), 1441 (s), 1317 (s), 1178 (m), 1074 (m), 981 (m), 954 (m), 769 (s), 691 (s), 658 (s); ^{1}H nmr (AC250, $CDCl_3$) δ: 7.52-7.23 (m, 20H); ^{13}C nmr (AC250, $CDCl_3$) δ: 158.88 (s), 138.15 (s), 135.50 (s), 129.55 (d), 129.30 (d), 128.64 (d), 127.99 (d), 127.84 (d); ms *m/z*: 361 ($M^{+\bullet}$+1, 13%), 360 (53), 359 (43), 283 (100), 257 (13), 256 (13), 205 (7), 180 (28), 165 (45), 77 (54), 51 (17); actual mass of ion $C_{26}H_{20}N_2$: 360.1626; measured: 360.1653.

Irradiation of p-cyanoacetophenone azine in dichloromethane through quartz

A solution of 0.61 g (2.1×10^{-3} mol) *p*-cyanoacetophenone azine in 80 mL dichloromethane was irradiated for 4 days through quartz with the 1-kW lamp. The reaction was followed by gc/ms and gc/fid. The solvent was evaporated and the starting material (azine; 40% recovered) was separated from the product by washing with ethanol. The product was identified as *p*-cyanoacetophenone (mass spectrum and retention time); yield: 55% based on reacted azine.

Irradiation of p-cyanoacetophenone azine in dichloromethane through Pyrex

A solution of 0.114 g (4.0×10^{-4} mol) *p*-cyanoacetophenone azine in 40 mL dichloromethane was irradiated for 4 days through Pyrex with the 1-kW lamp. The reaction was followed by gc/ms and gc/fid. Conversion of the starting material after 4 days as determined by gc/fid was 10%. A small amount of *p*-cyanoacetophenone was detected in the final product mixture.

Irradiation of benzophenone azine in dichloromethane through quartz

A solution of 0.50 g (1.8×10^{-3} mol) benzophenone azine in 200 mL dichloromethane was irradiated through quartz with the 1-kW lamp for 32 hours. The reaction was followed by gc/fid and gc/ms. The solvent was removed by rotary evaporation and the mixture was chromatographed on silica gel. Benzophenone azine (0.246 g, 51%) and benzophenone (0.152 g, 60%) were isolated from the mixture. Identification was based on mass spectra, retention time, and infrared spectra which were compared to those of the original compounds. Other products, tentatively identified on basis of their mass spectra and retention times, are benzophenone imine and triphenyl-isoindole.

Irradiation of benzophenone azine in dichloromethane through Pyrex

A solution of 60 mg (1.7×10^{-4} mol) benzophenone azine in 40 mL dichloro-methane was irradiated through Pyrex with the 1-kW lamp for 63 hours. The reaction was

monitored by gc/ms and gc/fid. Only the starting material could be detected. Evaporation of the solvent after completion of the reaction and analysis of the residue by gc/ms and gc/fid indicated the presence of a small amount of benzophenone.

Irradiation of benzophenone azine in dichloromethane through quartz in the presence of a radical scavenger

A solution of 73 mg (2.0×10^{-4} mol) benzophenone azine and 44 mg (2.2×10^{-4} mol) 2,6-di-*tert*-butyl-4-methylphenol in 40 mL dichloromethane was irradiated through quartz with the 1-kW lamp for 26 hours. Analysis of the reaction mixture revealed the presence of three major products: benzophenone, benzophenone imine, and triphenyl-isoindole. Identification was based on the mass spectra and retention times of the compounds. The phenol was no longer present in the mixture.

Irradiation of benzophenone azine in dichloromethane through quartz in the presence of an acid catalyst

A solution of 72 mg (2.0×10^{-4} mol) benzophenone azine and 26 mg (2.3×10^{-4} mol) trifluoroacetic acid in 40 mL dichloromethane was irradiated through quartz with the 1-kW lamp for 26 hours. Analysis of the reaction mixture by gc/fid and gc/ms revealed the presence of three major products: benzophenone, benzophenone imine, and triphenyl-isoindole. Identification was based on their mass spectra and retention times.

Irradiation of benzophenone imine in dichloromethane through quartz in the presence of tert-butylperoxide

A solution of 81 mg (4.4×10^{-4} mol) benzophenone imine and 583 mg (4.0×10^{-3} mol) *tert*-butyl peroxide in 40 mL dichloromethane was irradiated through quartz with the 1-kW lamp for 5 hours. Analysis of the reaction mixture by gc/fid and gc/ms indicated that the imine had largely reacted. The major product was not benzophenone.

Irradiation of benzophenone imine in dichloromethane through quartz

A solution of 80 mg (4.4×10^{-4} mol) benzophenone imine in 40 mL dichloromethane was irradiated through quartz with the 1-kW lamp for 5 hours. Analysis of the reaction mixture by gc/fid and gc/ms indicated that no significant reaction had taken place.

Irradiation of benzophenone imine in benzene through Pyrex in the presence of tert-butylperoxide

A solution of 10.5 mg (mol) benzophenone imine and 61.5 mg (mol) *tert*-butyl peroxide in 2 mL benzene was irradiated through Pyrex for 5 hours with the 1-kW lamp. Analysis of the mixture by gc/fid and gc/ms indicated the presence of three major products which were identified on basis of their mass spectra and their retention times as benzophenone, biphenyl, and benzophenone azine.

Irradiation of benzophenone imine in benzene-d_6 through Pyrex in the presence of tert-butylperoxide

A solution of 22 mg (mol) benzophenone imine and 129 mg (mol) *tert*-butyl peroxide in 2 mL benzene was irradiated through Pyrex for 5 hours with the 1-kW lamp.

Analysis of the mixture by gc/ms indicated that no deuterium had been incorporated in biphenyl.

Laser flash photolysis experiments

The nanosecond laser flash photolysis system that was used for these experiments is based on a standard system.[20] Details will be described elsewhere.[99] Quartz cells (7 × 7 mm^2) were used to contain the samples and were deaerated by nitrogen or purged with oxygen as required for at least 15 minutes. In other cases a flow system was used. The lasers used for sample excitation are a Lambda Physik CompEX 102 excimer laser (308 nm; 150 mJ/pulse; 10 ns/pulse) or a Continuum NY61-10 Nd:YAG laser (266 nm; 5 mJ/pulse; 8 ns/pulse).

Chapter 4

Photochemical reactions and electrochemical oxidation of methylenecyclopropane

4.1 Introduction

According to the calculations reported in Chapter 2, methylenecyclopropane radical cation ($\mathbf{1}^{+\bullet}$)* is the highest energy species of the five related compounds that were considered. From Scheme 3.1 it is clear that reaction of this radical cation with its neutral precursor is highly exothermic. Because of the large exothermicity of this reaction it is hard to make predictions about the ultimate outcome of the reaction, i.e. the type of product(s) that will be formed. The dimerization of $\mathbf{1}^{+\bullet}$ with **1** in the gas phase, as calculated by *ab initio* methods, leads to the formation of only one type of dimer (Scheme 4.1). However, doing these experiments in the liquid phase could have a dramatic effect on product formation. In Chapter 3, product formation from the radical cation of 1,4-bis(methylene)cyclohexane (**2**) was discussed. This isomer is the lowest energy species of this series and it is likely that some of the products arising from the reaction of $\mathbf{1}^{+\bullet}$ with **1** will resemble those from the reaction of $\mathbf{2}^{+\bullet}$.

* It must be noted that ring opening of $\mathbf{1}^{+\bullet}$ to give $\mathbf{1a}^{+\bullet}$ will proceed rapidly. It is most likely that in these reactions the reactive species is $\mathbf{1a}^{+\bullet}$, not $\mathbf{1}^{+\bullet}$.

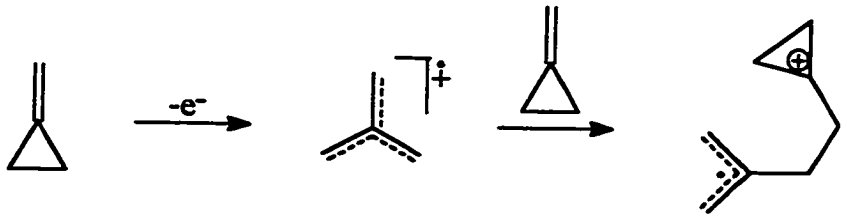

1 $1a^{\bullet+}$

Scheme 4.1. Dimerization of methylenecyclopropane radical cation in the gas phase leads to only one type of dimer.

Little experimental work has been done on the radical cations of MCP and TMM.[100-104] The parent molecules have never been studied, except for a recent ESR study.[104] Other studies have only involved substituted methylenecyclopropanes.

Blackstock and Painter[100] recently generated a TMM radical cation by using diazene (**75**) and tetracyanoethylene (TCNE) as the electron acceptor. The products from this reaction were found to be addition products (Scheme 4.2). The authors claimed that only product **78** was formed by a radical cation mechanism; **76** and **77** were the result of a biradical reaction. Evidence for this observation was the absence of an appreciable solvent effect on the formation of **76** and **77** and the fact that only **76** and **77** were formed in the thermal (dark) reaction.

The thermal reaction of 2-phenyl-1-methylenecyclopropane or 2,2-diphenyl-1-methylenecyclopropane with TCNE also results in the formation of cycloaddition products.[101] The mechanism for this reaction is believed to be a concerted pathway. Diradical intermediates or dipolar (zwitterionic) intermediates were ruled out on the basis

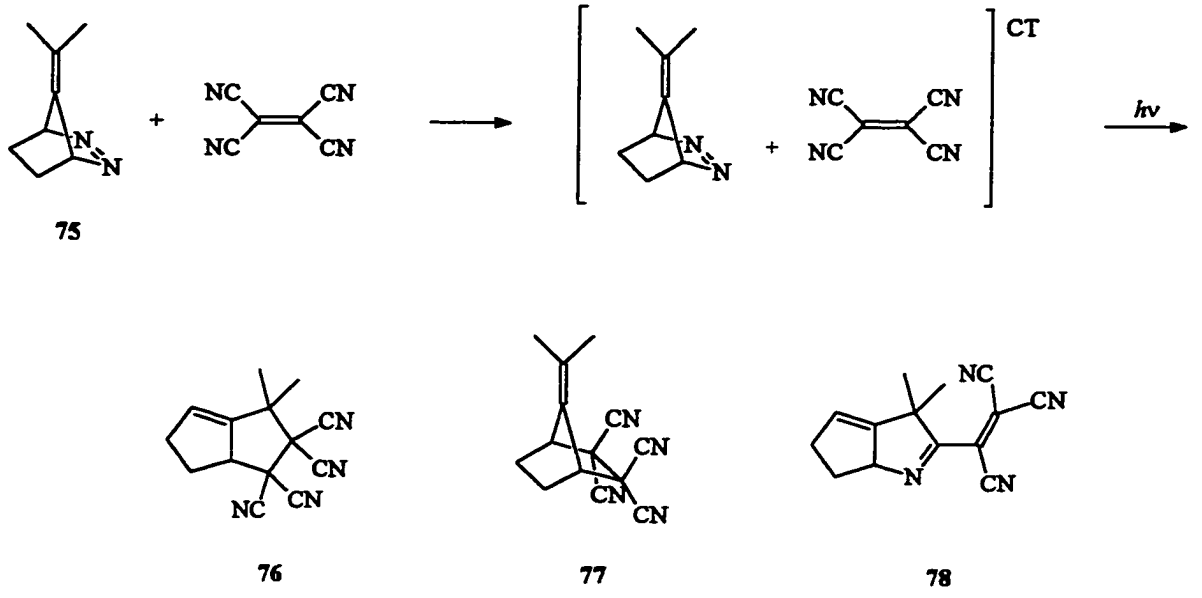

Scheme 4.2 Product formation in the photoreaction of diazene (**75**) with tetracyanoethylene.[100]

of the observation of a lack of a solvent effect and the fact that the reaction was not quenched by radical scavengers.

Earlier, Roth and co-workers studied the radical cation of 2,2-dianisyl-1-methylenecyclopropane.[102] The radical cation was generated by photoinduced electron transfer using chloranil (triplet) as the electron acceptor. The products from this reaction were also addition (MCP-chloranil) products (Scheme 4.3). CIDNP studies[102] indicated the presence of two different types of radical cations: (a) a ring-opened species in which the spin is delocalized in an allyl moiety and the charge is localized on the diarylmethylene group, and (b) a ring-closed species in which the spin is localized on the tertiary cyclopropane carbon and the charge is localized on the diarylmethylene group (Figure 4.1).

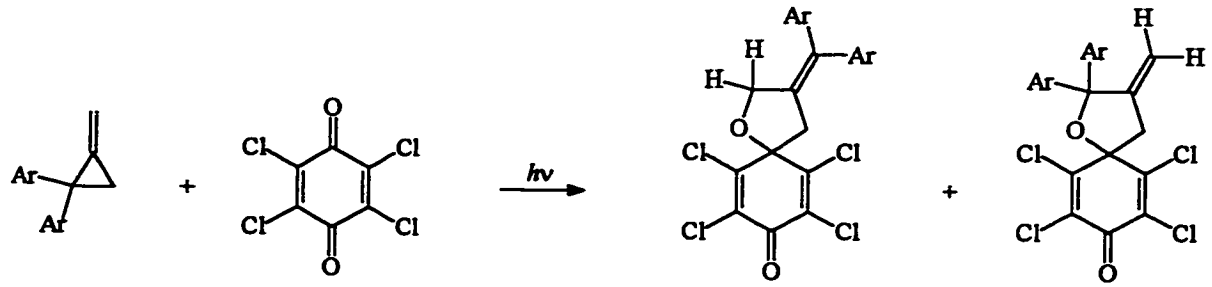

$Ar = C_6H_4OCH_3$

Scheme 4.3 Products from the photoreaction of 2,2-dianisyl-1-methylenecyclopropane with chloranil.[102]

Figure 4.1 Intermediates detected in the photoreaction of 2,2-dianisyl-1-methylenecyclopropane with chloranil using CIDNP.[102]

It is clear that the chemistry and behaviour of the radical cation of methylenecyclopropane as well as that of the trimethylenemethane radical cation are interesting and that there is some controversy regarding reaction pathways. More interesting, the reactions of the parent molecules (radical cations) have not been studied. Obviously, the structure and reactivity of these substituted species will be different from that of the unsubstituted compound.

In this Chapter, the results of the reactions of methylenecyclopropane (**1**) studied by photochemical and electrochemical methods in the presence and in the absence of nucleophiles are presented and the possible mechanisms for product formation are discussed.

4.2 Results and Discussion

Photochemistry of methylenecyclopropane (1) in the absence of a nucleophile.

It has been shown that radical cations undergo rapid nucleophilic addition (see for example Chapter 3). This is useful since the product distribution will enable us to assess spin and charge distributions in the radical cations. However, a main goal of this research is to determine whether the radical cation of methylenecyclopropane (MCP, **1**) undergoes dimerization and, if so, what is the structure(s) of the dimeric product(s). Addition of a nucleophile to the reaction mixture might compete with the dimerization as was observed before (Chapter 3). Dimerization is also more likely to occur when the concentration of MCP is greater. In order to favour dimerization, an attempt was made to generate the radical cation of MCP by photoinduced electron transfer using 1.4-dicyanobenzene as the electron acceptor, with the alkene present in excess (MCP:DCB = 5:1), and in the absence of a nucleophile.

Irradiation of a 0.5 M solution of methylenecyclopropane (**1**) in acetonitrile using 1,4-dicyanobenzene (**33**, 0.1 M) as the electron acceptor and biphenyl (**34**, 0.1 M) as the codonor, leads to the formation of photocycloaddition (*ortho*, *meta*, and *para*) products (Reaction [4.1]).

Reaction [4.1]

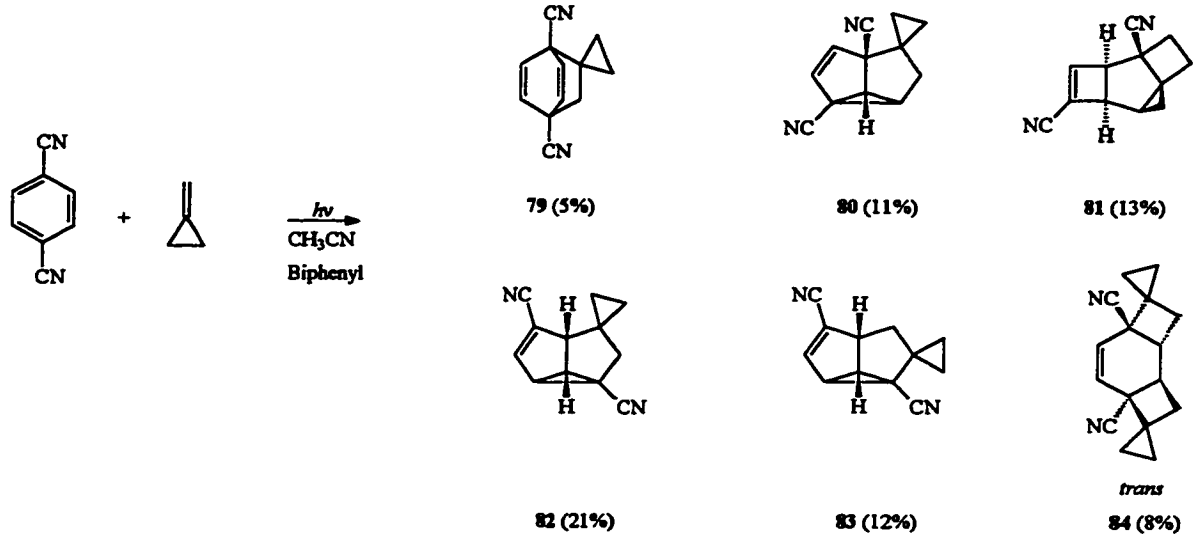

Identification of the products was initially made largely on the basis of the ^{1}H and ^{13}C nmr and mass spectra; X-ray crystallography confirmed the proposed structures (X-ray data is listed in Appendix II). Progress of the reaction was followed by gc/ms and gc/fid. The product ratios did not change over the duration of the irradiation (20 days). The final product ratios are **79**:**80**:**81**:**82**:**83**:**84** = 1.0:1.8:1.8:2.9:1.7:1.1. Formation of this type of cycloaddition product in the photoreactions of 1,4-dicyanobenzene is quite uncommon. The only previously reported example is that resulting from the irradiation of a mixture of **33** and 1,5-hexadiene (**36**) (Scheme 4.4).[48]

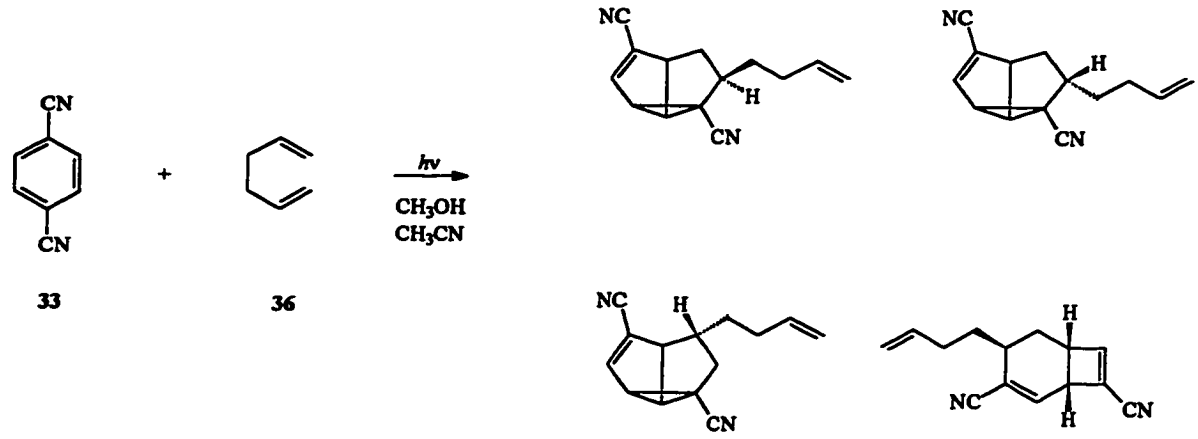

Scheme 4.4 Photocyclization products observed in the photoreaction of 1,5-hexadiene (**36**) with dicyanobenzene.[48]

Another interesting example is the formation of cycloaddition products in the photochemical reaction of 1,4-dicyanonaphthalene with 2,3-dimethyl-2-butene[105] (Scheme 4.5). However, in this reaction, the initial intermediates are believed to be the radical ions. Also, in this reaction there are several rearrangements taking place (deprotonation-reprotonation) which are inconsistent with a simple cycloaddition reaction.

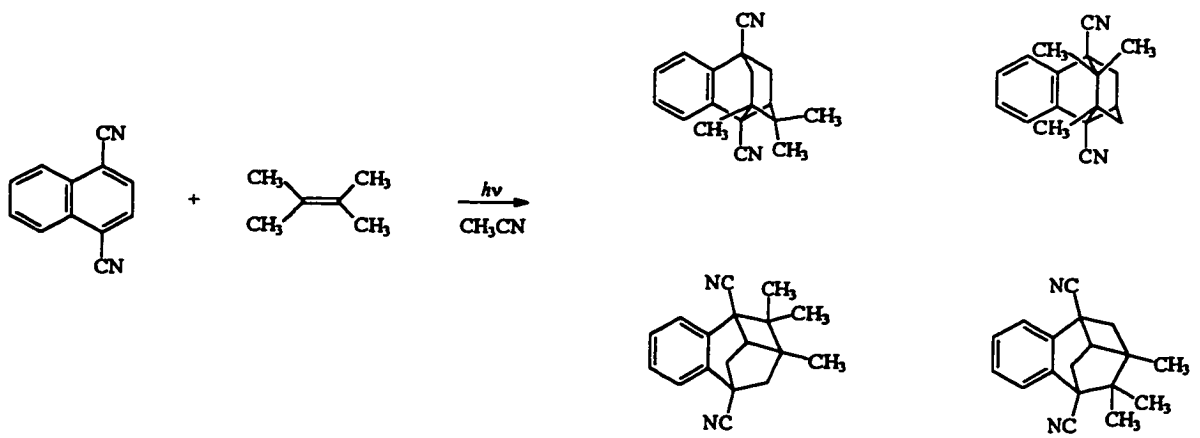

Scheme 4.5 Formation of cycloaddition products in the photoreaction of 1,4-dicyano-naphthalene with 2,3-dimethyl-2-butene.[105]

Photocycloaddition reactions generally do not occur with exocyclic double bonds. One reported example of such a reaction is that of methylenecyclobutane with benzene (Scheme 4.6).[106] Both products were formed in low yield.

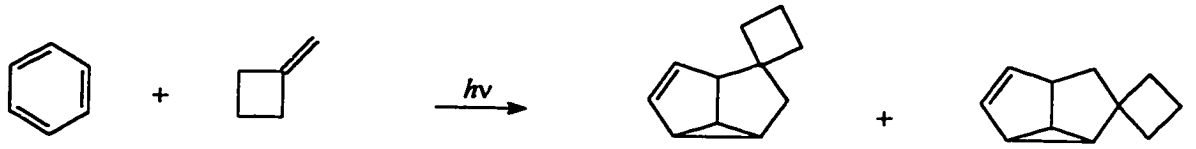

Scheme 4.6 Formation of cycloaddition products from the irradiation of methylenecyclobutane in benzene.[106]

Three of the major products (**80**, **82**, and **83**) in the photoreaction of MCP and **33** in acetonitrile are the result of a *meta* photocycloaddition. The mechanism for the formation of *meta* photocycloaddition products has been studied extensively and is believed to be as shown in Scheme 4.7.[107] Irradiation of a mixture of an arene and an alkene leads to the formation of an exciplex. Based on the energetics (which can be calculated using the Weller equation (Eq. 3.1)) a number of processes can now occur. If electron transfer is exergonic, a radical ion pair can be formed, in which case a substitution reaction usually takes place. However, if electron transfer is endergonic, other processes (cycloaddition) usually occur.

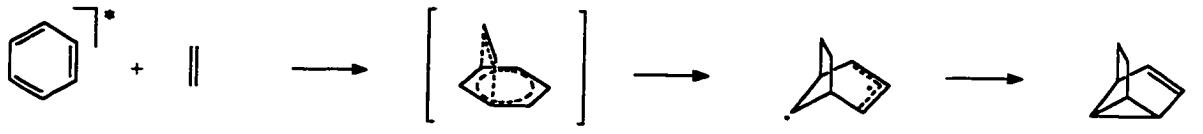

Scheme 4.7 Mechanism proposed for the *meta* photocycloaddition of ethylene to benzene.

From the observed *meta* addition products in the photoreaction of **1** with **33**, and the relative yields of the products, it can be concluded that there is a preference for 1,3 addition; in fact all three *meta* adducts that were isolated from this mixture are products of initial 1,3-bonding. This is in accord with studies on other disubstituted arenes carrying electron acceptor substituents.[107,109] Addition of the alkene moiety to the 1 and 3 positions of the arene allows for charge stabilization in the intermediate. To explain the high regioselectivity of these photocycloaddition reactions, the intermediates are sometimes represented as zwitterions. The favoured additions for **1** with **33** (^{1}S) are shown in Scheme 4.8. Clearly, the formation of **82** and **83** proceeds through the same intermediate, the only difference being the orientation of the MCP moiety.

Mattay and co-workers[108] have established guidelines for predicting the type of reaction that will take place upon irradiation of a mixture containing an arene and an alkene. The guidelines are based on the reduction potential of the arene and the oxidation potential of the alkene. The energetics can be calculated using the Weller equation (Eq. 3.1). It was shown that electron transfer and substitution take place when ΔG is less than 0 eV. *Ortho* cycloadditions take place when ΔG is between 0 and +1.5 eV, and *meta* cycloadditions when ΔG is larger than +1.5 eV. In order for *para* photocycloaddition to occur the energetics of the reaction must be highly endergonic and this mode of addition is rarely observed. It must be noted that these boundaries are not sharp, several exceptions to these guidelines are known. In the photoreaction of **1** with **33** one *para* cycloaddition product was observed. This could mean that the reaction is highly endergonic; however, using the Weller equation, an oxidation potential of >3.5 V for **1** would be required. The

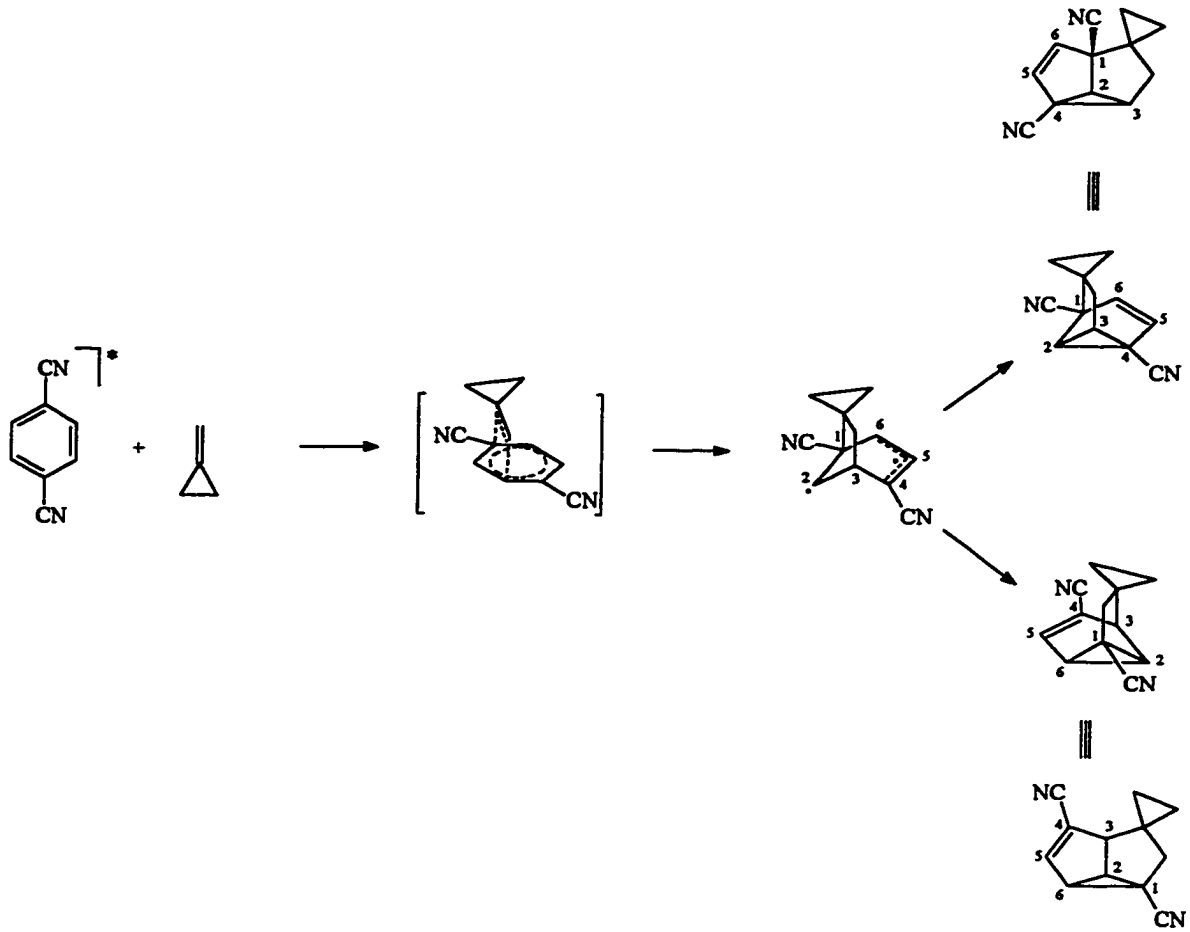

Scheme 4.8 Favoured addition pathway of MCP to **33** in the formation of *meta* photocycloaddition products.

measured oxidation potential (cyclic voltammetry, CV) was determined to be only 2.41 V.[§] Another possibility is the involvement of radical ions. Combination of the radical cation and the radical anion could lead to the observed cycloaddition product. This mechanism is also unlikely since it was shown in Chapter 2 that the MCP radical cation ($\mathbf{1}^{+\bullet}$) is likely to undergo a rapid ring opening to give the TMM radical cation ($\mathbf{1a}^{+\bullet}$). The

[§] It must be noted that the oxidation potentials of the alkenes studied in this thesis are irreversible, i.e. the number has no thermodynamic significance. Nevertheless, it has been well established that in many cases reliable values for the E_{ox} can be obtained from the measured peak potentials.[3]

formation of this *para* adduct must therefore be the result of a cycloaddition reaction with an energy demand less than expected on the basis of Mattay's guidelines.[108]

An interesting observation is the presence of the 2:1 (alkene:arene) adduct. Mattay and co-workers claim to have observed this type of adduct in the photoreaction of *m*-bis(trifluoromethyl)benzene with cyclopentene.[109a] The identification was based on mass spectra only; no attempt to isolate these 2:1 adducts was undertaken in this case, and their structural assignments remain tentative. Gilbert and co-workers claimed the formation of 2:1 adducts in the photoreaction of benzene and cyclopropene. No pure compounds were isolated but several possible structures were proposed, based on the assumption that the products are the result of a 1:1 addition of the cyclopropene dimer to benzene.[109b]

A single *ortho* photocycloaddition reaction of MCP to **33** can be used to explain the formation of product **81** (Scheme 4.9; pathway I). *Ortho* addition of MCP to **33** leads to the intermediate bicyclooctadiene **85** which can undergo a ring-opening to give the cyclooctatriene **86**. There are several examples in the literature for these types of (secondary) reactions.[110] Formation of the final product (**81**) can be accounted for by a modified cyclopropyl-π-methane rearrangement.[111] This reaction, discovered by Zimmerman and co-workers, proceeds by a mechanism (Scheme 4.10) that parallels that of the well-known di-π-methane rearrangement.[112] The cyclopropyl-π-methane rearrangement of **86**, however, would lead to compound **89** (Scheme 4.9, pathway II), which was not observed.[113] Instead, the 1,5-diradical intermediate (**87**) undergoes a ring-closure to give the observed product (**81**).

It is not clear why the observed product (**81**) is preferred over the expected product from the cyclopropyl-π-methane rearrangement (**89**). One possible explanation is that intermediate **88** is disfavoured due to the presence of two primary radical centres. Furthermore, the presence of two cyano groups could have a significant effect on the stability of the radical centres in **87** favouring pathway I rather than pathway II (Scheme 4.9).

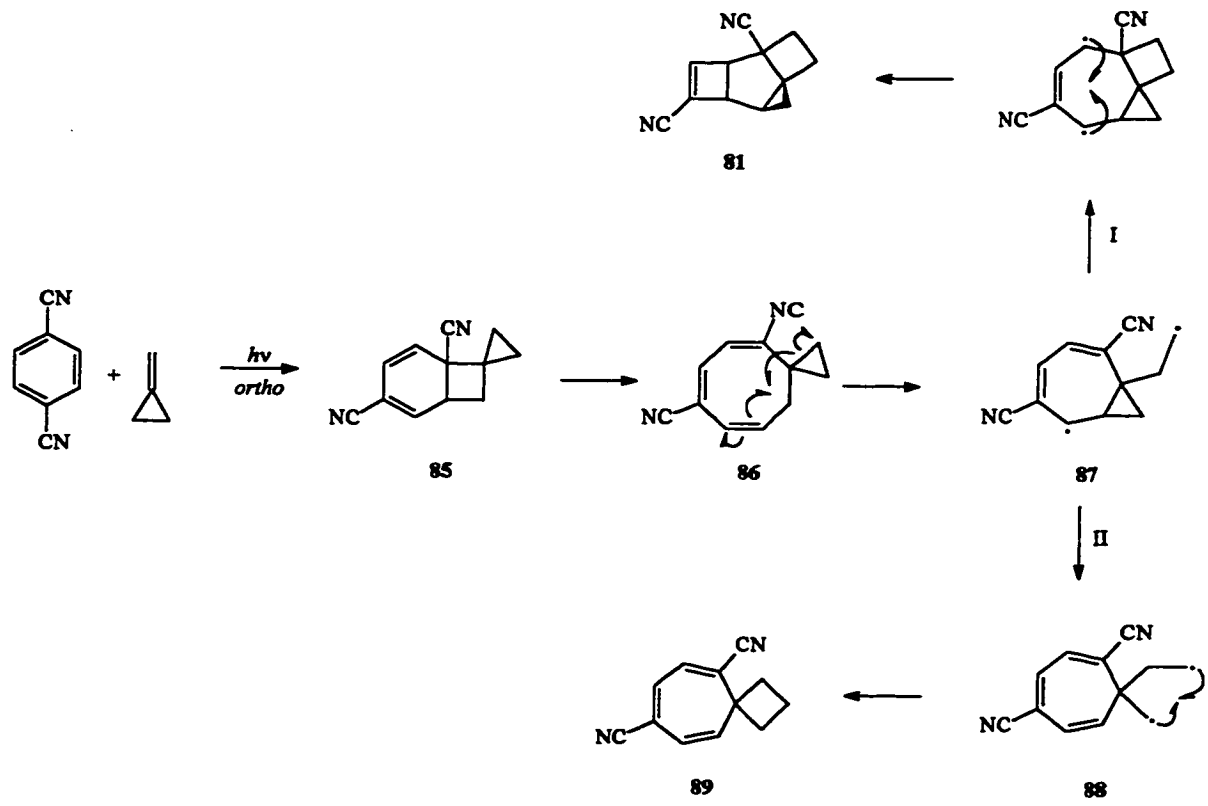

Scheme 4.9 Proposed mechanism for the formation of product **87** by a "modified" cyclopropyl-π-methane rearrangement.

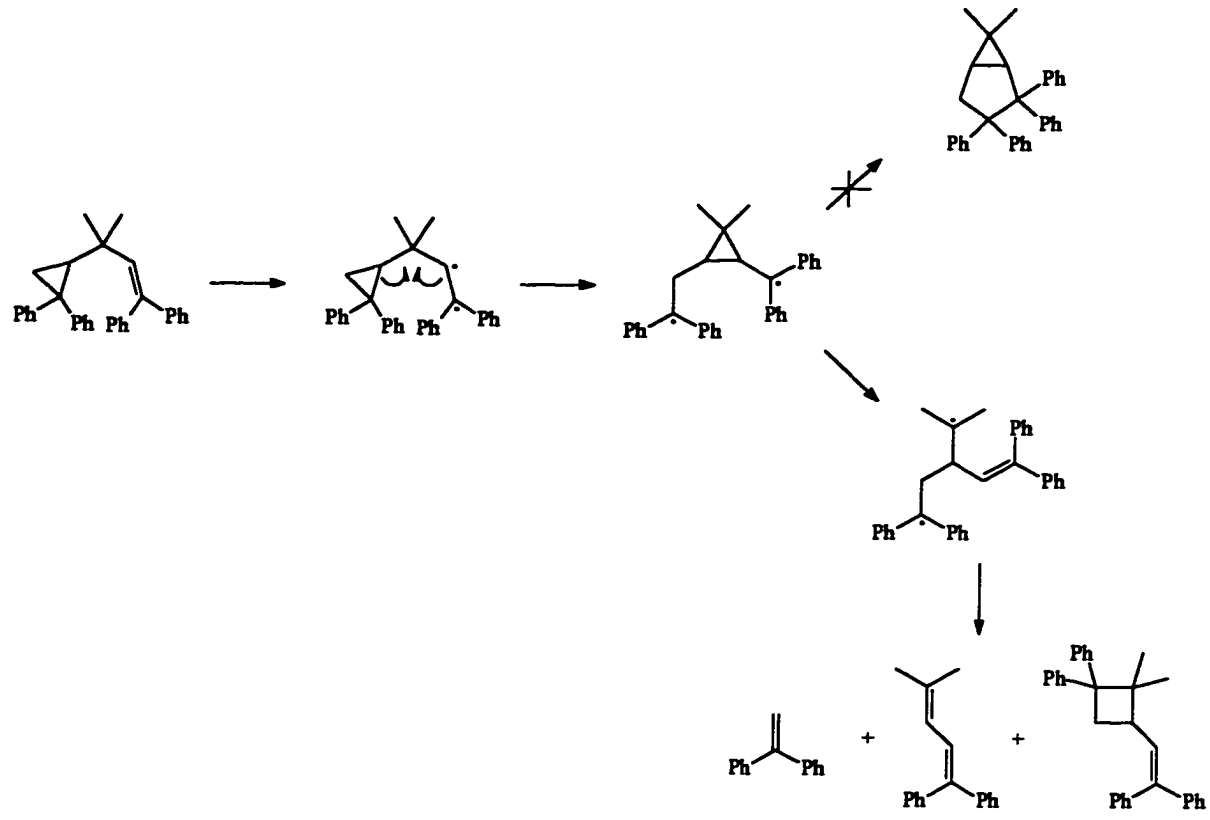

Scheme 4.10 Proposed mechanism for the cyclopropyl-π-methane rearrangement.[111]

As mentioned above, the measured (CV) oxidation potential of **1** is 2.41 V. Using the Weller equation this leads to a value of -5 kcal/mol for ΔG_{et}. Electron transfer is therefore expected to take place at the diffusion controlled rate. However, the product mixture clearly indicates that ET does not occur. Formation of the radical cation of **1** is expected to lead to the ring-opened trimethylenemethane radical cation.[65b,76] This was shown to be true by a recent ESR study on the MCP radical cation.[104] Even at temperatures as low as 4 K all the hydrogens in the radical cation were shown to be equivalent. This can only be explained by a ring-opened species. None of the isolated

products of the reaction of **1** with **33** show any indication of a ring-opened MCP unit, another good indication that electron transfer does not take place.

Lowering the MCP concentration to 0.1 M does not lead to different results, except for the fact that the reaction becomes less efficient. Increasing the biphenyl (**34**) concentration lowers the efficiency of the reaction as well. However, no other products are formed as a result of a higher biphenyl concentration.

It is well known that cycloadditions occur more rapidly in non-polar solvent since polar solvents favour electron transfer. When the photoreaction of **1** with **33** is carried out in a non-polar solvent ($CHCl_3$, $\varepsilon = 4.8$) rather than a polar solvent (CH_3CN, $\varepsilon = 35.7$) the same products are observed. The relative product ratios **79**:**80**:**81**:**82**:**83**:**84** are 1.0:1.8:1.2:2.8:1.4:0.3. These ratios fluctuated somewhat during the course of the irradiation (5 days) but the final values were very close to the initial values indicating that these numbers are reliable. With the exception of products **81** and **84** these ratios are very close to those observed for the reaction in acetonitrile, providing strong evidence that in both cases the same mechanism is operative.

Analysis of the product mixture shows that in all cases the cyclopropyl moiety remained closed. The rearrangement leading to product **81** does cleave the cyclopropyl unit but the initially formed *ortho* adduct must have had the original (ring-closed) cyclopropyl group (Scheme 4.9). This indicates that the mechanism does not proceed through a diradical, radical ionic, or zwitterionic intermediate, since these are expected to give mainly products resulting from addition of the ring-opened species to the arene.

In order to be able to understand the observation that no electron transfer takes place, even though the measured (CV) oxidation potential is low enough for the rate of electron transfer to be diffusion controlled, the ionization potential (IP, gas phase) of MCP was taken into account. It has been established that there is a good correlation between the oxidation potential (E_{ox}, solution) and the ionization potential (IP, gas phase) of a compound. Neikam et al.[114] measured the oxidation potentials and the ionization potentials of a large number of arenes and alkenes and determined the correlation to be as shown in Eq. 4.1.

$$E_{½}^{ox} = 0.827 \times IP - 5.40\ V \qquad (4.1)$$

This correlation gives the oxidation potential vs. Ag/Ag^{+}. In order to convert the oxidation potential relative to sce, 0.34 V has to be added to this calculated value. Using this correlation and the experimentally determined IP (vertical),[66a] the E_{ox} of **1** was calculated to be 2.88 V. Using the Weller equation (Eq. 3.1) the calculated ΔG for the reaction with **33** is now +5.8 kcal/mol (+0.25 eV). Based on these numbers it is clear that electron transfer is unlikely and that the major reaction pathway will be cycloaddition. Other alkenes were also considered in this study; the results are shown in Table 4.1.

Ab initio calculations (MP2/6-31G*//HF/6-31G*) were used to calculate the ionization potentials of the alkenes listed in Table 4.1. Both the adiabatic and the vertical ionization potentials were considered. The experimental (vertical) ionization potentials were found in the literature.[66a] Plotting the experimental (CV) oxidation potential against

Table 4.1. Comparison of the calculated and experimentally determined oxidation potentials (vs. sce) and ionization potentials of several alkenes.

Compound	IP_v[a] (eV)	IP_v[b] (eV)	IP_a[c] (eV)	$E_{ox,v}$[d] (V)	$E_{ox,v}$[e] (V)	$E_{ox,a}$[f] (V)	E_{ox}[g] (V)
methylenecyclopropane (1)	9.6	9.8[h]	8.89[h]	2.88	3.04	2.29	2.41[i]
2-methylpropene (84)	9.24	9.39[j]	8.81[j]	2.58	2.71	2.23	2.99[k]
1,4-bis(methylene)cyclohexane (2)	9.0	9.2[h]	8.51[h]	2.38	2.55	1.98	2.49[l]
2-methyl-2-butene	8.68	8.93[j]	8.27[j]	2.12	2.33	1.78	2.03[m]
2-methyl-1,2-butadiene	8.85	8.67[j]	8.45[j]	2.26	2.11	1.93	2.25[n]
4-methyl-1,3-pentadiene	8.28	8.23[j]	7.90[j]	1.79	1.75	1.47	1.51[j]
2,4-dimethyl-1,3-pentadiene	8.49	8.62[j]	7.58[j]	1.96	2.07	1.21	1.53[j]

[a] experimental (vertical) ionization potential (ref. 66a); [b] calculated (vertical) ionization potential (taken from the eigenvalue of the HOMO); [c] calculated adiabatic ionization potential (taken as the difference between the calculated total energy of the minimized neutral molecule and the minimized radical cation); [d] calculated oxidation potential (Eq. 4.1) using the experimental (vertical) ionization potential; [e] calculated oxidation potential (Eq. 4.1) using the calculated (vertical) ionization potential; [f] calculated oxidation potential (Eq. 4.1) using the calculated (adiabatic) ionization potential; [g] measured oxidation potential (vs. sce); [h] ref. 76a; [i] this work; [j] ref. 52i; [k] ref. 115 [l] ref. 76b; [m] ref. 50; [n] ref.52g.

the vertical ionization potential (Figure 4.2; r = 0.774) and against the adiabatic ionization potential (Figure 4.3; r = 0.903) shows that the correlation between the adiabatic IP and the experimental E_{ox} is better. It can be seen from Figure 4.2 that there are two points that deviate markedly from the expected oxidation potential based on the vertical IP (calculated). The oxidation potentials of these compounds (MCP and 2,4-dimethyl-1,3-pentadiene) show a much better correlation with the adiabatic IP (calculated) (Figure 4.3).

The measured E_{ox} of MCP is 2.41 V whereas based on the vertical IP it is expected to be close to 3 V. The calculated E_{ox} based on the adiabatic IP (2.29 V) is much closer to the measured (CV) value (2.41 V). Most of the other alkenes show a good correlation between the calculated and the measured E_{ox}. Only the measured E_{ox} of 2,4-

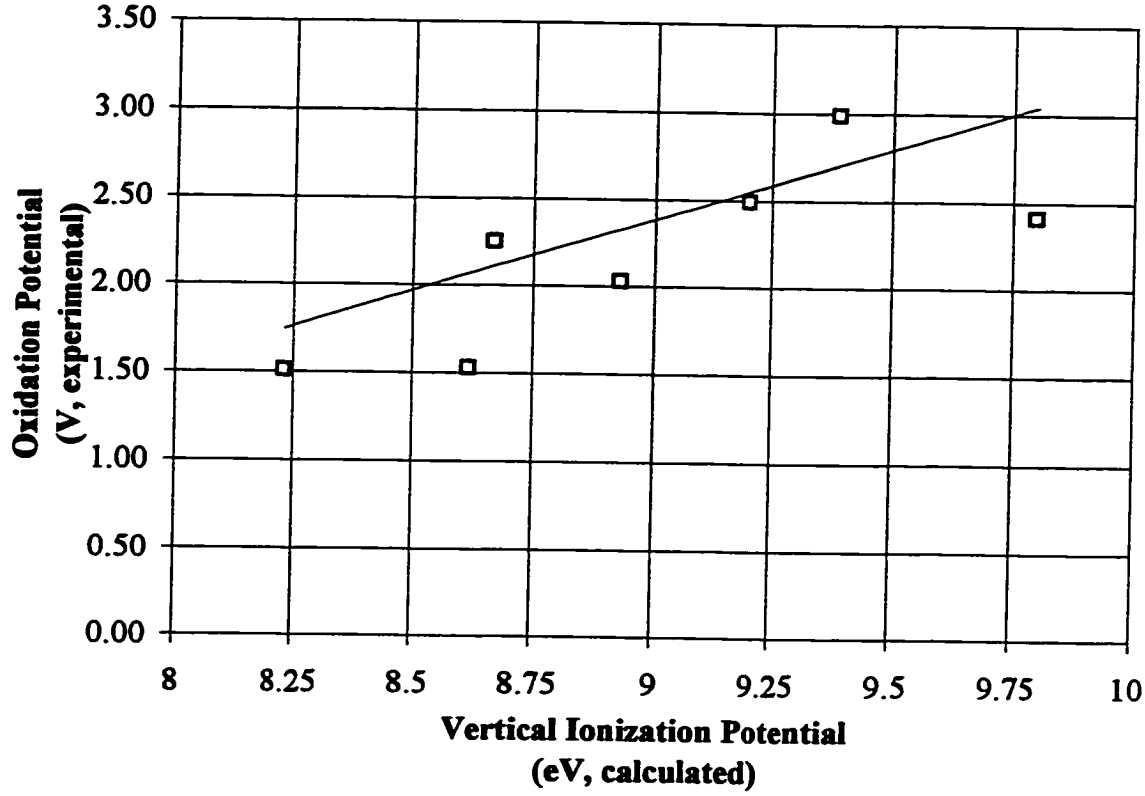

Figure 4.2 Correlation between the experimentally determined oxidation potentials (□) of the alkenes listed in Table 4.1 and the vertical ionization potentials (calculated). The line represents the expected oxidation potential based on the vertical ionization potential (calculated) using eq. 4.1.

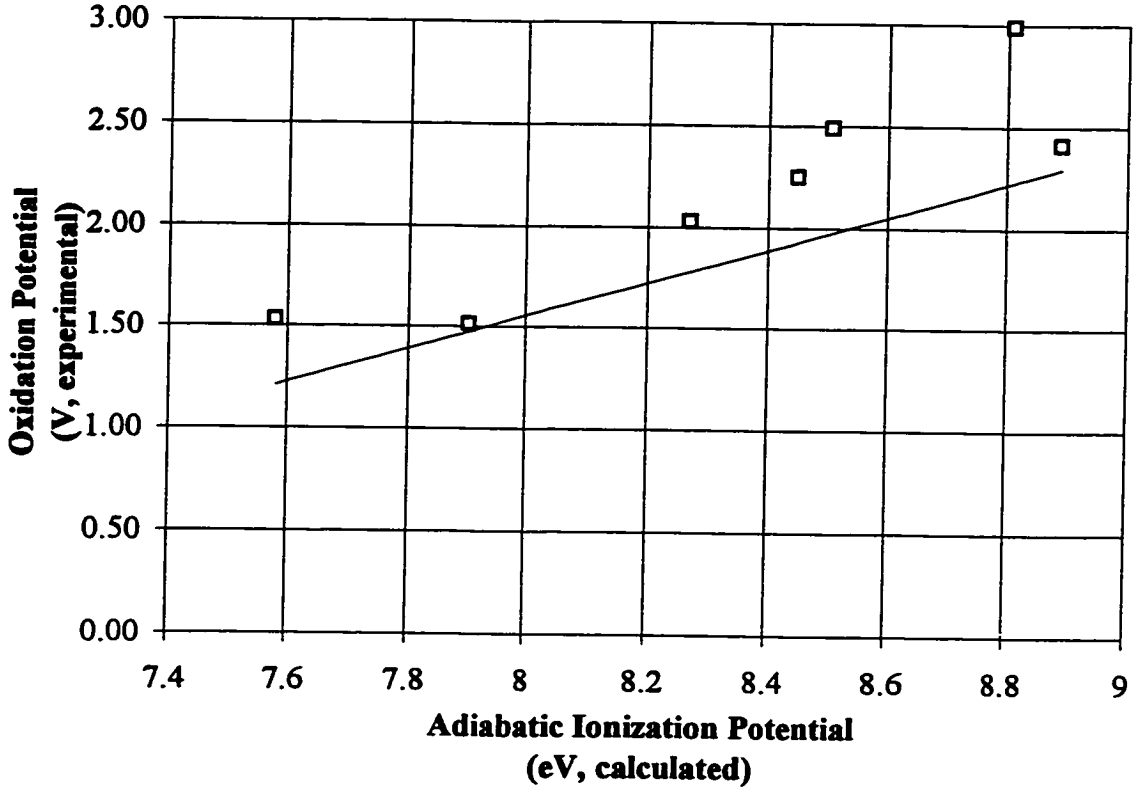

Figure 4.3 Correlation between the experimentally determined oxidation potentials (□) of the alkenes listed in Table 4.1and the adiabatic ionization potentials (calculated). The line represents the expected oxidation potential based on the adiabatic ionization potential (calculated) using eq. 4.1.

dimethyl-1,3-pentadiene (1.53 V) also significantly deviates from the calculated value (approximately 2 V).

It must be concluded that for MCP in the electrochemical experiments the measured E_{ox} reflects the adiabatic IP rather than the vertical IP. In the photochemical experiments the vertical IP determines the reactivity. This variation could result from the formation of a complex between the alkene and the Pt-electrode. MCP is a highly strained molecule and interaction with the electrode might lead to a relief of strain by a partial ring opening. This type of reaction has precedence. There are many examples of metal catalyzed ring opening reactions of methylenecyclopropanes.[74b,117] A commonly observed reaction is metal insertion. The metals frequently used for this type of reaction are Ni and Pd; however, there are also examples of Pt catalyzed reactions. Some examples of possible metal-catalyzed reactions of methylenecyclopropanes are shown in Scheme 4.11.[74b]

The other major exception listed in Table 4.1 is 2,4-dimethyl-1,3-pentadiene. This molecule has an E_{ox} of 1.53 V, a value close to that of 4-methyl-1,3-pentadiene (1.51 V). The major difference between these two neutral molecules is that the latter is planar (s-*trans*), conjugated whereas the former is not. The calculated dihedral angle between the double bonds in 2,4-dimethyl-1,3-pentadiene is ca. 50 degrees, i.e. significantly twisted from the s-*cis* conformation. It was shown by *ab initio* MO calculations that the global minimum of the radical cation of 2,4-dimethyl-1,3-pentadiene is planar.[52i] All four methyl groups stabilize the structure. However, rotations in the radical cation are subject to significant barriers and will therefore not occur easily. The initially formed radical cation

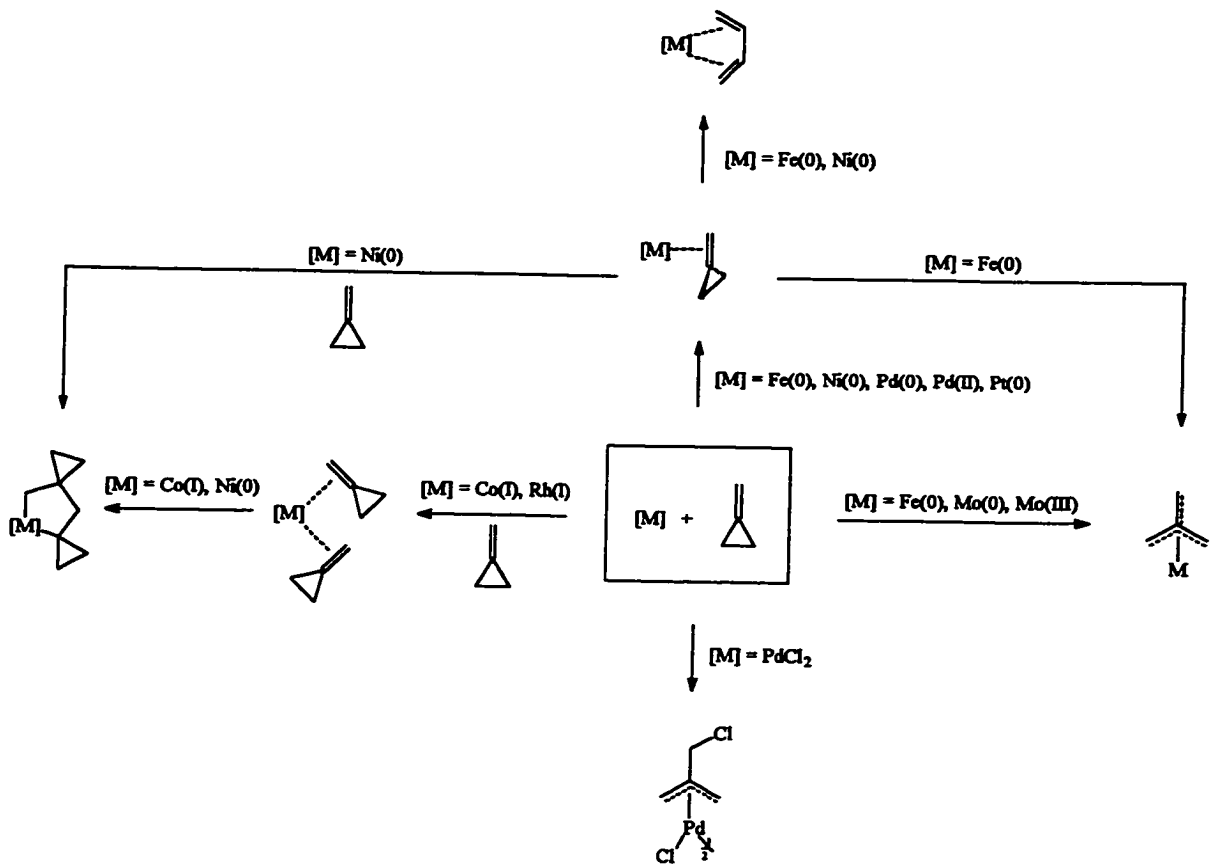

Scheme 4.11 Possible metal-catalyzed reactions of methylenecyclopropanes.[74b]

(vertical ionization) will have a twisted geometry (s-*cis*) and must overcome the barrier to become planar (adiabatic). Based on this data one would expect a much higher E_{ox} for 2,4-dimethyl-1,3-pentadiene than for 4-methyl-1,3-pentadiene. However, the measured (CV) values are practically the same. Interaction of the twisted diene with the electrode surface might reduce the twist of the dihedral angle, resulting in a lower oxidation potential (adiabatic) than expected on basis of the measured (vertical) ionization potential. However, in the photoinduced electron transfer reactions of this diene, there will be no assistance for the neutral molecule to become planar and therefore the electron transfer

will be governed by the vertical rather than the adiabatic IP. This is also evident from a comparison of the results of the irradiations of these two molecules (4-methyl-1,3-pentadiene and 2,4-dimethyl-1,3-pentadiene). The efficiency of the reaction of the twisted diene is significantly lower than that of the planar diene. In order for the twisted diene to reach the same amount of conversion as the planar diene it has to be irradiated almost twice as long as the planar diene even though the measured oxidation potentials are virtually the same.[52i] This once again indicates that, in the photochemical reactions, electron transfer is governed by the vertical ionization potential rather than the adiabatic IP.

It must be noted that there is another possible explanation for the observation that the oxidation potentials of certain alkenes are lower than expected. It is well known that oxidation potentials shift to lower potentials as a result of fast follow-up reactions or adsorption. The latter possibility was discussed above, but the former cannot be ruled out.

Electron transfer processes are often thought of in terms of inner-sphere and outer-sphere processes. For the outer-sphere processes the Marcus theory applies and therefore the reorganization energy becomes important. Also, MCP is a small species and oxidation (to give TMM) might be accompanied by a large solvent reorganization energy. A larger reorganization energy will shift the Marcus curve (Eq. 1.7) to a more negative ΔG_{ET}, i.e. the rate of electron transfer will become diffusion controlled at more negative ΔG values than under normal circumstances. This means that electron transfer might be taking place, however, due to a large reorganization energy it is not favoured.

Photochemistry of methylenecyclopropane (1) in the presence of a nucleophile.

Irradiation of a mixture of methylenecyclopropane (**1**, 0.1 M), biphenyl (**34**, 0.1 M), and 1,4-dicyanobenzene (**33**, 0.1 M) in acetonitrile-methanol (3:1) leads to the formation of essentially the same products as the irradiation without methanol. Progress of the reaction was followed by gc/ms and gc/fid; identification of the products was based on their retention times and mass spectra. A careful analysis of the chromatograms and the mass spectra revealed the presence of a few additional minor products. The mass spectra of these compounds were very similar to those of the cycloaddition products with the exception of the fact that the molecular ion was at m/z 184 rather than m/z 182. These compounds are most likely the reduced cycloaddition products. These products were not isolated from the mixture.

The observed ratios of the cycloaddition products are different from those obtained in the earlier experiments using acetonitrile or chloroform as the solvent. With methanol present the ratios are **79**:**80**:**81**:**82**:**83**:**84** = 1.0:1.8:0.1:1.4:0.6:1.7. The most significant difference is the almost complete absence of product **81** in the product mixture. The mechanism for the formation of this compound (a "modified" cyclopropyl-π-methane rearrangement) was discussed earlier (Scheme 4.8). The mechanism for the cyclopropyl-π-methane rearrangement shows that the fate of the reaction is determined by the pathway of the diradical intermediate (e.g. **87**). Opening of the cyclopropyl group followed by ring closure to give a cyclobutane moiety is the normal course of the reaction (Schemes 4.9 and 4.10). However, in a similar reaction, Zimmerman and Carpenter discovered that the

diradical intermediate reacted to give a very small amount of the cyclobutane product when the reaction was carried out in pentane but none when the solvent was *tert*-butanol.[111b] It is possible that the diradical (**87**) in the reaction of MCP with **33** is trapped by the solvent (methanol) leading ultimately to a reduced species.

The results of this reaction once again clearly indicate that, upon irradiation of a mixture of **33** and **1**, no electron transfer takes place. Under these conditions (i.e. the use of **33** as the electron acceptor) the energetic requirements for ET are not met. Formation of an exciplex between the first singlet excited state of **33** and MCP followed by cycloaddition is the preferred reaction pathway.

*Photochemistry of isobutylene (2-methylpropene, **90**) in the absence of a nucleophile.*

The structure of methylenecyclopropane (**1**) is similar to that of isobutylene (**90**). Obviously, MCP is a highly strained molecule and this will affect its reactivity. However, the calculated E_{ox} of isobutylene, based upon the (calculated) vertical IP, is ca. 2.7 V, high enough to inhibit electron transfer. The experimentally determined E_{ox} is 2.65 V vs. Ag/Ag^+ (i.e. 2.99 V vs. sce).[115]

An earlier investigation concluded that, in the absence of a nucleophile, irradiation of an acetonitrile solution containing isobutylene (**90**) and 1,4-dicyanobenzene (**33**) did not result in the formation of any products.[52c] In light of the results observed with MCP this lack of reactivity seems rather unlikely; one would expect substitution products in the case of electron transfer ($\Delta G < 0$ eV) or cycloaddition products in the case $\Delta G > 0$ eV. In the presence of a nucleophile (methanol) and a codonor (biphenyl, **34**) isobutylene (**90**)

reacts to give 1:1:1 (alkene:aromatic:nucleophile) substitution products, indicative of electron transfer, in good yield.[52d] These results prompted us to reinvestigate the reaction of isobutylene in the absence of nucleophile.

Irradiation of a solution of DCB (**33**, 0.1 M) and isobutylene (**90**, ca. 0.5 M) in acetonitrile resulted in the formation of only one major product (**91**, Reaction [4.2]).

Reaction [4.2]

33 **90** **91**

A possible mechanism for the formation of product **91** is as shown in Scheme 4.12. The most likely explanation for this observation is an ET process leading to the formation of the radical cation ($\mathbf{90}^{+\bullet}$) and radical anion ($\mathbf{33}^{-\bullet}$). Addition of $\mathbf{90}^{+\bullet}$ to acetonitrile yields a distonic radical cation which combines with $\mathbf{33}^{-\bullet}$. Loss of cyanide anion followed by cyclization and deprotonation yields the observed product (**91**).[‡] The proposed mechanism parallels the mechanism of the photo-NOCAS reaction with acetonitrile acting as the nucleophile. It also shows similarities to that of the addition of cations to acetonitrile (as is observed in electrochemical experiments (see Chapter 3)), except for the fact that no hydrolysis (to yield the acetamide) is observed. This type of reaction (photo-NOCAS

[‡] Another possible pathway (not shown) is formation of the distonic radical cation, combination with the radical anion ($\mathbf{33}^{-\bullet}$) followed by cyclization and loss of HCN.

reaction with acetonitrile as the nucleophile) has not been observed before under these conditions.

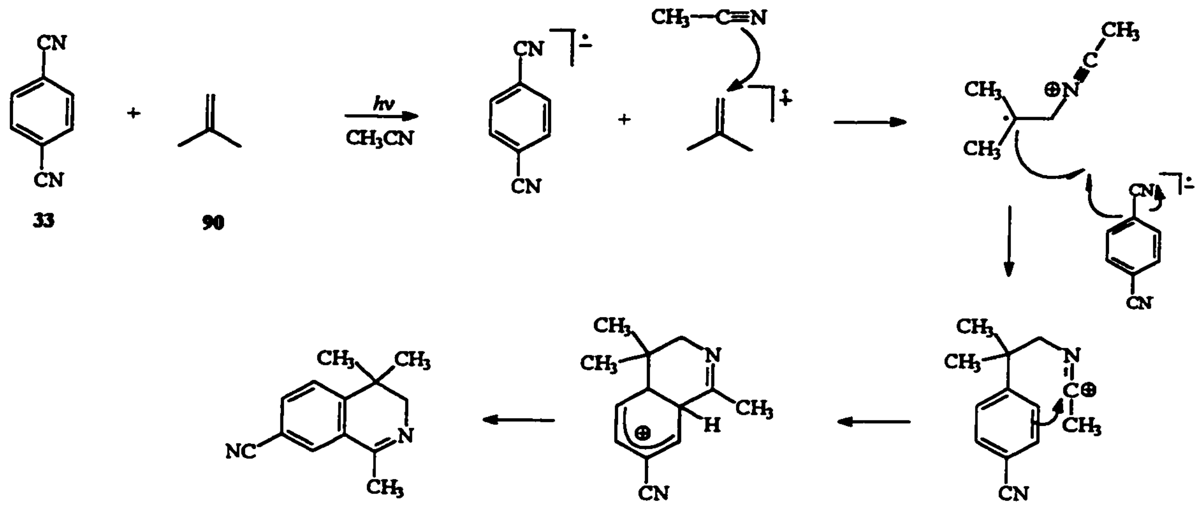

91

Scheme 4.12 Proposed mechanism for the formation of the major product (**91**) in the photoinduced electron transfer reaction of isobutylene (**90**) with 1,4-dicyanobenzene (**33**).

As shown earlier (Chapter 3), in the case of an unreactive alkene, the most common reaction upon oxidation in the absence of a nucleophile is deprotonation of the radical cation. The expected product(s) under these conditions are the 1:1 (alkene-aromatic) products which arise from deprotonation of the alkene followed by addition of the allylic radical to the radical anion and loss of cyanide anion (Scheme 4.13). The fact that this 1:1 product was only present in trace amounts indicates that the isobutylene radical cation is not acidic enough to protonate the base (acetonitrile). The resulting radical, although

allylic, is not expected to be stable since it is primary on both sides and deprotonation will therefore be less favourable.

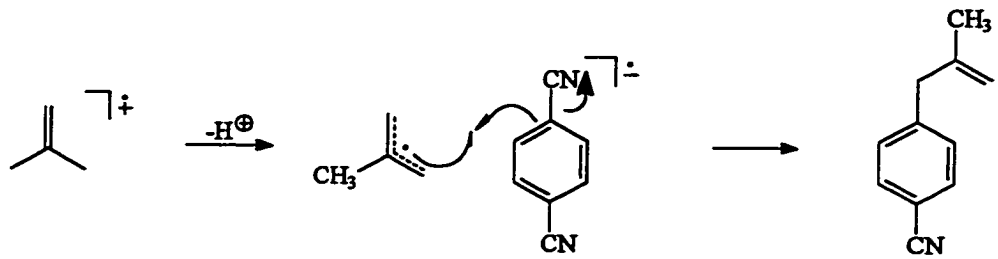

Scheme 4.13. Mechanism for the formation of 1:1 (alkene-aromatic) adducts; the final product is the expected product in the case of isobutylene acting as the electron donor.

Addition reactions to the solvent (acetonitrile) have been observed for radicals (addition to the carbon of the CN triple bond; Reaction [3.2]), and for cations (electrochemistry; addition to the nitrogen of the CN triple bond; Reaction [3.4]). One other example of a radical cation adding to acetonitrile has been observed. Product **46** in the photoinduced electron transfer reactions of 1,4-bis(methylene)cyclohexane (**2**) in the presence of **33** in acetonitrile (Reaction [3.2]) was the result of addition of the radical cation ($\mathbf{2}^{+\bullet}$) to acetonitrile. The intermediate distonic radical cation was trapped by cyanide anion rather than the 1,4-dicyanobenzene radical anion ($\mathbf{33}^{-\bullet}$), i.e. a tandem nucleophilic addition (Scheme 3.7). Nucleophilic addition of acetonitrile to radical cations is not commonly observed. As mentioned above, this reaction is only expected when the alkene radical cation does not undergo rapid deprotonation. Some examples of this type of reaction have been reported.[43a,44c,118] A particularly interesting example is the nucleophile-

assisted C-Si bond cleavage reaction of substituted benzylsilane radical cations.[118d] In this study acetonitrile and methanol were used as the nucleophiles in non-hydrogen bonding solvents. Under certain conditions, the reaction with acetonitrile was actually faster than the corresponding reaction with methanol. The rate constants for these bimolecular processes vary between 1.2×10^5 and 3.2×10^9 $M^{-1}s^{-1}$, depending on the substituents. However, in neat acetonitrile the rate constant for the reaction of the radical cation with methanol is 46 times faster than the reaction with acetonitrile.

Identification of product **91** was problematic. Based on earlier examples (addition of radicals to acetonitrile) an alternative mechanism, leading to a similar product, was proposed (Scheme 4.14). However, careful analysis of the NOESY (nmr) spectrum indicated clearly that there is an interaction between the single methyl (2.45 ppm) and the single proton on the phenyl ring (7.77 ppm). The two equivalent methyls (1.24 ppm) interact with the two neighbouring protons on the phenyl ring (7.49 (strong) and 7.71 (weak) ppm) but not with the single proton (7.77 ppm). The methylene protons (3.58 ppm) do not show any interaction with any of the phenyl protons. These results were confirmed by a nuclear Overhauser effect (nOe) experiment: irradiation of the *gem*-dimethyl group (1.24 ppm) led to an increase of the signal (doublet) at 7.49 ppm; irradiation of the single methyl group (2.45 ppm) led to an increase of the signal (doublet) at 7.77 ppm. Irradiation of the methylene protons (3.58 ppm) did not result in enhancement of any of the signals of the phenyl ring. These results rule out the product arising from the mechanism shown in Scheme 4.14 and confirm the structure of product **91**.

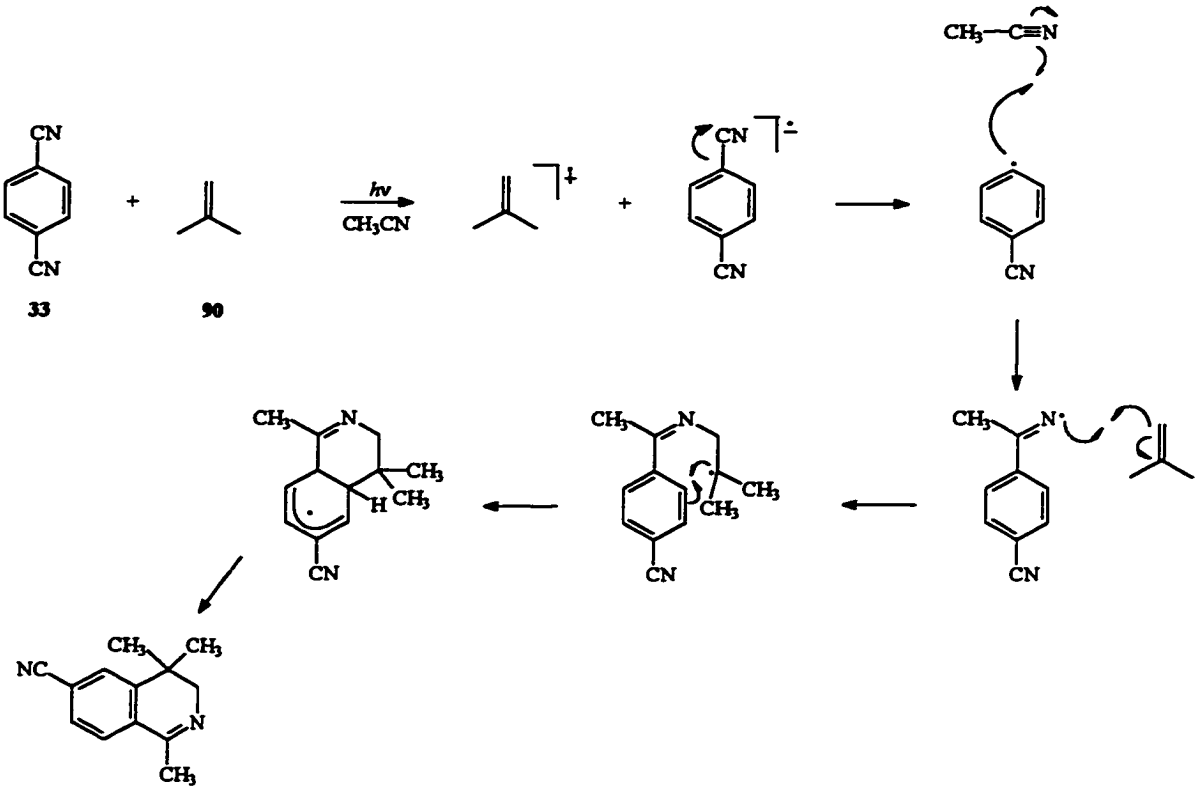

Scheme 4.14. Possible mechanism for the formation of a product similar to **91** (see text).

No cycloaddition products were isolated from this reaction mixture. There were indications (gc/ms) that some cycloaddition products were formed, however the amounts were too small to be of any significance.

When the irradiation is performed in chloroform as the solvent, only cycloaddition products were observed. The identification of these products is based on their mass spectra which show significant similarities to those observed in the reaction of MCP with **33**. Comparison of the final mixtures (gc/fid and gc/ms) of the reactions done in acetonitrile and in chloroform confirms the initial observation that in a polar solvent this reaction does not give any appreciable amounts of cycloaddition products.

From the results described above it can be concluded that electron transfer takes place even though the oxidation potential is high. This could mean that the measured value ($E_{½}^{ox}$ = 2.65 V vs. Ag/Ag^{+}; 2.99 V vs sce)[115] is incorrect. The expected value, based on the ionization potentials (experimental and calculated) is between 2.2 and 2.7 V. A value close to the latter is the most likely since small amounts of cycloaddition products were already observed, indicating that the value for ΔG (Eq. 3.1) is close to zero.

Unlike MCP (or 2,4-dimethyl-1,3-pentadiene) there is no significant strain or twisting in isobutylene and therefore the adiabatic IP is close to the vertical IP (Δ IP = 0.58 eV). The measured (CV) oxidation potential will, therefore, be close to the expected (calculated) value. In strained or twisted molecules the difference between these two values is significantly greater (Δ IP (MCP) = 0.9 eV; Δ IP (2,4-dimethyl-1,3-pentadiene) = 1.04 eV) and accordingly a lower oxidation potential is observed.

Electrochemical oxidation of methylenecyclopropane (1) in the absence of a nucleophile.

Attempts to generate the MCP radical cation by photoinduced electron transfer (see above) were not successful due to the high vertical IP of MCP. However, it was shown that the measured E_{ox} was only 2.41 V, close to the value expected, based on the adiabatic IP. Anodic oxidation of MCP at low potentials should therefore lead to the formation of the radical cation. Its reactivity can then be studied in the presence and absence of nucleophiles.

Anodic oxidation of MCP in acetonitrile (no methanol) results in the formation of one major product: *tert*-butylacetamide (**92**, Reaction [4.3]).

Reaction [4.3]

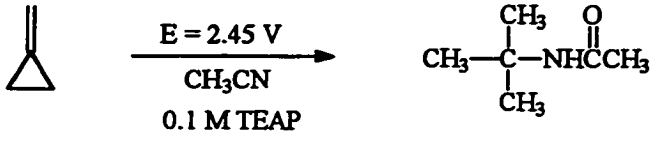

92

The product (*tert*-butylacetamide, **92**) is the result of the formation of the (relatively) stable *tert*-butyl cation which reacts with acetonitrile to give the final product (after hydrolysis). A possible mechanism for the formation of the *tert*-butyl cation is shown in Scheme 4.15.

It was shown in Chapter 3 that, under non-nucleophilic conditions, anodic oxidation of alkenes can lead to deprotonation. Even when methanol was present, one of the major products in the anodic oxidation of 1,4-bis(methylene)cyclohexane (**2**) was the result of a protonation of the methylene group. A recent ESR study on $\mathbf{1}^{+\bullet}$ showed that this species exists as the ring-opened TMM radical cation, $\mathbf{1a}^{+\bullet}$.[104] Upon warming of the matrix from 77 to 120 K, the radical cation lost a proton and underwent a ring closure to give the allylic 2-methylenecyclopropyl radical (Scheme 4.15, step 2).[¶]

[¶] The authors did not propose a mechanism for this reaction and it must be noted that, in principle, the radical cation $\mathbf{1a}^{+\bullet}$ could abstract a hydrogen atom from a neutral molecule (MCP, **1**) to yield the allylic radical and the allylic cation. Either way this reaction involves two species: the neutral (**1**) and the radical cation ($\mathbf{1a}^{+\bullet}$).

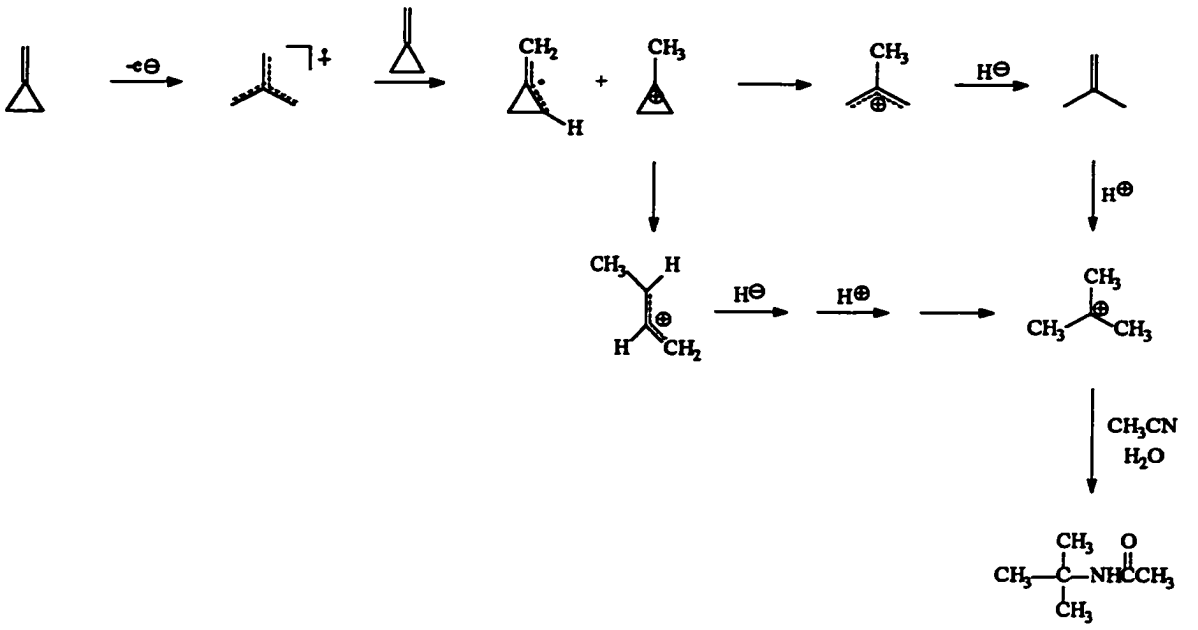

Scheme 4.15 Possible mechanisms for the formation of *tert*-butylacetamide (**92**) in the anodic oxidation of methylenecyclopropane (**1**).

Protonation of MCP (i.e. it acts as the base) leads to the methylcyclopropylium ion which can undergo a ring-opening to give the 2-methylallyl cation or the 1-methylallyl cation. Hydride transfer from a suitable donor (e.g. MCP) followed by protonation (and a rearrangement in the case of the 1-methylallyl cation pathway) leads to the *tert*-butyl cation. The pathway leading to isobutylene as an intermediate seems the most likely one since this involves less rearrangements. It has also been shown that *tert*-butylacetamide can be prepared from isobutylene and acetonitrile using an acid catalyst.[119] The formation of the *tert*-butyl cation through rearrangements has additional precedence. Anodic oxidation of bromoalkanes leads to the formation of their corresponding acetamido compounds.[120] For example, *tert*-butylacetamide was observed as a product in the

reactions of *s*-butyl bromide (trace) and *i*-butyl bromide (major).[120b] The anodic oxidation of n-pentyl bromide leads to the formation of *N*-1-pentylacetamide, *N*-2-pentylacetamide, and *N*-3-pentylacetamide in equal amounts, indicating that the initially formed carbocation undergoes multiple rearrangements.[120a]

The precursor to the methylcyclopropylium ion (1-bromo-1-methylcyclopropane) has not been studied by electrochemistry. However, a gas phase study (MS) on the radical cation revealed that loss of a bromine atom leads to the 1-methylcyclopropylium ion which then undergoes a ring opening to the 1-methylallyl cation rather than the 2-methylallyl cation.[121] The results were in agreement with MNDO calculations on these species. In solution, formation of the 2-methylallyl cation seems more likely (see above). As mentioned above, formation of the *tert*-butyl cation from MCP may involve one or more rearrangements. Both experimental[122] and theoretical[123] results on the $C_4H_7^+$ species have indicated that there is evidence for an equilibrium involving the nonclassical bicyclobutonium ion and the bisected cyclopropylcarbinyl cation. Rearrangements to other $C_4H_7^+$ species do not require much energy and are also expected to happen rapidly. For a four-carbon cationic species, the *tert*-butyl cation is the lowest energy structure that can be formed. The driving force for reaction towards this species will be large, even though this may involve several rearrangements, including hydride transfers.

Electrochemical oxidation of methylenecyclopropane (1) in the presence of a nucleophile.

In order to see whether any of the possible cation or radical cation intermediates could be trapped, the anodic oxidation of MCP was carried out in the presence of a nucleophile (methanol). Dimerization of the radical cation is not expected since nucleophilic attack usually competes effectively with that mode of reaction (see above). Under these conditions one major product and a number of minor products are formed. The major product was found to be 3-methoxy-2-(methoxymethyl)-1-propene (**93**) (Reaction [4.4]). Identification of **93** is based on its mass spectrum only, since it was not isolated.

Reaction [4.4]

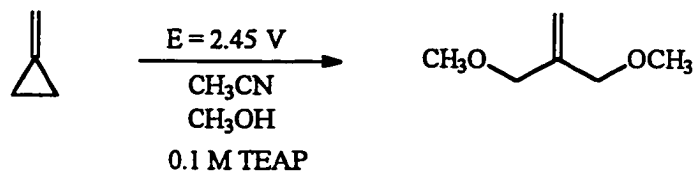

93

Based on the results of the anodic oxidation of **2** under similar conditions (Reaction [3.3]) this is not an unexpected product. Formation of the (ring-opened; TMM) radical cation (**1a**$^{+\bullet}$) followed by nucleophilic addition and loss of a proton from the distonic radical cation leads to the allylic radical. A second oxidation followed by a second nucleophilic addition and deprotonation yields the final product (Scheme 4.16). This sequence of

events parallels that of the formation of products **55**, **56**, **57**, and **58** described in Chapter 3 (Reaction [3.3]).

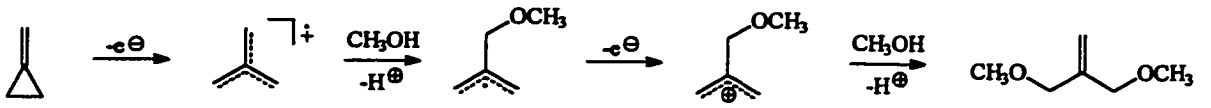

93

Scheme 4.16 Suggested mechanism for the formation of the major product (**93**) in the anodic oxidation of MCP in the presence of methanol.

It must be pointed out that most of the primary products of this reaction are probably too volatile to be observed with conventional gc/fid and gc/ms. For example, it was shown in Chapter 3 that anodic oxidation of alkenes in the presence of a nucleophile can lead to allylic substituted products (e.g. products **52** and **54**; Reaction [3.3]). Even though the formation of these types of products from MCP would require a ring-closed species ($\mathbf{1}^{+\bullet}$, an unlikely intermediate) their presence cannot be ruled out beforehand. It was also suggested that the ring-closed radical species that was observed by ESR upon warming of the matrix in which the TMM radical cation had been generated resulted from a hydrogen atom abstraction by the TMM radical cation from a neutral MCP molecule. Oxidation of this species and nucleophilic addition would also give the allylic substitution products (Scheme 4.17).

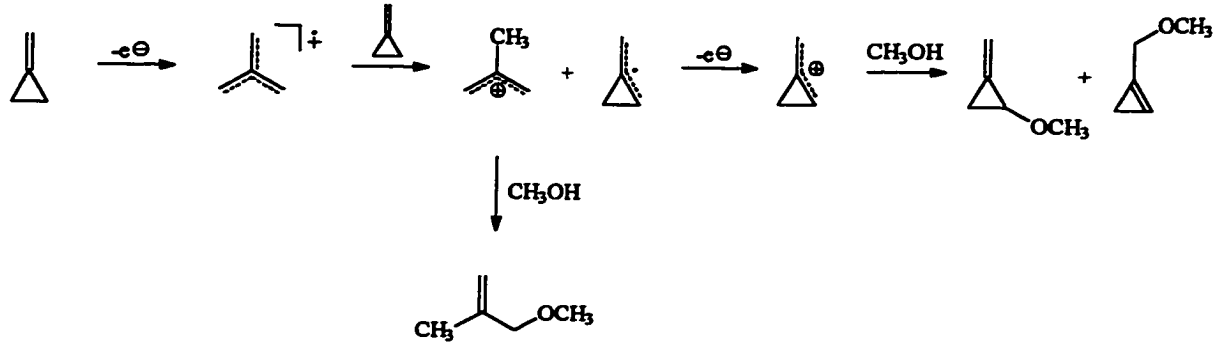

Scheme 4.17 Formation of volatile (low-boiling) products in the anodic oxidation of MCP in the presence of methanol.

The previous part described the anodic oxidation of MCP in the absence of methanol. It was shown that under those conditions the formation of the *tert*-butyl cation is favoured. Formation of this species in the presence of methanol is highly unlikely since it involves multiple rearrangements and the reactive intermediates would be trapped before the final intermediate (*tert*-butyl cation) is formed. However, the possible formation of the product resulting from this intermediate (*tert*-butyl methylether) cannot be ignored. Analysis of the pure compound (Aldrich) by gc/fid showed that the retention time is very short (< 1 minute) and its presence or absence in the reaction mixture can therefore not be proven. Besides the products discussed above there might be several others that fall into the same category. In order to obtain more reliable data for these types of reactions, other nucleophiles will have to be considered for future experiments.

4.3 Conclusions

The photochemical reactions of methylenecyclopropane (MCP, **1**) in the presence of an electron acceptor (1,4-dicyanobenzene, **33**) were studied under a number of

conditions. Using the measured (CV) oxidation potential of MCP, electron transfer was calculated to occur at the diffusion controlled rate. No products resulting from ET were detected; only photocycloaddition products were formed under these conditions. The mechanism is believed to be addition of MCP to the ^1S state of **33**. Only products with ring-closed MCP moieties were formed, indicating that no radical ions, diradicals or ionic species are involved. The product formation was shown to be independent of solvent (MeCN, MeOH, $CHCl_3$) and codonor concentration (biphenyl, **34**). It was shown that for PET reactions, the vertical IP must be considered. In many cases the measured E_{ox} reflects the vertical IP, however, for certain molecules (e.g. MCP) the difference between the vertical and the adiabatic IP is large. In those cases the initially generated (vertical) radical cation is expected to relax to a species with an energy reflecting that of the adiabatic IP. For these types of molecules the measured E_{ox} reflects the adiabatic IP rather than the vertical IP. This can be explained in terms of the formation of a complex (interaction) between the alkene and the Pt-electrode which will result in a partial release of strain. Anodic oxidation of MCP in the absence of a good nucleophile leads to several rearrangements resulting in the formation of the most stable C_4-cation possible: the *tert*-butyl cation. This species is then trapped by the solvent (MeCN) to give the final product *tert*-butylacetamide. In the presence of methanol this intermediate is not believed to be formed, however it cannot be completely ruled out. Under these conditions the major product is 3-methoxy-2-(methoxymethyl)-1-propene, a result of nucleophilic addition to the ring-opened radical cation followed by a second oxidation and nucleophilic addition.

This (reaction) pattern was also observed in the anodic oxidation of 1,4-bis(methylene)cyclohexane (**2**) in the presence of methanol.

The PET reaction of isobutylene in the absence of methanol gives rise to the formation of a photo-NOCAS product with MeCN acting as the nucleophile. The initially formed alkene radical cation adds to the solvent rather than undergoing a deprotonation. It is believed that deprotonation is unfavourable due to the fact that the resulting allylic radical is primary on both ends. This is the first example of this type of photo-NOCAS reaction. The addition of a radical cation to acetonitrile was observed in Chapter 3 as well. In fact, this work has provided examples of radicals, cations, and radical cations adding to acetonitrile. These reactions, incorporating acetonitrile in the final product, may have significant synthetic utility.

4.4 Experimental

General Information

For general procedures, equipment etc., see section 3.4

Materials

Methylenecyclopropane (**1**) was prepared as described below. Sodium amide, dibutylether, methallyl chloride (2-chloromethyl-1-propene), and potassium *tert*-butoxide (1.0 M solution in *tert*-butanol) were all received from Aldrich and used without further purification. 2-Methylpropene (isobutylene, **90**) was obtained from Matheson. For other materials, see section 3.4.

Irradiations

Irradiations were generally carried out on solutions of acetonitrile (with or without methanol as the nucleophile) with 1,4-dicyanobenzene, the alkene, and with or without a codonor. Solutions were irradiated in either 2 cm i.d. Pyrex tubes or 5 mm Pyrex nmr tubes, which were degassed by nitrogen ebullition. The samples were irradiated at 10°C using a CGE 1-kW medium-pressure mercury vapor lamp contained in a water-cooled quartz immersion well.

Cyclic Voltammetric Measurements

Cyclic voltammetry at a sweep rate of 100 mV/s was used to obtain the oxidation potential of the alkene. The apparatus has been described.[83] The working electrode was a platinum sphere (1 mm diameter) and the counter electrode was a platinum wire. The reference electrode was a saturated calomel electrode (sce), which was connected to the solution (TEAP 0.1 M, acetonitrile) through a Luggin capillary. The alkene concentration was ca. 0.005 M. Since the anodic wave was irreversible, the half-wave potential was taken as 0.028 V before the anodic peak potential.[3]

Controlled Potential Electrolyses

Controlled potential electrolyses of **1** were performed with a customized double wall two-electrode cell (total volume 200 mL), containing the working electrode and the reference electrode. The counter electrode compartment, containing the counter electrode,

was fitted into the cell; the two compartments are connected by means of fine glass frit. Both the working electrode and counter electrode were platinum mesh (6.5 cm^2). The reference electrode was the standard calomel electrode (sce). The cell was kept at a temperature of 10°C by means of a thermostated bath.

The electrochemical measurements were obtained with a Princeton Applied Research (PAR) 173 potentiostat in combination with a PAR 175 universal programmer and a PAR 179 digital coulometer.

Synthesis of methylenecyclopropane (1)

Methylenecyclopropane (1) was synthesized according to literature procedures with some minor modifications.[124] A 3-neck round bottom flask equipped with a pressure equalizing drop funnel (with a nitrogen inlet) and a condenser was charged with 20 g sodium amide and 50 mL dibutyl ether. This mixture was refluxed under nitrogen for ca. 15 minutes after which 40 mL of methallyl chloride was added dropwise over a period of 40 minutes. The volatile products were removed from the flask by a small nitrogen flow through a trap containing 50 mL 5N H_2SO_4 followed by an empty trap (kept at room temperature), and were then condensed in a trap cooled by an acetone/dry ice mixture. Analysis of this mixture by ^1H and ^{13}C nmr indicated the presence of both methylenecyclopropane and methylcyclopropene in a ratio of about 1:4. The mixture was transferred to a flask containing 50 mL dimethylsulfoxide after which 10 mL of a 1.0 M solution of potassium *tert*-butoxide in *tert*-butanol was added. The mixture was stirred for 1 h at room temperature and then 2 hours at reflux temperature. The volatiles were carried

over through an empty trap (room temperature) to a cold trap (cooled by an acetone/dry ice mixture) with a small nitrogen flow. The trap contained ca.10 mL of product (≈ 50% yield). Analysis of the contents of the trap by ^{1}H and ^{13}C nmr indicated the presence of pure methylenecyclopropane (**1**).

Irradiation of a mixture of methylenecyclopropane (1), 1,4-dicyanobenzene (33), and biphenyl (34) in acetonitrile.

A solution containing 6 g (1.1×10^{-1} mol) methylenecyclopropane (**1**), 3.1 g (2.4×10^{-2} mol) 1,4-dicyanobenzene (**33**), and 3.7 g (2.4×10^{-2} mol) biphenyl (**34**) dissolved in 240 mL anhydrous acetonitrile was irradiated for 20 days. After this period the solvent and the volatile products were removed by rotary evaporation. The residue was chromatographed on silica gel (mplc) using a hexanes-ether gradient. Further purification of the products was achieved by dcfc. Identification of the products was based on the ^{1}H and ^{13}C nmr spectra and the X-ray diffraction spectra (X-ray data is listed in Appendix II). The yields of the reaction were determined by calibrated gc/fid. All yields are based on the amount of 1,4-dicyanobenzene (**33**) that was consumed in the reaction.

2,5-Dicyanobicyclo[2.2.2]octa-3,7-diene spiro cyclopropane (**79**).

Recrystallized from cyclohexane; mp: 100 - 101°C; ir (KBr) ν: 3087 (s), 3074 (m), 3001 (m), 2978 (m), 2944 (m), 2879 (m), 2856 (w), 2255 (s), 1650 (w), 1603 (w), 1583 (w), 1463 (m), 1455 (m), 1426 (m), 1356 (s), 1324 (w), 1266 (m), 1236 (w), 1173 (m), 1160 (m), 1110 (w), 1056 (m), 1041 (m), 1023 (m), 1012 (m), 971 (m), 961 (m), 949 (m), 882

(m), 867 (m), 716 (s), 691 (s), 657 (w); ^{1}H nmr ($CDCl_3$, AC250) δ: 6.66-6.49 (m, 7.93 Hz, 12.82 Hz, 4H), 1.92 (s, 2H), 0.96 (m, 5.49 Hz, 6.10 Hz, 2H), 0.56 (t, 6.10 Hz, 2H); ^{13}C nmr ($CDCl_3$, AC250) δ: 133.82 (d), 133.40 (d), 120.70 (s), 118.53 (s), 45.57 (s), 42.75 (t), 38.68 (s), 24.77 (s), 10.15 (t); ms *m/z*: 182 ($M^{+\bullet}$, 4 %), 181 (19), 167 (12), 154 (19), 140 (19), 128 (30), 115 (10), 101 (13), 89 (5), 75 (17), 64 (16), 54 (100); actual mass of ion $C_{12}H_{10}N_2$: 182.0844; measured: 182.0843.

2,5-Dicyanotricyclo[3.3.0.^{2,6}0^{5,7}]oct-3-ene spiro cyclopropane (**80**).

Recrystallized from cyclohexane; mp: 90 - 91°C; ir (KBr) ν: 3095 (m), 3073 (m), 3006 (m), 2957 (m), 2943 (m), 2236 (s), 1695 (w), 1602 (w), 1452 (m), 1421 (s), 1360 (w), 1330 (w), 1317 (m), 1294 (w), 1075 (m), 1064 (m), 1031 (s), 1021 (s), 1002 (m), 989 (w), 969 (m), 948 (m), 931 (s), 919 (w), 896 (m), 871 (s), 846 (s), 811 (s), 782 (s), 764 (s), 710 (s); ^{1}H nmr ($CDCl_3$, AC250) δ: 5.81 (d, 5.47 Hz, 1H), 5.60 (d, 5.47 Hz, 1H), 3.56 (d, 7.3 Hz, 1H), 2.66 (dt (unresolved), 1.2 Hz, 6.7 Hz, 6.1 Hz, 1H), 2.05 (d, 14.0 Hz, 1H), 1.78 (dd, 6.7 Hz, 14.6 Hz, 1H), 1.15-1.03 (m, 1H), 0.72-0.49 (m, 3H); ^{13}C nmr ($CDCl_3$, AC250) δ: 132.75 (d), 125.67 (d), 118.33 (s), 116.54 (s), 55.23 (s), 47.28 (d), 37.56 (d), 36.59 (s), 31.62 (t), 27.90 (s), 13.07 (t), 4.90 (t); ms *m/z* 182 ($M^{+\bullet}$, 19%), 181 (70), 167 (38), 155 (56), 154 (100), 140 (67), 127 (37), 116 (41), 103 (25), 89 (17), 76 (29), 67 (55), 54 (40), 51 (50); actual mass of ion $C_{12}H_{10}N_2$: 182.0844; measured: 182.0835.

1,4-Dicyanotetracyclo[2.0.^{3,10}0.^{4,7}2.0.^{7,9}1]decene (**81**).

Recrystallized from cyclohexane; mp: 123 - 124°C; ir (KBr) ν: 3080 (w), 3063 (m), 3000 (m), 2976 (m), 2945 (m), 2869 (w), 2860 (w), 2227 (s), 2217 (s), 1601 (w), 1584 (w), 1448 (m), 1430 (m), 1286 (w), 1263 (w), 1248 (m), 1230 (w), 1196 (w), 1254 (w), 1135 (w), 1059 (m), 1043 (m), 1029 (m), 1006 (w), 966 (m), 955 (m), 909 (w), 873 (m), 865 (m), 848 (m), 838 (m), 652 (m), 641 (w); ^{1}H nmr ($CDCl_3$, AC250) δ: 6.83 (s, 1H), 4.23 (4 line multiplet: 3.05 Hz, 3.66 Hz, 4.27 Hz, 1H), 3.66 (dd, 1.22 Hz, 3.66 Hz, 1H), 2.75 (dd, 1.83 Hz, 10.38 Hz, 1H), 2.60-2.35 (m, 2H), 2.00-1.88 (m, 1H), 1.50-1.41 (m, 1H), 1.23-1.13 (m, 2H); ^{13}C nmr ($CDCl_3$, AC250) δ: 152.18 (d), 122.11 (s), 121.14 (s), 112.90 (s), 62.34 (d), 55.53 (d), 52.27 (s), 43.08 (s), 30.88 (t), 25.51 (t), 20.73 (d), 18.06 (t); ms *m/z:* 182 ($M^{+\bullet}$, 5%), 181 (37), 167 (26), 154 (100), 140 (88), 127 (59), 116 (53), 103 (44), 89 (19), 77 (38), 63 (37), 54 (18), 51 (57); actual mass of ion $C_{12}H_{10}N_2$: 182.0844; measured: 182.0849.

3,7-Dicyanotricyclo[3.3.0.^{2,6}0^{5,7}]oct-3-ene spiro cyclopropane (**82**).

Recrystallized from cyclohexane; mp: 106 - 107°C; ir (KBr) ν: 3084 (w), 3058 (w), 3004 (w), 2968 (w), 2937 (m), 2235 (s), 2216 (s), 1596 (m), 1443 (w), 1425 (m), 1305 (w), 1277 (w), 1247 (w), 1146 (w), 1059 (m), 1031 (m), 1019 (w), 998 (m), 950 (m), 903 (m), 882 (m), 854 (m), 788 (w), 629 (m); ^{1}H nmr ($CDCl_3$, AC250) δ: 6.53 (d, 3.05 Hz, 1H), 3.39 (t, 6.10 Hz, 1H), 2.82 (dd, 1.83 Hz, 5.48 Hz, 1H), 2.69 (dd, 2.44 Hz, 6.73 Hz, 1H), 2.26 (d, 14.05 Hz, 1H), 1.83 (dd, 1.23 Hz, 14.03 Hz, 1H), 0.93-0.54 (m, 4H); ^{13}C nmr ($CDCl_3$, AC250) δ: 140.73 (d), 119.11 (s), 115.18 (s), 58.65 (d), 44.86 (d), 40.35 (d),

35.36 (s), 34.98 (t), 24.37 (s), 14.21 (t), 5.75 (t); ms *m/z*: 182 ($M^{+\bullet}$, 29%), 181 (100), 167 (25), 155 (66), 154 (92), 140 (81), 127 (46), 116 (74), 103 (21), 89 (23), 77 (31), 63 (43), 54 (21), 51 (46); actual mass of ion $C_{12}H_{10}N_2$: 182.0844; measured: 182.0855.

4,6-Dicyanotricyclo[3.3.0.$^{3,7}0^{6,8}$]oct-4-ene spiro cyclopropane (**83**).

Recrystallized from cyclohexane; mp: 106 - 108°C; ir (KBr) ν: 3080 (m), 3054 (w), 2998 (w), 2985 (w), 2971 (w), 2954 (w), 2939 (w), 2870 (w), 2230 (s), 2217 (s), 1601 (m), 1505 (w), 1455 (m), 1430 (m), 1313 (w), 1293 (w), 1277 (w), 1261 (w), 1212 (w), 1153 (m), 1063 (m), 1029 (s), 1006 (m), 987 (w), 966 (s), 949 (w), 923 (w), 909 (m), 876 (s), 847 (s), 838 (s), 784 (w), 699 (w), 607 (w); ^{1}H nmr ($CDCl_3$, AC250) δ: 6.60 (3.05 Hz, 1H), 3.51 (6 line multiplet, 5.49 Hz, 6.11 Hz, 4.88 Hz, 11.60 Hz, 12.20 Hz, 1H + 1H), 2.84 (dd, 4.27 Hz, 12.20 Hz, 1H), 2.69 (dd, 2.44 Hz, 6.10 Hz, 1H), 1.53 (d, 12.20 Hz, 1H), 1.15-1.03 (m, 1H), 0.97-0.84 (m, 1H), 0.67-0.45 (m, 2H); ^{13}C nmr ($CDCl_3$, AC250) δ: 143.43 (d), 120.84 (s), 118.77 (s), 114.86 (s), 52.13 (d), 50.45 (t), 46.60 (d), 42.60 (d), 31.71 (s), 22.28 (s), 15.15 (t), 7.92 (t); ms *m/z:* 182 ($M^{+\bullet}$, 11%), 181 (28), 167 (27), 155 (15), 154 (23), 140 (16), 128 (14), 116 (21), 103 (12), 89 (2), 76 (12), 63 (10), 54 (100), 51 (17); actual mass of ion $C_{12}H_{10}N_2$: 182.0844; measured: 182.0850.

Dispiro[2.4.2.4]-11,14-dicyanotricyclo[2.2.2.0.$^{5,14}0^{6,11}$]tetradec-12-ene (**84**).

Recrystallized twice from cyclohexane and once from 95% ethanol; mp: 176 - 177°C; ir (KBr) ν: 3078 (w), 3001 (m), 2988 (w), 2967 (s), 2935 (m), 2925 (s), 2858 (m), 2237 (m), 2224 (m), 1446 (m), 1425 (m), 1244 (m), 1211 (w), 1177 (w), 1131 (w), 1118 (w),

1064 (w), 1060 (w), 1051 (w), 1033 (m), 1026 (m), 991 (w), 913 (m), 904 (w), 885 (m), 873 (m), 807 (m), 761 (s); ^{1}H nmr ($CDCl_3$, AC250) δ: 5.84 (s, 2H), 3.15 (m, 8.55 Hz, 9.15 Hz, 2H), 2.26 (m, 10.98 Hz, 9.77 Hz, 2H), 2.04 (m, 1.84 Hz, 9.15 Hz, 2H), 1.14-1.01 (m, 2H), 0.85-0.73 (m, 2H), 0.73-0.61 (m, 2H), 0.50-0.38 (m, 2H);^{13}C nmr ($CDCl_3$, AC250) δ: 124.43 (d), 119.85 (s), 35.94 (d), 35.77 (s), 30.62 (t), 26.23 (s), 12.02 (t), 6.78 (t); ms *m/z*: 236 ($M^{+\bullet}$, 1%), 235 (7), 221 (4), 207 (27), 194 (8), 179 (21), 167 (7), 154 (21), 140 (10), 129 (11), 116 (20), 104 (13), 91 (10), 77 (15), 63 (11), 54 (100), 51 (21); actual mass of ion $C_{16}H_{16}N_2$: 236.1313; measured: 236.1290.

Irradiation of methylenecyclopropane (1) and 1,4-dicyanobenzene (33) in acetonitrile.

A 0.1 M solution (40 mL) of MCP (**1**) in acetonitrile containing 0.5 g (3.9×10^{-3} mol) 1,4-dicyanobenzene (**33**) and 0.6 g (3.9×10^{-3} mol) biphenyl (**34**) was irradiated through Pyrex with the 1-kW lamp for 30 days. The reaction was followed by gc/fid and gc/ms. Analysis of the product mixture indicated the presence of the same products as in the reaction with a larger MCP concentration.

Influence of the biphenyl (34) concentration on the product formation in the irradiation of methylenecyclopropane (1) and 1,4-dicyanobenzene (33) in acetonitrile.

Solutions (2 mL) containing 0.1 M (50 μL) MCP (**1**) and 0.1 M (25 mg) 1,4-dicyanobenzene (**33**), as well as 0.1 M (30 mg) , 0.25 M (78 mg) , and 0.5 M (154 mg) biphenyl (**34**) were irradiated through Pyrex with the 1-kW lamp for 40 hours. The reactions were followed by gc/fid and gc/ms. Analysis of the product mixtures indicated

that the same products were formed in each reaction. Increasing the biphenyl concentration slows down the product formation. No other products were formed.

Irradiation of methylenecyclopropane (1) and 1,4-dicyanobenzene (33) in chloroform.

A solution of 0.7 g (1.3×10^{-2} mol) methylenecyclopropane (**1**) and 1.55 g (1.2×10^{-2} mol) 1,4-dicyanobenzene (**33**) in 200 mL chloroform was irradiated for 5 days through Pyrex with the 1-kW lamp. The reaction was followed by gc/ms and gc/fid. Analysis of the product mixture by gc/fid and gc/ms indicated the formation of the same products that were observed in the experiment with acetonitrile as the solvent.

Irradiation of a mixture of methylenecyclopropane (1) and 1,4-dicyanobenzene (33) in acetonitrile-methanol (3:1).

A solution of 0.2 g (3.7×10^{-3} mol) methylenecyclopropane (**1**), 0.5 g (3.9×10^{-3} mol) 1,4-dicyanobenzene (**33**), and 0.6 g (3.9×10^{-3} mol) biphenyl (**34**) in 40 mL acetonitrile-methanol (3:1 by volume) solution was irradiated through Pyrex with the 1-kW lamp for 40 days. The reaction was followed by gc/fid and gc/ms. Product identification was based on retention time (2 different columns) and mass spectra. Several other products were tentatively identified as the reduced 1:1 cycloadducts; the identification is based on their mass spectra.

Irradiation of a solution of 2-methylpropene (isobutylene, 90) and 1,4-dicyanobenzene (33) in acetonitrile.

2-Methylpropene (**90**) was bubbled for two minutes through a solution of 25 mg (2.0×10^{-4} mol) 1,4-dicyanobenzene (**33**) in 2 mL acetonitrile. The solution was irradiated for 41 hours through Pyrex with the 1-kW lamp. The reaction was followed by gc/fid and gc/ms. Analysis of the final product mixture revealed the presence of only one major product (**91**; ca. 70% yield at 60% conversion of **33**).

Irradiation of a solution of 2-methylpropene (isobutylene, 90) and 1,4-dicyanobenzene (33) in acetonitrile-d_3.

2-Methylpropene (**90**) was bubbled for two minutes through a solution of 25 mg (2.0×10^{-4} mol) 1,4-dicyanobenzene (**33**) in 2 mL acetonitrile-d_3. The solution was irradiated for 14 hours through Pyrex with the 1-kW lamp. The reaction was followed by gc/fid and gc/ms. Analysis of the final product mixture revealed the presence of only one major product. The mass spectrum (m/z ($M^{+\bullet}$) = 201) indicated that deuterium had been incorporated into the molecule (**91**-d_3).

Irradiation of a solution of 2-methylpropene (isobutylene, 90) and 1,4-dicyanobenzene (33) in acetonitrile.

2-Methylpropene (**90**) was added to a solution of 2.6 g (2.0×10^{-2} mol) 1,4-dicyanobenzene (**33**) in 200 mL acetonitrile by ebullition of the gas through the solution for 5 minutes. The mixture was irradiated through Pyrex with the 1-kW lamp for 8 days.

The reaction was followed by gc/fid and gc/ms. Only one product (**91**) was detected. The solvent was evaporated by rotary evaporation and the residue was chromatographed on silica gel (dcfc) using a hexanes-dichloromethane gradient. The isolated product was characterized by ^{1}H nmr, ^{13}C nmr, ir, and mass spectra and was identified as 7-cyano-1,4,4-trimethyl-2-benzazine (**91**).

7-Cyano-1,4,4-trimethyl-2-benzazine (**91**).

ir (Nicolet) ν: 2966 (m), 2931 (m), 2902 (w), 2231 (m), 1637 (m), 1465 (w), 1438 (w), 1387 (w), 1374 (m), 1307 (w), 1295 (m), 912 (m), 732 (s); ^{1}H nmr (AC250, $CDCl_3$) δ: 7.77 (d, 1.22 Hz, 1H), 7.71 (dd, 1.22 Hz, 7.93 Hz, 1H), 7.49 (d, 7.93 Hz, 1H), 3.58 (br. s, 2H), 2.45 (s, 3H), 1.24 (s, 6H); ^{13}C nmr (AC250, $CDCl_3$) δ: 162.48 (s), 151.26 (s), 134.51 (d), 129.19 (d), 128.30 (s), 124.82 (d), 118.39 (s), 110.55 (s), 59.46 (t), 32.06 (s), 25.86 (q), 23.01 (q); ms *m/z*: 198 ($M^{+\bullet}$, 52%), 197 (100), 183 (90), 168 (8), 154 (17), 140 (17), 127 (18), 116 (13), 101 (6), 89 (7), 77 (11), 63 (12), 51 (13); actual mass of ion $C_{13}H_{14}N_2$: 198.1157; measured: 198.1166.

Electrolysis of a solution of methylenecyclopropane (1) in acetonitrile.

A solution of 4.6 g (2.0×10^{-2} mol) tetraethylammonium perclorate (TEAP) in 200 mL acetonitrile was deaerated for 30 minutes by nitrogen ebullition. After this period 6.5 mL (9.6×10^{-2} mol) methylenecyclopropane (**1**) was added to the solution and a potential difference of 2.45 V was applied to the cell. The reaction was stopped after 1080 C had been consumed (ca. 10% conversion; calculated on basis of a 1-electron oxidation (Eq.

3.2)). The solvent was evaporated and the residue was washed with benzene to remove the residual TEAP. Evaporation of the benzene left the crude product which was identified as N-*tert*-butylacetamide (**92**, 25%) based on its ^{1}H nmr, ^{13}C nmr,[125a,b] and mass spectra.[125b]

N-tert-butylacetamide (**92**).

^{1}H nmr ($CDCl_3$, AC250) δ: 7.36 (s, 1H), 1.94 (s, 3H), 1.35 (s, 9H); ^{13}C nmr ($CDCl_3$, AC250) δ: 170.11 (s), 51.36 (s), 28.63 (q), 24.22 (q); ms *m/z*: 115 ($M^{+\bullet}$, 7%), 100 (10), 64 (5), 60 (21), 59 (17), 58 (100), 56 (7).

Electrolysis of a solution of methylenecyclopropane (1) in acetonitrile-methanol (3:1).

A solution of 4.6 g TEAP (2.0×10^{-2} mol) in 200 mL acetonitrile-methanol (3:1) was purged with nitrogen for 45 minutes. A potential difference of 2.45 V was applied to the cell for 2 hours for background correction. After this period the coulometer was reset and 6.5 mL MCP (5.2 g, 9.6×10^{-2} mol) was added to the solution after which the potential difference (2.45 V) was applied to the cell again. The reaction was allowed to continue until 2085 C had been consumed (ca. 11% conversion; calculated on basis of a 2-electron oxidation using Eq. 3.2). Analysis of the product mixture by gc/ms revealed the presence of one major product (**93**) and several minor products. Compound **93** was isolated from the mixture by distillation and further purified by prep-gc. Identification of product **93** (3-methoxy-2-(methoxymethyl)-1-propene) is based on its mass spectrum.

3-Methoxy-2-(methoxymethyl)-1-propene (93).

ms *m/z*: 116 ($M^{+\bullet}$, 0.1%), 115 (1), 101 (2), 85 (18), 84 (47), 75 (18), 71 (100), 69 (12), 58 (9), 56 (16), 55 (55), 53 (13).

Appendix I

Selected bond lengths, bond angles, and dihedral angles of methylenecyclopropane (1), 1,4-bis(methylene)cyclohexane (2), tricyclo[2.2.2.0^{1,4}]octane (3), dispiro[2.0.2.2]octane (4), dispiro[2.1.2.1]octane (5), and derived radical cations as calculated by AM1 and ab initio methods.

Table 2.8. Selected calculated (AM1) bond lengths, bond angles, and dihedral angles of methylenecyclopropane (**1**) and derived radical cations.[a]

	1	**1**$^{+\bullet}$	**1a**$^{+\bullet}$
bond length			
1-2	1.467	1.567	1.414
1-3	1.467	1.567	1.413
1-4	1.309	1.284	1.399
2-3	1.513	1.450	2.429
bond angle			
1-2-3	62.1	62.4	121.2
2-1-4	148.9	152.4	119.4
dihedral angle			
1-2-3-4	180.0	180.0	180.0

[a] All bond lengths are in angstroms; bond angles and dihedral angles are in degrees.

Table 2.9. Selected calculated (AM1) bond lengths, bond angles, and dihedral angles of 1,4-bis(methylene)cyclohexane (**2**) and derived radical cations.[a]

	2a	**2b**	**2a**$^{+\bullet}$	**2b**$^{+\bullet}$	**6**$^{+\bullet}$	**7**$^{+\bullet}$	**10**$^{+\bullet}$
bond length							
1-2	1.490	1.490	1.462	1.489	1.388	1.389	4.091
1-4	2.873	2.943	2.841	2.913	3.056	3.814	3.733
1-7	1.335	1.336	1.423	1.338	1.382	1.387	1.300
2-3	1.519	1.517	1.519	1.517	3.418	5.475	1.509
3-4	1.490	1.490	1.486	1.464	1.392	1.386	1.491
4-8	1.335	1.336	1.336	1.413	1.388	1.384	1.337
7-8	5.448	5.616	5.479	5.664	4.693	5.058	5.942
bond angle							
1-2-3	111.9	112.3	115.5	113.2	-	-	-
2-3-4	111.9	112.3	112.0	113.3	-	-	113.0
6-1-2	114.9	116.1	122.3	117.5	119.1	118.7	-
7-1-2	122.5	122.0	118.8	121.3	120.5	122.1	-
8-4-3	122.5	122.0	122.8	120.5	121.6	120.3	122.7
dihedral angle							
1-2-3-4	-49.5	-55.4	-37.7	-49.6	-	-	-
1-6-5-4	49.5	37.3	-55.4	-49.4	63.7	178.7	180.0
2-1-6-7	178.6	177.4	-180.0	180.0	-179.6	-179.0	-
3-4-5-8	-178.6	-177.1	180.0	-180.0	176.9	-179.9	176.5
6-1-2-3	51.0	26.9	23.8	24.7	-	-	-
7-1-2-3	-130.4	-153.1	-158.8	-155.4	-	-	-
8-4-3-2	-130.4	-152.8	-128.8	-155.7	-	-	116.6

[a] All bond lengths are in angstroms; bond angles and dihedral angles are in degrees.

Table 2.10. Selected calculated (AM1) bond lengths, bond angles, and dihedral angles of tricyclo[2.2.2.$0^{1,4}$]octane (**3**) and derived radical cations.[a]

	3	**3**$^{+\bullet}$	**12**$^{+\bullet}$
bond length			
1-2	1.528	1.488	3.300
1-4	1.616	2.271	1.547
1-6	1.528	1.488	1.469
1-7	1.528	1.488	1.470
2-3	1.568	1.598	1.461
3-4	1.528	1.476	1.491
4-5	1.528	1.475	1.564
4-8	1.528	1.475	1.564
5-6	1.568	1.597	1.582
7-8	1.568	1.597	1.581
bond angle			
1-2-3	90.9	104.7	98.8
4-5-6	90.9	101.6	91.6
5-6-1	90.9	104.7	85.9
6-1-7	120.0	113.9	138.8
8-4-5	120.0	115.9	119.2
dihedral angle			
3-2-1-6	-88.4	-67.0	56.0
4-5-6-1	-0.0(2)	0.8	-10.5
5-6-1-2	-88.4	65.9	-
7-1-6-2	176.9	132.9	-
8-4-5-6	88.5	70.1	89.4

[a] All bond lengths are in angstroms; bond angles and dihedral angles are in degrees.

Table 2.11. Selected calculated (AM1) bond lengths, bond angles, and dihedral angles of dispiro[2.0.2.2]octane (**4**) and derived the radical cations.[a]

	4	**4**$^{+\bullet}$	**13**$^{+\bullet}$	**15**$^{+\bullet}$	**16**$^{+\bullet}$	**17**$^{+\bullet}$	**18**$^{+\bullet}$	**19**$^{+\bullet}$
bond length								
1-2	1.502	1.460	1.477	1.516	1.517	1.518	1.460	1.489
1-3	1.495	1.559	1.527	1.455	1.458	1.456	1.578	1.528
2-3	1.494	1.558	1.527	1.458	1.459	1.457	1.579	1.524
3-4	1.507	1.451	1.451	3.148	3.063	3.721	1.378	1.489
3-8	1.528	1.524	1.538	1.414	1.434	1.432	1.508	1.449
4-5	1.495	1.560	2.457	1.391	1.457	1.457	1.459	1.597
4-6	1.494	1.558	1.443	1.388	1.455	1.455	1.461	1.612
4-7	1.528	1.524	1.503	1.495	1.415	1.410	3.172	1.382
5-6	1.502	1.460	1.467	2.429	1.516	1.516	1.515	1.449
7-8	1.550	1.530	1.558	1.520	1.523	1.524	1.462	3.375
bond angle								
1-2-3	60.3	62.1	61.1	62.7	62.7	62.8	62.5	60.9
1-3-4	128.0	128.8	128.5	-	-	-	117.8	118.4
2-3-4	128.0	129.0	128.6	-	-	-	117.3	-
3-4-7	90.8	91.9	93.0	101.2	101.0	149.0	107.0	119.1
4-5-6	60.3	62.1	115.2	121.9	62.8	62.8	62.5	63.7
4-7-8	89.2	88.1	88.3	112.2	115.7	115.9	104.4	119.5
6-4-3	128.0	129.0	135.6	-	-	-	149.5	116.3
dihedral angle								
1-3-4-5	-79.2	-74.3	-38.1	-	-	-	-149.4	107.8
2-3-4-5	0.0	-0.3	38.3	-	-	-	147.7	40.2
3-8-7-4	0.0(5)	-0.0(3)	0.0	-73.9	-68.8	179.5	-77.4	100.0
7-4-5-6	115.7	113.4	-179.9	177.4	179.9	-179.8	-	-103.5
8-3-1-2	115.7	113.4	114.7	-179.9	-156.0	-173.6	105.7	-106.1

[a] All bond lengths are in angstroms; bond angles and dihedral angles are in degrees.

Table 2.12. Selected calculated (AM1) bond lengths, bond angles, and dihedral angles of dispiro[2.1.2.1]octane (**5**) and derived radical cations.[a]

	5	**20**$^{+\bullet}$	**22**$^{+\bullet}$	**23**$^{+\bullet}$
bond length				
1-2	1.503	1.499	1.495	1.489
1-3	1.492	1.495	1.508	1.527
2-3	1.492	1.495	1.508	1.522
3-4	1.528	1.532	1.510	1.445
3-8	1.528	1.533	1.510	1.502
4-5	1.528	1.493	2.411	3.040
5-6	1.492	1.435	1.473	1.458
5-7	1.492	2.461	1.406	1.454
5-8	1.528	1.497	1.473	1.416
6-7	1.503	1.462	2.545	1.516
bond angle				
3-2-1	60.5	60.2	60.3	60.9
3-4-5	89.0	88.7	72.4	98.3
3-8-5	89.0	88.5	106.4	115.9
5-6-7	60.5	116.3	124.3	62.8
8-3-1	127.3	127.7	120.0	116.5
8-3-2	127.3	127.7	120.2	118.1
8-3-4	91.0	90.0	108.7	115.2
8-5-4	91.0	92.9	74.0	98.5
8-5-6	127.3	133.1	111.4	147.7
8-5-7	127.3	165.3	124.2	149.6
dihedral angle				
3-1-2-4	116.3	116.7	-109.9	106.6
4-5-6-7	116.3	0.0	-179.5	-
8-3-1-2	-116.3	-116.6	109.2	-105.4
8-3-4-5	0.0	0.0	-1.4	61.7
8-5-6-7	-116.4	-180.0	180.0	-179.8

[a] All bond lengths are in angstroms; bond angles and dihedral angles are in degrees.

Table 2.13. Selected calculated (HF/6-31G*) bond lengths, bond angles and dihedral angles of methylenecyclopropane (1) and derived radical cations.[a]

	1	$1^{+\bullet}$	$1a^{+\bullet}$
bond length			
1-2	1.462	1.616	1.385
1-3	1.462	1.616	1.385
1-4	1.308	1.299	1.452
2-3	1.527	1.425	2.321
bond angle			
2-1-3	58.5	63.8	113.8
4-1-2	148.6	153.8	123.1
dihedral angle			
1-2-3-4	-180.0	180.0	-180.0

[a] All bond lengths are in angstroms; bond angles and dihedral angles are in degrees.

Table 2.14. Selected calculated (HF/6-31G*) bond lengths, bond angles and dihedral angles of 1,4-bis(methylene)cyclohexane (**2**) and derived radical cations.[a]

	2a	**2b**	**2c**	**2a**$^{+\bullet}$	**2b**$^{+\bullet}$	**2c**$^{+\bullet}$	**6**$^{+\bullet}$	**7**$^{+\bullet}$
bond length								
1-2	1.511	1.519	1.509	1.508	1.519	1.475	1.387	1.394
1-4	2.901	2.987	2.803	2.864	2.959	2.734	3.039	3.886
1-7	1.321	1.320	1.320	1.321	1.318	1.372	1.368	1.394
2-3	1.540	1.533	1.542	1.560	1.537	1.607	3.742	5.232
3-4	1.511	1.519	1.522	1.486	1.484	1.482	1.400	1.377
4-8	1.321	1.320	1.320	1.417	1.418	1.372	1.393	1.377
7-8	5.412	5.627	4.942	5.466	5.694	4.646	4.276	5.232
bond angle								
3-2-1	111.0	111.5	110.5	110.8	112.2	106.7	-	-
4-3-2	111.0	111.5	112.1	110.0	112.3	111.9	-	-
6-1-2	114.1	115.1	114.4	114.1	116.0	115.1	121.7	119.0
7-1-2	123.0	122.5	123.0	122.0	122.0	122.4	114.4	122.0
8-4-3	123.0	122.5	122.6	121.1	121.0	122.1	121.3	114.0
dihedral angle								
1-6-5-4	52.0	58.9	-38.5	50.6	54.0	-37.5	59.5	180.0
3-2-1-6	53.7	-28.7	59.7	54.8	-26.4	63.3	-	-
3-4-5-8	178.5	-180.0	178.3	178.2	-180.0	172.1	-178.0	179.5
4-3-2-1	-52.0	58.9	-38.5	-50.5	54.1	-37.5	-	-
7-1-2-6	-178.5	-180.0	-178.3	-179.4	-180.0	-172.1	-180.0	178.4
8-4-3-2	-124.8	151.4	159.2	-125.9	153.4	147.6	-	-

[a] All bond lengths are in angstroms; bond angles and dihedral angles are in degrees.

Table 2.15. Selected calculated (HF/6-31G*) bond lengths, bond angles and dihedral angles of tricyclo[2.2.2.$0^{1,4}$]octane (**3**) and derived radical cations.[a]

	3	$\mathbf{3}^{+\bullet}$
bond length		
1-2	1.548	1.511
1-4	1.511	2.292
1-6	1.548	1.511
2-3	1.569	1.626
3-4	1.548	1.468
4-5	1.548	1.468
5-6	1.569	1.627
7-1	1.548	1.511
7-8	1.569	1.627
8-4	1.548	1.468
bond angle		
3-2-1	88.9	107.1
4-5-6	88.9	98.6
5-6-1	88.9	107.1
6-1-2	120.0	111.9
7-1-6	120.0	111.9
8-4-5	120.0	117.7
dihedral angle		
3-2-1-6	91.8	63.4
4-5-6-1	0.0	-0.2
5-6-1-2	-91.8	-63.1
7-1-6-2	183.7	126.5
8-4-5-6	-91.8	-75.0

[a] All bond lengths are in angstroms; bond angles and dihedral angles are in degrees.

Table 2.16. Selected calculated (HF/6-31G*) bond lengths, bond angles and dihedral angles of dispiro[2.0.2.2]octane (**4**) and derived radical cations.[a]

	4	**4a**$^{+\bullet}$
bond length		
1-2	1.502	1.462
1-3	1.491	1.728
2-3	1.491	1.492
3-4	1.521	1.423
3-8	1.533	1.523
4-5	1.491	1.728
4-6	1.491	1.492
4-7	1.533	1.523
5-6	1.502	1.462
7-8	1.553	1.554
bondangle		
1-2-3	60.5	71.6
1-3-4	128.3	117.0
3-4-5	128.3	117.0
4-7-8	89.4	87.4
6-4-7	126.6	132.8
7-8-3	89.4	87.4
8-3-2	126.6	132.8
dihedral angle		
1-2-3-4	-117.4	-93.9
1-3-4-5	-79.9	-114.0
3-4-7-8	-0.1	-6.1
4-5-6-7	115.6	99.8
6-4-3-8	-140.2	-176.0
6-4-7-8	141.3	176.1

[a] All bond lengths are in angstroms; bond angles and dihedral angles are in degrees.

Table 2.17. Selected calculated (HF/6-31G*) bond lengths, bond angles and dihedral angles of dispiro[2.1.2.1]octane (**5**) and derived radical cations.[a]

	5	**21**$^{+\bullet}$
bond length		
1-2	1.502	1.498
1-3	1.491	1.492
2-3	1.491	1.492
3-4	1.534	1.534
4-5	1.534	1.547
5-6	1.491	1.472
5-7	1.491	1.472
5-8	1.534	1.547
6-7	1.502	1.844
8-3	1.534	1.534
bond angle		
1-2-3	60.5	60.3
2-3-4	126.9	126.4
3-4-5	88.0	86.9
4-5-6	126.9	122.5
5-6-7	60.5	77.6
5-8-3	88.0	86.9
7-5-8	126.9	122.7
8-3-1	126.9	126.3
dihedral angle		
1-2-3-4	115.9	-115.2
2-3-4-5	141.0	-142.0
3-4-5-6	150.0	-131.4
4-5-6-7	115.9	-120.9
6-5-8-3	141.0	131.4
8-3-1-2	-115.9	115.2
8-3-4-5	-0.0(1)	0.4

[a] All bond lengths are in angstroms; bond angles and dihedral angles are in degrees.

Table 2.18. Selected calculated (HF/6-31G*) bond lengths, bond angles and dihedral angles of the dimeric radical cations $24^{+\bullet}$ - $31^{+\bullet}$.[a]

species	bond length		bond angle		dihedral angle	
$24^{+\bullet}$	1-2	1.491	2-1-3	130.0	1-2-3-4	121.5
	1-3	1.468	2-5-6	105.7	1-2-5-6	58.0
	1-4	1.476	3-1-4	62.0	2-5-6-7	-100.2
	1-6	2.884	5-2-1	113.0	5-6-7-8	-176.4
	2-5	1.578	5-6-7	149.2		
	3-4	1.516				
	5-6	1.449				
	6-7	1.444				
	6-8	1.446				
	7-8	1.515				

species	bond length		bond angle		dihedral angle	
$25^{+\bullet}$	1-2	1.392	1-3-5	114.3	1-2-3-4	-179.7
	1-3	1.518	2-1-3	118.9	1-3-5-6	59.8
	1-4	1.398	2-1-4	122.2	2-1-3-5	-111.1
	1-6	2.968	3-5-6	106.6	3-5-6-7	-95.3
	2-4	2.442	5-6-7	148.7	5-6-7-8	-176.2
	3-2	2.507	7-6-8	63.2		
	3-4	2.512				
	5-3	1.588				
	5-6	1.447				
	6-7	1.443				
	6-8	1.447				
	7-8	1.515				

Table 2.18 (cont.)

species	bond length		bond angle		dihedral angle	
$26^{+\bullet}$	1-2	1.453	1-2-3	123.2	1-2-3-4	179.3
	1-3	1.389	3-1-4	114.0	5-6-7-8	-179.9
	1-4	1.381	5-6-7	147.9		
	1-6	5.251	7-6-8	63.9		
	3-4	2.323				
	3-7	3.252				
	3-8	3.342				
	4-8	5.089				
	5-6	1.307				
	6-7	1.461				
	6-8	1.458				
	7-8	1.544				

species	bond length		bond angle		dihedral angle	
$27^{+\bullet}$	1-2	1.284	1-4-3	82.3	3-4-1-2	-6.1
	1-3	1.933	2-1-3	128.7	5-6-7-8	-174.5
	1-4	1.430	2-1-4	179.2		
	2-5	3.666	5-6-7	148.5		
	3-4	1.506	6-7-8	62.8		
	5-6	1.313				
	6-7	1.463				
	6-8	1.463				
	7-8	1.524				

Table 2.18 (cont.)

species	bond length		bond angle		dihedral angle	
28$^{+\bullet}$	1-2	1.398	1-4-5	114.3	1-2-3-4	179.7
	1-3	1.392	3-1-2	122.2	1-4-5-6	-59.8
	1-4	1.518	3-1-4	118.9	3-1-4-5	111.0
	1-6	2.969	4-5-6	106.6	4-5-6-7	-78.3
	2-3	2.442	5-6-7	148.0	5-6-7-8	-176.3
	4-5	1.588	6-7-8	63.2		
	5-6	1.447				
	6-7	1.447				
	6-8	1.443				
	7-8	1.515				

species	bond length		bond angle		dihedral angle	
29$^{+\bullet}$	1-2	1.519	1-2-5	108.5	1-2-3-4	-179.2
	1-3	1.394	1-3-4	123.0	1-2-5-6	-180.0
	1-4	1.394	2-5-6	104.1	2-5-6-7	-84.2
	1-6	3.736	3-1-2	118.5	3-1-2-5	-89.6
	2-5	1.599	5-6-7	148.2	5-6-7-8	-173.2
	3-4	2.449	6-7-8	63.2		
	5-6	1.439				
	6-7	1.446				
	6-8	1.446				
	7-8	1.515				

Table 2.18 (cont.)

species	bond length		bond angle		dihedral angle	
30$^{+\bullet}$	1-2	1.397	1-2-3	117.7	1-2-3-4	-180.0
	1-4	1.420	3-1-4	124.7	5-6-7-8	180.0
	1-3	1.423	5-6-7	148.0		
	1-6	5.927	6-7-8	63.6		
	3-8	5.106				
	3-4	2.518				
	4-7	3.944				
	5-6	1.307				
	6-7	1.461				
	7-8	1.539				

species	bond length		bond angle		dihedral angle	
31$^{+\bullet}$	1-2	1.519	1-2-5	108.5	1-2-5-6	-180.0
	1-3	1.394	2-5-6	104.1	2-5-6-7	-84.2
	1-4	1.394	3-1-2	118.5	3-1-2-5	-89.6
	1-6	3.736	3-1-4	123.0	2-1-3-4	-179.3
	2-5	1.599	5-6-7	148.2	5-6-7-8	-173.2
	3-4	2.449	7-6-8	63.2		
	5-6	1.439				
	6-7	1.446				
	6-8	1.446				
	7-8	1.515				

[a] All bond lengths are in angstroms; bond angles and dihedral angles are in degrees.

Appendix II

Determination of the structures of the photocycloaddition products obtained from the reaction between methylenecyclopropane (1) and dicyanobenzene (33) by X-ray crystallography.

Experimental.

The general description that follows corresponds to the structure determination for compound **79** and has specific information for that particular crystal. Similar data for the other compounds (**80** - **83**) can be found in the tables that follow this section. The experimental technique, however, was similar.

Data Collection

A colourless needle crystal of $C_{12}H_{10}N_2$ having approximate dimensions of 0.020 × 0.060 × 0.250 mm was mounted in a glass capillary. All measurements were made on a Rigaku AFC5R diffractometer with graphite monochromated Cu-Kα radiation and a 12 kW rotating anode generator.

Cell constants and an orientation matrix for data collection, obtained from a least-squares refinement using the setting angles of 25 carefully centered reflections in the range $40.66 < 2\theta < 52.20°$ corresponded to a primitive monoclinic cell with dimensions:

a = 10.7328(9) Å
b = 8.029(1) Å $\beta = 95.186(6)°$
c = 11.7230(8) Å
V = 1006.1(2) Å^3

For Z = 4 and F.W. = 182.22, the calculated density is 1.20 g/cm^3. The systematic absences of:

h01: $l \neq 2n$
0k0: $k \neq 2n$

uniquely determine the space group to be:

$P2_1/c$ (#14)

The data were collected at a temperature of 23 ± 1°C using the ω-2θ scan technique to a maximum 2θ value of 120.1°. Omega scans of several intense reflections, made prior to data collection, had an average width at half-height of 0.36° with a take-off angle of 6.0°. Scans of (1.26 + 0.35 tanθ)° were made at a speed of 8.0°/min (in omega). The weak reflections ($I < 15.0\sigma(I)$) were rescanned (maximum of 5 rescans) and the counts were accumulated to ensure good counting statistics. Stationary background

counts were recorded on each side of the reflection. The ratio of peak counting time to background counting time was 2:1. The diameter of the incident beam collimator was 0.5 mm and the crystal to detector distance was 400 mm.

Data Reduction

Of the 1750 reflections which were collected, 1613 were unique (R_{int} = 0.147). The intensities of three representative reflections were measured after every 150 reflections. Over the course of the data collection, the standards decreased by 14.6%. A linear correction factor was applied to the data to account for this phenomenon.

The linear absorption coefficient, μ, for Cu-Kα radiation is 5.4 cm^{-1}. Azimuthal scans of several reflections indicated nod need for an absorption correction. The data were corrected for Lorentz and polarization effects.

Structure Solution and Refinement

The structure was solved by direct methods[126] and expanded using Fourier techniques.[127] Some non-hydrogen atoms were refined anisotropically, while the rest were refined isotropically. Hydrogen atoms were included but not refined. The final cycle of full-matrix least-squares refinement[128] was based on 364 observed reflections ($I > 3.00\sigma(I)$) and 87 variable parameters and converged (largest parameter shift was 0.00 times its esd) with unweighted and weighted agreement factors of:

$$R = \Sigma||Fo| - |Fc||/\Sigma|Fo| = 0.069$$
$$R_w = \sqrt{(\Sigma w(|Fo| - |Fc|)^2/\Sigma wFo^2)} = 0.070$$

The standard deviation of an observation of unit weight[129] was 2.84. The weighting scheme was based on counting statistics and included a factor (p = 0.020) to downweight the intense reflections. Plots of $\Sigma w(|Fo| - |Fc|)^2$ versus $|Fo|$, reflection order in data collection, sin θ/λ and various classes of indices showed no unusual trends. The maximum and minimum peaks on the final difference Fourier map corresponded to 0.21 and -0.21 e^- / Å^3, respectively.

Neutral atom scattering factors were taken from Cromer and Waber.[130] Anomalous dispersion effects were included in Fcalc;[131] the values for $\Delta f'$ and $\Delta f''$ were those of Creagh and McAuley.[132] The values for the mass attenuation coefficients are those of Creagh and Hubbel.[133] All calculations were performed using the teXsan[134] crystallographic software package of Molecular Structure Corporation.

2,5-Dicyanobicyclo[2.2.2]octa-3,7-diene spiro cyclopropane (**79**)

A. Crystal Data

Empirical Formula	$C_{12}H_{10}N_2$
Formula Weight	182.22
Crystal Colour, Habit	colourless, needle
Crystal Dimensions	0.020 × 0.060 × 0.250
Crystal System	monoclinic
Lattice Type	P
No. of Reflections Used for Unit Cell Determination (2θ range)	25 (40.7 - 52.2°)
Omega Scan Peak Width at Half-height	0.36°
Lattice Parameters	a = 10.7328(9)Å b = 8.029(1) Å c = 11.7230(8) Å β = 95.186(6)° V = 1006.1(2) Å^3
Space Group	$P2_1/c$ (#14)
Z value	4
D_{calc}	1.203 g/cm^3
F_{000}	384.00
μ(MoKα)	5.36 cm^{-1}

B. Intensity Measurements

Diffractometer	Rigaku AFC5R
Radiation	CuKα (λ = 1.54178 Å) graphite monochromated
Attenuator	Ni foil (factors = 1.00, 3.65, 13.29, 49.39)
Take-off Angle	6.0°
Detector Aperture	6.0 mm horizontal 6.0 mm vertical
Crystal to Detector Distance	40 cm
Temperature	23.0°C
Scan Type	ω-2θ
Scan Rate	8.0°/min (in omega) (5 rescans)
Scan Width	(1.26 + 0.35 tanθ)
$2\theta_{max}$	120.1°
No. of Reflections Measured	Total: 1750 Unique: 1613 (R_{int} = 14.67)
Corrections	Lorentz-polarization Decay (14.55% decline)

C. Structure Solution and Refinement

Structure Solution	Direct Methods (SHELXS86)
Refinement	Full-matrix least-squares
Function Minimized	$\Sigma w(\|Fo\| - \|Fc\|)^2$
Least Squares Weights	$1/\sigma^2(Fo^2) = 4Fo^2/\sigma^2(Fo^2)$
p-factor	0.020
Anamolous Dispersion	All non-hydrogen atoms
No. Observations ($I > 3.00\sigma(I)$)	364
No. Variables	87
Reflection/Parameter Ratio	4.18
Residuals: R; Rw	0.069; 0.070
Goodness of Fit Indicator	2.84
Max Shift/Error in Final Cycle	0.00
Maximum peak in Final Diff. Map	0.21 $e^-/Å^3$
Minimum peak in Final Diff. Map	-0.21 $e^-/Å^3$

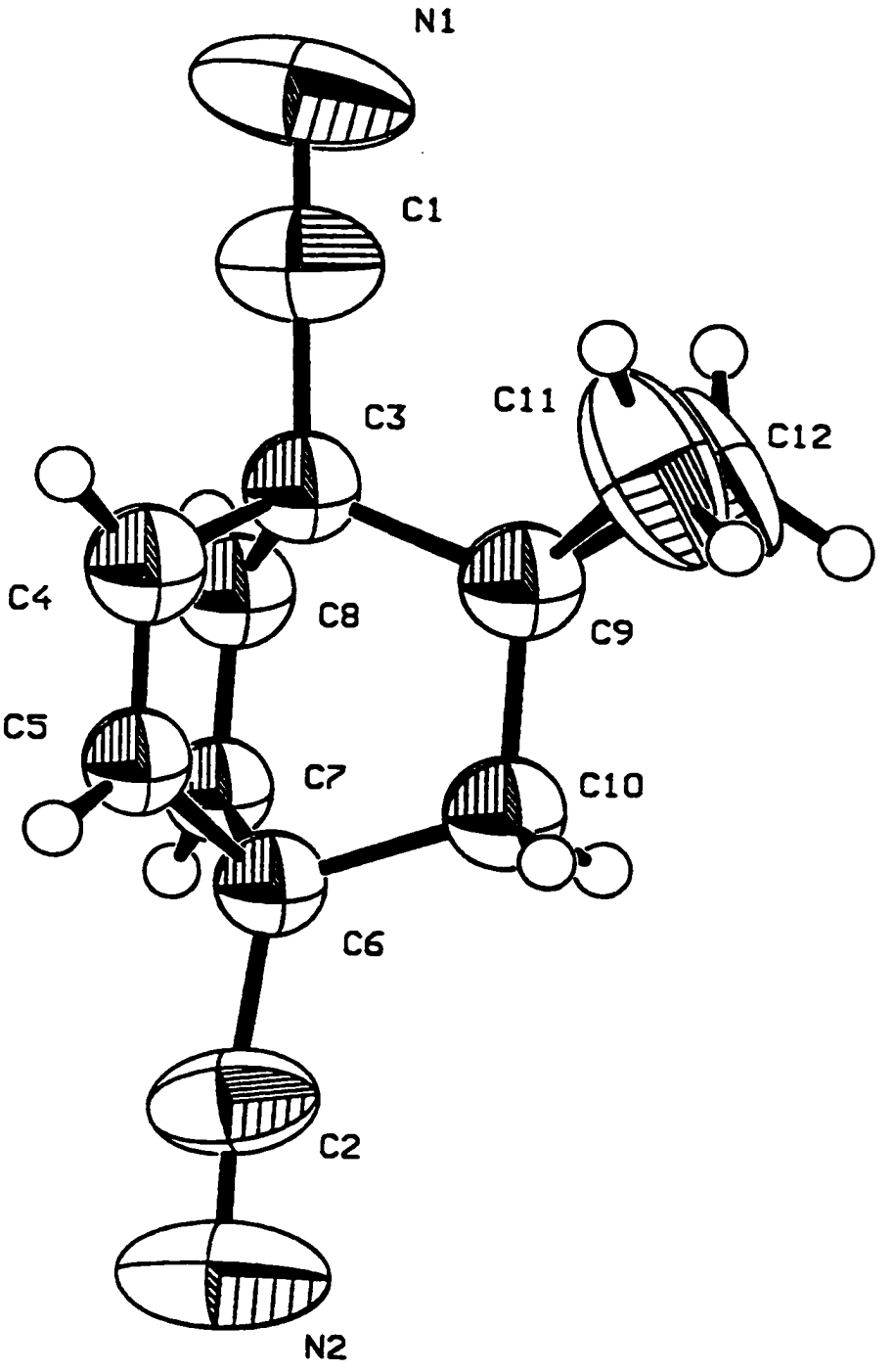

Figure 4.4 Structure of 79 determined by X-ray crystallograpy.

Table 4.2 Bond lengths (Å) in **79** determined by X-ray crystallography.[a]

atoms	distance	atoms	distance
N1-C1	1.12(2)	N2-C2	1.13(2)
C1-C3	1.46(2)	C2-C6	1.45(2)
C3-C4	1.56(2)	C3-C8	1.52(2)
C3-C9	1.54(2)	C4-C5	1.29(2)
C5-C6	1.55(2)	C6-C7	1.52(2)
C6-C10	1.54(2)	C7-C8	1.30(2)
C9-C10	1.52(2)	C9-C11	1.50(2)
C9-C12	1.49(2)	C11-C12	1.50(2)

[a] See Figure 4.4 for numbering of atoms.

Table 4.3 Bond angles (°) in **79** determined by X-ray crystallography.[a]

atoms	angle	atoms	angle
N1-C1-C3	178(2)	N2-C2-C3	173(2)
C1-C3-C4	111(1)	C1-C3-C8	112(1)
C1-C3-C9	114(1)	C4-C3-C8	106(1)
C4-C3-C9	103(1)	C8-C3-C9	107(1)
C3-C4-C5	112(1)	C4-C5-C6	117(1)
C2-C6-C5	111(1)	C2-C6-C7	115(1)
C2-C6-C10	115(1)	C5-C6-C7	105(1)
C5-C6-C10	103(1)	C7-C6-C10	104(1)
C6-C7-C8	116(1)	C3-C8-C7	113(1)
C3-C9-C10	110(1)	C3-C9-C11	117(1)
C3-C9-C12	118(1)	C10-C9-C11	120(1)
C10-C9-C12	122(1)	C11-C9-C12	60(1)
C6-C10-C9	110(1)	C9-C11-C12	59(1)
C9-C12-C11	60(1)		

[a] See Figure 4.4 for numbering of atoms.

Table 4.4 Torsion angles (°) in **79** determined by X-ray crystallography.[a]

atoms	angle	atoms	angle
N1-C1-C3-C4	-166.2	N1-C1-C3-C8	-46.5
N1-C1-C3-C9	76.6	N2-C2-C6-C5	-152(18)
N2-C2-C6-C7	87(19)	N2-C2-C6-C10	-34(19)
C1-C3-C4-C5	176(1)	C1-C3-C4-H1	-1.4
C1-C3-C8-C7	-174(1)	C1-C3-C8-H4	5.9
C1-C3-C9-C10	-178(1)	C1-C3-C9-C11	38(2)
C1-C3-C9-C12	-30(2)	C2-C6-C5-C4	-175(1)
C2-C6-C5-H2	5.3	C2-C6-C7-C8	174(1)

Table 4.4 (cont.)

atoms	angle	atoms	angle
C2-C6-C7-H3	-3.8	C2-C6-C10-C9	-175(1)
C2-C6-C10-H5	-54.4	C2-C6-C10-H6	64.1
C3-C4-C5-C6	-1(1)	C3-C4-C5-H2	177.4
C3-C8-C7-C6	0(2)	C3-C8-C7-H3	177.8
C3-C9-C10-C6	-3(1)	C3-C9-C10-H5	-124.1
C3-C9-C10-H6	117.0	C3-C9-C11-C12	-108(1)
C3-C9-C11-H7	1.9	C3-C9-C11-H8	143.1
C3-C9-C12-C11	107(1)	C3-C9-C12-H9	-143.5
C3-C9-C12-H10	-0.5	C4-C3-C8-C7	-52(1)
C4-C3-C8-H4	128.5	C4-C3-C9-C10	59(1)
C4-C3-C9-C11	-83(1)	C4-C3-C9-C12	-152(1)
C4-C5-C6-C7	-49(1)	C4-C5-C6-C10	60(1)
C5-C4-C3-C8	53(1)	C5-C4-C3-C9	-59(1)
C5-C6-C7-C8	51(1)	C5-C6-C7-H3	-127.2
C5-C6-C10-C9	-53(1)	C5-C6-C10-H5	67.5
C5-C6-C10-H6	-173.9	C6-C5-C4-H1	176.3
C6-C7-C8-H4	178.3	C6-C10-C9-C11	138(1)
C6-C10-C9-C12	-149(1)	C7-C6-C5-H2	131.2
C7-C6-C10-C9	56(1)	C7-C6-C10-H5	177.3
C7-C6-C10-H6	-64.2	C7-C8-C3-C9	57(1)
C8-C3-C4-H1	-124.5	C8-C3-C9-C10	-52(1)
C8-C3-C9-C11	164(1)	C8-C3-C9-C12	94(1)
C8-C7-C6-C10	-56(1)	C9-C3-C4-H1	122.6
C9-C3-C8-H4	-121.3	C9-C11-C12-H9	-108.4
C9-C11-C12-H10	111.7	C9-C12-C11-H7	-112.2
C9-C12-C11-H8	108.4	C10-C6-C5-H2	-119.2
C10-C6-C7-H3	124.4	C10-C9-C11-C12	112(1)
C10-C9-C11-H7	-137.6	C10-C9-C11-H8	3.7
C10-C9-C12-C11	-108(1)	C10-C9-C12-H9	-0.2
C10-C9-C12-H10	142.8	C11-C9-C10-H5	18.3
C11-C9-C10-H6	-100.6	C11-C9-C12-H9	108.6
C11-C9-C12-H10	-108.4	C12-C9-C10-H5	90.1
C12-C9-C10-H6	-28.8	C12-C9-C11-H7	109.9
C12-C9-C11-H8	-108.9	H1-C4-C5-H2	-4.5
H3-C7-C8-H4	-3.0	H7-C11-C12-H9	139.4
H7-C11-C12-H10	-0.5	H8-C11-C12-H9	0.0
H8-C11-C12-H10	-139.9		

[a] See Figure 4.4 for numbering of atoms.

2,5-Dicyanotricyclo[3.3.0.^{2,6}0^{5,7}]oct-3-ene spiro cyclopropane (**80**)

A. Crystal Data

Empirical Formula	$C_{12}H_{10}N2$
Formula Weight	182.22
Crystal Colour, Habit	colourless, block
Crystal Dimensions	0.150 × 0.200 × 0.200
Crystal System	monoclinic
Lattice Type	P
No. of Reflections Used for Unit Cell Determination (2θ range)	25 (51.1 - 78.4°)
Omega Scan Peak Width at Half-height	0.28°
Lattice Parameters	a = 7.1821(7) Å b = 13.6319(8) Å c = 10.3611(6) Å β = 106.633(6)° V = 972.0(1) Å^3
Space Group	$P2_1/c$ (#14)
Z value	4
D_{calc}	1.245 g/cm^3
F_{000}	384.00
μ(MoKα)	5.89 cm^{-1}

B. Intensity Measurements

Diffractometer	Rigaku AFC5R
Radiation	CuKα (λ = 1.54178 Å) graphite monochromated
Attenuator	Ni foil (factors = 1.00, 3.65, 13.29, 49.39)
Take-off Angle	6.0°
Detector Aperture	6.0 mm horizontal 6.0 mm vertical
Crystal to Detector Distance	40 cm
Temperature	23.0°C
Scan Type	ω-2θ
Scan Rate	8.0°/min (in omega) (5 rescans)
Scan Width	(1.26 + 0.35 tanθ)
$2\theta_{max}$	120.1°
No. of Reflections Measured	Total: 1656 Unique: 1524 (R_{int} = 4.89)
Corrections	Lorentz-polarization Absorption

(trans factors: 0.4550 - 1.0000)
Secondary Extinction
(coefficient: 1.95237e-05)

C. Structure Solution and Refinement

Structure Solution	Direct Methods (SHELXS86)
Refinement	Full-matrix least-squares
Function Minimized	$\Sigma w(\|Fo\| - \|Fc\|)^2$
Least Squares Weights	$1/\sigma^2(Fo^2) = 4Fo^2/\sigma^2(Fo^2)$
p-factor	0.006
Anamolous Dispersion	All non-hydrogen atoms
No. Observations ($I > 3.00\sigma(I)$)	602
No. Variables	128
Reflection/Parameter Ratio	4.70
Residuals: R; Rw	0.044; 0.061
Goodness of Fit Indicator	2.51
Max Shift/Error in Final Cycle	0.00
Maximum peak in Final Diff. Map	0.15 $e^-/Å^3$
Minimum peak in Final Diff. Map	-0.20 $e^-/Å^3$

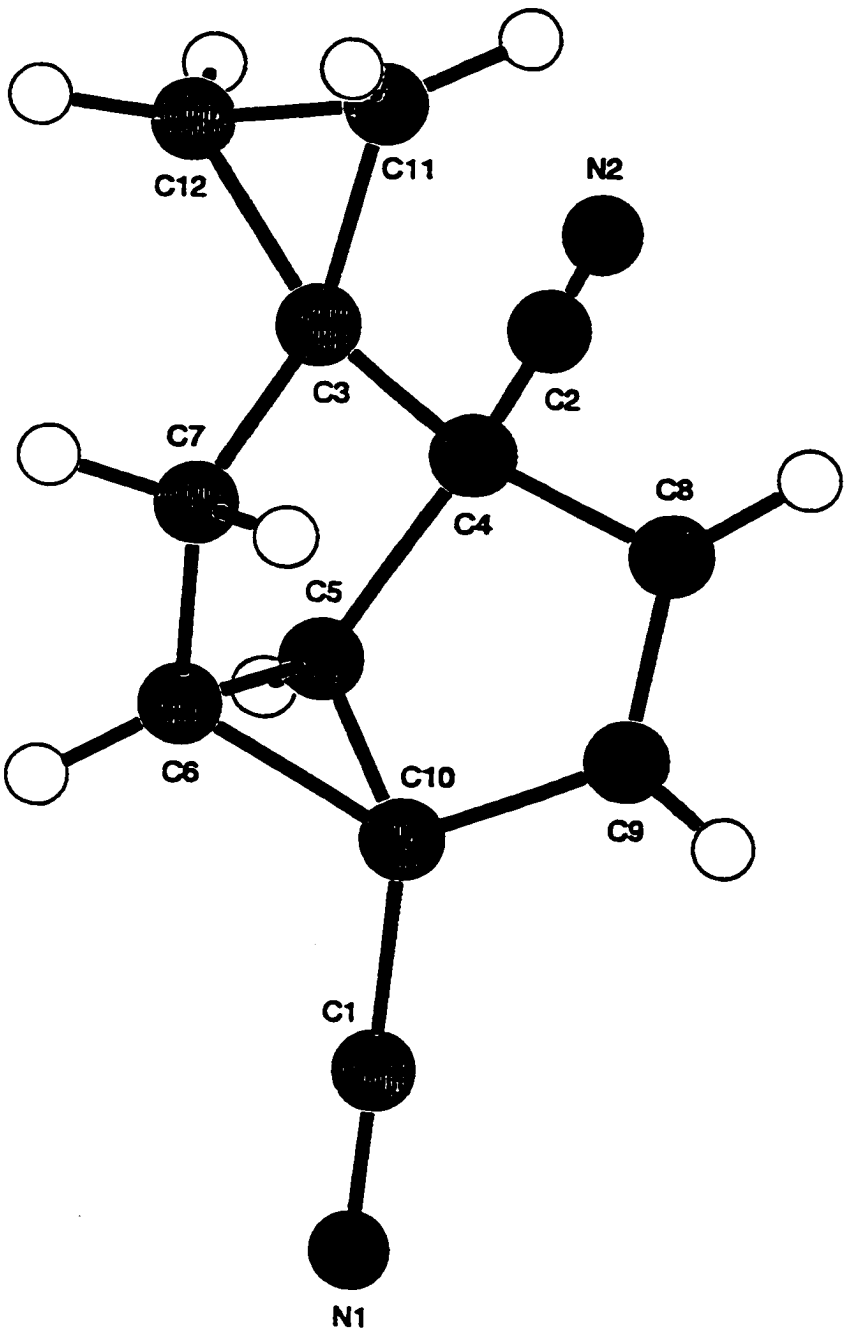

Figure 4.5 Structure of **80** determined by X-ray crystallography.

Table 4.5 Bond lengths (Å) in **80** determined by X-ray crystallography.[a]

atoms	distance	atoms	distance
N1-C1	1.137(9)	N2-C2	1.132(9)
C1-C10	1.46(1)	C2-C4	1.46(1)
C3-C4	1.536(9)	C3-C7	1.525(10)
C3-C11	1.492(10)	C3-C12	1.497(10)
C4-C5	1.545(9)	C4-C8	1.528(10)
C5-C6	1.508(9)	C5-C10	1.498(10)
C6-C7	1.523(10)	C6-C10	1.547(9)
C8-C9	1.316(10)	C9-C10	1.493(10)
C11-C12	1.493(10)		

[a] See Figure 4.5 for numbering of atoms.

Table 4.6 Bond angles (°) in **80** determined by X-ray crystallography.[a]

atoms	angle	atoms	angle
N1-C1-C10	179.2(9)	N2-C2-C4	178.4(9)
C4-C3-C7	105.0(6)	C4-C3-C11	122.7(6)
C4-C3-C12	120.6(6)	C7-C3-C11	122.5(6)
C7-C3-C12	121.3(6)	C11-C3-C12	60.0(5)
C2-C4-C3	115.3(6)	C2-C4-C5	113.2(6)
C2-C4-C8	113.3(6)	C3-C4-C5	102.9(6)
C3-C4-C8	107.8(6)	C5-C4-C8	103.2(6)
C4-C5-C6	104.8(6)	C4-C5-C10	105.1(6)
C6-C5-C10	61.9(4)	C5-C6-C7	109.1(6)
C5-C6-C10	58.7(4)	C7-C6-C10	119.7(6)
C3-C7-C6	104.5(6)	C4-C8-C9	111.3(7)
C8-C9-C10	111.3(7)	C1-C10-C5	120.0(6)
C1-C10-C6	117.9(6)	C1-C10-C9	119.9(7)
C5-C10-C6	59.3(5)	C5-C10-C9	106.4(6)
C6-C10-C9	117.8(6)	C3-C11-C12	60.2(5)
C3-C12-C11	59.9(5)		

[a] See Figure 4.5 for numbering of atoms.

Table 4.7 Torsion angles (°) in **80** determined by X-ray crystallography.[a]

atoms	angle	atoms	angle
N1-C1-C10-C5	-74(62)	N1-C1-C10-C6	-5(62)
N1-C1-C10-C9	150(62)	N2-C2-C4-C3	-76(30)
N2-C2-C4-C5	41(30)	N2-C2-C4-C8	158(29)
C1-C10-C5-C4	-154.4(7)	C1-C10-C5-C6	106.6(7)
C1-C10-C6-C5	-110.1(7)	C1-C10-C6-C7	154.5(7)
C1-C10-C9-C8	146.6(7)	C2-C4-C3-C7	161.2(6)
C2-C4-C3-C11	-52.3(10)	C2-C4-C3-C12	19.6(10)
C2-C4-C5-C6	-156.7(6)	C2-C4-C5-C10	139.0(6)
C2-C4-C8-C9	-136.1(7)	C3-C4-C5-C6	-31.5(7)
C3-C4-C5-C10	-95.9(6)	C3-C4-C8-C9	95.1(8)
C3-C7-C6-C5	8.8(8)	C3-C7-C6-C10	73.0(8)
C4-C3-C7-C6	-28.7(7)	C4-C3-C11-C12	109.1(8)
C4-C3-C12-C11	-112.6(8)	C4-C5-C6-C7	14.3(8)
C4-C5-C6-C10	-99.5(6)	C4-C5-C10-C6	99.0(6)
C4-C5-C10-C9	-14.0(8)	C4-C8-C9-C10	4.8(9)
C5-C4-C3-C7	37.5(7)	C5-C4-C3-C11	-176.1(6)
C5-C4-C3-C12	-104.2(8)	C5-C4-C8-C9	-13.3(9)
C5-C6-C10-C9	93.4(7)	C5-C10-C6-C7	-95.4(7)
C5-C10-C9-C8	6.2(9)	C6-C5-C4-C8	80.5(7)
C6-C5-C10-C9	-113.0(6)	C6-C7-C3-C11	-175.3(7)
C6-C7-C3-C12	112.6(7)	C6-C10-C9-C8	-57.3(9)
C7-C3-C4-C8	-71.1(7)	C7-C3-C11-C12	-110.1(8)
C7-C3-C12-C11	112.0(8)	C7-C6-C5-C10	113.8(7)
C7-C6-C10-C9	-2(1)	C8-C4-C3-C11	75.3(8)
C8-C4-C3-C12	147.2(7)	C8-C4-C5-C10	16.2(8)

[a] See Figure 4.5 for numbering of atoms.

1,4-Dicyanotetracyclo[2.0.^{3,10}0.^{4,7}2.0.^{7,9}1]decene (**81**)

A. Crystal Data

Empirical Formula	$C_{12}H_{10}N2$
Formula Weight	182.22
Crystal Colour, Habit	colourless needle plate
Crystal Dimensions	0.050 × 0.250 × 0.300
Crystal System	monoclinic
Lattice Type	C
No. of Reflections Used for Unit Cell Determination (2θ range)	25 (40.2 - 55.7°)
Omega Scan Peak Width at Half-height	0.30°
Lattice Parameters	a = 23.193(2) Å b = 6.271(2) Å c = 13.482(2) Å β = 94.85(1)° V = 1954.0(8) Å^3
Space Group	$C2_1/c$ (#15)
Z value	8
D_{calc}	1.239 g/cm^3
F_{000}	768.00
μ(MoKα)	5.52 cm^{-1}

B. Intensity Measurements

Diffractometer	Rigaku AFC5R
Radiation	CuKα (λ = 1.54178 Å) graphite monochromated
Attenuator	Ni foil (factors = 1.00, 3.65, 13.29, 49.39)
Take-off Angle	6.0°
Detector Aperture	6.0 mm horizontal 6.0 mm vertical
Crystal to Detector Distance	40 cm
Temperature	23.0°C
Scan Type	ω-2θ
Scan Rate	8.0°/min (in omega) (5 rescans)
Scan Width	(1.10 + 0.35 tanθ)
2θ_{max}	120.1°
No. of Reflections Measured	Total: 1649 Unique: 1601 (R_{int} = 10.52)
Corrections	Lorentz-polarization Absorption (trans factors: 0.5805 - 1.0000)

C. Structure Solution and Refinement

Structure Solution	Direct Methods (SHELXS86)
Refinement	Full-matrix least-squares
Function Minimized	$\Sigma w(\|Fo\| - \|Fc\|)^2$
Least Squares Weights	$1/\sigma^2(Fo^2) = 4Fo^2/\sigma^2(Fo^2)$
p-factor	0.001
Anamolous Dispersion	All non-hydrogen atoms
No. Observations ($I > 3.00\sigma(I)$)	329
No. Variables	77
Reflection/Parameter Ratio	4.27
Residuals: R; Rw	0.044; 0.045
Goodness of Fit Indicator	1.53
Max Shift/Error in Final Cycle	0.08
Maximum peak in Final Diff. Map	0.12 $e^-/Å^3$
Minimum peak in Final Diff. Map	-0.16 $e^-/Å^3$

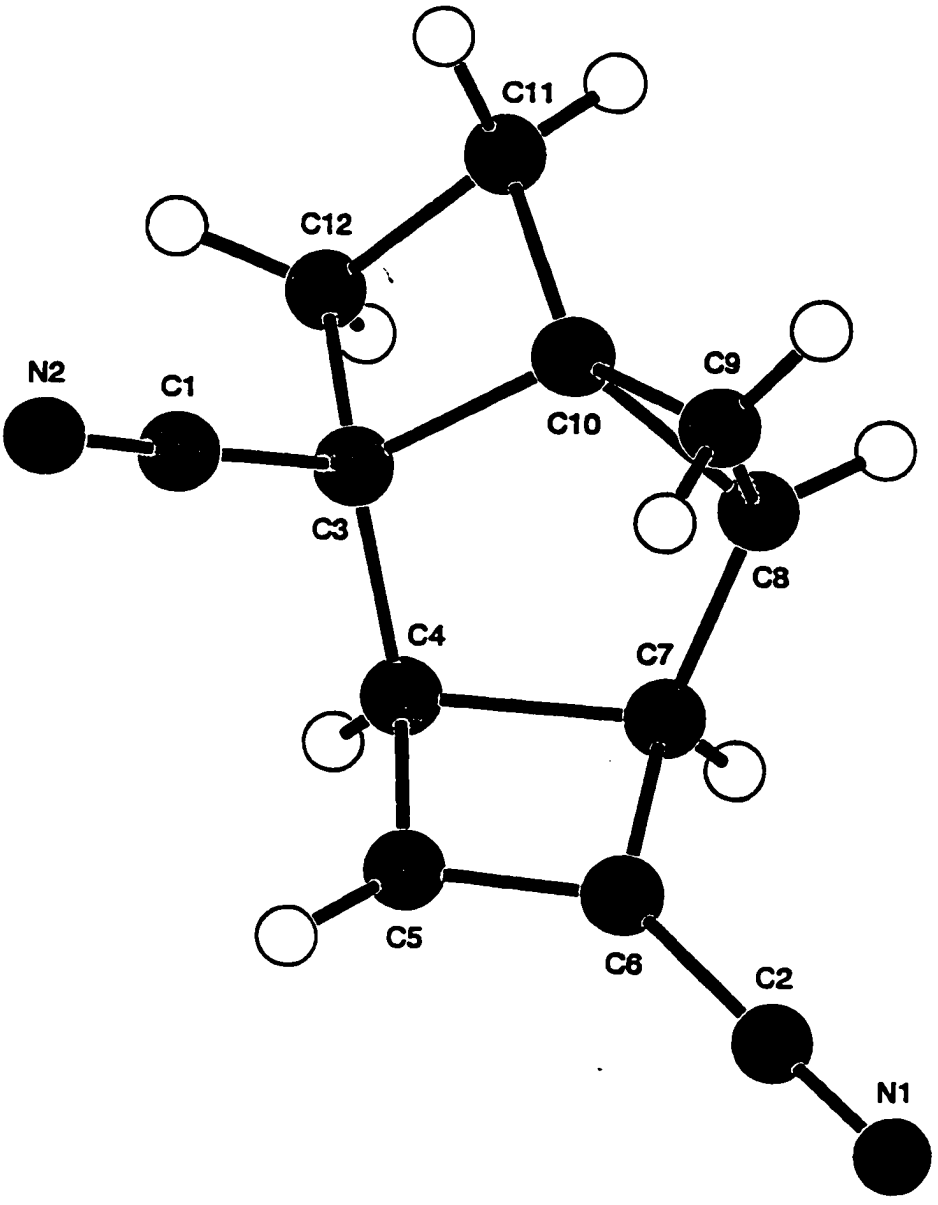

Figure 4.6 Structure of **81** determined by X-ray crystallography.

Table 4.8 Bond lengths (Å) in **81** determined by X-ray crystallography.[a]

atoms	distance	atoms	distance
N1-C2	1.13(1)	N2-C1	1.16(1)
C1-C3	1.48(1)	C2-C6	1.45(1)
C3-C4	1.52(1)	C3-C10	1.54(1)
C3-C12	1.56(1)	C4-C5	1.50(1)
C4-C7	1.59(1)	C4-H1	0.99
C5-C6	1.32(1)	C5-H2	0.99
C6-C7	1.52(1)	C7-C8	1.49(1)
C7-H3	1.00	C8-C9	1.52(1)
C8-C110	1.50(1)	C8-H4	0.97
C9-C10	1.48(1)	C9-H5	0.97
C9-H6	0.97	C10-C11	1.53(1)
C11-C12	1.55(1)	C11-H7	1.01
C11-H8	0.96	C12-H9	0.99
C12-H10	0.97		

[a] See Figure 4.6 for numbering of atoms.

Table 4.9 Bond angles (°) in **81** determined by X-ray crystallography.[a]

atoms	angle	atoms	angle
N2-C1-C3	178(1)	N1-C2-C6	178(1)
C1-C3-C4	112.2(8)	C1-C3-C10	114.3(8)
C1-C3-C12	112.2(8)	C4-C3-C10	108.9(8)
C4-C3-C12	120.0(9)	C10-C3-C12	87.0(7)
C3-C4-C5	120.1(9)	C3-C4-C7	105.6(8)
C3-C4-H1	115.1	C5-C4-C7	85.1(7)
C5-C4-H1	113.1	C7-C4-H1	113.5
C4-C5-C6	95.7(8)	C4-C5-H2	132.6
C6-C5-H2	131.5	C2-C6-C5	134.0(10)
C2-C6-C7	131.4(8)	C5-C6-C7	94.6(7)
C4-C7-C6	84.6(6)	C4-C7-C8	107.8(8)
C4-C7-H3	116.1	C6-C7-C8	119.5(8)
C6-C7-H3	113.7	C8-C7-H3	112.3
C7-C8-C9	121.4(7)	C7-C7-C10	110.0(7)
C7-C8-H4	120.4	C9-C8-C10	58.8(6)
C9-C8-H4	114.5	C10-C8-H4	115.5
C8-C9-C10	59.9(6)	C8-C8-H5	120.5
C8-C9-H6	123.0	C10-C9-H5	120.9
C10-C9-H6	121.8	C5-C9-H6	105.7
C3-C10-C8	107.4(8)	C3-C10-C9	123.7(8)
C3-C10-C11	91.0(7)	C8-C10-C9	61.3(6)
C8-C10-C11	128.6(8)	C9-C10-C11	141.9(9)
C10-C11-H8	87.9(8)	C10-C11-H7	113.5

Table 4.9 (cont.)

C10-C11-H8	118.5	C12-C11-H7	113.7
C12-C11-H8	119.5	H7-C11-H8	104.0
C3-C12-C11	89.6(7)	C3-C12-H9	115.8
C3-C12-H10	116.9	C11-C12-H9	113.0
C11-C12-H10	117.4	H9-C12-H10	104.4

[a] See Figure 4.6 for numbering of atoms.

Table 4.10 Torsion angles (°) in **81** determined by X-ray crystallography.[a]

atoms	angle	atoms	angle
N1-C2-C6-C5	172(47)	N1-C2-C6-C7	-3(49)
N2-C1-C3-C4	147(40)	N2-C1-C3-C10	22(40)
N2-C1-C3-C12	-74(40)	N1-C3-C4-C5	-38(1)
C1-C3-C4-C7	-132.0(8)	C1-C3-C10-C8	131.7(8)
C1-C3-C10-C9	64(1)	C1-C3-C10-C11	-97.1(9)
C1-C3-C12-C11	99.3(8)	C2-C6-C5-C4	-175(1)
C2-C6-C7-C4	175(1)	C2-C6-C7-C8	-76(1)
C3-C4-C5-C6	-106.9(10)	C3-C4-C7-C6	121.3(8)
C3-C4-C7-C8	2.0(10)	C3-C10-C8-C7	-4(1)
C3-C10-C8-C9	-119.4(9)	C3-C10-C9-C8	92.6(10)
C3-C10-C11-C12	-16.1(7)	C3-C12-C11-C10	15.9(7)
C4-C3-C10-C8	5.1(1)	C4-C3-C10-C9	-61(1)
C4-C3-C10-C11	136.7(8)	C4-C3-C12-C11	-125.9(9)
C4-C5-C6-C7	1.7(9)	C4-C7-C6-C5	-1.6(8)
C4-C7-C8-C9	66(1)	C4-C7-C8-C10	1(1)
C5-C4-C3-C10	88.9(10)	C5-C4-C3-C12	-173.4(8)
C5-C4-C7-C6	1.4(7)	C5-C4-C7-C8	-117.9(8)
C5-C6-C7-C8	105.8(10)	C6-C5-C4-C7	-1.6(8)
C6-C7-C8-C9	-27(1)	C6-C7-C8-C10	-92.6(10)
C7-C4-C3-C10	-4(1)	C7-C4-C3-C12	93.1(9)
C7-C8-C9-C10	-95.6(9)	C7-C8-C10-C9	115.3(8)
C7-C8-C10-C11	-110(1)	C8-C9-C10-C11	-117(1)
C8-C10-C3-C12	-115.3(8)	C8-C10-C11-C12	97(1)
C9-C8-C10-C11	134(1)	C9-C10-C3-C12	178.0(9)
C9-C10-C11-C12	-171(1)	C10-C3-C12-C11	-15.8(7)
C11-C10-C3-C12	15.9(8)		

[a] See Figure 4.6 for numbering of atoms.

3,7-Dicyanotricyclo[3.3.0.^{2,6}0^{5,7}]oct-3-ene spiro cyclopropane (**82**)

A. Crystal Data

Empirical Formula	$C_{12}H_{10}N_2$
Formula Weight	182.22
Crystal Colour, Habit	colourless needle
Crystal Dimensions	0.020 × 0.170 × 0.500
Crystal System	monoclinic
Lattice Type	P
No. of Reflections Used for Unit Cell Determination (2θ range)	24 (30.7 - 48.3°)
Omega Scan Peak Width at Half-height	0.43°
Lattice Parameters	a = 5.61(1) Å b = 25.81(2) Å c = 6.792(9) Å β = 98.8(2) Å
Space Group	$P2_1/c$ (#14)
Z value	4
D_{calc}	1.244 g/cm^3
F_{000}	384.00
μ(MoKα)	5.54 cm^{-1}

B. Intensity Measurements

Diffractometer	Rigaku AFC5R
Radiation	CuKα (λ = 1.54178 Å) graphite monochromated
Attenuator	Ni foil (factors = 1.00, 3.65, 13.29, 49.39)
Take-off Angle	6.0°
Detector Aperture	6.0 mm horizontal 6.0 mm vertical
Crystal to Detector Distance	40 cm
Temperature	23.0°C
Scan Type	ω-2θ
Scan Rate	8.0°/min (in omega) (5 rescans)
Scan Width	(1.37 + 0.35 tanθ)
$2\theta_{max}$	120.3°
No. of Reflections Measured	Total: 1662 Unique: 1501 (R_{int} = 13.25)
Corrections	Lorentz-polarization

C. Structure Solution and Refinement

Structure Solution	Direct Methods (SHELXS86)
Refinement	Full-matrix least-squares
Function Minimized	$\Sigma w(\|Fo\| - \|Fc\|)^2$
Least Squares Weights	$1/\sigma^2(Fo^2) = 4Fo^2/\sigma^2(Fo^2)$
p-factor	0.003
Anamolous Dispersion	All non-hydrogen atoms
No. Observations ($I > 3.00\sigma(I)$)	349
No. Variables	87
Reflection/Parameter Ratio	4.01
Residuals: R; Rw	0.056; 0.059
Goodness of Fit Indicator	2.96
Max Shift/Error in Final Cycle	0.03
Maximum peak in Final Diff. Map	0.15 $e^-/Å^3$
Minimum peak in Final Diff. Map	-0.18 $e^-/Å^3$

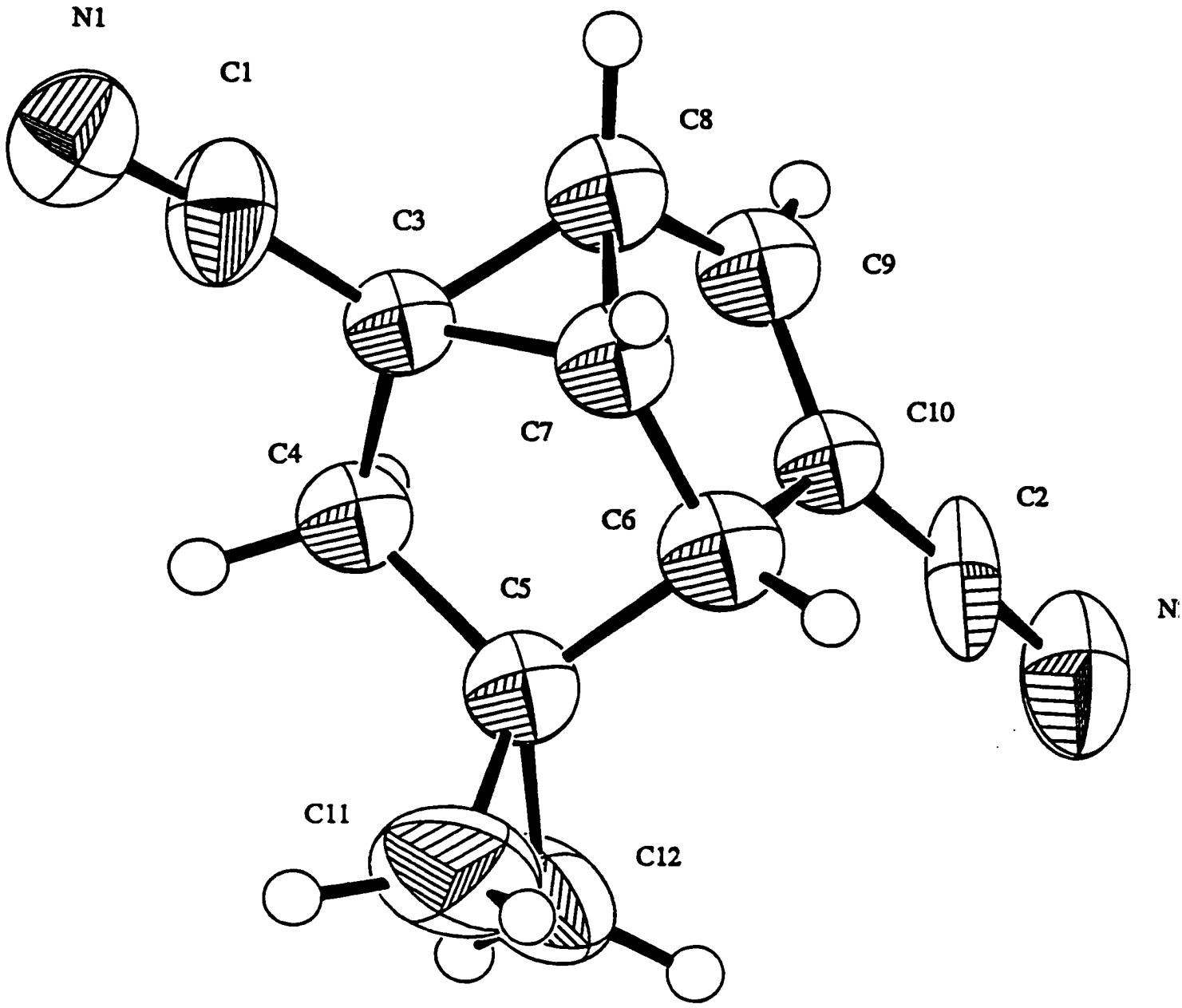

Figure 4.7 Structure of **82** determined by X-ray crystallography.

Table 4.11 Bond lengths (Å) in **82** determined by X-ray crystallography.[a]

atoms	distance	atoms	distance
N1-C1	1.14(1)	N2-C2	1.14(2)
C1-C3	1.39(1)	C2-C10	1.39(2)
C3-C4	1.53(1)	C3-C7	1.51(1)
C3-C8	1.54(1)	C4-C5	1.55(2)
C5-C6	1.56(1)	C5-C11	1.45(2)
C5-C12	1.48(2)	C6-C7	1.52(2)
C6-C10	1.49(1)	C7-C8	1.47(1)
C8-C9	1.51(2)	C9-C10	1.33(2)
C11-C12	1.52(2)		

[a] See Figure 4.7 for numbering of atoms.

Table 4.12 Bond angles (°) in **82** determined by X-ray crystallography.[a]

atoms	angle	atoms	angle
N1-C1-C3	174(1)	N2-C2-C10	177(1)
C1-C3-C4	119(1)	C1-C3-C7	122(1)
C1-C3-C8	116(1)	C4-C3-C7	107.6(9)
C4-C3-C8	117.0(10)	C7-C3-C8	57.7(7)
C3-C4-C5	105.7(10)	C4-C5-C6	102(1)
C4-C5-C11	122(1)	C4-C5-C12	123(1)
C6-C5-C11	119(1)	C6-C5-C12	123(1)
C11-C5-C12	62.6(10)	C5-C6-C7	103.8(9)
C5-C6-C10	107(1)	C7-C6-C10	104(1)
C3-C7-C6	106.4(10)	C3-C7-C8	62.1(7)
C6-C7-C8	105(1)	C3-C8-C7	60.1(7)
C3-C8-C9	119(1)	C7-C8-C9	105(1)
C8-C9-C10	109(1)	C2-C10-C6	123(1)
C2-C10-C9	123(1)	C6-C10-C9	111(1)
C5-C11-C12	59.7(9)	C5-C12-C11	57.7(9)

[a] See Figure 4.7 for numbering of atoms.

Table 4.13 Torsion angles (°) in **82** determined by X-ray crystallography.[a]

atoms	angle	atoms	angle
N1-C1-C3-C4	62(15)	N1-C1-C3-C7	-79(15)
N1-C1-C3-C8	-164(62)	N2-C2-C10-C6	-70(37)
N2-C2-C10-C9	119(36)	C1-C3-C4-C5	-134(1)
C1-C3-C7-C6	157(1)	C1-C3-C7-C8	-102(1)
C1-C3-C8-C7	113(1)	C1-C3-C8-C9	-153(1)
C2-C10-C6-C5	-75(1)	C2-C10-C6-C7	174(1)
C2-C10-C9-C8	176(1)	C3-C4-C5-C6	-30(1)
C3-C4-C5-C11	107(1)	C3-C4-C5-C11	-176(1)
C3-C7-C6-C5	-30(1)	C3-C7-C6-C10	81(1)
C3-C7-C8-C9	-114(1)	C3-C8-C7-C6	100(1)
C3-C8-C9-C10	-57(1)	C4-C3-C7-C6	11(1)
C4-C3-C7-C8	111(1)	C4-C3-C8-C7	-94(1)
C4-C3-C8-C9	-2(1)	C4-C5-C6-C7	37(1)
C4-C5-C6-C10	-72(1)	C4-C5-C11-C12	113(1)
C4-C5-C12-C11	-112(1)	C5-C4-C3-C7	12(1)
C5-C4-C3-C8	74(1)	C5-C6-C7-C8	-95(1)
C5-C6-C10-C9	96(1)	C6-C5-C11-C12	-115(1)
C6-C5-C12-C11	109(1)	C6-C7-C3-C8	-99(1)
C6-C7-C8-C9	-14(1)	C6-C10-C9-C8	4(1)
C7-C3-C8-C9	92(1)	C7-C6-C5-C11	-101(1)
C7-C6-C5-C12	-176(1)	C7-C6-C10-C9	-13(1)
C7-C8-C9-C10	6(1)	C8-C7-C6-C10	16(1)
C10-C6-C5-C11	148(1)	C10-C6-C5-C12	73(1)

[a] See Figure 4.7 for numbering of atoms.

4,6-Dicyanotricyclo[3.3.0.$^{3,7}0^{6,8}$]oct-4-ene spiro cyclopropane (**83**)

A. Crystal Data

Empirical Formula	$C_{12}H_{10}N_2$
Formula Weight	182.22
Crystal Colour, Habit	colourless needle
Crystal Dimensions	0.050 × 0.100 × 0.200
Crystal System	monoclinic
Lattice Type	P
No. of Reflections Used for Unit Cell Determination (2θ range)	22 (41.4 - 56.7°)
Omega Scan Peak Width at Half-height	0.49°
Lattice Parameters	a = 7.872(3) Å b = 9.168(2) Å c = 13.967(2) Å β = 105.36(1) Å
Space Group	$P2_1/n$ (#14)
Z value	4
D_{calc}	1.368 g/cm^3
F_{000}	424.00
μ(MoKα)	7.16 cm^{-1}

B. Intensity Measurements

Diffractometer	Rigaku AFC5R
Radiation	CuKα (λ = 1.54178 Å) graphite monochromated
Attenuator	Ni foil (factors = 1.00, 3.65, 13.29, 49.39)
Take-off Angle	6.0°
Detector Aperture	6.0 mm horizontal 6.0 mm vertical
Crystal to Detector Distance	40 cm
Temperature	23.0°C
Scan Type	ω-2θ
Scan Rate	16.0°/min (in omega) (5 rescans)
Scan Width	(1.57 + 0.35 tanθ)
$2\theta_{max}$	120.1°
No. of Reflections Measured	Total: 1679 Unique: 1553 (R_{int} = 5.40)
Corrections	Lorentz-polarization Absorption (trans. factors: 0.6201 - 1.0000) Decay (0.59% decline)

	Secondary Extinction (coefficient: 1.19642e-06)

C. Structure Solution and Refinement

Structure Solution	Direct Methods (SHELXS86)
Refinement	Full-matrix least-squares
Function Minimized	$\Sigma w(\|Fo\| - \|Fc\|)^2$
Least Squares Weights	$1/\sigma^2(Fo^2) = 4Fo^2/\sigma^2(Fo^2)$
p-factor	0.004
Anamolous Dispersion	All non-hydrogen atoms
No. Observations ($I > 3.00\sigma(I)$)	329
No. Variables	78
Reflection/Parameter Ratio	4.22
Residuals: R; Rw	0.073; 0.075
Goodness of Fit Indicator	3.02
Max Shift/Error in Final Cycle	0.02
Maximum peak in Final Diff. Map	0.67 $e^-/Å^3$
Minimum peak in Final Diff. Map	-0.59 $e^-/Å^3$

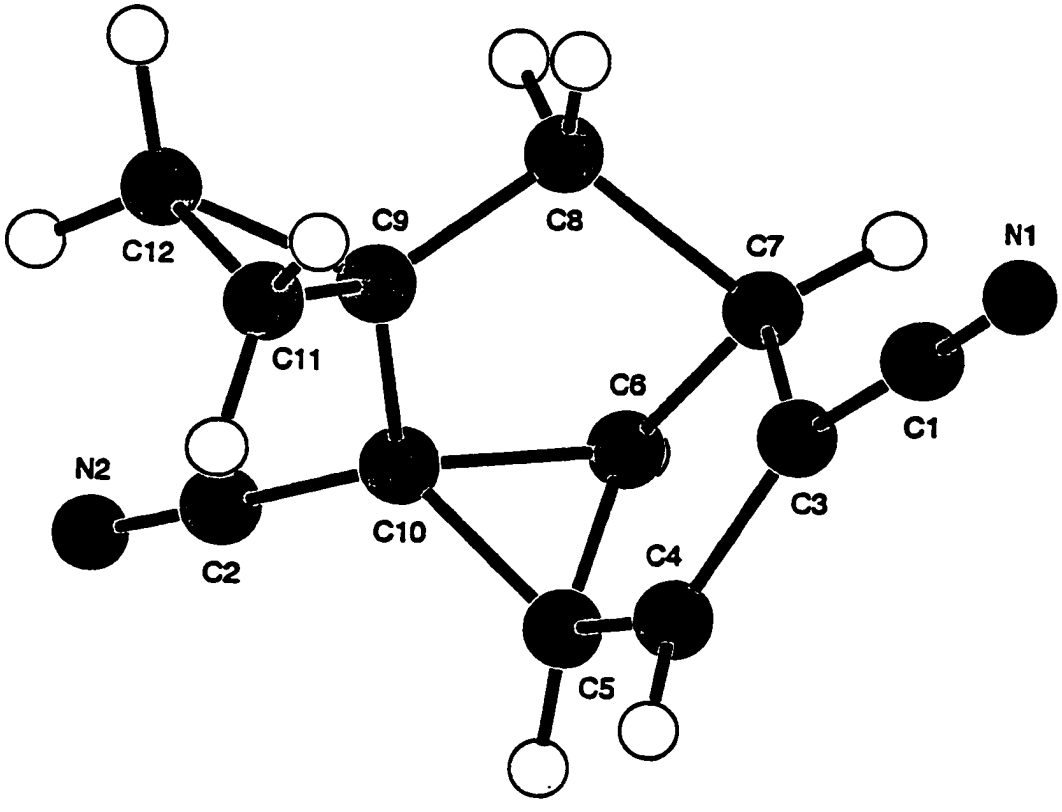

Figure 4.8 Structure of **83** determined by X-ray crystallography.

Table 4.14 Bond lengths (Å) in **83** determined by X-ray crystallography.[a]

atoms	distance	atoms	distance
N1-C1	1.13(2)	N2-C2	1.13(2)
C1-C3	1.44(2)	C2-C11	1.42(2)
C3-C4	1.52(2)	C3-C5	1.55(2)
C3-C8	1.50(2)	C4-C5	1.50(2)
C4-C12	1.49(3)	C5-C6	1.53(3)
C6-C7	1.61(2)	C6-C11	1.50(2)
C7-C8	1.53(2)	C8-C9	1.42(2)
C8-C10	1.44(2)	C9-C10	1.47(3)
C11-C12	1.32(2)		

[a] See Figure 4.8 for numbering of atoms.

Table 4.15 Bond angles (°) in **83** determined by X-ray crystallography.[a]

atoms	angle	atoms	angle
N1-C1-C3	176(3)	N2-C2-C11	172(3)
C1-C3-C4	116(1)	C1-C3-C5	119(2)
C1-C3-C8	117(1)	C4-C3-C5	58.3(10)
C4-C3-C8	121(1)	C5-C3-C8	109(1)
C3-C4-C5	61(1)	C3-C4-C12	114(1)
C5-C4-C12	104(2)	C3-C5-C4	59(1)
C3-C5-C6	105(1)	C4-C5-C6	106(2)
C5-C6-C7	99(1)	C5-C6-C11	104(1)
C7-C6-C11	105(1)	C6-C7-C8	105(1)
C3-C8-C7	104(1)	C3-C8-C9	123(1)
C2-C8-C10	123(1)	C7-C8-C9	120(1)
C7-C8-C10	119(1)	C9-C8-C10	61(1)
C8-C9-C10	59(1)	C8-C10-C9	58(1)
C2-C11-C6	121(2)	C2-C11-C12	127(2)
C6-C11-C12	110(1)	C4-C12-C11	113(1)

[a] See Figure 4.8 for numbering of atoms.

Table 4.16 Torsion angles (°) in **83** determined by X-ray crystallography.[a]

atoms	angle	atoms	angle
N1-C1-C3-C4	-139(39)	N1-C1-C3-C5	-72(40)
N1-C1-C3-C8	65(40)	N2-C2-C11-C6	-11(19)
N2-C2-C11-C12	179(17)	C1-C3-C4-C5	110(2)
C1-C3-C4-C12	-156(1)	C1-C3-C5-C4	-104(2)
C1-C3-C5-C6	155(1)	C1-C3-C8-C7	-131(2)
C1-C3-C8-C9	85(2)	C1-C3-C8-C10	9(3)
C2-C11-C6-C5	176(1)	C2-C11-C6-C7	-78(2)
C2-C11-C12-C4	175(1)	C3-C4-C5-C6	99(1)
C3-C4-C12-C11	-60(2)	C3-C5-C4-C12	-110(1)
C3-C5-C6-C7	-31(1)	C3-C5-C6-C11	76(1)
C3-C8-C7-C6	-30(1)	C3-C8-C9-C10	-113(2)
C3-C8-C10-C9	113(2)	C4-C3-C5-C6	-100(2)
C4-C3-C8-C7	74(2)	C4-C3-C8-C9	-68(2)
C4-C3-C8-C10	-144(2)	C4-C5-C3-C8	115(1)
C4-C5-C6-C7	-94(1)	C4-C5-C6-C11	14(2)
C4-C12-C11-C6	4(2)	C5-C3-C8-C12	93(2)
C5-C3-C8-C7	10(1)	C5-C3-C3-C9	-132(2)
C5-C3-C8-C10	151(2)	C5-C4-C7-C8	-94(2)
C5-C4-C12-C11	4(2)	C5-C6-C9-C8	39(1)
C5-C6-C11-C12	-11(2)	C7-C5-C3-C8	15(2)
C6-C5-C4-C12	-11(2)	C6-C7-C8-C9	113(2)
C6-C7-C8-C10	-173(1)	C6-C6-C11-C12	92(1)
C7-C8-C9-C10	109(2)	C7-C8-C10-C9	-110(2)
C8-C3-C4-C12	-1(2)	C8-C7-C6-C11	-68(1)

[a] See Figure 4.8 for numbering of atoms.

Dispiro[2.4.2.4]-11,14-dicyanotricyclo[2.2.2.0.^{5,14}0^{6,11}]tetradec-12-ene (**84**)

The structure of product **84** was firmly established by X-ray crystallography (see Figure 4.9). However, the data that was obtained from the X-ray analysis is not sufficient to permit publication.

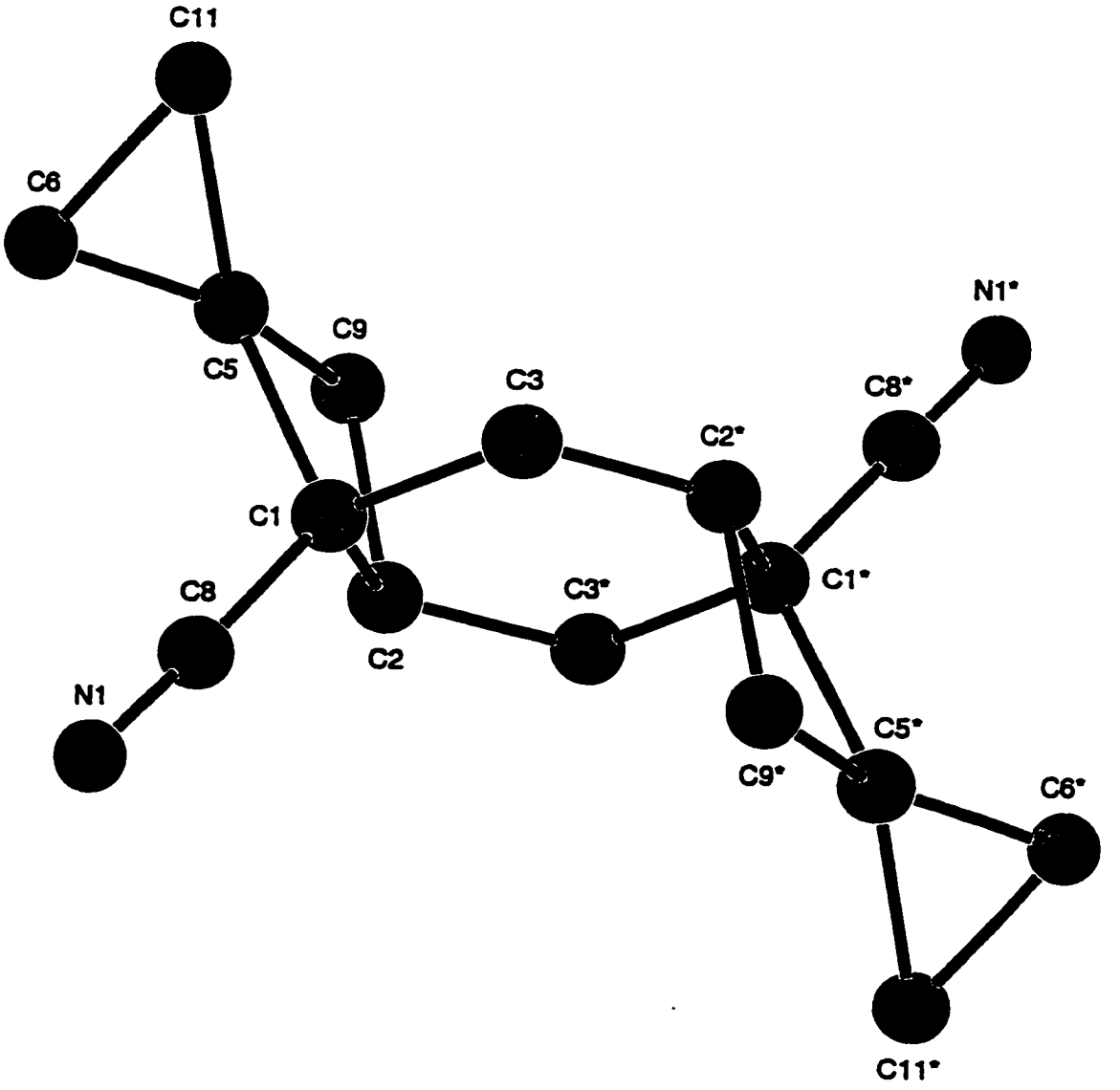

Figure 4.9 Structure of **84** determined by X-ray crystallography.

References

0 Hobbes commenting on Calvin's observation that no important lesson was learned from the replicator failure (*Scientific Progress goes "boink"*).
B. Watterson, *The Indispensable Calvin and Hobbes*, p.190 (1992).

1 H.D. Roth, *Top. Curr. Chem.*, **163**, 131 (1992).

2 (*a*) A.J. Fry, *Synthetic Organic Electrochemistry*, 2nd ed., John Wiley & Sons, 1989.
(*b*) K. Yoshida, *Electrooxidation in Organic Chemistry*, John Wiley & Sons, 1984.
(*c*) C.K. Mann and K.K. Barnes, *Electrochemical Reactions in Nonaqueous Systems*, Marcel Dekker, Inc., New York, 1970.
(*d*) D. Kyriacou, *Modern Electroorganic Chemistry*, Springer-Verlag, New York, 1994.
(*e*) L. Eberson, J.H.P. Utley, and O. Hammerich in: *Organic Electrochemistry*, p. 505, eds. H. Lund and M.M. Baizer, 3rd ed., Marcel Dekker, Inc, New York, 1991.
(*f*) N.L. Weinberg and H.R. Weinberg, *Chem. Rev.*, **68**, 449 (1968).

3 (*a*) R.S. Nicholson and I. Shain, *Anal. Chem.*, **36**, 706 (1964).
(*b*) R.S. Nicholson and I. Shain, *Anal. Chem.*, **37**, 178 (1965).

4 D.D.M. Wayner, Ph.D. thesis, Dalhousie University (1984).

5 T. Shida, E. Haselbach, and T. Bally, *Acc. Chem. Res.*, **17**, 180 (1984).

6 M.C.R. Symons, *Chem. Soc. Rev.*, 393 (1984).

7 (*a*) L.B. Knight, *Acc. Chem. Res.*, **19**, 313 (1986).
(*b*) L.B. Knight and J. Steadman, *J. Chem. Phys.*, **80**, 1018 (1984).

8 M. Tabata and A. Lund, *Chem. Phys.*, **75**, 379 (1983).

9 (*a*) X.-Z. Qin, L.D. Snow, and F. Williams, *J. Am. Chem. Soc.*, **107**, 3366 (1985).
(*b*) L.D. Snow, J.T. Wang, and F. Williams, *Chem. Phys. Lett.*, **100**, 193 (1983).
(*c*) X.-Z. Qin, L.D. Snow, and F. Williams, *J. Phys. Chem.*, **89**, 3602 (1985).

10 (*a*) R.H. Nobes, W.J. Bouma, J.K. Macleod, and L. Radom, *Chem. Phys Lett.*, **135**, 78 (1987).
(*b*) T. Bally, S. Nitsche, and E. Haselbach, *Helv. Chim. Acta*, **67**, 86 (1984).

(*c*) W.J. Bouma, D. Poppinger, S. Saebø, J.K. MacLeod, and L. Radom, *Chem. Phys. Lett.*, **104**, 198 (1984).

11 (*a*) X.-Z. Qin,and F. Williams, *Chem. Phys. Lett.*, **112**, 79 (1984).
(*b*) X.-Z. Qin, L.D. Snow, and F. Williams, *J. Am. Chem. Soc.*, **106**, 7640 (1984).
(*c*) X.-Z. Qin and F. Williams, *Tetrahedron*, **42**, 6301 (1986).

12 (*a*) S. Lunell, L. Yin, and M.-B Huang, *Chem. Phys.*, **139**, 293 (1989).
(*b*) P. Du, D.A. Hrovat, and W.T. Borden, *J. Am. Chem. Soc.*, **110**, 3405 (1988).
(*c*) D.D.M. Wayner, R.J. Boyd, and D.R. Arnold, *Can. J. Chem.*, **63**, 3283 (1985).
(*d*) D.D.M. Wayner, R.J. Boyd, and D.R. Arnold, *Can. J. Chem.*, **61**, 2310 (1983).

13 (*a*) D.R. Arnold and R.W.R. Humphreys, *J. Am. Chem. Soc.*, **101**, 2743 (1979).
(*b*) V.R. Rao and S.S. Hixson, *J. Am. Chem. Soc.*, **101**, 6458 (1979).
(*c*) K. Mizuno, J. Ogawa, H. Kagano, and Y. Otsuji, *Chem. Lett.*, 437 (1981).
(*d*) K. Mizuno, J. Ogawa, and Y. Otsuji, *Chem. Lett.*, 741 (1981).
(*e*) P.G. Gassman, K.D. Olsen, L. Walter, adn R. Yamaguchi, *J. Am. Chem. Soc.*, **103,** 4977 (1981).
(*f*) P.G. Gassman and K.D. Olsen, *J. Am. Chem. Soc.*, **104**, 3740 (1982).

14 (*a*) *Photoinduced Electron Transfer*, Parts A-D, eds. M.A. Fox and M. Chanon, Elsevier, Amsterdam, 1988.
(*b*) S.L. Mattes and S. Farid in: *Organic Photochemistry*, Vol.6, p.233, ed. A. Padwa, Marcel Dekker, Inc., New York, 1983.
(*c*) G.J. Kavernos and N.J. Turro, *Chem. Rev.*, **86**, 401 (1986).
(*d*) G.J. Gavernos, *Top. Curr. Chem.*, **163**, 131 (1992).
(*e*) J. Mattay, *Angew. Chem., Int. Ed. Engl.*, **26**, 825 (1987).
(*f*) A. Albini, M. Mella, and M. Freccero, *Tetrahedron*, **50**, 575 (1994).

15 D. Rehm and A. Weller, *Isr. J. Chem.*, **8**, 259 (1970).

16 (*a*) I.R. Gould, D. Ege, J.E. Moser, and S. Farid, *J. Am. Chem. Soc.*, **112**, 4290 (1990).
(*b*) I.R. Gould and S. Farid, *Acc. Chem. Res.*, **29**, 522 (1996).
(*c*) B.R. Arnold, D. Noukakis, S. Farid, J.L. Goodman, and I.R. Gould, *J. Am. Chem. Soc.*, **117**, 4399 (1995).
(*d*) B.R. Arnold, S. Farid, J.L. Goodman, and I.R. Gould, *J. Am. Chem. Soc.*, **118**, 5482 (1996).
(*e*) S.B. Karki, J.P. Dinnocenzo, S. Farid, J.L Goodman, I.R. Gould, and T.A. Zona, *J. Am. Chem. Soc.*, **119**, 431 (1997).

17 (*a*) R.A. Marcus, *J. Chem. Phys.*, **24**, 966 (1956).
(*b*) R.A. Marcus, *Can. J. Chem.*, **37**, 155 (1959).

18 (*a*) G.L. Closs, L.T. Calcaterra, N.J. Green, K.W. Penfield, and J.R. Miller, *J. Phys. Chem.*, **90**, 3673 (1986).
(*b*) K. Ishiguro, T. Nakano, H. Shibata, and Y. Sawaki, *J. Am. Chem. Soc.*, **118**, 7255 (1996).
(*c*) D.P. DeCosta and J.A. Pincock, *J. Am. Chem. Soc.*, **111**, 8948 (1989).
(*d*) J.W. Hilborn, E. MacKnight, J.A. Pincock, and P.J. Wedge, *J. Am. Chem. Soc.*, **116**, 3337 (1994).

19 (*a*) S.L. Mattes and S. Farid, *J. Am. Chem. Soc.*, **108**, 7356 (1986).
(*b*) D.R. Arnold and M.S. Snow, *Can. J. Chem.*, **66**, 3012 (1988).
(*c*) L.J. Lamont and D.R. Arnold, *Can. J. Chem.*, **68**, 390 (1990).

20 L.M. Hadel in: *CRC Handbook of Photochemistry*, Vol.I, p. 279, ed. J.C. Scaiano, CRC Press, Inc. Boca Raton, Florida (1989).

21 (*a*) L.J. Johnston and N.P. Schepp, *Adv. Electron Transfer Chem.*, **5**, 41 (1996).
(*b*) N.P. Schepp and L.J. Johnston, *J. Am. Chem. Soc.*, **116**, 6895 (1994).
(*c*) N.P. Schepp and L.J. Johnston, *J. Am. Chem. Soc.*, **118**, 2872 (1996).
(*d*) L.J. Johnston and N.P. Schepp, *Pure & Appl. Chem.*, **67**, 71 (1995).

22 A.J. Bard, A. Ledwith, and H.J. Shine, *Adv. Phys. Org. Chem.*, **13**, 155 (1976).

23 P.S. Engel, A.K.M.M. Hoque, J.N. Scholz, H.J. Shine, and K.H. Whitmire, *J. Am. Chem. Soc.*, **110**, 7880 (1988).

24 W. Yueh and N.L. Bauld, *J. Chem. Soc., Perkin Trans. 2*, 1761 (1996).

25 N.L. Bauld, D.J. Bellville, B. Harirchian, K.T. Lorenz, R.A. Pabon, Jr., D.W. Reynolds, D.D. Wirth, H.-S. Chiou, and B.K. Marsh, *Acc. Chem. Res.*, **20**, 371 (1987).

26 P.S. Engel, D.M. Robertson, J.N. Scholz, and H.J. Shine, *J. Org. Chem.*, **57**, 6187 (1992).

27 (*a*) N.L.Bauld, *Tetrahedron*, **45**, 5307 (1989).
(*b*) N.L. Bauld, *Adv. Electron Transfer Chemistry*, **2**, 1 (1992).

28 (*a*) *Ion-Molecule Reactions*, ed. J.L. Franklin, Plenum Press, New York, 1972.
(*b*) *Tandem Mass Spectrometry*, ed. F.W. McLafferty, John Wiley & Sons, 1983.
(*c*) J.R. O'Lear, L.G. Wright, J.N. Louris, and R.G. Cooks, *Org. Mass Spectrom.*, **22**, 348 (1987).
(*d*) J.L. Holmes, *Org. Mass Spectrom.*, **20**, 169 (1985).
(*e*) P.C. Burgers and J.K. Terlouw, *Mass Spectrom.*, **10**, 35 (1989).

29 R.G. Cooks, J.H. Beynon, R.M. Caprioli, and G.R. Lester, *Metastable Ions*, Elsevier, Amsterdam (1973).

30 K. Levsen and H. Schwartz, *Angew. Chem. Int. Ed. Engl.*, **15**, 509 (1976).

31 (*a*) B.F. Yates, W.J. Bouma, and L. Radom, *J. Am. Chem. Soc.*, **106**, 5805 (1984).
(*b*) B.F. Yates, W.J. Bouma, and L. Radom, *Tetrahedron*, **42**, 6225 (1986).

32 V.H. Wysocki and H.I. Kenttämaa, *J. Am. Chem. Soc.*, **112**, 5110 (1990).

33 K.M. Stark, L.K.M. Kiminkinen, and H.I. Kenttämaa, *Chem. Rev.*, **92**, 1649 (1992).

34 (*a*) J.W. Orton, *Electron Paramagnetic Resonance*, London Iliffe Books, Ltd. (1968).
(*b*) T.H. Lowry and K.S. Richardson, *Mechanism and Theory in Organic Chemistry*, 3rd ed., Harper & Row, New York (1987).
(c) A.G. Davies, *Chem. Soc. Rev.*, 299 (1993).
(*d*) N.S. Isaacs, *Physical Organic Chemistry*, Longman Scientific & Technical (1987).
(*e*) N.J. Bunce, *J. Chem. Ed.*, **64**, 907 (1987).

35 (*a*) F.D. Lewis. *Acc. Chem. Res.* **19**, 401 (1986).
(*b*) F.G. Bordwell, J.-P. Cheng, and M.J. Bausch. *J. Am. Chem. Soc.* **110**, 2867 (1988).
(*c*) L.M. Tolbert and R.K. Khanna. *J. Am. Chem. Soc.* **109**, 3477 (1987).
(*d*) L.M. Tolbert, R.K. Khanna, A.E. Popp, L. Gelbaum, and L.A. Bottomley. *J. Am. Chem. Soc.* **112**, 2373 (1990).
(*e*) F.G. Bordwell and M.J. Bausch, *J. Am. Chem. Soc.*, **108**, 2473 (1986).

36 A.M. de P. Nicholas and D.R. Arnold. *Can. J. Chem.* **60**, 2165 (1982).

37 S. Ege, *Organic Chemistry, Structure and Reactivity*, p. 363, 3rd ed., D.C. Heath and Company (1994).

38 A.L. Perrott and D.R. Arnold, *Can. J. Chem.*, **70**, 272 (1992).

39 (*a*) D.R. Arnold and A.J. Maroulis. *J. Am. Chem. Soc.* **98**, 5931 (1976).
(*b*) D.F. Eaton. *Pure Appl. Chem.* **56**, 1191 (1984).
(*c*) L.W. Reichel, G.W. Griffin, A.J. Muller, P.K. Das, and S.N. Ege. *Can. J. Chem.* **62**, 424 (1984).
(*d*) H.F. Davis, P.K. Das, L.W. Reichel, and G.W. Griffin. *J. Am. Chem. Soc.* **106**, 6968 (1984).
(*e*) A. Okamoto and D.R. Arnold. *Can. J. Chem.* **63**, 2340 (1985).
(*f*) A. Okamoto, M.S. Snow, and D.R. Arnold, *Tetrahedron*, **42**, 6175 (1986).

(*g*) D.R. Arnold, B.J. Fahie, L.J. Lamont, J. Wierzchowski, and K.M. Young. *Can. J. Chem.* **65**, 2734 (1987).
(*h*) D.R. Arnold and L.J. Lamont. *Can. J. Chem.* **67**, 2119 (1989).
(*i*) D.R. Arnold, L.J. Lamont, and A.L. Perrott. *Can. J. Chem.* **69**, 225 (1991).
(*j*) F.D. Saeva, *Top. Curr. Chem.* **156**, 59 (1990).
(*k*) P. Maslak, *Top. Curr. Chem.* **168**, 1 (1993).

40 R. Popielarz and D.R. Arnold. *J. Am. Chem. Soc.* **112**, 3068 (1990).

41 A.L. Perrott, H.J.P. de Lijser, and D.R. Arnold, *Can. J. Chem.*, **75**, 000 (1997).

42 D.R. Arnold, X. Du, and H.J.P. de Lijser, *Can. J. Chem.* **73**, 522 (1995).

43 (*a*) D.R. Arnold and X. Du, *Can. J. Chem.*, **72**, 403 (1994).
(*b*) D.R. Arnold and X. Du, *J. Am. Chem. Soc.*, **111**, 7666 (1989).

44 (*a*) J.P. Dinnocenzo, W.P. Todd, T.R. Simpson, and I.R. Gould, *J. Am. Chem. Soc.*, **112**, 2462 (1990).
(*b*) S.S. Shaik and J.P. Dinnocenzo, *J. Org. Chem.*, **55**, 3434 (1990).
(*c*) J.P. Dinnocenzo, D.R. Lieberman, and T.R. Simpson, *J. Am. Chem. Soc.*, **115**, 366 (1993).
(*d*) J.P. Dinnocenzo, T.R. Simpson, H. Zuilhof, W.P. Todd, and T. Heinrich, *J. Am. Chem. Soc.*, **119**, 987 (1997).
(*e*) J.P. Dinnocenzo, H. Zuilhof, D.R. Lieberman, T.R. Simpson, and M.W. McKechney, *J. Am. Chem. Soc.*, **119**, 994 (1997).

45 (*a*) A.L.J. Beckwith, *Tetrahedron*, **37**, 3073 (1981).
(*b*) A.L.J. Beckwith and C.H. Schiesser, *Tetrahedron*, **41**, 3925 (1985).
(*c*) A.L.J. Beckwith, I.A. Blair, and G. Phillipou, *Tetrahedron Lett.*, 2251 (1974).
(*d*) A.L.J. Beckwith, C.J. Easton, and A.K. Serelis, *J. Chem. Soc., Chem. Commun.*, 482 (1980).
(*e*) A.L.J. Beckwith, T. Lawrence, and A.K. Serelis, *J. Chem. Soc., Chem. Commun.*, 484 (1980).
(*f*) A.L.J. Beckwith and T. Lawrence, *J. Chem. Soc., Perkin Trans.* 2, 1535 (1979).
(*g*) A.L.J. Beckwith, G. Phillipou, and A.K. Serelis, *Tetrahedron Lett.*, **22**, 2811 (1981).
(*h*) A.L.J. Beckwith and G. Moad, *J. Chem. Soc., Chem. Commun.*, 472 (1974).

46 (*a*) J.E. Baldwin, *J. Chem. Soc., Chem. Commun.*, 734 (1976).
(*b*) J.E. Baldwin, *J. Chem. Soc., Chem. Commun.*, 738 (1976).

47 S. Hintz, A. Heidbreder, and J. Mattay, *Top. Curr. Chem.*, **177**, 77 (1996).

48 D.R. Arnold, K.A. McManus, and X. Du, *Can. J. Chem.*, **72**, 415 (1994).

49 D.A. Connor, D.R. Arnold, P.K. Bakshi, and T.S. Cameron, *Can. J. Chem.*, **73**, 762 (1995).

50 K.A. McManus and D.R. Arnold, *Can. J. Chem.*, **73**, 2158 (1995).

51 D.R. Arnold, D.A. Connor, K.A. McManus, P.K. Bakshi, and T.S. Cameron, *Can. J. Chem.*, **74**, 602 (1996).

52 (*a*) R.A. Neunteufel and D.R. Arnold, *J. Am. Chem. Soc.*, **95**, 4080 (1973).
(*b*) A.J. Maroulis, Y. Shigemitsu, and D.R. Arnold, *J. Am. Chem. Soc.*, **100**, 535 (1978).
(*c*) R.M. Borg, D.R. Arnold, and T.S. Cameron. *Can. J. Chem.*, **62**, 1785 (1984).
(*d*) D.R. Arnold and M.S. Snow. *Can. J. Chem.*, **66**, 3012 (1988).
(*e*) D.R. Arnold, X. Du, and K.M. Henseleit, *Can. J. Chem.*, **69**, 839 (1991).
(*f*) K. McMahon and D.R. Arnold, *Can. J. Chem.*, **71**, 450 (1993).
(*g*) K.A. McManus and D.R. Arnold, *Can. J. Chem.*, **72**, 2291 (1994).
(*h*) D.R. Arnold, X. Du, and J. Chen. *Can. J. Chem.*, **73**, 307 (1995).
(*i*) D.R. Arnold, M.S.W. Chan, and K.A. McManus. *Can. J. Chem.*, **74**, 2143 (1996).

53 (*a*) H.D. Roth, *Acc. Chem. Res.*, **20**, 343 (1987).
(*b*) N.L. Bauld, D.J. Bellville, R. Pabon, R. Chelsky, and G. Green, *J. Am. Chem. Soc.*, **105**, 2378 (1983).
(*c*) R.A. Pabon and N.L. Bauld, *J. Am. Chem. Soc.*, **106**, 1145 (1984).
(*d*) M. Kojima, A. Kakehi, A. Ishida, and S. Takamuku, *J. Am. Chem. Soc.*, **118**, 2612 (1996).
(*e*) F.D. Lewis and M. Kojima, *J. Am. Chem. Soc.*, **110**, 8664 (1988).

54 (*a*) D.R. Arnold and S.A. Mines, *Can. J. Chem.*, **65**, 2312 (1987).
(*b*) D.R. Arnold and S.A. Mines, *Can. J. Chem.*, **67**, 689 (1989).

55 (*a*) J.P. Dinnocenzo and D.A. Conlon, *J. Am. Chem. Soc.*, **110**, 2324 (1988).
(*b*) J.P. Dinnocenzo and D.A. Conlon, *Tetrahedron*, **36**, 7415 (1995).

56 (*a*) G.-F. Chen and F. Williams, *J. Am. Chem. Soc.*, **113**, 7792 (1991).
(*b*) D. Vollmer, D.L. Rempel, M.L. Gross, and F. Williams, *J. Am. Chem. Soc.*, **117**, 1669 (1995).

57 *Radical Ionic Systems*, ed. A. Lund and M. Shiotani, Kluwer Academic Publishers, Dordrecht, 1991.

58 (*a*) L.A. Eriksson and S. Lunell, *J. Chem. Soc. Faraday Trans.*, **86**, 3287 (1990).
(*b*) T. Bally, *J. Mol. Struct.* (THEOCHEM), **227**, 249 (1991).
(*c*) X. Du, D.R. Arnold, R.J. Boyd, and Z. Shi, *Can. J. Chem.*, **69**, 1365 (1991).

(*d*) M.N. Paddon-Row and M.C.R. Symons, *J. Chem. Soc. Faraday Trans.*, **88**, 667 (1992).
(*e*) N.L. Bauld, *J. Am. Chem. Soc.*, **114**, 5800 (1992).
(*f*) T. Bally, L. Truttmann, S. Dai, J.T. Wang, and F. Williams, *Chem. Phys. Lett.*, **212**, 141 (1993).
(*g*) P. Jungwirth, P. Cársky, and T. Bally, *J. Am. Chem. Soc.*, **115**, 5776 (1993).
(*h*) P. Jungwirth and T. Bally, *J. Am. Chem. Soc.*, **115**, 5783 (1993).
(*i*) J.P. Alvarez-Idaboy, L.A. Eriksson, and S. Lunell, *J. Phys. Chem.*, **97**, 12742 (1993).
(*j*) H.D. Roth and P.S. Lakkaraju, *J. Phys. Chem.*, **97**, 13403 (1993).
(*k*) H.D. Roth, X.-M. Du, H. Weng, P.S. Lakkaraju, and C.J. Abelt, *J. Am. Chem. Soc.*, **116**, 7744 (1994).
(*l*) J.J. Dannenberg, *Angew. Chem. Int. Ed. Engl.*, **15**, 519 (1976).
(*m*) H. Zipse, *J. Am. Chem. Soc.*, **117**, 11798 (1995).
(*n*) S. Lunell, D. Feller, and E.R. Davidson, *Theor. Chim. Acta*, **77**, 111 (1990).
(*o*) G. Frenking, *Int. J. Mass. Spectrom. Ion. Processes*, **95**, 109 (1989).
(*p*) D.D.M. Wayner, B.A. Sim, and J.J. Dannenberg, *J. Org. Chem.*, **56**, 4853 (1991).

59 (*a*) J.B. Foresman and Æ. Frisch, *Exploring Chemistry with Electronic Structure Methods: A Guide to using Gaussian*, Gaussian, Inc., Pittsburgh, PA 15213 USA, 1993.
(*b*) W.J. Hehre, L. Radom, P. v. R. Schleyer, and J.A. Pople, *Ab Initio Molecular Orbital Theory*, John Wiley & Sons, 1986.
(*c*) T. Clark, *A Handbook of Computational Chemsitry*, Wiley-Interscience, 1985.

60 R.S. Mulliken, *J. Chem. Phys.*, **23**, 1833, 1841, 2338, 2343 (1955).

61 C. Møller and M.S. Plesset, *Phys. Rev.*, **46**, 618 (1934).

62 (*a*) R.C. Bingham, M.J.S. Dewar, and D.H. Lo, *J. Am. Chem. Soc.*, **97**, 1285, 1294, 1302, 1307 (1975).
(*b*) M.J.S. Dewar and D.M. Storch, *J. Am. Chem. Soc.*, **107**, 3898 (1985).
(*c*) M.J.S. Dewar, E.G. Zoebisch, E.F. Healy, and J.J.P. Stewart, *J. Am. Chem. Soc.* **107**, 3902 (1985).

63 Gaussian 92/DFT, Revision F.2, M.J. Frisch, G.W. Trucks, H.B. Schlegel, P.M.W. Gill, B.G. Johnson, M.W. Wong, J.B. Foresman, M.A. Robb, M. Head-Gordon, E.S. Replogle, R. Gomperts, J.L. Andres, K. Raghavachari, J.S. Binkley, C. Gonzalez, R.L. Martin, D.J. Fox, D.J. Defrees, J. Baker, J.J.P. Stewart, and J.A. Pople, Gaussian Inc., Pittsburgh PA, 1993.

64 PC Model, Serena Software, Bloomington, IN 4702-3076.

65 (*a*) D. Feller, K. Tanaka, E.R. Davidson, and W.T. Borden, *J. Am. Chem. Soc.*, **104**, 967 (1982).
(*b*) P. Du and W.T. Borden, *J. Am. Chem. Soc.*, **109**, 5330 (1987).
(*c*) M.A. McAllister and T.T. Tidwell, *J. Am. Chem. Soc.*, **114**, 5362 (1992).
(*d*) V.W. Laurie and W.M. Stigliani, *J. Am. Chem. Soc.*, **92**, 1485 (1970).

66 (*a*) G. Bieri, F. Burger, E. Heilbronner, and J.P. Maier, *Helv. Chim. Acta*, **60**, 2213 (1977).
(*b*) P. Hemmersbach and M. Klessinger, *Tetrahedron*, **36**, 1337 (1980).

67 (*a*) R.G. Doerr and P.S. Skell, *J. Am. Chem. Soc.*, **89**, 3062 (1967).
(*b*) P.S. Skell and R.G. Doerr, *J. Am. Chem. Soc.*, **89**, 4688 (1967).
(*c*) F. Weiss, *Quart. Rev., Chem. Soc.*, **24**, 278 (1970).
(*d*) J.J. Gajewski, A. Yeshurun, and E.J. Bair, *J. Am. Chem. Soc.*, **94**, 2138 (1972).
(*e*) G. Maier, D. Jürgen, R. Tross, H.P. Reisenauer, B.A. Hess Jr., and L.J. Schaad, *Chem. Phys.*, **189**, 383 (1994).

68 Cyclization to triplet methylenecyclopropane is endothermic (25-50 kcal/mol) and while cyclization to singlet (ground state) methylenecyclopropane is exothermic (20 kcal/mol), this reaction is strongly spin forbidden.[67]

69 (*a*) J.J. Gajewski, L.K. Hoffman, and C.N. Shih, *J. Am. Chem. Soc.*, **96**, 3705 (1974).
(*b*) D.S. Bailey and J.B. Lambert, *J. Org. Chem.*, **38**, 134 (1973).

70 In fact, of all semi-empirical methods used (CNDO, INDO, MNDO, MINDO/3, PM3, and AM1) for calculations on **14**, only AM1 gave results that were in good agreement with the results of the *ab initio* calculations.

71 (*a*) W.-D. Stohrer and R. Hoffmann, *J. Am. Chem. Soc.*, **94**, 779 (1972).
(*b*) M.D. Newton and J.M. Schulman, *J. Am. Chem. Soc.*, **94**, 4391 (1972).
(*c*) J.J. Dannenberg and T.M. Prociv, *J. Chem. Soc. Chem. Commun.*, 291 (1973).
(*d*) A.R. Gregory, M.N. Paddon-Row, L. Radom, and W.-D. Stohrer, *Aust. J. Chem.*, **30**, 473 (1977).
(*e*) M.L. Herr, *Tetrahedron*, **33**, 1897 (1977).
(*f*) K.B. Wiberg, *J. Am. Chem. Soc.*, **105**, 1227 (1983).
(*g*) K.B. Wiberg, R.F.W. Bader, and C.D.H. Lau, *J. Am. Chem. Soc.*, **109**, 985, 1001 (1987).
(*h*) D. Feller and E.R. Davidson, *J. Am. Chem. Soc.*, **109**, 4133 (1987).
(*i*) T. Ushio, T. Kato, K. Ye, and A. Imamura, *Tetrahedron*, **45**, 7743 (1989).

72 (*a*) P.E.Eaton and G.H. Temme III, *J. Am. Chem. Soc.*, **95**, 7508 (1973).
(*b*) K.B.Wiberg, G.A. Epling, and M. Jason, *J. Am Chem. Soc.*, **96**, 912 (1974).
(*c*) J.J. Dannenberg, T.M. Prociv, and C. Hutt, *J. Am. Chem. Soc.*, **96**, 914 (1974).

(d) K.B. Wiberg, W.E. Pratt, and W.F. Bailey, *J. Am. Chem. Soc.*, **99**, 2297 (1977).
(*e*) K.B. Wiberg and M.G. Matturro, *Tetrahedron Lett.*, **22**, 3481 (1981).
(*f*) K.B.Wiberg, *Acc. Chem. Res.*, **17**, 379 (1984).
(*g*) K.B. Wiberg, J.J. Caringi, and M.G. Matturro, *J. Am. Chem. Soc.*, **112**, 5854 (1990).

73 (*a*) E. Buchta and A. Kröniger, *Chimia*, 225 (1969).
(*b*) P. Binger, *Angew. Chem. Int. Ed. Engl.*, **11**, 309, 433 (1972).
(*c*) W.R. Dolbier Jr., D. Lomas, T. Garza, C. Harmon, and P. Tarrant, *Tetrahedron*, **28**, 3185 (1972).
(*d*) M. Randic and L. Kumar, *J. Molec. Struct.*, **26**, 145 (1975).
(*e*) M.J. Doyle, J. McMeeking, and P. Binger, *J. Chem. Soc. Chem. Commun.*, 376 (1976).
(*f*) J.M. Denis, P. Le Perchec, and J.M. Conia, *Tetrahedron*, **33**, 399 (1977).
(*g*) P. Binger, M.J. Doyle, and R. Benn, *Chem. Ber.*, **116**, 1 (1983).
(*h*) P. Binger, A. Brinkmann, and P. Wedemann, *Chem. Ber.*, **116**, 2920 (1983).
(*i*) K. Rasmussen and C. Tosi, *J. Molec. Struct. (Theochem)*, **121**, 233 (1985).

74 (*a*) Examples of metal catalyzed (C1-C3) bond cleavage reactions exist. these oxidative insertion reactions of low valent complexes of Pt^0, Pt^{II}, Rh^I, and Fe^0 are well known.[74b] However, there seem to be no examples available of the uncatalyzed process.
(*b*) P. Binger and H.M. Büch, *Top. Curr. Chem.*, **135**, 77, (1987) and cited references.

75 D.R. Arnold and A.J. Maroulis, *J. Am. Chem. Soc.*, **98**, 5931 (1976).

76 (*a*) H.J.P. de Lijser and D.R. Arnold, *J. Phys. Chem.*, **100**, 3996 (1996).
(*b*) H.J.P. de Lijser and D.R. Arnold, *J. Chem. Soc., Perkin Trans. 2*, 1369 (1997).

77 D.D.M. Wayner and D.R. Arnold, *Can. J. Chem.*, **63**, 871 (1985).

78 (*a*) Q.-X. Guo, X.-Z. Qin, J.T. Wang, and F. Williams, *J. Am. Chem. Soc.*, **110**, 1974 (1988).
(*b*) F. Williams, Q.-X. Guo, D.C. Bebout, and B.K. Carpenter, *J. Am. Chem. Soc.*, **111**, 4133 (1989).

79 L.S. Prasad, R. Ding, E.G. Bradford, L.D. Kispert, and H. Wang, *Isr. J. Chem.*, **29**, 33 (1989).

80 M. St-Jacques and M. Bernard, *Can. J. Chem.*, **47**, 2911 (1969).

81 (*a*) T. Shono and A. Ikeda, *J. Am. Chem. Soc.*, **94**, 7892 (1972).

(*b*) T. Shono, A. Ikeda, J. Hayashi, and S. Hakozaki, *J. Am. Chem. Soc.*, **97**, 4261 (1975).
(*c*) P.G. Gassman and R. Yamaguchi, *Tetrahedron*, **38**, 1113 (1982).

82 L.M. Harwood, *Aldrichimica Acta*, **18**, 25 (1985).

83 D.R. Arnold and D.D.M. Wayner, *Can. J. Chem.*, **64**, 100 (1986).

84 C.L. Perris and R.M. Christenson, *J. Org. Chem.*, **25**, 1888 (1960).

85 (*a*) R.A. Kaba, D. Griller, and K.U. Ingold, *J. Am. Chem. Soc.*, **96**, 6202 (1974).
(*b*) J.R. Shelton and C.W. Uzelmeier, *J. Am. Chem. Soc.*, **88**, 5222 (1966).
(*c*) See for example: A.L.J. Beckwith, D.M. O'Shea, and S.W. Westwood, *J. Am. Chem. Soc.*, **110**, 2565 (1988).
(*d*) Yu.N. Ogibin, E.I. Troyanskii, and G.I. Nikishin, *Izv. Akad. Nauk. SSSR Ser. Khim.*, 1461 (1975).

86 P.S. Engel, W.-K. Lee, G.E. Marschke, and H.J. Shine, *J. Org. Chem*, **52**, 2813 (1987).

87 (*a*) P. Neta, G.R. Holdren, and R.H. Schuler, *J. Phys. Chem.*, **75**, 449 (1971).
(*b*) G.V. Buxton, C.L. Greenstock, W.P. Helman, and A.B. Ross, *J. Phys. Chem. Ref. Data*, **17**, 513 (1988).
(*c*) J.A. Baban, V.P.J. Marti, and B.P. Roberts, *J. Chem. Soc., Perkin Trans. 2*, 1723 (1985).
(*d*) V. Paul and B.P. Roberts, *J. Chem. Soc., Perkin Trans. 2*, 1183 (1988).
(*e*) J.N. Kirwan and B.P. Roberts, *J. Chem. Soc., Perkin Trans. 2*, 539 (1989).
(*f*) V.P.J. Marti and B.P. Roberts, *J. Chem. Soc., Perkin Trans. 2*, 1613 (1986).
(*g*) D. Wittneben and H.-F. Grützmacher, *Int. J. Mass Spectrom. Ion Processes*, **100**, 545 (1990).

88 (*a*) A.R. Forrester, M. Gill, J.S. Sadd, and R.H. Thomson, *J.C.S. Chem. Comm.*, 291 (1975)
(*b*) J. Boivin, E. Fouquet, and S.Z. Zard, *Tetrahedron*, **50**, 1745, 1757 (1994).
(*c*) J. Boivin, E. Fouquet, A.-M. Schiano, and S.Z. Zard, *Tetrahedron*, **50**, 1769 (1994).
(*d*) M.L. Poutsma and P.A. Ibarbia, *J. Org. Chem.*, **34**, 2848 (1969).
(*e*) J. Hofmann, K. Schulz, and G. Zimmermann, *Tetrahedron Lett.*, **37**, 2399 (1996).
(*f*) C.J. Rhodes and H. Agirbas, *J. Chem. Soc., Faraday Trans.*, **86**, 3303 (1990).

89 (*a*) R.F. Hudson, A.J. Lawson, and E.A.C. Lucken, *Chem. Comm.*, 807 (1971);
(*b*) M.C.R. Symons, *Tetrahedron*, **29**, 615 (1973);
(*c*) H. Sakuragi, S. Ishikawa, T. Nishimura, M. Yoshida, N. Inamoto, and K. Tokumaru, *Bull. Chem. Soc. Jap.*, **49**, 1949 (1976);

(*d*) A.R. Forrester, M. Gill, C.J. Meyer, J.S. Sadd, and R.H. Thomson, *J.C.S. Perkin 1*, 606 (1979);
(*e*) B.P. Roberts and J.N. Winter, *J.C.S. Perkin 2*, 1353 (1979);
(*f*) P.R. Marriott and D. Griller, *J. Am. Chem. Soc.*, **103**, 1521 (1981);
(*g*) J. Lub, M.L. Beekes, and Th.J. de Boer, *J. Chem. Soc., Perkin Trans. 2*, 721 (1983);
(*h*) T.S.V. Buys, H. Cerfontain, J.A.J. Geenevasen, and F. Stunnenberg, *Recl. Trav. Chim. Pays-Bas*, **109**, 491 (1990).

90 D. Griller, G.D. Mendenhall, W. Van Hoof, and K.U. Ingold, *J. Am. Chem. Soc.*, **96**, 6068 (1974).

91 T. Suehiro, Y. Matsui, and Y. Inogushi, *Bull. Chem. Soc. Jap.*, **51**, 2609 (1978).

92 (*a*) R.W. Binkley, *J. Org. Chem.*, **33**, 2311 (1968).
(*b*) R.W. Binkley, *J. Org. Chem.*, **34**, 2072 (1969).
(*c*) R.W. Binkley, *J. Org. Chem.*, **34**, 931 (1969).
(*d*) R.W. Binkley, *J. Org. Chem.*, **35**, 2796 (1970).

93 R.F. Hudson, A.J. Lawson, and K.A.F. Record, *J. Chem. Soc., Chem. Comm.*, 488 (1974).

94 J. Gorse, III and R.W. Binkley, *J. Org. Chem.*, **37**, 575 (1972).

95 J.C. Scaiano and L.C. Stewart, *J. Am. Chem. Soc.*, **105**, 3609 (1983).

96 (*a*) *Ab initio* calculations[96b] have shown that the spin and charge distributions in phenyl radical and in *p*-cyanophenyl radical are very similar; their behaviour is, therefore, expected to be similar as well.
(*b*) A.L. Perrott, unpublished results. *Ab initio* calculations (MP2/6-31G*//HF/6-31G*) were performed on phenyl radical and *p*-cyanophenyl radical using Gaussian 92.[63]

97 An X-Ray crystal structure of *p*-cyanoacetophenone azine has been reported: R. Glaser, G.S. Chen, and C.L. Barnes, *J. Org. Chem.*, **58**, 7446 (1993)

98 The X-ray crystal structure was recently reported: A.K. Saha, M.M. Hossain, D.S. Grubisha, and D.W. Bennett, J. Chem. Cryst., **25**, 383 (1995).

99 F.L. Cozens and N.P. Schepp, Manuscript in preparation.

100 S.L. Painter and S.C. Blackstock, *J. Am. Chem. Soc.*, **117**, 1441 (1995).

101 R. Noyori, N. Hayashi, and M. Katô, *J. Am. Chem. Soc.*, **93**, 4948 (1971).

102 T. Miyashi, Y. Takahashi, T. Mukai, H.D. Roth, and M.L.M. Schilling, *J. Am. Chem. Soc.*, **107**, 1079 (1985).

103 (*a*) Y. Takahashi, T. Miyashi, and T. Mukai, *J. Am. Chem. Soc.*, **105**, 6511 (1985).
(*b*) T. Miyashi, M. Kamata, and T. Mukai, *J. Am. Chem. Soc.*, **108**, 2755 (1986).
(*c*) T. Miyashi, M. Kamata, and T. Mukai, *J. Am. Chem. Soc.*, **109**, 2780 (1987).
(*d*) T. Miyashi, Y. Takahashi, M. Kamata, K. Yokogowa, H. Ohaku, and T. Mukai, *Studies in Organic Chemistry*, **31**, 363 (1987).

104 K. Komaguchi, M. Shiotani, and A. Lund, *Chem. Phys. Lett.*, **265**, 217 (1997).

105 D.R. Arnold, P.C. Wong, A.J. Maroulis, and T.S. Cameron, *Pure Appl. Chem.*, **52**, 2609 (1980).

106 R. Srinivasan, *Tetrahedron Lett.*, **32**, 2725 (1974).

107 (*a*) J. Cornelisse, *Chem. Rev.*, **93**, 615 (1993).
(*b*) F. Müller and J. Mattay, *Chem. Rev.*, **93**, 99 (1993).
(*c*) P. A. Wender, L. Siggel, and J.M. Nuss, *Organic Photochemistry* (Ed. E. Padwa), Vol. **10**, 357 (1989).

108 (*a*) J. Mattay, *Tetrahedron*, **41**, 2293 (1985).
(*b*) J. Mattay, *Tetrahedron*, **41**, 2405 (1985).
(*c*) J. Mattay, *J. Photochem.*, **37**, 167 (1987).

109 (*a*) G. Weber, J. Runsink, and J. Mattay, *J. Chem. Soc., Perkin Trans. 1*, 2333 (1987).
(*b*) D. Bryce-Smith, B. Foulger, J. Forrester, A. Gilbert, B.H. Orger, and H.M. Tyrrell, *J.C.S. Perkin I*, 55, 1980.

110 For example see:
(*a*) P.J. Wagner and K. Nahm, *J. Am. Chem. Soc.*, **109**, 6528 (1987).
(*b*) K.B. Cosstick, M.G.B. Drew, and A. Gilbert, *J. Chem. Soc., Perkin Trans. 1*, 1867 (1987).

111 (*a*) H.E. Zimmerman and C.J. Samuel, *J. Am. Chem. Soc.*, **97**, 4025 (1975).
(*b*) H.E. Zimmerman and C.W. Carpenter, *J. Org. Chem.*, **53**, 3298 (1988).
(*c*) S.M. Nevill, A.L. Pincock, and J.A. Pincock, *J. Org. Chem.*, in press (1997).

112 H.E. Zimmerman and G.L. Grunewald, *J. Am. Chem. Soc.*, **88**, 448 (1966).

113 It must be noted that the six isolated products are the major products of the photoreaction of MCP with **33**. Analysis of the final product mixture indicated the presence of at least six other products with mass spectra very similar to those of the isolated products. It can, therefore, not be ruled out that the product from the

cyclopropyl-π-methane rearrangement is not formed. However, since all of these "extra" products are only minor products, it can be concluded that the "normal" cyclopropyl-π-methane rearrangement is not an important pathway in this reaction.

114 W.C. Neikam, G.R. Dimeler, and M.M. Desmond, *J. Electrochem. Soc.*, **111**, 1190 (1964).
There are several correlations available. For others see references 115 and 116.

115 L.L. Miller, G.D. Nordblum, and E.A. Mayeda, *J. Org. Chem.*, **37**, 916 (1972).

116 (*a*) L. Eberson, Adv. *Phys. Org. Chem.*, **18**, 79 (1982).
(*b*) L. Eberson, *Electron Transfer Reactions in Organic Chemistry*, Springer-Verlag (1987).

117 M. Lautens, Y. Ren, and H.M. Delanghe, *J. Am. Chem. Soc.*, **116**, 8821 (1994).

118 (*a*) T. Herbertz, and H.D. Roth, *J. Am. Chem. Soc.*, **118**, 10954 (1996).
(*b*) H. Weng, Q. Sheik, and H.D. Roth, *J. Am. Chem. Soc.*, **117**, 10655 (1995).
(*c*) T.A. Zona and J.L. Goodman, *J. Am. Chem. Soc.*, **115**, 4925 (1993).
(*d*) K.P. Dockery, J.P. Dinnocenzo, S. Farid, J.L. Goodman, I.R. Gould, and W.P. Todd, *J. Am. Chem. Soc.*, **119**, 1876 (1997).

119 D.Z. Samedova, K.Ya. Alieva, S.S. Avanesova, F.K. Ismailov, Z.A. Ekhtibarova, and T.N. Shakhtakhtinskii, *Dokl. Akad. Nauk. Az. SSR*, **32**, 42 (1976); Chemical Abstracts **87**: 52718f (1977).

120 (*a*) J.Y. Becker and M. Münster, *Tetrahedron Lett.*, 455 (1977).
(*b*) J.Y. Becker and D. Zemach, *J.C.S. Perkin II*, 336 (1981).

121 R.D. Bowen, J. Chandrasekhar, G. Frenking, P. v. R. Schleyer, H. Schwartz, C. Wesdemiotis, and D.H. Williams, *Chem. Ber.*, **113**, 1084 (1980).

122 J.S. Staral, I. Yavari, J.D. Roberts, G.K.S. Prakash, D.J. Donovan, and G.A. Olah, *J. Am. Chem. Soc.*, **100**, 8016 (1978).

123 H. Kollmar and H.O. Smith, *Tetrahedron Lett.*, 3133 (1970).

124 (*a*) I.S. Krull and D.R. Arnold, *Org. Prep. Proced.*, **1**, 283 (1969).
(*b*) J.R. Salaun, J. Champion, and J.M. Conia, *Org. Synth.*, **57**, 36 (1977).
(*c*) R. Köster, S. Arora, and P. Binger, *Angew. Chem.*, **8**, 205 (1969).
(*d*) R. Köster, S. Arora, and P. Binger, *Synthesis*, 322 (1971).
(*e*) R. Köster, S. Arora, and P. Binger, *Liebigs Ann. Chem.*, 1219 (1973).

125 (*a*) J. Llinarés, J. Elguero, R. Faure, and E.-J. Vincent, *Org. Magn. Res.*, **14**, 20 (1980).

(*b*) N. Kalayanam and S. Sivaram, *Org. Mass Spectrom.*, **22**, 43 (1987).

126 *SHELXS86*: G.M. Sheldrick, In: *Crystallographic Computing* (Eds. G.M. Sheldrick, C. Kruger, and R. Goddard), Oxford University Press, pp. 175-189 (1985).

127 *DIRDIF92*: P.T. Beurskens, G. Admiraal, G. Beurskens, W.P. Bosman, S. Garcia-Granda, R.O. Gould, J.M.M. Smits, and C. Smykalla. *The DIRDIF program system*, Technical support of the Crystallographic Laboratory, University of Nijmegen, The Netherlands (1992).

128 Least-Squares:

Function minimized: $\Sigma w(|Fo| - |Fc|)^2$

where $w = 1/\sigma^2(Fo^2) = 4Fo^2/\sigma^2(Fo^2)$

$\sigma^2(Fo^2) = [S^2(C+R^2B)+(pFo^2)^2]/Lp^2$

S = Scan rate
C = Total Integrated Peak Count
R = Ratio of Scan Time to background counting time
B = Total Background Count
Lp = Lorentz-polarization factor
p = p-factor

129 Standard deviation of an observation of unit weight:

$\sqrt{(\Sigma w(|Fo| - |Fc|)^2/(No-Nv))}$

where: No = number of observations
Nv = number of variables

130 D.T. Cromer and J.T. Weber, *International Tables for X-ray Crystallography*, Vol. IV, The Kynoch Press, Birmingham, England, Table 2.2 A (1974).

131 J.A. Ibers and W.C. Hamilton, *Acta Crystallogr.* **17**, 781 (1964).

132 D.C. Creagh, W.J. McAuley, *International Tables for Crystallography*, Vol. C, (Ed. A.J.C. Wilson), Kluwer Academic Publishers, Boston, Table 4.2.6.8, pp. 219-222 (1992).

133 D.C. Creagh and J.H. Hubbell, *International Tables for Crystallography*, Vol. C, (Ed. A.J.C. Wilson), Kluwer Academic Publishers, Boston, Table 4.2.4.3, pp. 200-206 (1992).

134 *teXsan*: Crystal Structure Analysis Package, Molecular Structure Corporation (1985 & 1992)

IMAGE EVALUATION TEST TARGET (QA-3)

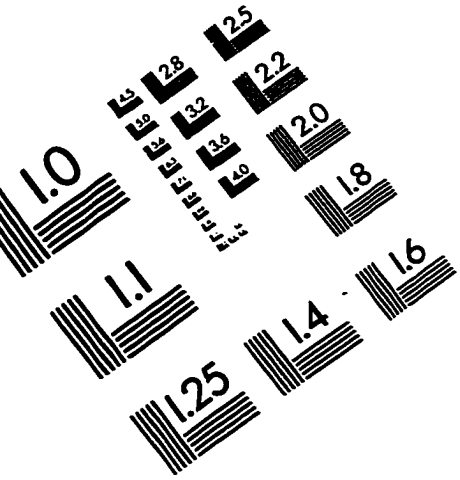

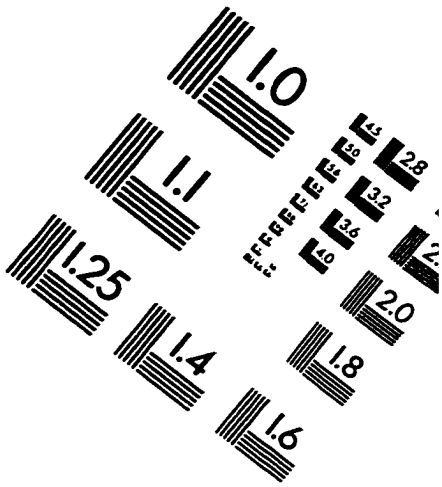

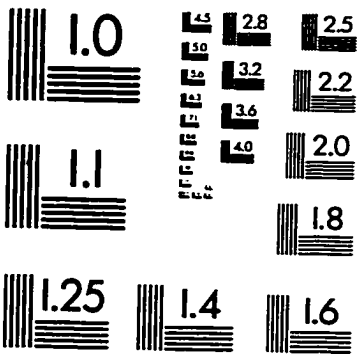

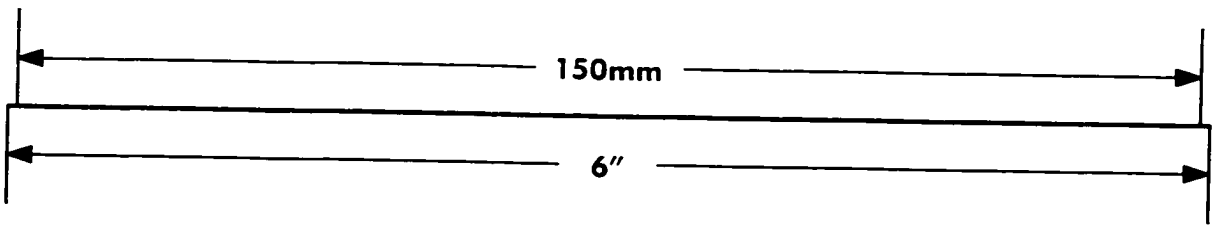

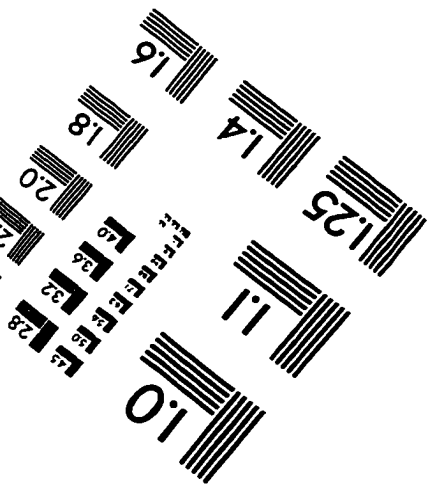

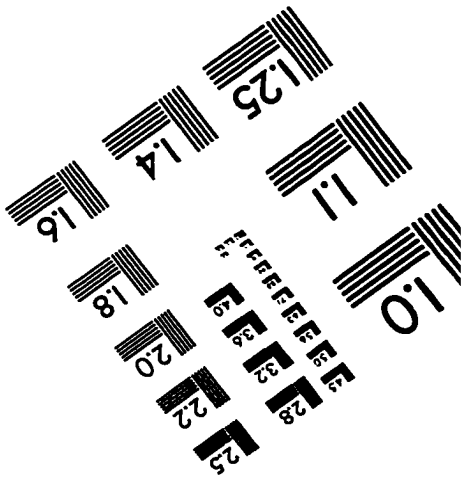

APPLIED IMAGE, Inc
1653 East Main Street
Rochester, NY 14609 USA
Phone: 716/482-0300
Fax: 716/288-5989